Alfred J. Klapperich
131 Walker Ave
Clarendon Hills Ill.
10-19-59
DEC 10 1959

АКАДЕМИЯ НАУК СССР
AKADEMIIA NAUK SSSR

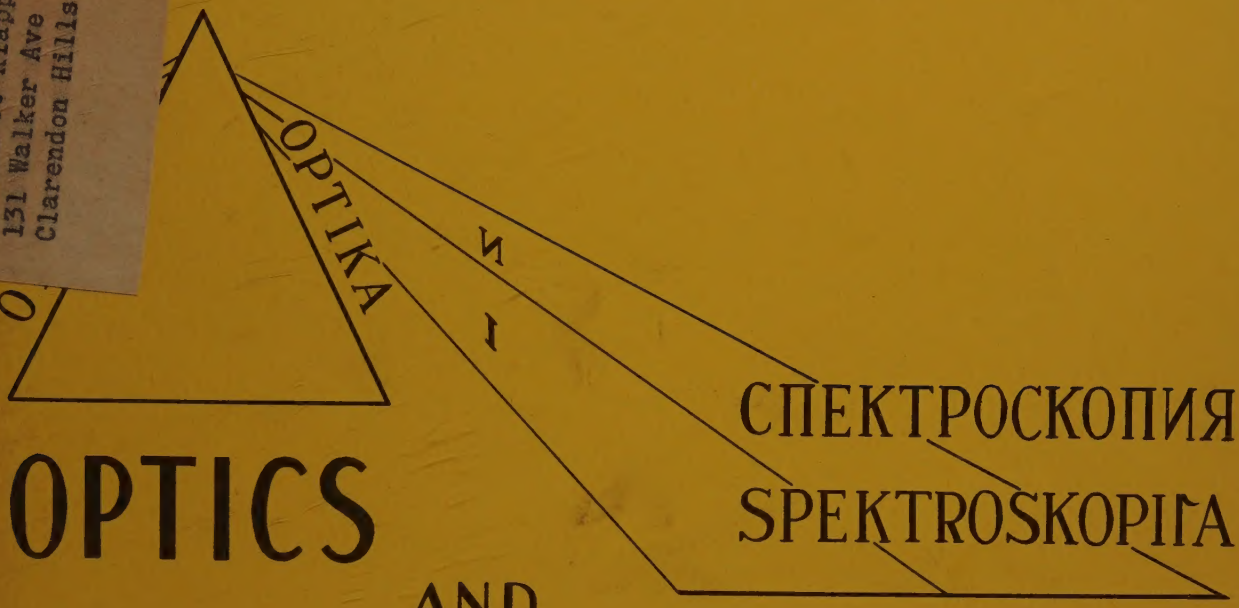

OPTICS AND SPECTROSCOPY

MAY 1959 - VOL. VI - NO. 5
MAI 1959 - TOM. VI - VYP. 5

Translated on the Initiative of
THE OPTICAL SOCIETY OF AMERICA, INC.
With a Grant-in-Aid from
THE NATIONAL SCIENCE FOUNDATION
by MORRIS D. FRIEDMAN, INC.

RUSSIAN EDITORIAL STAFF

Editor: S. E. FRISH

Assistant Editor: P. P. FEOFILOV

Corresponding Secretary: L. S. SAZONOV

Associate Editors:

M. M. GUREVICH M. A. EL'IASHEVICH A. A. LEBEDEV V. P. LINNIK
S. L. MANDEL'SHTAM I. V. OBREIMOV V. K. PROKOF'EV
N. N. SOBOLEV A. N. TERENIN A. I. TUDOROVSKII

Translation Editorial Staff

MORRIS D. FRIEDMAN

DR. JAMES R. ARONSON, *Arthur D. Little, Inc.*
FRED W. BEHNKE, *Perkin-Elmer Corp.*
DR. RICHARD DALVEN, *Raytheon Company, Research Division,*
DR. SUMNER P. DAVIS, *University of California*
CYRUS FELDMAN, *Oak Ridge National Laboratory*
DR. CONRAD J. RAUCH, *Massachusetts Institute of Technology — Lincoln Laboratory*
DR. JOHN S. WAUGH, *Massachusetts Institute of Technology*

Published semi-monthly by the Optical Society of America, Inc. Business and Editorial office: 33 University Road, Cambridge 38, Mass. Society officies: 121 Lincoln Avenue, Rochester, New York. Subscriptions for one year to members of the Society: Associates $13.00; Regular members and Fellows $17.00. Subscriptions for non-members of the Society: One year U.S. and Possessions, $25.00; Foreign $28.00. Back numbers: $3.00 per copy. Lithoprinted in the USA.

Application for 2nd Class mailing privileges pending at Post Office, Boston, Mass.

АКАДЕМИЯ НАУК СССР
AKADEMIIA NAUK SSSR

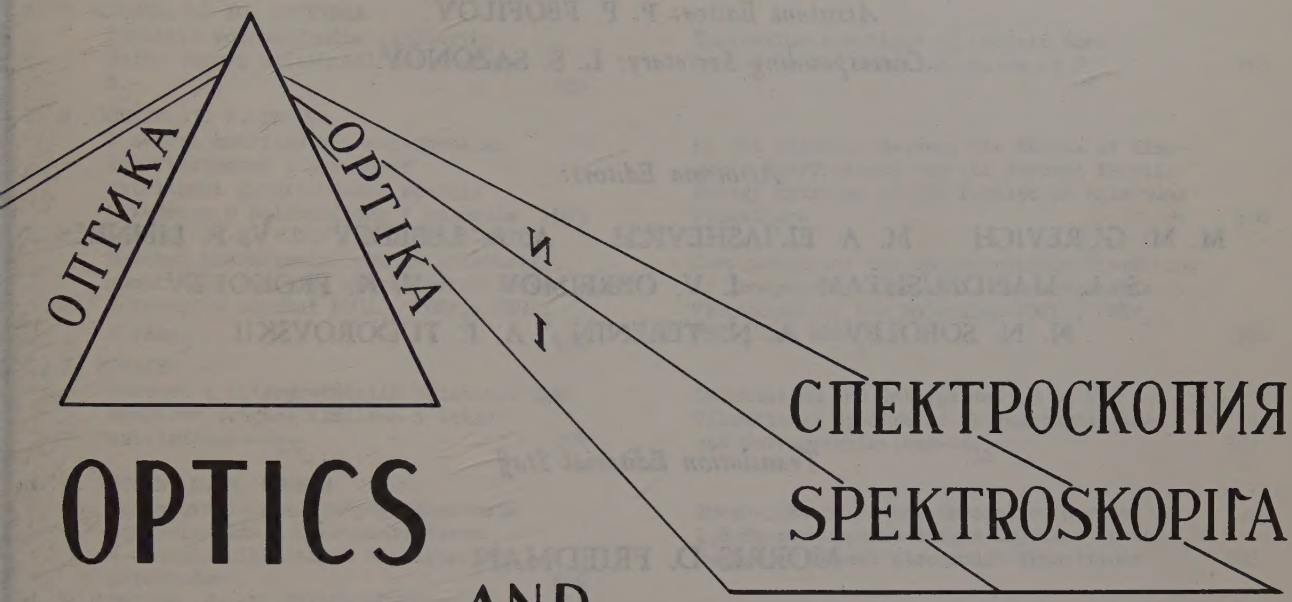

OPTICS AND SPECTROSCOPY

MAY 1959 - VOL. VI - NO. 5
MAI 1959 - TOM. VI - VYP. 5

Translated on the Initiative of
THE OPTICAL SOCIETY OF AMERICA, INC.
With a Grant-in-Aid from
THE NATIONAL SCIENCE FOUNDATION
by MORRIS D. FRIEDMAN, INC.

RUSSIAN EDITORIAL STAFF

Editor: S. E. FRISH

Assistant Editor: P. P. FEOFILOV

Corresponding Secretary: L. S. SAZONOV

Associate Editors:

M. M. GUREVICH M. A. EL'IASHEVICH A. A. LEBEDEV V. P. LINNIK
S. L. MANDEL'SHTAM I. V. OBREIMOV V. K. PROKOF'EV
N. N. SOBOLEV A. N. TERENIN A. I. TUDOROVSKII

Translation Editorial Staff

MORRIS D. FRIEDMAN

DR. JAMES R. ARONSON, *Arthur D. Little, Inc.*
FRED W. BEHNKE, *Perkin-Elmer Corp.*
DR. RICHARD DALVEN, *Raytheon Company, Research Division,*
DR. SUMNER P. DAVIS, *University of California*
CYRUS FELDMAN, *Oak Ridge National Laboratory*
DR. CONRAD J. RAUCH, *Massachusetts Institute of Technology — Lincoln Laboratory*
DR. JOHN S. WAUGH, *Massachusetts Institute of Technology*

Published semi-monthly by the Optical Society of America, Inc. Business and Editorial office: 33 University Road, Cambridge 38, Mass. Society officies: 121 Lincoln Avenue, Rochester, New York. Subscriptions for one year to members of the Society: Associates $13.00; Regular members and Fellows $17.00. Subscriptions for non-members of the Society: One year U.S. and Possessions, $25.00; Foreign $28.00. Back numbers: $3.00 per copy. Lithoprinted in the USA.

Application for 2nd Class mailing privileges pending at Post Office, Boston, Mass.

TOM VI, Vyp. 5
VOL. VI, No. 5

OPTIKA I SPEKTROSKOPIIA
OPTICS AND SPECTROSCOPY

Mai, 1959
May, 1959

SODERZHANIE

Plan razvitiia narodnogo khoziaistva SSSR i zadachi sovetskoi optiki 573

F. A. KOROLEV, B. A. KOZLOV, A. I. ODINTSOV
K voprosu o forme kontura linii v atomnom puchke 576

S. M. KISHKO, M. IU. KUCHINKA
Funktsii vozbuzhdeniia nekotorykh polos vtoroi polozhitel'noi sistemy N_2 580

I. N. GODNEV, I. V. ORLOVA
O sviazi matritsy kinematicheskikh koeffitsientov s obratnymi matritsami kineticheskoi energii v zadache o kolebaniiakh v molekule 583

L. S. MAIANTS, E. M. POPOV, M. I. KABACHNIK
Raschet kharakteristichnykh kolebanii soedinenii fosfora. Kharakteristichnye kolebaniia molekul $POCl_3$, $POBr_3$, $PSCl_3$ i $PSBr_3$ 589

I. F. KOVALEV
Raschet i interpretatsiia kolebatel'nykh spektrov tetrametilsilana i tetrametilsilana--d_{12} 594

M. S. BRODIN, M. S. SOSKIN
Issledovanie spektra pogloshcheniia monokristalla 1,2-benzantratsena v oblasti nizhaishikh elektronnykh perekhodov 600

M. P. LISITSA, IU. P. TSIASHCHENKO
Kolichestvennye issledovaniia infrakrasnogo pogloshcheniia i dispersii khloroforma 605

V. E. ESKIN, I. A. BARANOVSKAIA
Akusticheskoe dvoinoe luchepreломlenie fenil-etilovogo spirta pri nizkikh temperaturakh 616

V. M. PIVOVAROV, N. D. ORDYNTSEVA
Vliianie kontsentratsii i tipa rastvoritelia na intensivnost' linii kombinatsionnogo rasseianiia polnosimmetrichnogo kolebaniia nitrogruppy i na elektronnye spektry pogloshcheniia aromaticheskikh nitrosoedinenii 620

P. A. BAZHULIN AND L. P. OSIPOVA
Raznost' energii povorotnykh izomerov v zhidkom i gazoobraznom 1, 2 -ftorkhloretane 625

I. V. ASTAF'EV, A. I. SHATENSHTEIN
Spektry pogloshcheniia karbanionov 631

B. I. SUKHORUKOV, A. I. FINKEL'SHTEIN
Opticheskoe issledovanie molekuliarnogo stroeniia tsianamida i ego proizvodnykh. I. Molekuliarnoe stroenie ditsiandiamida 637

V. L. ERMOLAEVA
Zavisimost' veroiatnosti perenosa energii pri sensibilizovannoi fosforestsentsii ot sily ostsilliatora triplet-singuletnogo perekhoda v molekule aktseptora energii 642

V. M. AGRANOVICH, IU. V. KONOBEEV
Vliianie reabsorbtsiina vykhod i dlitel'nost' liuminestsentsii molekuliarnykh kristallov. I. 648

N. A. TOLSTOI, A. M. TKACHUK
Issledovanie spektraal'nogo raspredeleniia vremeni zatukhaniia svecheniia rubina metodom impul'snogo taumetra 659

CONTENTS

The Plan for the Development of the National Economy of the USSR and the Tasks of Soviet Optics 373

On the Line Shape in an Atomic Beam 375

Excitation Functions of Certain Bands of the Second Positive System of N_2 378

On the Relation Between the Matrix of Kinematic Coefficients and the Inverse Kinetic Energy Matrices in the Problem of Molecular Vibrations 380

Computation of the Characteristic Vibrations of Phosphorus Compounds. Characteristic Vibrations of the Molecules $POCl_3$, $POBr_3$, $PSCl_3$ and $PSBr_3$ 384

Calculation and Interpretation of the Vibrational Spectra of Tetramethylsilane and Tetramethylsilane--d_{12} 387

Investigation of the Absorption Spectra of 1,2-Benzanthracene Single Crystals in the Region of Lowest Electronic Transitions 392

Quantitative Investigations of the Infrared Absorption and Dispersion of Chloroform 396

Acoustic Birefringence of Phenylethyl Alchohol at Low Temperatures 401

The Influence of Concentration and Type of Solvent on the Raman Line Intensity of Totally Symmetric Vibrations of the Nitro Group and on the Electronic Absorption Spectra of Aromatic Nitro Compounds 403

Difference in Energy of Rotational Isomers in Liquid and Gaseous 1,2-Chlorofluoroethane 406

Absorption Spectra of Carbanions 410

Optical Investigation of the Molecular Structure of Cyanamide and its Derivatives I. Molecular Structure of Dicyanamide 414

Dependence of the Probability of Energy Transport in Sensitized Phosphorescence on the Oscillator Strength of a Triplet-Singlet Transition in an Energy Acceptor Molecule 417

Influence of Reabsorption on the Yield and Duration of Luminescence of Molecular Crystals. I. 421

Investigation of the Spectral Distribution of the Luminescence Decay Time of Ruby by The Pulse Taumeter Method 427

N. A. TOLSTOI
Formal'nyi analiz teorii dvukhstupenchatogo vozbuzhdeniia fosforestsentsii i fotoprovodimosti. III. Sravnenie teorii s opytom (svechenie ZnS-Cu) 665
O. N. KAZANKIN, F. M. PEKERMAN, L. N. PETOSHINA
Elektroliminofory na sul'fidselenidnoi osnove 672
I. N. SHKLIAREVSKII, A. A. AVDEENKO
Prosvetlenie metallicheskikh pokrytii 678

A. P. LUKIRSKII AND I. A. KARPOVICH
Opredelenie absoliutnoi chuvstvitel nosti nekotorykh fotomaterialov k ul tramiagkomu rentgenovskomu izlucheniiu 685
S. I. LEVIKOV AND L. P. SHISHATSKAIA
O vodorodnoi i rtutno-gelievoi lampakh dlia spektrofotometrov SF-4 688

KRATKIE SOOBSHCHENIIA

V. A. LOGINOV
Tochnost' opredeleniia dlin voln pri razlichnykh formulakh interpolirovaniia na difraktsionnom spektrografe DFS-3 692
M. P. LISITSA, V. N. MALINKO
O temperaturenoi zavisimosti intensivnostei sostavnykh tonov $\nu_1 + \nu_3$ i $\nu_1 + (\nu_1 + \nu_4)$ gazoobraznogo CCl_4 694
E. V. SHUVALOVA
Vliianie elektronodonornykh rastvoritelei na polusu pogloshcheniia valentnogo CH-kolebaniia atsetilena 696
V. B. GLASKO, V. P. MASLOV, V. I. PANIKAR, N. D. SOKOLOV
O vide korreliatosionnoi funktsii dlia atoma gelii 698
A. N. ZAKHAR'EVSKII, L. A. FEDIN
Izmerenie dvoinogo lucheprelomleniia volokon 701
G. S. KRINCHIK, M. V. CHETKIN
K teorii rasprostraneniia elektromagnitnykh voln v girotronykh sredakh 703
B. A. VEKLENKO
K teorii rezonansnogo islucheniia gazovogo razriada 705
M. BANCIE-GRILLOT, E. F. GROSS, E. GRILLOT B. S. RAZBIRIN
Issledovanie lineichaoi fluorestsentsii i pogloshcheniia kristallov chistogo sernistogo kadmiia pri temperature 4.2°K 707
E. F. GROSS, E. GRILLOT, B.P. ZAKHARCHENIA, M. BANCIE-GRILLOT
Vliianie magnitnogo polia na linii sinei fliuorestsentsii i na linii pogloshcheniia nekotorykh kristallov chistogo sernistogo kadmiia pri temperature 4.2°K 710
M. L. VEINGEROV, A. A. SIVKOV, A. P. PETROV
Radiometr Kruksa v kachestve modulatora izlucheniia 713
I. V. PEISAKHSON
Pis'mo v redaktsiiu 713

RETSENZII

D. IU. GAL PERN
Optika anizotropnykh sred. F. I. Fedorov 714

NEKROLOG

M. F. ROMANOVA 716

Lithoprinted in the U.S.A. by Blackburn Printing Co., West Concord, Mass.

Formal Analysis of the Theory of Two-Step Excitation of Phosphorescence and Photo Conduction III. Comparison of Theory and Experiment (ZnS-Cu Luminescence) 430

Electro-luminophors on a Sulphide-Selenide Base 435

Increasing the Transparency of Metallic Coatings 439

Determination of the Absolute Sensitivity of Certain Photographic Materials to Ultra-Soft X-Radiation 444

Hydrogen and Mercury-Helium Light Sources for SF-4 Spectrophotometers 446

BRIEF REPORTS

Accuracy of Wavelength Determination on a DFS-3 Grating Spectograph with Various Interpolation Formulas 449

On the Temperature Dependence of the Intensities of the Summation Tones $\nu_1 + \nu_3$ and $\nu_1 + (\nu_1 + \nu_4)$ of Gaseous CCl_4 450

The Influence of Electron-donating Solvents on the C-H Stretching Absorption Band of Acetylene 452

The Form of the Correlation Function for the Helium Atom 453

The Measurement of Birefringence of Fibers 455

On the Theory of Electromagnetic Wave Propagation in Gyrotropic Media 457

The Theory of Resonance Radiation of a Gas Discharge 459

Investigation of Linear Fluorescence and Absorption of Pure Cadmium Sulfide Crystals at a Temperature of 4.2°K 461

Influence of a Magnetic Field on the Blue Fluorescence Lines and On the Absorption Lines of Certain Pure Cadmium Sulfide Crystals at a Temperature of 4.2°K 462

The Crookes Radiometer as a Radiation Chopper 464

Letter to the Editor 464

BOOK REVIEW

Optics of Anisotropic Media by F. I. Fedorov AN BSSR Press, Minsk, 1958 465

OBITUARY

M. F. ROMANOVA 466

Abbreviations Often Encountered and Used Herein 467

Affiliations of Authors from Issue 5 468

TOM VI, Vyp. 5
VOL. VI, No. 5

OPTIKA I SPEKTROSKOPIIA
OPTICS AND SPECTROSCOPY

Mai, 1959
May, 1959

The Plan for the Development of the National Economy of the USSR and the Tasks of Soviet Optics

The special Twenty-first Congress of the Communist Party of the Soviet Union formulated a mighty plan for the development of the national economy of the USSR. The main task of the coming period will be the development of a comprehensive economic technical base of communism, the strengthening of the economic power of our motherland, and the fuller satisfaction of the growing material and spiritual requirements of the Soviet people. Compared with the year 1958, the average industrial production for the seven-year period 1959 to 1965 will increase by approximately 80%, including an increase in the production of manufacturing facilities by 85 to 88%. Basically, this will permit us to solve the main economic problem of catching up with and outdistancing the most highly developed capitalistic countries in productive capacity per worker.

Currently, progress in the industrial field is to a great degree determined by progress in technology, based on the latest achievements in physics and other natural sciences. Therefore the development of physics is a necessary prerequisite for the successful fulfillment of the seven-year plan for the economy of the USSR.

Comrade N. S. Khrushchev, in his report at the Twenty-first Congress of the Communist Party of the Soviet Union, emphasized that physical sciences occupy a leading position in natural science, on the successful development of which depends the advance in allied sciences and that of the national economy. He pointed out that the efforts of Soviet physicists will be concentrated on the solving of problems of cosmic rays, nuclear reactions and semiconductors. In the field of chemical sciences, the most important task will be the broadening of theoretical research, instrumental in the development of new technological processes and the creation of synthetic materials.

The problems indicated are of primary importance. It should be kept in mind, however, that all parts of physics and chemistry are closely linked with each other and progress in one area is impossible without progress in other areas. In particular, new divisions of physics can not be developed without developments in optics and spectroscopy, which provide the most delicate methods for research on matter in all its states of aggregation, methods of exact measurement, production quality control and the analysis of materials according to their composition.

Progress in Soviet optics has been significant. Suffice it to mention that in the pre-revolutionary period the number of original studies in physics completed in one year did not exceed 50, of which 5 to 6 per year were devoted to optics. Currently, in our journal "Optics and Spectroscopy" alone there are published yearly approximately 300 reports on studies completed in the various divisions of optics. During the years of Soviet rule, research in atomic spectroscopy has been greatly developed, the foundation of this field having been laid by D. C. Rozhdestvenskii. In the field of molecular spectroscopy, L. I. Mandel'shtam and G. S. Landsberg, independently of and concurrently with the Indian physicist Raman, discovered the effect of the "combination scattering" of light. The S. I. Vavilov school conducted fundamental experiments in the field of luminescence of liquids and solids and to it we owe the discovery of the effect known as the Vavilov-Cherenkov effect. Progress in applied optics in the construction of a large variety of optical instruments has been significant.

Soviet optics possesses all prerequisites necessary to fulfill the great tasks which are arising before it.

In the field of atomic and molecular spectroscopy, the task ahead is to investigate, by optical methods, the structure of solids, liquids and gases. The study of spectra of absorption and luminescence is an aid in understanding the structure of semiconductors and in clarifying a number of their properties, especially such properties as photoconductivity and the photo-electric effect. This research may be of very great significance in the solution of the problem of converting light energy into electrical energy directly. Optical methods contribute greatly to the understanding of the nature of liquids and solutions. Spectroscopy should occupy a significant place in the study of properties of gas-discharge plasmas, including the so-called "hot plasma." It may be assumed that a sufficiently thorough and many-sided study of the properties of the "hot plasma" will permit us to find a way to achieve controllable nuclear fusion, which would become the basic source of energy for peaceful uses in the future. Spectroscopic methods may prove suitable for the study of processes of excitation, ionization, and transport of particles in the plasma as well as for settling the nature of the rapidly changing effects which take place in it. Spectroscopy of high resolving power and radio-spectroscopy should receive wide application in the determination of such important characteristics of atomic nuclei as their spins and magnetic and quadrupole moments.

Methods of molecular spectroscopy, the study of Raman spectra and absorption spectra in the ultraviolet and, especially, in the infrared region, play an exceptionally important part in the study of the structure of complex organic molecules and the nature of chemical compounds. Investigation of the processes of photosynthesis and photocatalysis is of particular interest. The study of these processes opens a wide perspective for the understanding of the borderline region between physics and chemistry and between physics and biology. A close association of efforts by physicists, chemists, and biologists should bring beneficial results; this is the goal toward which efforts should be directed.

Spectroscopic analysis plays an important role in the growth of industry. Modern technology has introduced completely new problems: the manufacture of superpure materials, the analysis of gases, the analysis of the isotopic composition of elements.

From this also stems a need for new types of spectroscopic analysis. Not so long ago a substance containing admixtures of 0.1% was considered pure. Contemporary requirements of nuclear power and of the technology of semiconductors have advanced far: now frequently the presence of admixtures in a quantity of 10^{-5}%, and sometimes even smaller, is considered inadmissible. This calls for the development of new methods of spectroscopic analysis.

The problems with which molecular spectral analysis is confronted are extremely extensive and varied. Although emission spectroscopy as a means

of analysis has already been widely introduced here into many areas of our industry, e. g. in ferrous and non-ferrous metallurgy, the introduction of spectroscopic analysis in the chemical industry may be considered inadequate. It is essential to speed up the introduction of optical methods of research in chemistry which, undoubtedly, will be of substantial help in the creation of new synthetic materials of high quality.

The extensive introduction of optical methods into all areas of industry requires the creation of instruments which will guarantee quick and accurate measurements. In this connection Soviet optics has indeed progressed; suffice it to indicate the development of excellent diffraction gratings. In general, however, our instrument manufacture is still faced with many unsolved problems. It is necessary to introduce photoelectric methods into spectrocopy more quickly, to produce automatic instruments, and to utilize electronic computers in all divisions of scientific and applied optics.

Soviet optics must combine the working out of principally theoretical problems with the cultivation of problems having an important applied significance. Soviet scientists have always realized the necessity for a broad perspective on the connection between science and technology. Without the development of broad scientific research the development of new technology is impossible. In its turn, technology offers science new problems and supplies it with powerful means of studying nature. The results of research must be brought to a conclusion and quickly put into practice.

The grand plan for the development of the national economy of the USSR places a great and responsible obligation before Soviet opticians and spectroscopists. There is no doubt that they will fulfill them with honor.

ТОМ VI, Vyp. 5 | ОПТИКА И СПЕКТРОСКОПИЯ | Mai, 1959
VOL. VI, No. 5 | OPTICS AND SPECTROSCOPY | May, 1959

On the Line Shape in an Atomic Beam

F. A. KOROLEV, B. A. KOZLOV, A. I. ODINTSOV

Abstract: The influence of the evaporator slit width on the shape of the spectral line observed in an atomic beam has been investigated theoretically. The general expression obtained for the distribution of intensity along the line contour includes earlier formulas as special cases.

The shape of the spectral line in an atomic beam has been investigated theoretically by Minkowski and Bruck [1]. They obtained an expression for the distribution of the intensity in the contour under the assumption that the long dimension of the output slit of the evaporator is parallel to the line along which the radiation is observed and the slit width a_1 is a small quantity. No quantitative estimate of the influence of the slit width a_1 on the line contour is presented in [1] although it has been shown that this influence should be slight.

It has recently been shown [2] that for intense beams the exit slit of the evaporator must be located perpendicular to the line of observation. So that the dimension a_1 of the evaporator slit (now the slit length) in the direction perpendicular to the line of observation must assume a large value. In this connection, it is interesting to investigate the influence of a_1 on the line contour in more detail.

The expression obtained by Minkowski and Bruck for the distribution of intensity in an atomic beam, in which the collimating slit and the oven slit are visualized as rectangles with mutually parallel sides, can easily be generalized to the case of arbitrary a_1. Hence, the following expression is obtained for the intensity distribution

$$I(\nu)d\nu = C\frac{n_0}{2\pi^{\frac{3}{2}}}\,h\,\frac{|\nu-\nu_0|}{b}\exp\left[-\left(\frac{\nu-\nu_0}{b}\right)^2\right]\frac{d\nu}{b}\,X$$

$$(1)\qquad X\int_{-t}^{+t}\left\{\frac{\exp[-p^2(1+\eta^2)]}{p}-\frac{\exp[-q^2(1+\eta^2)]}{q}+\right.$$

$$\left.+\sqrt{\pi}\sqrt{1+\eta^2}\,[\Phi(p\sqrt{1+\eta^2})-\Phi(q\sqrt{1+\eta^2})]\right\}\frac{d\eta}{1+\eta^2}\,,$$

where $p=\frac{2h}{s_2+s_1}\cdot\frac{|\nu-\nu_0|}{b}$, $q=\frac{2h}{|s_2+s_1|}\cdot\frac{|\nu-\nu_0|}{b}$,

$t=\frac{a_1}{2l}$ and $b=\nu_0\frac{\bar{v}}{c}$, where s_1 and s_2 are the dimensions of the oven slit and the collimating slit of the beam in the direction of the line of observation (the line NN' on fig. 1); a_1 is the size of the oven slit in the direction perpendicular to the line of observation; h is the distance between the slits; l is the distance from the furnace slit to the line of observation; $\bar{v}$ is the most probable atom velocity at the furnace temperature; c is the speed of light; n_0 the atom density in the furnace. The coefficient C includes the probability of excitation of the atoms in the beam, the transition probability and the quantum yield for the spectral line under consideration.

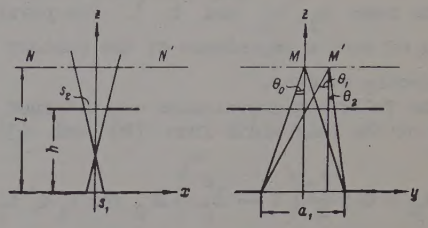

Figure 1. Diagram of an Atomic Beam. (Explanation in the text).

The so-called error function is denoted by $\Phi(x)=\frac{2}{\sqrt{\pi}}\int_0^x \exp[-\xi^2\,d\,\xi^2]$ For simplicity, it is assumed that the line of observation of the luminescence intersects the beam axis (the z axis in fig. 1), however, the expression (1) is easily generalized to the case of arbitrary position of the line of observation.

It appears to be impossible to integrate (1) in the general case but, if the relation $\left(\frac{a_1}{2l}\right)^2 \ll 1$* holds, then the following approximate expression can be obtained for $I(\nu)$:

$$(2)\qquad I(\nu)d\nu = C\frac{n_0 a_1}{2\pi^{\frac{3}{2}}}\cdot\frac{h}{l}\cdot\frac{|\nu-\nu_0|}{b}\exp\left[-\left(\frac{\nu-\nu_0}{b}\right)^2\right]\frac{d\nu}{b}\,X$$

$$X\left\{\frac{\exp[-p^2]}{p}-\frac{\exp[-q^2]}{q}+\sqrt{\pi}\,[\Phi(p)-\Phi(q)]\right.$$

$$\left.-\frac{t^2}{3}\left[\frac{\exp[-p^2]}{p}-\frac{\exp[-q^2]}{q}+\frac{\sqrt{\pi}}{2}(\Phi(p)-\Phi(q))\right]\right\}$$

In the particular case when $s_1 \ll s_2$, the expression (2) is simplified and becomes

$$(3)\qquad I(\nu)d\nu = C\frac{n_0 s_1}{2\pi^{\frac{3}{2}}}\cdot\frac{a_1}{l}\exp\left\{-\left(\frac{\nu-\nu_0}{b}\right)^2\left[1+\left(\frac{2h}{s_2}\right)^2\right]\right\}\,X$$

$$X\,\frac{d\nu}{b}\left[1-\frac{t^2}{3}(1+p^2)\right].$$

Formulas (1), (2) and (3) transform into the Minkowski-Bruck formulas for $t\to 0$.

Analyzing (2) and (3), the conclusion can be drawn that the dimension a_1 of the oven slit in the direction perpendicular to the line of observation does not exert a noticeable influence

* This condition is always satisfied in practice; thus, for example, $\left(\frac{a_1}{2l}\right)^2 = 0.046$ in the apparatus described in [2].

on the shape of the line (at least as long as $a_1 < l$). The shape of the line in the beam depends in a first approximation only on the dimensions s_1 and s_2 of the slits along the line of observation and on the spacing h between the slits. Only for very large values of a_1 ($a_1 \geqslant l$) does noticeable deformation of the contour (a narrowing) arise; in the limiting case *, when $a_1 \gg l$, a contour almost twice as narrow as when $a_1 \ll l$ is obtained (for the same s_1, s_2 and h). The physical meaning of such a dependence of the contour on a_1 is perfectly evident.

The following expressions are obtained for the values of the half-width from (2) and (3)

$$\Delta_S = 0.5\,\frac{s_2}{h}\left(1 - \frac{t^2}{6}\right)\Delta_G \quad \text{for } s_1 \ll t, \tag{4}$$

and

$$\Delta_S = 0.41\,\frac{s}{h}\left(1 - \frac{t^2}{6}\right)\Delta_G \quad \text{for } s_1 = s_2 = s \tag{5}$$

where Δ_S is the Doppler half-width of a line in the beam and Δ_G is the Doppler half-width of the line in the gas at the oven temperature.

If the exit slit of the oven is perpendicular to the line of observation ($a_1 > s_1$), then there is a practical possibility of using different s_1 for fixed s_2 and h since the beam intensity in this case is independent of the slit width s_1 [2]. The contour shape will then change. Presented in figure 2 are line contours in a beam for different values of the ratio s_2/s_1. As is seen from figure 2, the line shape depends strongly on the

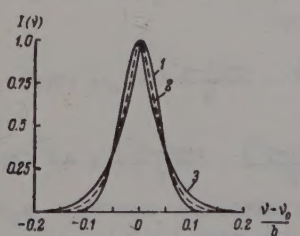

Figure 2. Dependence of the line contour in a beam on the ratio $\frac{s_2}{s_1}$.

1 - $\frac{s_2}{s_1} = \infty$; 2 - $\frac{s_2}{s_1} = 1.5$; 3 - $\frac{s_2}{s_1} = 1$; $\frac{s_2}{h} = 0.1, a_1 \quad l$.

relation of the slit dimensions s_1 and s_2. The contour which occurs for $s_1 = s_2$ permits somewhat greater resolution to be obtained in a number of cases than does the contour for $s_1 \ll s_2$. The advantage of the contour for $s_1 \ll s_2$, besides the more rapid drop in the intensity at the wings, is its simple analytic form which permits, in particular, the apparatus width to be taken into account more easily.

It is interesting to note that a sharply asymmetric shape can be obtained for $s_1 \ll s_2$ if, as is shown on figure 3, the beam is inclined to the line of observation (the line NN' on figure 3). Such a contour guarantees that very high resolution, corresponding to a steep drop in one side of the contour, will be obtained. It might be expedient in some cases to use an arrangement giving an asymmetric contour of this type in addition to using very well collimated beams.

Exact formulas were obtained from the general expression (1) for the intensity distribution in the contour, for the integral line intensity and for the line intensity at the maximum. The formula obtained for the integral intensity is rather complex and consequently is not presented. Under the conditions $s_1 \ll h$, $s_2 \ll h$, it can be written as

$$E = C\,\frac{n_0 s_1}{2}\cdot\frac{s_2}{h}\,\sin\theta_0\left[1 - \frac{s_1^2 + s_2^2}{8h^2}\left(1 - \frac{\sin^2\theta_0}{3}\right)\right] \tag{6}$$

where $\theta_0 = \tan^{-1}\frac{a_1}{2l}$

This expression agrees with the approximate formula for the integral intensity obtained in [2] by another method.

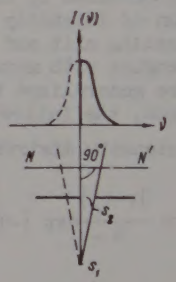

Figure 3 Formation of an asymmetric contour because of the deviation of the beam axis from the line of observation for $s_2 \gg s_1$.

In the particular case of $a_1 \ll l$ and $s_1 = s_2$, formula (6) transforms into the Minkowski-Bruck [1] formula (if terms of order $(\frac{s}{h})^4$ are neglected in the latter). The expression obtained for the line intensity at the maximum agrees with that presented in [2].

The formulas for the radiation intensity in a beam were derived under the assumption that the line of observation intersects the beam axis. Displacement of the line of observation to the beam periphery (from the point M to M' on fig. 1) leads to a diminution in the intensity. It can be shown that the maximum line intensity decreases proportionally to $\theta_1 + \theta_2$ (i. e., in proportion to the angle subtended by the length a_1 of the oven slit at the

* This case is not included in formulas (2) and (3) and was investigated separately.

observation point) and the integral intensity is proportional to $\sin\theta_1 + \sin\theta_2$. Hence, if $MM' \ll l$, the beam intensity at the points M and M' is practically the same.

June 2, 1958

References

1. R. MINKOWSKI, H. BRUCK: Z. Phys., 95, 274 (1935)
2. A. I. ODINTSOV: OiS, 6, 389 (1959) (see this journal page 250)

TOM VI, Vyp. 5
VOL. VI, No. 5

OPTIKA I SPEKTROSKOPIIA
OPTICS AND SPECTROSCOPY

Mai, 1959
May, 1959

Excitation Functions of Certain Bands of the Second Positive System of N_2

by

S. M. KISHKO AND M. IU. KUCHINKA

Abstract: A photoelectrical investigation is made of the optical excitation functions for the bands $0 \rightarrow 3$, $1 \rightarrow 4$ and $2 \rightarrow 6$ of the second positive system of molecular nitrogen. It is shown that the positions of the maxima of the excitation functions depend on the nitrogen pressure. The results obtained are compared with data from other investigations.

Optical excitation functions of the stronger bands of the second positive system of N_2 have been investigated before [1], employing the photographic method, at high nitrogen pressures (0.1 mm Hg) and at large currents of exciting electrons (0.3 ma) which were not monoenergetic. Under these conditions in the excitation tube, one had multiple collisions between the exciting electrons and the nitrogen molecules, and large deviations from the nominal electron velocity. Therefore the optical excitation functions of the bands could be obtained only with certain distortions. As we know [2], in order to obtain optical excitation functions without any distortions, one has to conduct the experiments at such pressures and at such an electron current density that multiple collisions, collisions of the second kind and step excitations do not take place. The optical excitation functions of the bands of the second positive system of N_2 have not yet been studied under such conditions.

We investigated the optical excitation functions of the $0 \rightarrow 3$ ($\lambda = 4059.4$Å), $1 \rightarrow 4$ ($\lambda = 3998.4$Å) and $2 \rightarrow 6$ ($\lambda = 4700.5$Å) bands of the second positive system of N_2, corresponding to the transition $C^3\Pi \rightarrow B^3\Pi$, in the pressure range from 10^{-2} to $4 \cdot 10^{-3}$ mm Hg for a current density of the order 10^{-3} amp/cm^2.

A sketch of the experimental set-up is shown in figure 1.

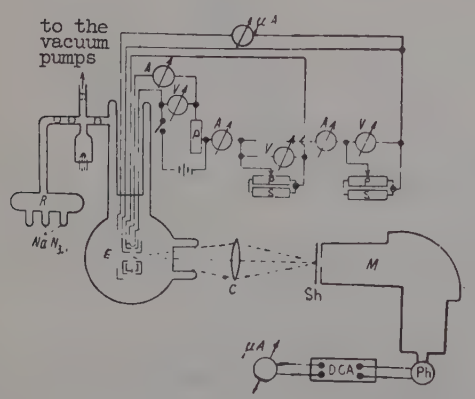

Figure 1. Layout of instruments and electrical diagram of power supply for the excitation tube.

A-Ammeters, V-Voltmeters, A-Microammeters, E- Excitation tube, C- Condenser, Sh- Shutter, M- Monochromator, Ph- Photomultiplier FEU-17, DCA- DC Amplifier, R-Vessel where the nitrogen was generated, P- Potentiometers, S- Voltage stabilizers.

The excitation of the N_2 molecular spectrum took place in a discharge tube E, made from molybdenum glass. The tube contained a multi-electrode system, consisting of a directly heated equipotential oxide cathode, two cylindrical anodes an electron receiver and a screening cylinder. Inside the receiver were three grids of nickel wire with small meshes which had the function of retaining secondary and reflected electrons in the receiver. The distance between cathode and receiver was 18 mm and the length of the equipotential space between the second anode and the receiver was 10 mm. All of the electrodes were made from thin nickel sheets and spot welded. Before being welded into the tube they were boiled in distilled water and washed carefully with ethyl alcohol. The oxide layer was made by depositing a double barium-strontium carbonate, dissolved in acetone onto a core of 1.5 mm diameter. The discharge tube was outgassed at 400° C until a vacuum of 10^{-5} mm Hg was obtained. Then, after the temperature was lowered to 200° C, the oxide cathode was activated. At a heating current of 1.1 amp and anode potentials of 30 V the electron current to the receiver was 20 μa.

We determined how monoenergetic the electrons were by using a retarding potential, and found that the velocities of more than 90 % of the electrons of the exciting beam had velocities in a spectrum less than 1 eV wide.

We obtained the molecular nitrogen in the cylinder R as follows: All three appendages of the cylinder R were filled with sodium nitride (NaN_3). Then, after obtaining a high vacuum, under slow heating, the sodium azide dissociated according to the reaction $NaN_3 \rightarrow Na + 3/2\ N_2$ into nitrogen and metallic sodium. The latter condensed on the walls of the vessel. The nitrogen obtained from the first two appendages was used for a careful flushing of the vessel R, the discharge tube and the connecting tubes. The nitrogen from the third was used for filling the discharge tube in its working condition. The discharge tube was filled with nitrogen by means of a valve system (metering system). The nitrogen pressure was measured with a thermo-manometric tube and a vacuum gauge VMB-1.

The purity of the sodium azide as well as that of the nitrogen obtained was checked by the spectral method. The discharge tube was not disconnected from the vacuum pump system, but was sealed off by a good vacuum valve. In order to diminish absorption of the radiation from the nitrogen, the window of the discharge tube was made from molybdenum glass which transmits radiation to 3100 Å without noticeable absorption.

The light passing through the window of the discharge tube was focussed with the aid of a

condenser lens onto the entrance slit of the monochromator. As such, we used an ISP-51 spectral instrument with a 270 mm camera lens where an exit slit was substituted for the film adapter. Immediately behind the exit slit was a photoelectric photometer. The radiation was recorded with an FEU-17 photomultiplier of 150 amp/mm sensitivity and with a dark current of $7 \cdot 10^{-11}$ amp. The photomultiplier was cooled with dry ice by means of a two-sided copper cooling cup. The photocurrent was measured with a galvanometer of the type M-21 which had a current sensitivity of $0.6 \cdot 10^{-9}$ amp/mm. min. The voltage to the discharge tube was supplied by a set of acid batteries of high capacity and with voltage stabilizers; the electron current was measured with a type LM microammeter and the voltage to the electrodes with MVA-47 voltmeters.

The method of our measurement was essentially a determination of the intensities of the $0 \rightarrow 3$, $1 \rightarrow 4$ and $2 \rightarrow 6$ bands of the second positive system of N_2, excited by an electron beam in a rarefied gas, for different energies of the exciting electrons. Since the current to the receiver increased gradually with increasing accelerating potential, the intensity values obtained by photometric evaluation were normalized to a constant value of the exciting current equal to 10 μa. The accelerating potential was varied in 1 V steps from 10 to 33 V, in the region of the maximum of the excitation function in 0.3 V steps. In the graphical representation of the results of our measurements we corrected for the contact potential difference between the oxide layer and the nitrogen, which was 3.5 V. The accuracy of our measurements was 2%.

The results of our investigation are shown in Figure 2.

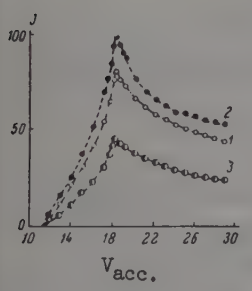

Figure 2. Optical excitation functions for the $0 \rightarrow 3$, $1 \rightarrow 4$, and $2 \rightarrow 6$ bands of the second positive system N_2.

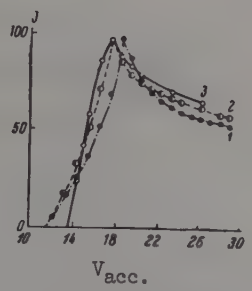

Figure 3. Influence of the pressure on the optical excitation function of the $1 \rightarrow 4$ band of the second positive system of N_2.

1) $p = 4.5 \cdot 10^{-3}$ mm Hg; 2) $p = 10^{-2}$ mm Hg; 3) Curve of Langstroth.

One can see that the optical excitation functions of the $0 \rightarrow 3$, $1 \rightarrow 4$, and $2 \rightarrow 6$ bands of the second positive system of molecular nitrogen each have one sharp maximum. The excitation function of all the bands which we investigated starts immediately after the excitation potential of the C^3 level which is equal to 11 V [3] and the maximum lies at 18 V. If we increase the energy of the exciting electrons the radiation intensities decrease at first rapidly, and then slowly. We obtained these results at a nitrogen pressure of $4.5 \cdot 10^{-3}$ mm Hg and less; the density of the electron beam was of the order 10^{-3} amp/cm^2. With increasing pressure, the position of the maximum is displaced towards lower potentials. This occurs due to the appearance of multiple collisions. Figure 3 shows the excitation functions of the $1 \rightarrow 4$ band ($\lambda = 3998.4$ Å) of the second positive system of N_2 for different pressures. From the results shown in this figure one can see that for pressures around 10^{-2} mm Hg the curve of the optical excitation function almost agrees with that of Langstroth. The maximum of the excitation function occurs in this case near an accelerating potential of 17 V and not at 18 V as was the case at lower pressures. Thus, in our investigation we have determined the optical excitation function of the bands of the second positive system of N_2 without any distortions. We have also clarified the influence of the nitrogen pressure on the position of the maxima of the excitation functions of these bands.

The authors express their sincere gratitude to I. P. Zapesochnyi for suggesting the topic and for his guidance.

June 16, 1958

References

1. L. S. ORNSTEIN, G. O. LANGSTROTH: Proc. Roy. Acad. Sci. Amst., 36, 384 (1933)
G. O. LANGSTROTH: Proc. Roy. Soc., 146A, 166 (1934)
O. THIEME: Z. Phys., 78, 412 (1932)
2. I. P. ZAPESOCHNYI: Vestnik, Leningrad Univ., No. 11, 67 (1954)
3. G. HERZBERG: Molecular Spectra and Molecular Structure (IL, Moscow, 1949)

TOM VI, Vyp. 5
VOL. VI, No. 5

OPTIKA I SPEKTROSKOPIIA
OPTICS AND SPECTROSCOPY

Mai, 1959
May, 1959

On the Relation Between the Matrix of Kinematic Coefficients and the Inverse Kinetic Energy Matrices in the Problem of Molecular Vibrations

I. N. GODNEV, I. V. ORLOVA

Abstract: The use of the Lagrange equations with included holonomic constraints to solve the problem of molecular vibrations in coupled coordinates has been analyzed. Formulas have been derived which relate the matrix of the kinematic coefficients A to the T^{-1} and T_o^{-1} matrices, where T and T_o are the kinetic energy matrices corresponding to the coupled and independent coordinates.

As is well known, use of the kinematic coefficients makes the solution of the problem of vibrations in molecules extremely simple [1,2]. The matrix A of these coefficeints equals T^{-1} in the case of independent coordinates [1-4], where T is the kinetic energy matrix. The column (or row) elements of the matrix A are linearly dependent in the case of coupled (dependent) vibrational coordinates [1,2]; consequently, this matrix has no inverse while the matrix T^{-1} generally exists. Naturally, it is expedient to consider the question of the relation between the matrices A and T^{-1} when using dependent coordinates. As will be shown herein, such a relation can easily be established by using Lagrange equations with included constraints. An analysis of the abovementioned dependence will also be useful to obtain simple formulas expressing the kinematic coefficients matrix A in terms of T_o^{-1}, where T_o is the kinetic energy matrix in independent coordinates.

To solve the problem of vibrations of a molecule with n-l vibrational degrees of freedom, let n natural interdependent coordinates $q_1, q_2, \ldots, q_n$ be used which satisfy the condition*

$$a_1q_1 + a_2q_2 + \ldots + a_nq_n = 0 \tag{1}$$

Let the kinetic and potential energies of our problem of small vibrations be described in matrix form by means of the dependent coordinates

$$2T = \sum_{i,j} t_{ij}\dot{q}_i\dot{q}_j = \tilde{\dot{q}}T\dot{q} \tag{2}$$

$$2U = \sum_{i,j} u_{ij}q_iq_j = \tilde{q}Uq \tag{3}$$

where q is a column matrix with elements $q_1, q_2, \ldots, q_n$; t_{ij} and u_{ij} are constants and the symbol $\sim$ denotes transposition.

When using coupled coordinates** we cannot use the usual Lagrange equations but must use them in the form with included constraints. Such equations, when one holonomic constraint exists, take the form [5,6]

$$\frac{d}{dt}\left(\frac{\partial L}{\partial \dot{q}i}\right) - \frac{\partial L}{\partial qi} = \alpha a_i, \tag{4}$$

where i=1, 2,..., n and α is a Lagrange parameter.

Substitution of T and U from (2) and (3) into the Lagrange equations (4) yields

$$T\ddot{q} + Uq = \alpha a, \tag{5}$$

where a is a column matrix with elements $a_1, a_2, \ldots, a$

The matrix equation (5) can be represented in another way, which is convenient for the solution of th vibrational problem in dependent coordinates if the parameter α is eliminated. Actually, differentiating the equation of constraint (1) twice and writing the result in matrix form, we obtain

$$\tilde{a}\ddot{q} = 0. \tag{6}$$

obtaining the column matrix $\ddot{q}$ from (5) and substituting it into (6) we will have

$$-\tilde{a}T^{-1}Uq + \tilde{a}T^{-1}a\alpha = 0, \tag{7}$$

from which

$$\alpha = \frac{\tilde{a}T^{-1}U}{\tilde{a}T^{-1}a}q, \tag{8}$$

since $\tilde{a}T^{-1}a$ is a number.

After the substitution of α, (5) becomes

$$T\ddot{q} + \left(E - \frac{a\tilde{a}T^{-1}}{\tilde{a}T^{-1}a}\right)Uq = 0. \tag{9}$$

Multiplication of this equation on the left by T^{-1} yields

$$\ddot{q} + T^{-1}\left(E - \frac{a\tilde{a}T^{-1}}{\tilde{a}T^{-1}a}\right)Uq = 0. \tag{10}$$

Having defined the matrix A as follows:

$$A = T^{-1} - \frac{T^{-1}a\tilde{a}T^{-1}}{\tilde{a}T^{-1}a}, \tag{11}$$

we obtain the El'iashevich equations [7,1] in matrix form

$$\ddot{q} + AUq = 0. \tag{12}$$

An investigation of these equations shows [1] that the elements A_{ij} of the matrix A are the kinematic coefficients defined by the expression

$$A_{ij} = \sum_{\alpha} \frac{\vec{e}_{i\alpha}\vec{e}_{j\alpha}}{m_\alpha} \tag{13}$$

where m_α - is the mass of atom α and $\vec{e}_{i_\alpha}$ and $\vec{e}_{j_\alpha}$ are vectors introduced by El'iashevich [1]

It follows from the above that a relation, expressible by means of (11), exists between the kinematic coefficients matrix A and the matrix T^{-1} in the case of coupled coordinates.

---

* Subsequent reasoning can be generalized to the case of several constraints.

** The elimination of redundant coordinates at the very beginning of the solution of the problem of molecular vibrations is often very inconvenient (see [1]).

Let us note that the linear dependence of the columns (or rows) of the matrix A can easily be proved on the basis of (11). Actually, to do this let us calculate the matrix Aa

$$(14)\quad Aa = \left(T^{-1} - \frac{T^{-1}a\tilde{a}T^{-1}}{\tilde{a}T^{-1}a}\right)a = T^{-1}a - T^{-1}a = \begin{pmatrix}0\\0\\\vdots\\0\end{pmatrix}.$$

On the other hand

$$(15)\quad Aa = \begin{pmatrix} a_1A_{11} + a_2A_{12} + \ldots + a_nA_{1n} \\ a_1A_{21} + a_2A_{22} + \ldots + a_nA_{2n} \\ \ldots\ldots\ldots\ldots \\ a_1A_{n1} + a_2A_{n2} + \ldots + a_nA_{nn} \end{pmatrix}$$

From a comparison of (14) and (15) it follows that

$$(16)\quad a_1\begin{pmatrix}A_{11}\\A_{21}\\\cdot\\\cdot\\\cdot\\A_{n1}\end{pmatrix} + a_2\begin{pmatrix}A_{12}\\A_{22}\\\cdot\\\cdot\\\cdot\\A_{n2}\end{pmatrix} + \ldots + a_n\begin{pmatrix}A_{1n}\\A_{2n}\\\cdot\\\cdot\\\cdot\\A_{nn}\end{pmatrix} = \begin{pmatrix}0\\0\\\cdot\\\cdot\\\cdot\\0\end{pmatrix}$$

i.e., the columns of the matrix A satisfy the same linear relations as do the coordinates. The dependence between the rows is also proved in an analogous manner if the matrix $\tilde{a}A$ is calculated.

The symmetry of the matrix A (for the case that T is symmetric) also results from (11), i.e.,

$$(17)\quad \tilde{A} = A$$

Now let us establish a relation between the matrix A and the matrix T_o which is obtained upon elimination of a given redundant coordinate and let us show that the matrix A, definable by (11), will be identical, for prescribed $a_1, a_2, \ldots, a_n$, for all those matrices T which yield the same matrix T_o upon elimination of a given redundant coordinate.

Elimination of the redundant coordinate q_n can be considered as the linear transformation

$$(18)\quad \begin{aligned} q_1 &= Q_1 \\ q_2 &= Q_2 \\ &\cdots\cdots \\ q_{n-1} &= Q_{n-1} \\ q_n &= -\frac{a_1}{a_n}Q_1 - \frac{a_2}{a_n}Q_2 - \ldots - \frac{a_{n-1}}{a_n}Q_{n-1}, \end{aligned}$$

where $Q_1, Q_2, \ldots, Q_{n-1}$ are the independent coordinates of our problem. To this transformation

$$(19)\quad q = MQ$$

there corresponds the rectangular matrix

$$(20)\quad M = \left.\begin{bmatrix} 1 & 0 & \ldots & 0 \\ 0 & 1 & \ldots & 0 \\ \cdots & \cdots & \cdots & \cdots \\ 0 & 0 & \ldots & 1 \\ \underbrace{-\frac{a_1}{a_n} & -\frac{a_2}{a_n} & \ldots & -\frac{a_{n-1}}{a_n}}_{n-1} \end{bmatrix}\right\} n.$$

After elimination of the redundant coordinate q_n, the kinetic energy matrix will be

$$(21)\quad T_o = \tilde{M}TM,$$

where, because of the independence of the coordinates $Q_1, Q_2, \ldots, Q_{n-1}$,

$$(22)\quad T_o = A_o^{-1}.$$

Using the matrix M, a transformation can be accomplished from the momenta p_i corresponding to the dependent coordinates q_i

$$(23)\quad p = T\dot{q},$$

to the momenta $\mathcal{P}_i$, corresponding to the independent coordinates Q_i

$$(24)\quad \mathcal{P} = T_o\dot{Q},$$

where $p = (p_1, p_2, \ldots, p_n)$ and $\mathcal{P} = (\mathcal{P}_1, \mathcal{P}_2, \ldots, \mathcal{P}_{n-1})$ are column matrices.

Differentiating (2) with respect to $\dot{Q}_i$ and taking (1) into account yields

$$(25)\quad \mathcal{P}_i = \frac{\partial T}{\partial \dot{q}_1}\cdot\frac{\partial \dot{q}_1}{\partial \dot{Q}_i} + \frac{\partial T}{\partial \dot{q}_2}\cdot\frac{\partial \dot{q}_2}{\partial \dot{Q}_i} + \ldots + \frac{\partial T}{\partial \dot{q}_n}\cdot\frac{\partial \dot{q}_n}{\partial \dot{Q}_i},$$

that is

$$(26)\quad \begin{aligned} \mathcal{P}_1 &= p_1 - \frac{a_1}{a_n}p_n, \\ \mathcal{P}_2 &= p_2 - \frac{a_2}{a_n}p_n, \\ &\cdots\cdots\cdots \\ \mathcal{P}_{n-1} &= p_{n-1} - \frac{a_{n-1}}{a_n}p_n. \end{aligned}$$

It is seen from (26) that the matrix of this transformation will be the transpose of the matrix (20).

Hence *

$$(27)\quad \mathcal{P} = \tilde{M}p.$$

The kinetic energy in terms of the independent momenta $\mathcal{P}_i$ will be

$$(28)\quad 2T = \tilde{\mathcal{P}}A_o\mathcal{P}.$$

---

* Because of the linear dependence of the momenta $p_1, p_2, \ldots, p_n$, there exists a family of other rectangular matrices, $\tilde{M}', \tilde{M}'', \ldots$ with the aid of which a transformation such as (27) can be accomplished. However, we shall use a tranformation with the definite matrix $\tilde{M}$ in (27).

Formula (27) can also be obtained by substituting T_o from (21) into (24) while taking (19) and (23) into account.

Substitution of the column matrix $\mathcal{P}$ from (27) into (28) yields

$$2T = \tilde{p}\, A'\, p, \tag{29}$$

$$A' = MA_o\tilde{M}. \tag{30}$$

Formula (29) expresses the kinetic energy in terms of the dependent momenta, where the matrix A' is defined uniquely for prescribed $a_1, a_2, \ldots a_n$ by the matrix A_o.

Let us note that use of the dependent momenta permits the kinetic energy to be written also by using a series of other matrices:*

$$2T = \tilde{p}A'p = \tilde{p}A''p = \tilde{p}A'''p = \ldots \tag{31}$$

Among such matrices appears the matrix A' which is identical to the kinematic coefficients matrix A (see Appendix), i.e.,

$$A' = A. \tag{32}$$

Substituting the value of A_o from (22) into (30), we will have

$$A = MT_o^{-1}M \tag{33}$$

Formula (33) now establishes the relation between the kinematic coefficients matrix and the matrix T_o^{-1}. It follows from this formula that the matrix A (for prescribed $a_1, a_2, \ldots a_n$) will be identical for all those matrices T which yield the same matrix T_o upon the elimination of a given redundant coordinate.

Let us present a simple example illustrating the above**

Let the connection between the coordinates be prescribed by the condition

$$q_1 + 2q_2 - q_3 = 0, \tag{34}$$

and let the kinetic energy be defined by the matrix

$$T_1 = \begin{pmatrix} \frac{5}{2} & \frac{1}{4} & -1 \\ \frac{1}{4} & 1 & -\frac{1}{4} \\ -1 & -\frac{1}{4} & \frac{1}{2} \end{pmatrix} \tag{35}$$

The matrix M will be [see (20)]

$$M = \begin{pmatrix} 1 & 0 \\ 0 & 1 \\ 1 & 2 \end{pmatrix} \tag{36}$$

Eliminating the coordinate q_3, we will obtain

$$T_o = \begin{pmatrix} 1 & -1 \\ -1 & 2 \end{pmatrix} \tag{37}$$

The same matrix T_o (with the elimination of the coordinate q_3) is given also by

$$T_2 = \begin{pmatrix} \frac{8}{3} & \frac{1}{2} & -1 \\ \frac{1}{2} & \frac{4}{3} & -\frac{1}{6} \\ -1 & -\frac{1}{6} & \frac{1}{3} \end{pmatrix} \tag{38}$$

Upon substitution into (11), T_1 and T_2 yield one and the same matrix

$$A = \begin{pmatrix} 2 & 1 & 4 \\ 1 & 1 & 3 \\ 4 & 3 & 10 \end{pmatrix} \tag{39}$$

The same matrix is also obtained if M and T_o^{-1} are substituted into (33). In conclusion, let us note that formulas similar to (11) and (33) can be obtained for the force constants also.

APPENDIX

To prove the equality of the matrices A and A', let us note that because of the linear dependence of the rows and columns of A [see (16)], this matrix can be represented, as can easily be verified by direct multiplication, as

$$A = MB_o\tilde{M}, \tag{40}$$

where B_o is a matrix of rank n-1, obtained from A by cancellation of the n-th row and column.

Let us introduce a matrix C which will be used to accomplish the transformation from the independent momenta $\mathcal{P}_i$ to the momenta p_i:

$$p = C\mathcal{P}. \tag{41}$$

To do this, let us replace the column matrix q in (23) by an expression which is obtained by differentiating the equality (19). We will have

$$p = T\dot{Q}. \tag{42}$$

Obtaining $\dot{Q}$ from (24) and substituting into (42), we obtain

$$p = TMT_o^{-1}\mathcal{P}, \tag{43}$$

---

* An infinite set of such matrices exists because of the linear dependence of the momenta. Hence, it follows that it is impossible to define the kinematic coefficients matrix as any matrix of the quadratic form (31) for the dependent coordinate (momenta) case, as has regrettably been done in the monograph of Wilson et al. [2], p.308.

** For simplicity, we will present an abstract example rather than an example referring to a molecule.

that is

$$C = \tilde{M}T_o^{-1} \tag{44}$$

Multiplication of the rectangular matrices $\tilde{M}$ and C or $\tilde{C}$ and M yields the unit matrix E of rank n-1:

$$\tilde{M}C = E, \tag{45}$$

$$\tilde{C}M = E. \tag{46}$$

Actually, for example

$$\tilde{M}C = \tilde{M}TMT_o^{-1} = T_o T_o^{-1} = E \tag{47}$$

because the product of the first three cofactors in (47) equals T_o because of (21).

Let us also note that the matrix M satisfies the relation

$$\tilde{M}a = \begin{pmatrix} 0 \\ 0 \\ \vdots \\ 0 \end{pmatrix} \Big\}n-1 \tag{48}$$

whose validity may be established by direct multiplication of the transposed matrix (20) by a.

The relations (45) and (46) permit B_o to be expressed in terms of A. Multiplying (40) on the right by C and on the left by $\tilde{C}$, we obtain on the basis of these relations

$$B_o = \tilde{C}AC \tag{49}$$

Substituting A from (11) in this expression and using (48) and (21), we will have

$$B_o = T_o^{-1}\tilde{M}T\left(T^{-1} - \frac{T^{-1}a\tilde{a}T^{-1}}{\tilde{a}T^{-1}a}\right)TMT_o^{-1} = T_o^{-1}, \tag{50}$$

that is [see (22)]

$$B_o = A_o \tag{51}$$

Now it follows from a comparison of (30) and (40) that

$$A' = A. \tag{52}$$

July 2, 1958

References

1. M. V. VOL'KENSHTEIN, M. A. EL'IASHEVICH, B. I. STEPANOV: Kolebaniia molekul (Vibrations of molecules) 1, Gostekhizdat, Moscow, 1949
2. E. B. WILSON, J. C. DECIUS, P. C. CROSS: Molecular Vibrations, N.Y., 1955
3. L. S. MAIANTS: Tr. FIAN, 5, 63 (1950)
4. V. M. TATEVSKII: ZETF, 15, 445 (1945)
5. L. NORDHEIM: Handbuch d. Phys., 5, 43-90, 1927
6. L. G. LOITSIANSKII, A. I. LUR'E: Kurs teoreticheskoi mekhaniki (Course in theoretical mechanics) 2, Gostekhizdat, Moscow, 1955
7. M. A. EL'IASHEVICH: DAN USSR, 28, 604 (1940) ZFKH, 15, 847 (1941) (See LC RT-1141, 23 pp.)

TOM VI, Vyp. 5
VOL. VI, No. 5

OPTIKA I SPEKTROSKOPIIA
OPTICS AND SPECTROSCOPY

Mai, 1959
May, 1959

Computation of the Characteristic Vibrations of Phosphorus Compounds. Characteristic Vibrations of the Molecules $POCl_3$, $POBr_3$, $PSCl_3$ and $PSBr_3$

L. S. MAIANTS, E. M. POPOV, M. I. KABACHNIK

Abstract: The frequencies and forms of the normal vibrations have been calculated for the molecules $POCl_3$, $POBr_3$, $PSCl_3$ and $PSBr_3$, for certain specially chosen values of the force constants. The sensitivity of these frequencies to changes in the force constants, the masses of the atoms, and the bond lengths and angles have also been calculated. We have considered the question of the characteristic vibrations corresponding to the so-called P = O and P = S frequencies.

There is a large fund of experimental data in the literature of the vibrational spectra of phosphorus compounds. This material is used for comparisons with new spectra in order to determine the existence in the molecule of certain definite bonds or groups of bonds. It can be seen from the experimental data that the so-called characteristic frequencies of these bonds change considerably with any change in the environment of the bonds which may be considered due to a change in the force constant of the given bond or to a change in the corresponding vibration of nearby bonds and angles.

Table 1

Designation of the Force Constants

Co-ordinates	Q	q_1	q_2	q_3	γ_1	γ_2	γ_3	δ_1	δ_2	δ_3
Q	K_Q	h_{Qq}	h_{Qq}	h_{Qq}	$b_{Q\gamma}$	$b_{Q\gamma}$	$b_{Q\gamma}$	$a_{Q\delta}$	$a_{Q\delta}$	$a_{Q\delta}$
q	h_{Qq}	K_q	h_{qq}	h_{qq}	$b_{q\gamma}$	$a_{q\gamma}$	$a_{q\gamma}$	$a_{q\delta}$	$b_{q\delta}$	$b_{q\delta}$
γ	$b_{Q\gamma}$	$b_{q\gamma}$	$a_{q\gamma}$	$a_{q\gamma}$	K_γ	$l_{\gamma\gamma}$	$l_{\gamma\gamma}$	$0_{\gamma\delta}$	$l_{\gamma\delta}$	$l_{\gamma\delta}$
δ	$a_{Q\delta}$	$a_{q\delta}$	$b_{q\delta}$	$b_{q\delta}$	$0_{\gamma\delta}$	$l_{\gamma\delta}$	$l_{\gamma\delta}$	K_δ	$l_{\delta\delta}$	$l_{\delta\delta}$

Table 2

Force Constants (in units of 10^6 cm^{-2})

Molecule	K_Q	K_q	K_γ	K_δ	h_{Qq}	h_{qq}	$a_{Q\delta}$	$a_{q\gamma}$	$a_{q\delta}$	$l_{\gamma\gamma}$	$l_{\delta\delta}$	$l_{\gamma\delta}$
$POCl_3$	18.61	5.23	1.29	1.80	0.85	0.70	0.85	0.34	0.34	−0.10	−0.10	−0.10
$POBr_3$	17.52	4.00	0.83	1.42	0.85	0.20	0.60	0.20	0.20	−0.10	−0.10	−0.10
$PSCl_3$	9.50	4.24	0.90	2.14	0.85	0.70	0.60	0.20	0.20	−0.10	−0.10	−0.10
$PSBr_3$	9.10	3.30	0.70	1.75	0.70	0.20	0.60	0.10	0.10	−0.05	−0.05	−0.05

Remarks; The coefficients $b_{Q\gamma}$, $b_{q\gamma}$, $b_{q\delta}$ and $0_{\gamma\delta}$ are assumed as equal to 0.

It has become apparent that it is necessary to undertake a theoretical treatment of the experimental data on the vibrational spectra of phosphorus compounds so as to be able to interpret correctly the changes in these spectra as one progresses from one molecule to another. In this connection we have undertaken to compute the characteristic frequencies of a series of phosphorus compounds, including a numerical analysis of the dependence of these frequencies on the force constants and kinematic parameters, using the theory of characteristic vibrations [1].

In the present communication we set forth the results of a computation of the vibrations of the simplest molecules containing the bonds P = O and P = S, namely in the molecules $POCl_3$, $POBr_3$, $PSCl_3$ and $PSBr_3$.

On the basis of the experimental data one may assume that the equilibrium configuration of all these molecules (general formula ZPY_3) belongs to the group C_{3v} (see insert). Accordingly, in the vibrational spectra of the molecules of the type ZPY_3 six fundamental frequencies should be observed; three totally symmetric and three doubly degenerate frequencies. In the calculation use is made of the interpretation of Raman spectra on the basis of polarization measurements [3 - 6].

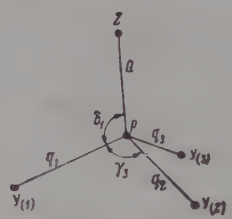

As generalized coordinates we chose (Q) and (q_i), which are the changes corresponding to the lengths of the bonds P-Z and P-Y_i (i = 1, 2, 3) respectively; furthermore γ_k and δ_i are taken as the changes corresponding to the angles $Y_{(i)}PY_{(j)}$ ($k \neq i, j$; i, j = 1, 2, 3) and $ZPY_{(i)}$ (i = 1, 2, 3). The generalized angular coordinates are connected by the relation $\gamma_1 + \gamma_2 + \gamma_3 + \delta_1 + \delta_2 + \delta_3 = 0$. The matrix elements T^{-1} were calculated from the appropriate tables [7]. The calculation was made with the following values of the bond lengths: $S_{(P=O)} = 1.58$ Å, $S_{(P-Cl)} = 2.02$ Å, $S_{(P=S)} = 1.94$ Å, $S_{(P-Br)} = 2.18$ Å. The angles $Y_{(i)}PY_{(j)}$ and $ZPY_{(i)}$ (i,j = 1,2,3) were taken to be tetrahedral. As the unit of bond length we chose the length of the C-H bond in methane $S_{(C-H)} = 1.09$ Å. As the unit of mass we chose the mass of hydrogen $m_H = 1.008$

Table 3

The Vibrations ν_1

Molecule	Observed frequencies in cm^{-1}		calc. frequency in cm^{-1}	Form of vibrations									Partial derivatives $\frac{\partial \nu_i}{\partial t}(t = K_Q, K_q, \ldots, \delta)$														
	Raman spectra	Infra-red spectra		Q	q_1	q_2	q_3	γ_1	γ_2	γ_3	δ_1	δ_2	K_Q	K_q	K_γ	K_δ	h_{Qq}	h_{qq}	$a_{Q\delta}$	$a_{q\gamma}$	$a_{q\delta}$	$l_{\gamma\gamma}$	$l_{\delta\delta}$	$l_{\gamma\delta}$	σ_Y*	σ_Z*	γ	δ
$POCl_3$	1292	1292	1295	1	−0.18	−0.18	−0.18	0.28	0.28	0.28	−0.28	−0.28	37	2	5	5	−31	4	−49	−12	6	10	10	−20	0	0	3	5
$POBr_3$	1260	—	1260	1	−0.15	−0.15	−0.15	0.26	0.26	0.26	−0.26	−0.26	38	1	3	3	−20	2	−34	− 6	3	6	6	−12	0	0	6	−16
$PSCl_3$	748	748	748	1	−0.31	−0.31	−0.31	0.47	0.47	0.47	−0.47	−0.47	43	4	9	9	−43	8	−66	−22	11	18	18	−36	−4	0	6	32
$PSBr_3$	718	—	721	1	−0.27	−0.27	−0.27	0.41	0.41	0.41	−0.41	−0.41	43	3	7	7	−32	6	−52	−42	21	14	14	−28	0	0	10	10

* σ_Y and σ_Z are reciprical, respectively, to the length of the P - Y and P - Z bonds expressed in the units of length used.

Table 4

The Vibrations $\nu_2 - \nu_6$

Molecule	Vibration	Symmetry	Frequency in cm^{-1}		Form of vibration									Partial derivatives $\frac{\partial \nu_i}{\partial t}(t = K_Q, K_q, \ldots, \sigma_Z)$													
			Observed Raman spectra	Calculated	Q	q_1	q_2	q_3	γ_1	γ_2	γ_3	δ_1	δ_2	K_Q	K_q	K_γ	K_δ	h_{Qq}	h_{qq}	$a_{Q\delta}$	$a_{q\gamma}$	$a_{q\delta}$	$l_{\gamma\gamma}$	$l_{\delta\delta}$	$l_{\gamma\delta}$	σ_Y	σ_Z
$POCl_3$	ν_2	A_1	486	488	−0.03	1	1	1	−0.38	−0.38	−0.38	0.38	0.38	1	44	7	7	− 66	88	− 24	− 70	35	14	14	− 28	65	0
	ν_3		268	255	0.03	0.11	0.11	0.11	1	1	1	−1	−1	4	− 8	92	92	18	−16	−198	−118	59	184	184	−368	514	0
	ν_4	E	582	582	0	1	−1	0	0.52	−0.52	0	−0.72	0.72	0	69	8	6	0	−69	0	− 49	− 50	− 8	− 6	30	− 35	−139
	ν_5		191	200	0	−0.06	0.06	0	1	−1	0	0.08	−0.08	0	− 8	157	− 7	0	8	0	−162	20	−157	7	120	585	− 55
	ν_6		337	362	0	0.22	−0.22	0	−0.08	0.08	0	1	−1	0	−23	4	169	0	23	0	5	− 83	− 4	−169	76	132	2240
$POBr_3$	ν_2	A_1	340	344	−0.07	1	1	1	−0.53	−0.53	−0.53	0.53	0.53	3	45	10	10	− 80	90	− 39	− 86	43	20	20	− 40	− 35	0
	ν_3		173	168	0.02	0.21	0.21	0.21	1	1	1	−1	−1	2	−18	113	113	45	−36	−268	−154	77	226	226	−452	683	0
	ν_4	E	488	486	0	1	−1	0	0.57	−0.57	0	−0.77	0.77	0	57	9	9	0	−57	0	− 58	− 59	− 9	− 9	20	− 25	− 71
	ν_5		118	118	0	−0.06	0.06	0	1	−1	0	0.06	−0.06	0	−12	200	−13	0	12	0	−241	21	−200	13	199	445	− 4
	ν_6		267	254	0	0.27	−0.27	0	−0.05	0.05	0	1	−1	0	−33	3	189	0	33	0	14	−108	− 3	−189	102	130	710
$PSCl_3$	ν_2	A_1	430	436	0.03	1	1	1	−0.26	−0.26	−0.26	0.26	0.26	−2	53	7	7	− 74	106	− 18	− 94	47	14	14	− 28	10	0
	ν_3		245	246	−0.03	0.13	0.13	0.13	1	1	1	−1	−1	−3	− 7	101	101	29	−14	−200	−146	73	202	202	−404	1089	0
	ν_4	E	540	532	0	1	−1	0	0.48	−0.48	0	−0.55	0.55	0	70	10	7	0	−70	0	− 52	− 49	− 10	− 7	16	− 18	− 23
	ν_5		170	170	0	−0.07	0.07	0	1	−1	0	0.03	−0.03	0	−11	179	− 4	0	11	0	−185	12	−179	4	129	491	0
	ν_6		(250)	255	0	0.32	−0.32	0	−0.17	0.17	0	1	−1	0	−39	12	141	0	39	0	− 4	−102	− 12	−141	98	74	635
$PSBr_3$	ν_2	A_1	299	301	−0.03	1	1	1	−0.44	−0.44	−0.44	0.44	0.44	2	53	10	10	−103	106	− 40	116	− 58	20	20	− 40	20	0
	ν_3		165	161	0	0.25	0.25	0.25	1	1	1	−1	−1	0	−24	119	119	68	−48	−276	− 44	22	238	238	−476	798	0
	ν_4	E	438	452	0	1	−1	0	0.59	−0.59	0	−0.67	0.67	0	65	11	11	0	−65	0	− 50	− 54	− 11	− 11	10	2	− 50
	ν_5		115	109	0	−0.01	0.01	0	1	−1	0	0.17	−0.17	0	0	229	−53	0	0	0	−266	60	−229	53	60	390	−192
	ν_6		179	173	0	0.39	−0.39	0	−0.28	0.28	0	1	−1	0	−64	23	168	0	64	0	− 5	−142	− 23	168	98	303	789

The force constants are identified in Table 1. The values of the force constants (see Table 2) were chosen in such a way as to assure satisfactory agreement between the calculated and measured frequencies. It is however necessary to view these values as highly provisional. The remaining symmetry relations are taken into account by well-known methods [8, 9]. The secular equations are solved by the method of "iterated roots", [1], from which one obtains both the square of the frequencies and the forms of vibrations. The partial derivatives of the frequencies by various parameters are calculated with the aid of an advanced method [10]. The results of these calculations are given in Tables 3, 4 and 5.

In Table 3 are given the results of the calculation of the totally symmetric vibrations ν_1, corresponding to the so-called P = O frequencies in $POCl_3$ and $POBr_3$ and the so-called P = S frequencies in $PSCl_3$ and $PSBr_3$. From Table 3 it is clear that for all four molecules the vibration ν_1 is not uniquely characterized by the form of the coordinate Q which determines the change in the length of the P = O or P = S bond, since in this mode the coordinates q, γ and δ change considerably as well. One should notice that in the molecules $PSCl_3$ and $PSBr_3$ this vibrational mode is less uniquely characterized by the form of the coordinate Q than in the molecules $POCl_3$ and $POBr_3$.

From the values given in Table 3 for the partial derivatives of the frequencies with respect to various parameters it follows that a similar change in the values of all the parameters would not significantly change the value of the frequency ν_1. And also it is possible to assert confidently that the experimental determination of this frequency has been made correctly and that also in the corresponding modes of the molecules $POCl_3$, $POBr_3$, and $PSBr_3$, the coordinate Q is the one with the largest variation. This also confirms the quantitative estimate of the "uniqueness" of the frequency α and the form of the vibration β for the coordinate Q; this is clear from Table 5 in which we give the results of a calculation of the corresponding "non-characteristic coefficients" of the frequency α and the coefficients for the form of the vibration β [1].

Table 5

Characterization of the Vibration ν_1 in terms of the Coordinate Q

Molecule	α	β
$POCl_3$	−0.03	0.70
$POBr_3$	0.01	0.63
$PSCl_3$	0.00	1.18
$PSBr_3$	0.00	1.06

In Table 4 are listed the results of a calculation of the remaining normal vibrations of the molecules $POCl_3$, $POBr_3$, $PSCl_3$ and $PSBr_3$. It is clear from Table 4 that not one of these modes is uniquely characterized by the form of any particular coordinate. The modes best characterized by the form of any particular coordinate. The modes best characterized by the form of the coordinates are the vibrations ν_3 and ν_4.

June 11, 1958

References

1. L. S. MAIANTS: Tr. FIAN, 5, 63 (1950)
2. P. W. ALLEN, L. E. SUTTON: Acta Cryst. 3 46 (1950)
3. A. SIMON, G. SCHULZE: Naturwiss., 25, 669 (1937)
4. V. N. THATTE: Nature, 138, 468 (1936)
5. J. CABANNES, A. ROUSSET: Ann. de Phys., Series 10, 19, 229 (1933)
6. M.-L. DELWAULLE, F. FRANCOIS: C.R., 220, 817 (1945); 224, 1422 (1947)
   M.-L. DELWAULLE: C.R., 222, 1391 (1946)
7. M. A. EL'IASHEVICH: ZFKh, 15(7-8), 847-864 (1941) (See LC RT-1141, 23 pp.)
8. L. S. MAIANTS: ZETF, 25, 393 (1953)
9. L. S. MAIANTS: DAN USSR, 89(3), 423-426 (1953) (See OTS RT-33, 4 pp.)
10. L. S. MAIANTS: OiS, 5, 378 (1958)

TOM VI, Vyp. 5 OPTIKA I SPEKTROSKOPIIA Mai, 1959
VOL. VI, No. 5 OPTICS AND SPECTROSCOPY May, 1959

Calculation and Interpretation of the Vibrational Spectra of Tetramethylsilane and Tetramethylsilane--d_{12}

I. F. KOVALEV

Abstract: The methods of Vol'kenshtein, El'iashevich, Stepanov [1], and Maiants [2] are employed for the computation and evaluation of the potential energy constants (force coefficients and influence coefficients) and the forms of the normal vibrations of tetramethylsilane. The frequencies of the vibrational spectra of $Si(CH_3)_4$ and $Si(CD_3)_4$ are computed and interpreted.

INTRODUCTION

Studies of methylsilane are of great importance for theoretical and experimental chemistry. In particular, there is great interest in knowledge of the potential functions and the normal vibration frequencies. With this aim we carried out earlier theoretical studies of Si_2H_6 [3] (this has no Si-C bond) and of CH_3SiH_3 [4] (this has one Si-C bond). In this paper the analogous question is solved for tetramethylsilane (which has four Si-C bonds).

References [3,4] mention the work of other authors touching on these compounds. The results are said to be incomplete. We note in addition that other investigations of the force field of $Si(CH_3)_4$ accomplished up to now are also incomplete. The first computations were carried out by Wall and Eddy [5] and by Silver [6]. They determined the frequencies of the molecular skeleton, regarding the methyl group as a simple atom with atomic weight 15. They also calculated the vibrations of the group with respect to the Si atom under the assumption that the latter represented an infinite mass. By this means they obtained the simple valence potential. Wall and Eddy obtained the following values of the force coefficients (in 10^5 dyne/cm): $K_{Si-C}=3.31$; $K_{Si-CH_3}=3.14$; $K_{C-H}=4.76$; $k_\epsilon(C_i\text{-}Si\text{-}C_j)=0.120$; $k_\alpha(H_i\text{-}C\text{-}H_j)=0.468$. Silver obtained the following: $K_{Si-C}=3.31$; $K_{C-H}=4.79$; $k_\epsilon=0.137$; $k_\alpha(H_i\text{-}C\text{-}H_j)=k_\beta(Si\text{-}C\text{-}H_i)=0.468$.

Siebert [7] computed the force constants and the vibration spectrum of $Si(CH_3)_4$ and some other tetramethyl compounds. He also employed a simplified valence-force coordinate system: he considered the diagonal coefficients plus the interaction constants between similar coordinates only. He found for tetramethylsilane the following set of coefficients (in 10^5 dyne/cm): $K_{Si-C}=2.93$; $H(Si\text{-}C_i,\ Si\text{-}C_j)=0.16$; $K_{C-H}=4.74$; $h(C\text{-}H_i,\ C\text{-}H_j)=0.08$; $k_\epsilon=0.166$; $l_\epsilon(C_i\text{-}Si\text{-}C_j,\ C_j\text{-}Si\text{-}C_i)=0.015$; $k_\beta=0.357$; $l_\beta(H_i\text{-}C\text{-}Si,\ H_j\text{-}C\text{-}Si)=-0.041$ and $k_\alpha=0.438$.

Recent important experimental and theoretical work [7--17] permits a much more complete treatment of $Si(CH_3)_4$ than that accomplished up to now.

DISCUSSION OF THE FREQUENCIES IN EXPERIMENTALLY OBSERVED VIBRATION SPECTRA

We found at our disposal experimental data on the Raman and infrared spectra of tetramethylsilane given in references [8--17]. In addition to the frequencies, the intensities and extent of depolarization of the spectral lines were measured. The results of measurement and a referral of the frequencies to the normal vibrations are given in Table 1.

The tetramethylsilane molecule belongs to the symmetry point group T_d. The 45-th order representation matrix decomposes under symmetry considerations into an irreducible representation of the form:

$$(1)\quad \Gamma = 3A_1 + A_2 + 4E + 4F_1 + 7F_2.$$

By the selection rules the wholly symmetric (A_1) and doubly degenerate (E) vibrations are resolved into the Raman spectrum only. The triply degenerate vibrations (F_2) are resolved into the Raman and infrared spectra. The A_2 and F_1 vibrations do not appear in either spectrum.

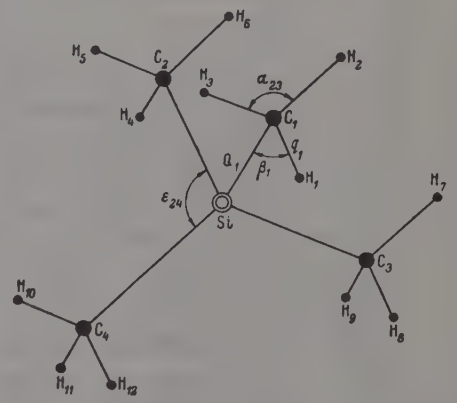

Equilibrium configuration of the tetramethylsilane molecule

Thus, fourteen distinct fundamental frequencies may be observed. In fact, 10 lines are observed in the Raman spectrum, and about 40 in the infrared. A few interpretive remarks are in order. The opinion of the various authors varies with respect to two lines, at 1249 and 859 cm^{-1}. In [9] and [10] the line at 1249 cm^{-1} is attributed to vibrations of the methyl group. It seems to us that such a frequency is rather high for a vibration of this kind.

Table 1

Vibrational Spectra of Tetramethylsilane and Tetramethylsilane-d_{12} (Frequencies in cm^{-1})

Designation	Coordinate	Vibration type	$Si(CH_3)_4$ Experimental frequencies: Raman spectrum [8]	Raman spectrum [9] liquid	Raman spectrum [10]	Raman spectrum [14]	Raman spectrum [11]***	Infrared spectra [9] gas	Infrared spectra [12] solid	Infrared spectra [12] gas	Infrared spectra [13] gas	Infrared spectra [14]	Infrared spectra [15] gas	Infrared spectra [17] solution	Calculated frequencies	Form of the vibrations	$Si(CD_3)_4$ Calculated frequencies
ν_1	q	A_1	2905(10b)	2900(100)	2898(20b)	2900(100p)	2919	-	-	-	-	-	-	-	2900	Q= -0.048q α= -0.041q	2108
ν_2	α= -β	A_1	1264(10b)	1263(8)	1260(2d)	1263(8p)	1254	-	-	-	-	-	-	-	1266	Q= 0.129α q= -0.035α	1009
ν_3	Q	A_1	598(20)	593(40)	590 (20n)	593(40p)	598	-	-	-	-	-	-	-	598	q= -0.036Q α= 0.214Q	511
ν_5	q	E	2963(10b)	2955(88)	2957(20b)	-	2963	-	-	-	-	-	-	-	2968	ε= -0.087q α= 0.072q	
ν_6	α	E	-	1418(40)	-	1418(40dp)	1430	-	-	-	-	-	-	-	1415	β= -0.081q q= 0.029α ε= -0.040α	2218
ν_7	β	E	863(10b)**	-	859(7b)**	-	869	-	-	-	-	-	-	-	855	β= 0.234α q= -0.046β ε= 0.142β	1035
ν_8	ε	E	202(20b)	199(80)	199(10b)	199(80dp)	202	-	-	-	-	-	-	-	200	α= -0.290β q= 0.023 α= 0.088ε	663
ν_{13}	q_b	F_2	-	2957(88)	-	2957(88dp)	2967	2957(s)	-	-	2969	2957(vs)	2967	-	2967	β= -0.310 Q= -0.002q_b q_a= -0.701q_b	173
ν_{14}	q_a	F_2	-	-	-	-	2919	-	-	-	2904	-	2900	2899	2899	ε= -0.084q_b α_a= -0.051q_b α_b= 0.071q_b β_a= 0.056q_b Q= -0.059q_a q_b= 0.703q_a	2221
ν_{15}	α_a= -β_b	F_2	1427(15b)	-	1418(7d)	-	1430	1430(s)	-	-	1413P 1425Q 1432R	1430(s)	1429	1439	1418	ε= 0.002q_a α_a=-0.040q_a α_b= -0.028q_a β_a= 0.039q_a Q = 0.016α_a q_a= 0.029α_a	2101
ν_{16}	α_b= -β_b	F_2	-	-	-	-	1254	1285(m)	1255	1257	1241P 1250Q 1256R	1285(m)	1265	-	1261	q_b=-0.040α_a ε = 0.043α_a α_b= -1.404α_a β_a= 0.240α_a Q = 0.228α_b q_b=-0.050α_b	1036
ν_{17}	β_a= -β_b	F_2	-	1250(8)	1249(2d)	1250(8dp)	869	1250(s)	852 880	871	865P 870Q 875R	1253(s)	848 879	1258	895	q_b=-0.034α_b ε= -0.015α_b α_a= 1.375α β_a=-1.378α_b Q = 0.242β_a q_a=-0.040β_a	1003
ν_{18}	Q	F_2	696(15b)	694(33)	690(10b)	694(33dp)	696	694(vs)	694	693	689P 698Q 707R	696(vs)	690	-	705	Q_b= 0.058β_a ε = -0.356β_a α_a=-0.350β_a α_b= 0.398β_a qα = 0.047Q q_b=-0.014Q ε = -0.278Q α_a=-0.011Q	746
ν_{19}	ε	F_2	239(15b)	245(46)	243(10b)	245(46dp)	239	-	-	-	-	-	-	-	244	α_b=-0.260Q β_a=-0.394Q Q = -0.019ε q_a=-0.013ε q_b= 0.021ε α_a=-0.054ε α_b= 0.079ε β_a= 0.185ε	604 216
ν_4	τ	A_2	-	-	-	-	-	-	-	-	-	-	-	-	145		
ν_9	q	F_1	-	-	-	-	-	-	-	-	-	-	-	-	2966		
ν_{10}	α	F_1	-	-	-	-	-	-	-	-	-	-	-	-	1416		
ν_{11}	β	F_1	-	-	-	-	-	-	-	-	-	-	-	-	829		
ν_{12}	τ	F_1	-	-	-	-	-	-	-	-	-	-	-	-	145		

Abbreviations. b--broad; n--narrow; d--diffuse; m--medium; s--strong; vs--very strong; p--polarized; dp--depolarized; P,Q,R--branch designation (our interpretation).

* The notation is the same as that of reference [11].

** This is assumed to be a combination frequency.

It is more reasonable to assume that there is a shift toward lower frequencies, as compared to tetramethylmethane, when the methyl group is added to a heavier atom, and to attribute the line under discussion to vibrations connected with the deformation of the H--C--H and H--C--Si angles, as is done in [9,11,13,14]. The postulation of such a shift is supported by computation in the case of CH_3SiH_3 [4]. In general, bands in the range from about 1240 to 1280 cm^{-1} are characteristic of compounds in which the CH_3 group is directly bound to the silicon atom.

The line 859 cm^{-1} is considered in [9] as a combination of two harmonics $\nu_8(e)$ and $\nu_{18}(f_2)$; this seems less than plausible. The observed frequency, 859 cm^{-1}, is not in good agreement with the appropriate combination frequency, 889 cm^{-1}. The line at 859 cm^{-1} can be very satisfactorily interpreted as a fundamental arising from the degenerate vibration $\nu_7(e)$.

In the infrared absorption spectra, as published by various authors, there are differing numbers of bands. For example, one of the most recent investigations, by Smith [13], yields 44 minima.

The tetramethylsilane molecule may be considered to be a spherical top. If we take the equilibrium interatomic distances to be $r_{Si-C} = 1.888$ Å, $r_{C-H} = 1.09$ Å [18] and the angles to be tetrahedral, the moment of inertia will be $I = 271.75 \times 10^{-40}$ gm cm^2, and the rotational constant $A \approx 0.1$ cm^{-1}. Therefore, under the conditions of measurement of the spectra [13] the rotational band structure was not resolved. The observation of six infrared bands is related to the triply degenerate (F_2) fundamental oscillation, (Table 1), and the rest are due to harmonics and combination frequencies (Table 2).

Table 2

Interpretation of the Combination Frequencies and Harmonics of Tetramethylsilane

Infrared Spectrum (in cm^{-1})		Interpretation	Infrared Spectrum (in cm^{-1})		Interpretation
4530	VW	$\nu_4+\nu_5+\nu_{15}(F_1+F_2)$	1879	VW	$2\nu_3+\nu_{18}(F_2)$
3813	VW	$\nu_2+\nu_{13}(F_2)$	1834	W	$\nu_3+\nu_{16}(F_2)$
4240	VW	$\nu_{11}+\nu_{13}(A_2+E+F_1+F_2)$	1654	VW	$\nu_6+\nu_{19}(F_1+F_2)$
			1589	VW	$\nu_{17}+\nu_{18}(A_1+E+F_1+F_2)$
3655	VW	$\nu_5+\nu_{18}(F_1+F_2)$	1570		
3212	W	$\nu_{13}+\nu_{19}(A_1+E+F_1+F_2)$	1474	W	$\nu_{17}+\nu_{19}(A_1+E+F_1+F_2)$
3090	W	$\nu_8+\nu_{14}(F_1+F_2)$			
3037	W	$\nu_6+\nu_8+\nu_{10}(F_1+F_2+F_1+F_2)$	1382	W	$2\nu_{18}(A_1+E+F_1+F_2)$
			1335	VW	$\nu_7+2\nu_{19}(A_1+E+F_1+F_2+A_2+E+F_1+F_2)$
2827	W	$\nu_6+\nu_{15}(F_1+F_2)$			
2477	VW	$2\nu_{16}(A_1+E+F_1+F_2)$	1282	W	$\nu_3+\nu_{18}(F_2)$
2361	VW	$\nu_2+\nu_7+\nu_{19}(F_1+F_2)$	1180	VW	$\nu_6-\nu_{19}(F_1+F_2)$
2215	VW	$\nu_2+\nu_{18}+\nu_{19}(A_1+E+F_1+F_2)$			
2133	W	$\nu_{15}+\nu_{18}(A_1+E+F_1+F_2)$	1113	VW	$\nu_7+\nu_{19}(F_1+F_2)$
			1105		
2082	VW	$\nu_4+\nu_{16}+\nu_{18}(A_2+E+F_1+F_2)$	1070	W	$\nu_8+\nu_{17}(F_1+F_2)$
			1030	VW	$\nu_8+\nu_{11}(F_1+F_2)$
2050	VW	$\nu_3+\nu_{15}(F_2)$	945	W	$\nu_{18}+\nu_{19}(A_1+E+F_1+F_2)$
1945	W	$\nu_{16}+\nu_{18}(A_1+E+F_1+F_2)$			

Abbreviations. w--weak; vw--very weak; The high frequencies (in the range 4530 to 2050 cm^{-1}) are approximate [13].

CALCULATION OF THE COEFFICIENTS OF THE FORCE FIELD, FREQUENCY, AND FORM OF THE OSCILLATIONS

The calculation of the force coefficients, frequency, and form of the normal vibrations of tetramethylsilane was based on the methods of Vol'kenshtein, El'iashevich, Stepanov [1] and Maiants [2]. Forty-six natural coordinates were introduced, as follows: Q_i ($i = 1,\ldots,4$) as variations in the length of the Si—C bonds; q_i ($i = 1,\ldots 12$) as variations in the length of the C--H bonds; ϵ_{ij} ($i,j = 1,\ldots,4$; 6 variables) as variations in the C—Si—C angles; α_{ij} and β_i ($i, j = 1,\ldots, 12$) as respectively the variations in the H--C--H and H--C--Si angles. [The equilibrium configuration of the $Si(CH_3)_4$ molecule is shown schematically in the figure]. Ultimately five variables are eliminated by means of five auxiliary relations among the angles

$$(2)\quad \epsilon_{12}+\epsilon_{13}+\epsilon_{14}+\epsilon_{23}+\epsilon_{24}+\epsilon_{34}=0,$$
$$\alpha_{12}+\alpha_{23}+\alpha_{13}+\beta_1+\beta_2+\beta_3=0,$$
$$\alpha_{45}+\alpha_{56}+\alpha_{46}+\beta_4+\beta_5+\beta_6=0,$$
$$\alpha_{78}+\alpha_{89}+\alpha_{79}+\beta_7+\beta_8+\beta_9=0,$$
$$\alpha_{10\,11}+\alpha_{11\,12}+\alpha_{10\,12}+\beta_{10}+\beta_{11}+\beta_{12}=0.$$

Anharmonics were calculated by introduction of the spectroscopic masses of hydrogen and deuterium. After symmetry reductions and calculation of side conditions, the potential and kinetic energy coefficient matrices were obtained: of third order for vibrations of types A_1 and F_1, of fourth order for vibrations of type E, and of seventh order for vibrations of type F_2*

In calculating the potential energy function we used results obtained for CH_3SiH_3 [4]. In the first approximation four auxiliary coefficients (i.e. as compared to [4]) were introduced, corresponding to newly considered interactions: k_ϵ(C--Si--C); H_ϵ(Si--C_i, Si--C_j); $A = A_\epsilon - B_\epsilon$ (which describes the interaction of the Si--C_i bond with the angles C_i--Si--C_j and C_j--Si--C_k) and $l_{\epsilon\epsilon}$ (the interaction of the angle C_i--Si--C_j with the angle C_j--Si--C_k--Si--C_l). Ultimately, in order to secure better agreement between the calculated and experimental values of the vibration spectra, the values of certain constants were adjusted. The following are the finally adopted values of the force coefficients (in 10^6 cm^{-2}):**

$K_q=4.62$, $K_q=8.05$, $k_\epsilon=0.856$, $k_\alpha=0.675$, $k_\beta=0.660$

$H_\epsilon=0.15$, $h_\alpha=0.070$, $A_{\alpha\beta}=0.225$, $A=A_\epsilon-B_\epsilon=0.300$,

$a=0.350$, $l_{\alpha\alpha}=l_{\alpha\beta}=-0.035$, $l_{\beta\beta}=-0.040$,

$m_{\beta\epsilon}=0.080$, $n_{\beta\epsilon}=-0.010$, $l_{\epsilon\epsilon}=0.081$.

*The rotation of the CH_3 group with respect to the Si—C axis was neglected.

**The notation is the same as in [4].

The frequencies and the form of the normal vibrations, calculated on the basis of the system of constants given above, are shown in Table 1. The secular equations for $Si(CH_3)_4$ were solved by the iteration method of Maiants [2], and the equations for $Si(CD_3)_4$ were solved by successive diagonalizations.

The influence coefficients, calculated by the method of determinants, are as follows (in 10^{-6} cm^2):

K_Q^{-1}=0.2310, K_q^{-1}=0.1287, $\bar{k}_\alpha^{-1}$=1.2257, h_α^{-1}= -0.0026,

α_α^{-1} = -0.0339, b_α^{-1}=0.0344, α_β^{-1}=-0.0357, b_β^{-1}=0.0346,

$\bar{l}_{\alpha\alpha}^{-1}$ =-0.2210, $\bar{l}_{\alpha\beta}^{-1}$= -0.2244, H_ϵ^{-1}= -0.0097,

$o_{\alpha\beta}^{-1}$ = -0.335, H'^{-1} =-0.0003, H''^{-1}=0.0002, H_β^{-1} =-0.0016,

B_α^{-1} = 0.0377, B'^{-1}=0.0015, B''^{-1}=-0.0007, A_ϵ^{-1}=-0.0415,

B_ϵ^{-1} =0.0415, $\bar{l}_{\beta\beta}^{-1}$ = -0.2365, $\bar{k}_\beta^{-1}$ =1.2561, u_β^{-1}=0.0031,

t_β^{-1} = -0.0055, s_β^{-1} =0.0118, v_β^{-1} =0.0012, $p_{\beta\epsilon}^{-1}$ = -0.0083,

$r_{\beta\epsilon}^{-1}$ =0.0077, $m_{\beta\epsilon}^{-1}$ = -0.1232, $n_{\beta\epsilon}^{-1}$ =0.0580, A_β^{-1} =-0.0377,

C_β^{-1} = 0.0083, D_β^{-1} = -0.0026, $\bar{k}_\epsilon^{-1}$ = 1.1225,

$\bar{l}_{\epsilon\epsilon}^{-1}$ = -0.2487, o_ϵ^{-1} = -0.1278, $p_{\alpha\epsilon}^{-1}$ =0.0111,

$r_{\alpha\epsilon}^{-1}$ = -0.0020, $l'^{-1}_{\alpha\epsilon}$ = -0.0016, $l''^{-1}_{\alpha\epsilon}$ =-0.0028,

c_ϵ^{-1} =0.0056, d_ϵ^{-1} = -0.0029, b'^{-1}_ϵ =0.0006, b''^{-1}_ϵ =-0.0001.

DISCUSSION OF RESULTS

The calculations have shown that the potential energy coefficients as derived do adequately account for the actual force field of the tetramethylsilane molecule; the calculated frequencies agree well with the experimentally observed frequencies. In characterizing the force field it is necessary to neglect certain interactions (as in Siebert [7]) primarily those between the Si--C bonds and the H--C--H and H--C--Si ($A_{\alpha\beta}$) angles, and also the interactions between the C--H bonds and the same angles (a).

Comparison of the potential energy functions shows that in going from methylsilane to tetramethylsilane there are certain changes in the force field corresponding to the Si--CH_3 group:

	K_Q^{-1}	K_q^{-1}	$\bar{k}_\alpha^{-1}$	$\bar{k}_\beta^{-1}$	A_β^{-1}
CH_3SiH_3[4]	0.2278	0.1283	1.1570	1.1190	-0.0735
$Si(CH_3)_4$	0.2310	0.1287	1.2257	1.2561	-0.0377

	H_β^{-1}	α_α^{-1}	α_β^{-1}	b_α^{-1}	b_β^{-1}
CH_3SiH_3[4]	-0.0032	-0.0320	-0.0294	0.0310	0.0311
$Si(CH_3)_4$	-0.0016	-0.0339	-0.0357	0.0344	0.0346

	$\bar{l}_{\alpha\alpha}^{-1}$	$\bar{l}_{\alpha\beta}^{-1}$	h_α^{-1}	$\bar{l}_{\beta\beta}^{-1}$	$o_{\alpha\beta}^{-1}$
CH_3SiH_3[4]	-0.1955	-0.2261	-0.0021	-0.1765	-0.3139
$Si(CH_3)_4$	-0.2210	-0.2244	-0.0026	-0.2365	-0.3335

For example, the influence coefficient K_q^{-1}, corresponding to an extension of the Si-C bond, is 1.4% greater in tetramethylsilane. The stability of the bond is correpondingly decreased. It must be noted that the Si-C bond in $Si(CH_3)_4$ is approximately 1,7% longer than in CH_3SiH_3.

The influence coefficient K_q, however, scarcely changes its value. Accordingly, the C—H bond changes very little as to its stability. The diagonal coefficients k_α and k_β in tetramethylsilane are approximately 6% and 12% greater. The $Si(CH_3)_4$ molecule is less stable with respect to deformations of the corresponding angles. The vibration frequencies $\nu(\alpha)$ and $\nu(\beta)$ are reduced to some extent in tetramethylsilane. Also in tetramethylsilane the Si—C influence is reduced by a factor of 2, and the influence of the C—H bond on the angles of the methyl group is slightly increased. The mutual influences of the H—C—Si angles are increased.

Consideration of the secular equations and the form of the normal vibrations shows (as was to be expected) that there is a very strong coupling among the type F_2 normal vibrations, connected with deformations of the H—C—H and H—C—Si angles:

$$\alpha_b = -1.404\alpha_\alpha,\ \alpha_\alpha = 1.375\ \alpha_b,\ \beta_\alpha = -1.378\ \alpha_b,$$

$$\beta_\alpha = 0.240\ \alpha_\alpha,\ \alpha_\alpha = -0.350\ \beta_\alpha \text{ and } \alpha_b = 0.398\ \beta$$

Both these angles are simultaneously and strongly deformed especially for vibrations with the frequencies ν_{16} and ν_{17}. In the case of the doubly degenerate vibrations ν_6 and ν_7 the coupling is a little less strong: the change in the H-C-Si angle, amounts to approximately 23% of the change in the H-C-H angle, and the H-C-H angle changes by approximately 29% of the change in the H-C-H angle. These angles are also appreciably deformed in the ν_3 and ν_{18} vibrations, which refer to changes in the length of the Si-C bond; and conversely, in the case of the vibrations connected with changes in these angles (ν_2,ν_{16},ν_{17}) the length of the Si—C bond changes appreciably. In vibrations of type ν_8 and ν_{19} only the H--C--Si angles change strongly. The inverse influence is of the same order.

Let us compare the values of the frequencies calculated by taking into account the coupling among normal vibrations (ν_c) with the zero-approximation values (ν_o) calculated by neglecting these couplings; the comparison is given below (frequencies in cm^{-1}):

	q	α=-β	Q	q	α	β	ϵ
ν_c	2900	1266	598	2968	1415	855	200
ν_o	2899	1248	634	2974	1378	873	275
Δ	1	18	-36	-6	37	-18	-75

	q_b	q_a	α_a=-β_b	α_b=-β_b	β_a=-β_b	Q	ϵ
ν_c	2967	2899	1418	1261	895	705	244
ν_o	2949	2925	1386	1239	895	744	316
Δ	18	-26	32	22	0	-39	-72

The magnitude of the difference $\Delta = \nu_c - \nu_o$ is especially great for vibrations of type $\nu(\epsilon)$.

The author wishes to express his deepest gratitude to M. M. Sushchinskii for his interest in this work.

July 7, 1958

References

1. M. V. VOL'KENSHTEIN, M. A. EL'IASHEVICH, B. I. STEPANOV: Kolebaniia molekul (Vibrations of molecules), 1. GITTL, Moscow, 1949
2. L. S. MAIANTS: Tr. FIAN USSR, 5, 63 (1950); DAN USSR, 89, 423 (1953) (See RT-33, 4 pp. from OTS); ZETF, 25, 393 (1953)
3. I. F. KOVALEV: OiS, 3, 552 (1957)
4. I. F. KOVALEV: OiS, 4, 560 (1958)
5. F. T. WALL, C. R. EDDY: J. Chem. Phys., 6, 107 (1938)
6. S. SILVER: J. Chem. Phys. 8, 919 (1940)
7. H. SIEBERT: Zs. anorg. allgem. Chem., 268, 177 (1952); 271, 75 (1952)
8. K. W. F. KOHLRAUSCH: Ramenspektren, Leipzig, Akad. Verlagsgesell. Becker und Erler, 1943 (IL, 1952, p. 171)
9. D. H. RANK, B. D. SAKSENA, E. R. SHULL: Disc. Faraday Soc., No. 9, 187, 219 (1950)
10. V. A. KOLESOVA, E. V. KUKHARSKAIA, D. N. ANDREEV: IAN USSR, OKhN, No. 2, 294 (1953) (See CB BULLETIN)
11. C. W. YOUNG, J. S. KOEHLER, D. S. MC KINNEY: J. Amer. Chem. Soc., 69, 1410 (1947)
12. I. SIMON, H. O. MC MAHON: J. Chem. Phys., 20, 905 (1952)
13. A. L. SMITH; J. Chem. Phys., 21, 1997 (1953)
14. E. R. SHULL, T. S. OAKWOOD, D. H. RANK: J. Chem. Phys., 21, 2024 (1953)
15. S. KAYE, S. TANNENBAUM: J. Org. Chem., 18, 1750 (1953)
16. S. TANNENBAUM, S. KAYE, G. F. LEWENZ: J. Amer. Chem. Soc., 75, 3753 (1953)
17. A. P. KRESHKOV, IU. IA. MIKHAILENKO, G. F. IAKIMOVICH: ZFKh, 28, 537 (1954)
18. A. C. BOND, L. O. BROCKWAY: J. Amer. Chem. Soc., 76, 3312 (1954)

TOM VI, Vyp. 5
VOL. VI, No. 5

OPTIKA I SPEKTROSKOPIIA
OPTICS AND SPECTROSCOPY

Mai, 1959
May, 1959

Investigation of the Absorption Spectra of 1,2-Benzanthracene Single Crystals in the Region of Lowest Electronic Transitions

M. S. BRODIN, M. S. SOSKIN

Abstract: Absorption curves have been obtained of 1,2-benzanthracene single crystals for 20 and 290° K in polarized light* for the region of lowest electronic transitions. The integrated absorption of the separate bands and the corresponding polarization relation have been determined. Conclusions have been drawn relative to the polarization of electronic transitions in a molecule on the basis of a comparison of the results obtained with theoretical considerations.

INTRODUCTION

There are more or less complete data in the literature on the spectral and optical properties of crystals of the simplest aromatic hrdrocarbons. The spectrum of the benzene crystal [1] has been investigated in sufficient detail, there are data for various temperatures on naphthalene, anthracene and, partially, phenanthrene crystals [2-4]. Of the tetracyclic compounds, naphthacene, chrysene and pyrene have been subjected to spectral investigation, however, the data obtained are far from complete. Hence, the extent to which compounds have been investigated decreases with the passage to the more complex compounds. We have not found any data in the literature on the 1,2-benzanthracene crystal and consequently, we undertook a study of this crystal with the idea of subsequently classifying the optical and spectral properties of crystals of the aromatic hydrocarbons after sufficient experimental material had been accumulated. There is such a classification in the literature for electronic absorption spectra of solutions of these compounds, for example, which indicates regularities in the location of their electronic levels, the magnitude of the transition probabilities, etc. [5].

Absorption curves of the 1,2-benzanthracene crystal in polarized light have been obtained herein at 20 and 290°.

1. EXPERIMENTAL PART

The 1,2-benzanthracene crystal belongs to the monoclinic system, to the space group $C_2^2(P_{21})$, i.e. it has only one symmetry element, a second order screw axis parallel to the monoclinic b axis of the crystal. Its cell parameters are [6]: a = 7.95 A, b = 6.5 A, c = 12.12 A, $\beta = 100.5^\circ$; the number of molecules per cell is 2. The molecule in the crystal retains a flat configuration but the length of the C-C bonds is rather distorted. The structure of the molecule is shown diagrammatically on figure 1, 1. Coordinates of the carbon atoms in the crystalline cell are also presented in [6]. On the basis of these data, we determined the orientation of the molecule in the crystal. It appears that the plane of the molecule is approximately parallel to the ac plane of the crystal cell.

In connection with the absence of a plane of symmetry and a center of inversion in the crystal, the crystal should be optically active on the basis of theoretical predictions [7]. We made attempts to detect this effect experimentally and to measure the rotation constant. The lack of sufficiently thick single crystals did not permit this question, which is of independent interest, to be investigated in detail. However, rather rough, approximate measurements made by using a polarizing microscope on 200 μ thick crystals afford the possibility of assuming the presence of activity in a 1,2-benzanthracene crystal with a rotation constant equal to 15-20 deg/mm in the 5460 Å region.

Single-crystal flakes of 1,2-benzanthracene were grown from pure material by sublimation (t_m = 160° C). These were very perfect platelets with mirror-like surfaces of uniform thickness. As before in [3], they were placed in optical contact with plane parallel quartz plates. In this case, stresses dependent on the difference in the values of the thermal expansion coefficient of the substrate and the crystal can arise during the crystal cooling and can lead to changes in the spectrum [8]. However, a comparison of the absorption spectra of crystals of different thickness (0.29 - 0.6μ), photographed under identical conditions, did not disclose any noticeable changes in the case of 1,2-benzanthracene.

Multiple investigations on a Federov stage show that the plane of the crystalline platelets, obtained by growing under sublimation, coincides with the N_mN_p plane of the refractive index ellipsoid, where N_m is the middle axis of the ellipsoid and N_p is the minor axis. According to x-ray structural results [9], this plane is the crystallographic ab plane, wherein N_m coincides with the monoclinic b axis and N_p approximates the a axis.

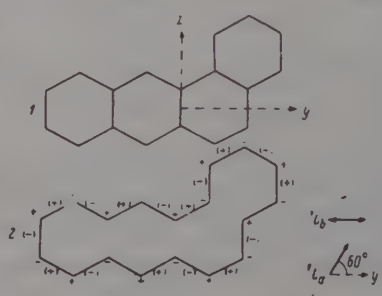

Figure 1. 1- structural formula of 1,2-benzanthracene molecule; 2- "polarization diagram".

2. EXPERIMENTAL RESULTS AND DISCUSSION

Absorption spectra have been obtained of two components (a and b) of a 1,2-benzanthracene crystal at 290 and 20° in the 25000 - 33000 cm^{-1} range, which corresponds to the region of lowest singlet electronic transitions. The absorption curves [$\kappa(\nu)$] for these conditions are shown on figures 2

* Unless specified otherwise, the temperatures herein will be in degrees K.

and 3. As is seen, the absorption curves at 20° are similar, in their general features, to the curves at room temperature but, as should also have been expected, show considerably more structure. The values of the absorption coefficients at the band maxima also change. Thus, for example, the altitude of the first maximum in the b component (ν = 25400 cm^{-1}) is 0.14 at 290° and 0.18 at 20° and 0.03 and 0.065, respectively, for the a component.

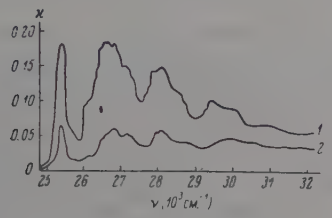

Figure 2. Absorption curves of a 1,2-benzanthracene crystal at 20°.

1- b-component; 2- a-component.

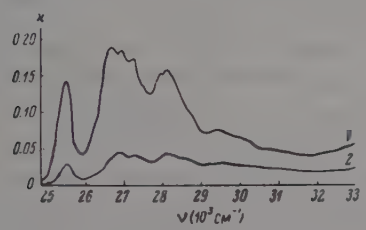

Figure 3. Absorption curves of a 1,2-benzanthracene crystal at 290°.

1- b-component; 2- a-component.

Let us dwell in more detail on the absorption curves of the b and a components at 20° (see fig. 2). Basically, they have the same configuration and consist of four sharp bands with supplementary structure. The first, at the frequency ν = 25400 ± 20 cm^{-1}, is sharpest and isolated. This band corresponds to a transition at the lowest excited electronic level. The luminescence spectrum of the crystal at 20°, which we obtained, confirms this (see fig. 4). Actually, the maximum of the initial luminescence band is 370 cm^{-1} away from the maximum of the first absorption band, i.e., is separated by approximately the magnitude of the band half-width which is 320 cm^{-1}. The absorption edge of a thick crystal (d = 70μ) coincided, in practice, with the absorption edge of the thin crystals (tenths of a micron) and there are no indications of the presence of impurity absorption at the location of the first luminescence band maximum. The second broad band is located in the 26000 - 27600 cm^{-1} range and is comparable to the first band in the maximum value of its absorption coefficient but exceeds it by far in its integrated absorption. The maximum and integrated absorption intensities of the next bands gradually fall off as the transition is made to higher frequencies.

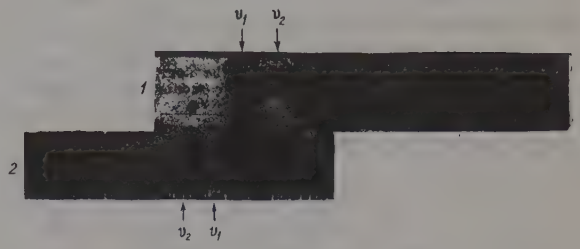

Figure 4. Absorption (1) and luminiescence (2) spectra of a 1,2-benzanthracene crystal at 20°. Arrows mark luminescence ν_1 = 25 030 cm^{-1} and ν_2 = 24 700 cm^{-1}, to which correspond the absorption bands ν_1 = 25 400 cm^{-1} and ν_2 = 25 730 cm^{-1}.

A series of five terms, with approximately 1400 cm^{-1} spacings between adjacent terms, namely: 25400, 26800, 28150, 29500 and 30900 cm^{-1}, is easily separated out of the spectrum. This series is usually ascribed to vibrations of the C-C bond [4]. There is also a second, less well-defined series with the same period: 25730 (?), 27160, 28550 and 30000 cm^{-1}. The two series mentioned are also observed in the spectrum of a frozen solution of 1,2-benzanthracene at 77°, which was obtained and [10] and duplicated by us.

3. ORIENTATION OF THE TRANSITION DIPOLES

In order to determine the polarization of the transitions in the molecule, and also to compare the absorption intensity of a crystal and a solution, the integrated intensity (the area S under the curve) was determined for separate absorption bands and for the portion of the spectrum under consideration as a whole. The results of the calculations for the separate bands of the a and b components 20° are presented in table 1.

Table 1

Band No.	ν_0(cm^{-1})	S_b (cm^{-2})	S_a (cm^{-2})	$\frac{S_b}{S_a}$
1	25400	38.4	12	3.2
2	26800	115	32.4	3.5
3	28100	81	30	2.7
4	29700	59	27.5	2.1
	Σ . .	293	102	2.9

The scales on the axes of the curve were the following: 200 cm^{-1} per cm along the horizontal and 0.01 of the absorption coefficient κ per cm along the vertical. It is seen from table 1 that the polarization ratio $\frac{S_b}{S_a}$, which equals 3.2 and 3.5 for the first two bands, respectively, diminishes as the transition is made to higher frequencies. As is shown in the work of Craig and Hobbins [3], the polarization ratio should remain constant for all electronic-vibrational bands in the absence of substantial splitting in both components of the spectrum.

The change observed in this ratio can indicate that we do not deal with just one electronic transition. We will return to this question later.

As the temperature rises to room temperature, not only the heights of the maxima but also the polarization ratio change for the separate bands. Values of S in the same units and the polarization ratio for 290° are presented in table 2.

Table 2

Band No.	$\nu_o=(cm^{-1})$	S_b (cm^{-2})	S_a (cm^{-2})	$\frac{S_b}{S_a}$
1	25500	37.4	6.8	5.5
2	26900	124	23	5.4
3	28200	89	25	3.6
4	29700	46	18.6	2.5
	Σ . .	296	73	4

It follows therefrom that the total absorption intensity drops somewhat at room temperature because of the a component. Moreover, the polarization ratio increases substantially for the initial bands, especially the first. A comparison of the total absorption spectrum intensities of a crystal and a solution [5] shows reasonable agreement.

The polarization ratio in combination with the "oriented gas model" ** permits a conclusion to be drawn on the direction of the electric transition moment in a molecule. On the other hand, the transition polarization and its intensity can be determined qualitatively on the basis of computations by means of the so-called "polarization diagram" and use of the molecule structure [5]. The "polarization diagram" for the lowest electronic transitions under consideration here yields two possible variations of the distribution of the electronic density of the π-electrons in the molecule when zeroes, or maximuma and minima of the electronic density coincide with the carbon atoms (see fig. 1, 2). The plus and minus charges arranged around the perimeter of the molecule at the maxima and minima of the electronic density, respectively, form elementary dipoles. Their vector sum also defines the orientation of the electronoptic transition and its intensity, qualitatively. The orientations thus obtained of the first electronic transitions in the molecule of 1,2-benzanthracene are shown diagrammatically on figure 1, 2 by heavy arrows. The designations of the levels are according to Platt [5]. As is seen, one of the transitions (^1L_b) is oriented along the molecule y axis and the other (^1L_a) makes a 60° angle therewith. According to the "polarization diagram", the ^1L_a transition is hardly responsive to a change in the molecule configuration because of deformation. The intensity of the ^1L_b transition in the ideal molecule case, i. e., when all the C-C bonds and valence angles are equal, would be zero. Since the molecule is somewhat deformed in a crystal [6], the probability of this transition is not zero, wherein not only the transition intensity but also the transition orientation changes as the deformation changes. Hence the "polarization diagram" permits the hypothesis that the absorption intensity at the ^1L_b level must be larger for a crystal, where the molecule can be deformed substantially, than for a solution, where this deformation is considerably less, while the absorption intensity at the ^1L_a level should not alter substantially. A comparison of the absorption spectra of a frozen solution and a crystal actually shows a change in the absorption intensity which is sharpest for the first band. Consequently, a transition at the ^1L_b band can be attributed thereto. At the same time, the observed high intensity of the electronic-vibrational bands of this level as compared with a purely electronic transition is clarified since the molecule vibrations lead to magnification of its deformation.

An analysis of the polarization ratio can also assist in the clarification of the question of the identification of bands observed in absorption spectra. The ratio can be determined theoretically by knowing the direction of the transition in the molecule and its location in the crystalline lattice. Thus, the values 6 and 2 have been obtained for ^1L_b and ^1L_a, respectively. As is seen from the table, the ratio obtained experimentally for the first band is 5.5 at room temperature and 3.2 at the hydrogen temperature. Comparing these values with those computed, a transition at the ^1L_b level can be assigned to the first band, which agrees with the assumption expressed above on the basis of comparing the intensities of the crystal and solution absorption spectra. The decrease in the polarization ratio observed experimentally for the higher spectrum frequencies apparently indicates that bands of the ^1L_a transition with a polarization ratio of 2 are superposed on the electronic-vibrational series of the ^1L_b transition. As regards the change in the polarization of the initial bands of the spectrum upon passage from 290 to 20°, it can be explained by the supplementary temperature deformation of the molecule in the crystal. A different mutual perturbation near the arranged ^1L_b and ^1L_a levels could lead to the same result [3]. It is seen from the spectrum of the solution that the band of the hypothesized second transition ^1L_a is significantly more intense than the bands of the first transition ^1L_b. A reverse situation occurs in a crystal, which is explained not only by the magnification of the intensities of the ^1L_b transition because of the molecule deformation, as has been remarked earlier, but also by a certain redistribution of the intensities of the ^1L_b and ^1L_a transitions which is related to the mutual perturbation of the appropriate levels in the crystal.

The question of the beginning of the second electronic transition cannot possibly be considered finally resolved. In [10] it is attributed to two possible beginnings, which corresponds to the 27160 cm^{-1} or the 25730 cm^{-1} bands in crystal. Information on the crystal luminescence aids in

**As is known [3], this model can be used for molecular crystals when no Davydov splitting is observed in the absorption spectra. The 1,2-benzanthracene crystal satisfies such a condition.

solving this question, to a considerable extent. In the luminescence spectrum at 20° which we obtained, there is an additional maximum at 24700 cm^{-1} in the initial band, in addition to the fundamental 25030 cm^{-1} maximum corresponding to a maximum in absorption in the first electronic transition at 25400 cm^{-1}, but at a distance of approximately 330 cm^{-1} away. It corresponds to a 25730 cm^{-1} maximum in the absorption spectrum. Hence, the 25730 cm^{-1} band does not correspond to a transition in the second excited electronic level but is a vibrational frequency of the first level.

Thus, on the basis of the experimental material explained above and by using certain theoretical considerations, a conclusion can be drawn on the presence of bands of two electronic transitions in the region studied of the absorption spectrum of a 1, 2-benzanthracene crystal and their orientation in the molecule can be determined, where the beginning of the second transition most probably corresponds to the frequency 27160 cm-1.

In conclusion, the authors are grateful to A. F. Prikhot'ko for useful discussions.

May 12, 1958

References

1. V. L. BROUDE, V. S. MEDVEDEV, A. F. PRIKHOT'KO: ZETF, 21, 665 (1951)
2. A. F. PRIKHOT'KO: ZETF, 19, 383, 487 (1949)
3. D. P. CRAIG, P. C. HOBBINS: J. Chem. Soc. 539, 2302, 2309 (1955)
M. S. BRODIN, A. F. PRIKHOT'KO: OiS, 2, 448 (1957)
4. D. S. MC CLURE: J. Chem. Phys., 25, 481 (1956)
5. J. R. PLATT: J. Chem. Phys., 17, 470 (1949)
H. B. KLEVENS, J. R. PLATT: J. Chem. Phys., 17, 470 (1949)
6. P. H. FRIEDLANDER, D. SAYRE: Nature, 178, 999 (1956)
7. V. M. AGRANOVICH: OiS, 1(3), 338-347 (1956) (See LC 59-15176; mi $2.40; ph $3.30)
8. V. L. BROUDE, O. S. PAKHOMOVA, A. F. A. F. PRIKHOT'KO: OiS, 2(3), 323-329 (1957) (See ATS RJ-1162 , 8 pp.)
9. J. IBALL: Z. Kristall., 99, 230 (1938)
10. C. SANDORFY, R. N. JONES: Canad. J. Chem., 34, 888 (1956)

TOM VI, Vyp. 5
VOL. VI, No. 5

OPTIKA I SPEKTROSKOPIIA
OPTICS AND SPECTROSCOPY

Mai, 1959
May, 1959

Quantitative Investigations of the Infrared Absorption and Dispersion of Chloroform

M. P. LISITSA AND IU. P. TSIASHCHENKO

Abstract: Absorption coefficients of liquid $CHCl_3$ were measured in the region of 470-11500 cm^{-1}. The integral absorption and half-width were calculated for the fundamental vibrations of some combination frequencies and overtones. The identification of vibrational frequencies was carried out in the interval 250-16500 cm^{-1}. A dispersion curve was obtained within the most intense band corresponding to the fundamental vibration ν_5 and its neighborhood (460-840 cm^{-1}).

INTRODUCTION

To this day there is no full and systematic information in the literature concerning the infrared spectra of $CHCl_3$ and the interpretation of its absorption bands. Particularly few quantitative measurements have been made. The authors of previous papers have limited themselves in most cases to the study of transmission of liquid $CHCl_3$ in the near infrared [1-9] and photographic [10-12] spectral regions without attempting a full identification of the observed bands. Only in [13-15] was the spectrum studied in the region containing the fundamental vibrations. However the authors of these papers did not succeed in clarifying all details. Even in the comparatively complete paper [15] many of the bands are not mentioned, a circumstance which apparently arises from failure to study this liquid in layers of sufficient thickness.

All cited measurements evaluated the intensity of absorption bands qualitatively. Only in [9,16-18] are quantitative data given; in [9, 18] they are obtained only for the overtones of the C-H stretching vibration of chloroform in solution. In [16,17] the peak intensity for the same vibration was determined.

The dispersion of chloroform has been studied to an even smaller extent; only two papers [19, 20], to our knowledge, are devoted to this matter. Both deal with regions of comparatively weak absorption, and the data of the second paper are not distinguished by particularly high accuracy.

The present paper is undertaken with the intention of obtaining complete vibrational data on the absorption of liquid $CHCl_3$, and also to bring them into systematic correspondence with information found in the literature.

METHOD AND EXPERIMENTAL ACCURACY

All measurements were performed on an IKS-6 infrared spectrometer. The positions of absorption maxima were determined with different accuracies in different spectral regions, as can be judged from the data in table 1.

Absorption coefficients K were calculated according to the familiar formula

$$(1) \qquad \frac{I_1}{I_2} = \exp\left[-K(d_1 - d_2)\right]$$

in which I_1 and I_2 designate the intensity of radiation emerging from liquid layers of thicknesses d_1 and d_2, respectively.

Table 1

Accuracy of determination of the position of absorption maxima.

Spectral interval (in cm^{-1})	480 to 650	650 to 950	950 to 1800	1800 to 2300	2300 to 3900	4000 to 10000
Error (in cm^{-1})	0.3 to 0.5	0.5 to 1.5	1.5 to 3	1 to 2	2 to 5	20 to 50

The use of two cells instead of one diminishes to a considerable degree the errors which arise from the presence of multiple reflection at the boundaries between the liquid and the surface of the cell window. However, for their full calculation it is necessary to make use of a more complex relation obtained by various authors for interference [21,22] as well as for thick layers [23]. The absence of a complex vibrational structure * of the absorption bands of $CHCl_3$ has allowed us to use the conventional formula (1) for the investigation of regions of weak absorption. For the region of very intense absorption (where the influence of multiple reflection grows considerably, and which can be investigated only in liquid layers whose thickness is comparable to the wavelength of the incident radiation) estimates were made of the errors which arise from the use of (1). The following exact formula was used [21,22]

$$(2) \qquad \frac{I_1}{I_2}\cdot\frac{1+R^2\exp[-2Kd_1]-2R\exp[-Kd_1]\cos 2(\alpha_1+\gamma)}{1+R^2\exp[-2Kd_2]-2R\exp[-Kd_2]\cos 2(\alpha_2+\gamma)} = \exp[-K(d_1-d_2)]$$

$$R = \frac{(n-n_1)^2+\kappa^2}{(n+n_1)^2+\kappa^2}, \quad \tan\gamma = \frac{2n_1\kappa}{n^2-n^2+\kappa^2}, \quad \alpha_i = \frac{2\pi n d_i}{\lambda}, \quad \kappa = \frac{K\lambda}{4\pi},$$

n and κ are the optical constants of the layer examined, n_1 is the refractive index of the material of the cell windows.

The results showed that the error introduced by using (1) for the calculation of K at the maximum of the most intense band ν_5, does not exceed 8-10%

* As was shown in [23], the application of the usual formula (1) for the calculation of such a structure can lead not only to quantitative errors, but also to a qualitative distortion of the absorption curve.

and is negligible for all other bands. The experimental error in the determination of K at the maximum by methods described earlier [24] reaches 15-20% for the band mentioned, so that the use of (1) proves to be permissible.

The thickness of the cells was always selected to give conditions under which the best accuracy was obtained in the determination of the optical density [25]. They varied between 5.6 μ and 10 cm. The thinnest spacers (5.6-50 μ) were prepared by dusting a layer of Selenium over a carefully polished sodium chloride cell window. The measurements of the thickness* of the cells were carried out with an error not exceeding 1%. Therefore, the accuracy of the measurements was mainly limited to reproducibility of spectral records. In the overwhelming majority of cases (excluding the vibration ν_5) K and $\int K_\nu d\nu$ are given with an error of 6-10%.

For the measurement of the $CHCl_3$ dispersion within the absorption band ν_5 a special reflection method was devised [26], eliminating the influence of vapor, since its absorption considerably distorts the result obtained during measurements of the reflection coefficient at a free surface of a volatile liquid. In the neighborhood of the ν_5 band the index of refraction was determined by improved interference methods [26]. The error in the measurement of n does not exceed 12-15% within the band, and 5-8% in its neighborhood.

THE ABSORPTION SPECTRUM OF CHLOROFORM

The absorption curves of liquid $CHCl_3$ are given in figures 1 - 7. The vibration frequencies, their interpretation, their symmetry, the absorption coefficients at the maxima, the integrated absorption and the halfwidth are given in table 2. For comparison [2,3,5,6,10-15] frequencies measured by other authors are listed as well. The other data are not contained in the cited papers; the identification of certain maxima, given in part in [2,5,11,13,15, 16], agrees almost with ours, which represents an attempt to give a most comprehensive interpretation of the infrared spectrum of chloroform.

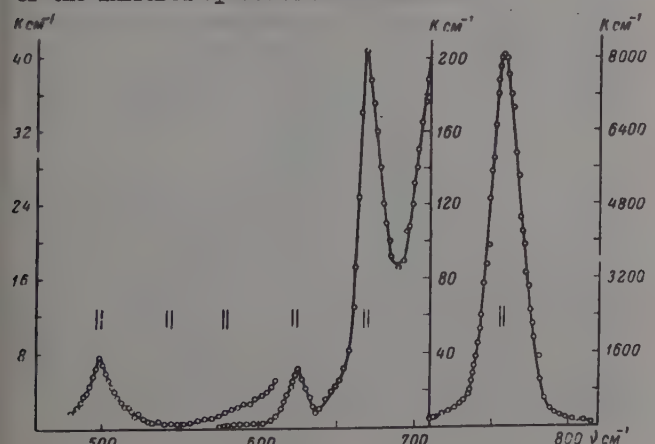

Figure 1. Absorption of Chloroform in the region 475-820 cm^{-1}

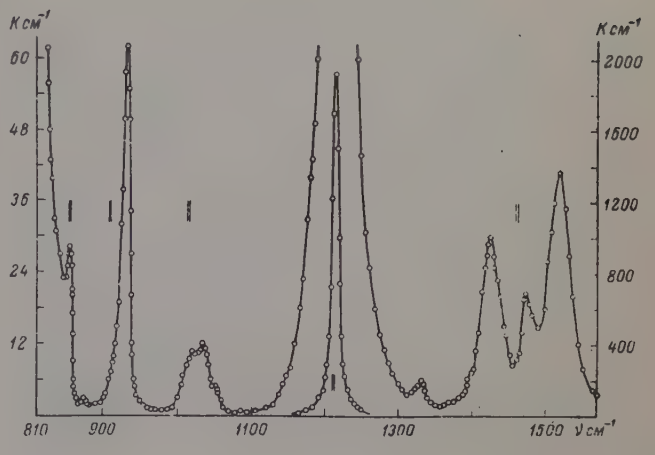

Figure 2. Absorption of Chloroform in the region 810 - 1560 cm^{-1}.

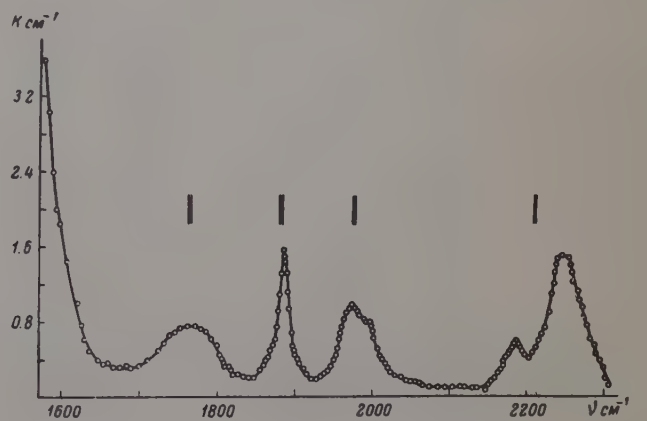

Figure 3. Absorption of Chloroform in the region 1560 - 2300 cm^{-1}.

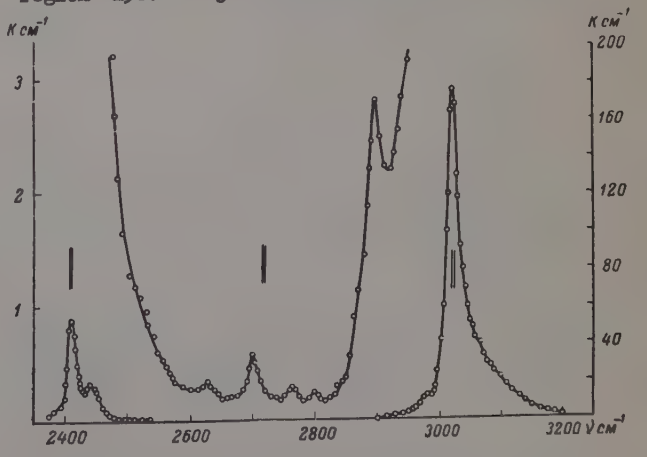

Figure 4. Absorption of Chloroform in the region 2375 - 3200 cm^{-1}.

* The cell thicknesses of 5.6 to 400μ were measured by an interference method.

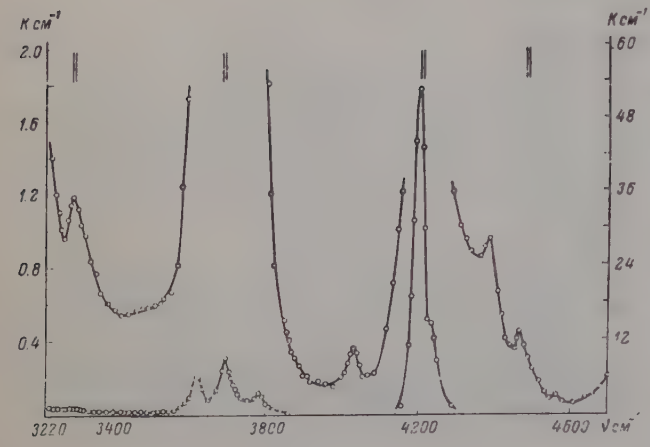

Figure 5. Absorption of Chloroform in the region 3220 - 4700 cm^{-1}.

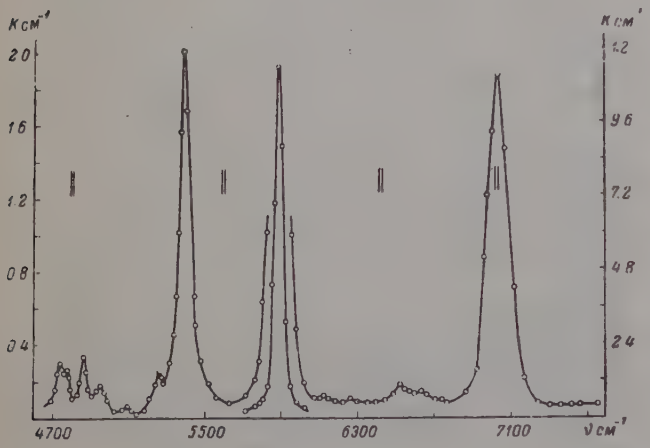

Figure 6. Absorption of Chloroform in the region 4700 - 7550 cm-1.

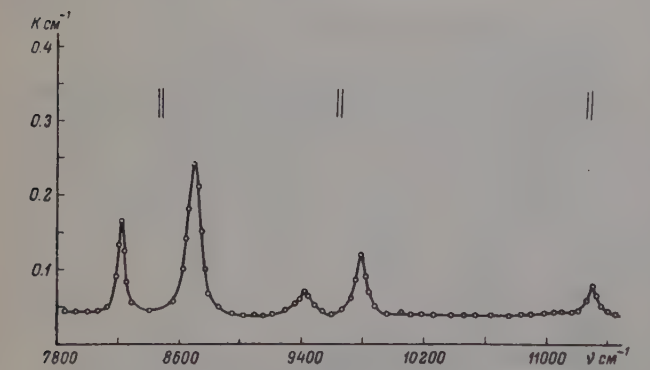

Figure 7. Absorption of Chloroform in the region 7800 - 11450 cm-1.

As a basis for identification we used the conventional model of the molecule $CHCl_3$ belonging to symmetry group C_{3v}. The six fundamental vibration frequencies of this molecule used for the calculation of overtones and combinational tones and for comparison with observed frequencies, were taken from Raman spectra [28], where they have been determined most precisely. Inasmuch as all the fundamental frequencies and all overtones are permitted by the selection rules [27, 28] in the infrared spectrum of $CHCl_3$, we failed to find a unique interpretation for some bands. For these all the most reliable references are found in square brackets in table 2. One must note that in calculating frequencies of the type $N\nu_i + \nu_k$ and $(N\nu_i + \nu_k) + \nu_j$ the frequencies $N\nu_i$ and $N\nu_i + \nu_k$ were taken from experimental data of the present work and the works of other authors: from [5] where they are given with an error of 5-10 cm^{-1}, for $2\nu_1$, $3\nu_1$, $3\nu_1 + \nu_4$, $2\nu_1 + \nu_4$ and from [11] for $4\nu_1$ and $5\nu_1$.

As seen from figure 2, the overwhelming majority of bands are identified satisfactorily and particularlarly in the region 470-4000 cm^{-1}, where we obtained many for the first time. The calculated and the experimentally found frequencies do not quite coincide in the glass prism region, however in the majority of cases they do not fall outside the experimental error. Some observed absorption maxima could not be interpreted according to conventional rules.

These include some maxima in the visible region and some shortwave satellites of intense vibrations arising from the C-H bond (the corresponding frequencies being 2442, 3066, 4240 cm-1): these are the first overtone of bending vibration ν_4, the stretching vibration ν_1 and the combination tone $\nu_1 + \nu_4$. The nature of these satellites probably can be explained to a certain degree by an investigation of the absorption of chloroform in other states of aggregation.

The integral absorption $\int K_\nu d\nu$ and the half-width were calculated for all isolated bands and those which split uniquely into symmetrical components. In some cases the integral absorption was determined for bands which do not split into fully resolved components* . In calculations in the region 5000-10000 cm^{-1} the background, averaging 0.05 cm^{-1}, was not taken into consideration.

The spectrum shown in figures 1-7 and the data given in table 2 show that the degenerate vibration of the C-Cl bond, corresponding to the frequency ν_5, is most intense. The integral absorption of the fully symmetric vibration ν_1, measured together with the shortwave component, is much smaller (in the first and second order) than the integral absorption of the vibrations ν_5 and ν_4. This can be explained by the fact that the C-H bond has basically a homopolar character, while the C-Cl bond is much nearer to ionic.

*The corresponding frequencies are combined in table 2 in brackets.

Table 2

Data of the Present Study						Data of other Authors									
Interpretation	Symmetry	Frequ. calc. (cm^{-1})	Frequ. exper. (cm^{-1})	K (max.) (cm^{-1})	$\int K(\nu)d\nu$ (cm^{-2})	Γ (cm^{-1})	[15]	[14]	[13]	[6]	[3]	[2,10]	[8]	[5]	[12]	[11]
—	—	—	—	—	—	—	—	230	—	—	—	—	—	—	—	—
ν_6	E	262.0	—	—	—	—	—	260	—	—	—	—	—	—	—	—
$\nu_2 - \nu_3$	A_1	302	—	—	—	—	—	303	—	—	—	—	—	—	—	—
ν_3	A_1	365.9	—	—	—	—	370	364	—	—	—	—	—	—	—	—
$\nu_2 - \nu_6$	E	406	—	—	—	—	392	—	—	—	—	—	—	—	—	—
$\nu_5 - \nu_6$	$A_1 + A_2 + E$	499	498	7.5	190	20	488	488	—	—	—	—	—	—	—	—
$\nu_6 + \nu_3$	E	628	625	33	580	16	629	—	625	—	—	—	—	—	—	—
ν_2	A_1	668.3	668	190	3 600	12	667	—	667	—	—	—	—	—	—	—
ν_5	E	761.2	759	8 000	222 000	24	755	—	760	—	—	—	—	—	—	—
$\nu_4 - \nu_3$	E	850	851	28	—	—	849	—	—	—	—	—	—	—	—	—
$\nu_5 + \nu_3 - \nu_6$	$A_1 + A_2 + E$	865	874	2.5	—	—	—	—	—	—	—	—	—	—	—	—
$\nu_6 + \nu_2$	E	930	928	62	1 000	13	929	—	924	—	—	—	—	—	—	—
$\nu_6 + \nu_5$	$A_1 + A_2 + E$	1023	1 020	10	} 540	—	—	—	—	—	—	—	—	—	—	—
$\nu_3 + \nu_2$	A_1	1034	1 032	12		—	1 031	—	1 024	—	—	—	—	—	—	—
$\nu_5 + \nu_2 - \nu_3$	E	1063	1 051	5		—	1 049	—	—	—	—	—	—	—	—	—
$\nu_5 + \nu_3$	E	1123	—	—	—	—	1 145	—	—	—	—	—	—	—	—	—
ν_4	E	1215.6	1 213	1 800	27 000	9.5	1 214	—	1 205	—	—	—	—	—	—	—
$2\nu_2$	A_1	1337	1 332	6.0	160	16	1 333	—	—	—	—	—	—	—	—	—
$\nu_6 + \nu_5 + \nu_3$	$A_1 + A_2 + E$	1389	1 394	6.0	—	—	1 393	—	—	—	—	—	—	—	—	—
$\nu_2 + \nu_5$	E	1429	1 425	30	1 200	31	1 420	—	—	—	—	—	—	—	—	—
$\nu_4 + \nu_6$	$A_1 + A_2 + E$	1476	1 473	20 (14) *	260	14	—	—	—	—	—	—	—	—	—	—
$2\nu_5$	$A_1 + E$	1522	1 520	41	1 900	34	1 524	—	—	—	—	—	—	—	—	—
$2\nu_5 + \nu_6$	$A_1 + A_2 + 2E$	1782	1 770	0.75	71	87	—	—	—	—	—	—	—	—	—	—
$\nu_4 + \nu_2$	E	1884	} 1 884	1.5	39	17	—	—	—	—	—	—	—	—	—	—
$2\nu_5 + \nu_3$	$A_1 + E$	1886					—	—	—	—	—	—	—	—	—	—
$\nu_5 + \nu_4$	$A_1 + A_2 + E$	1977	1 976	1.0	} 61	—	—	—	—	—	—	—	—	—	—	—
$3\nu_3$	A_1	2005	} 1 995	0.80		—	—	—	—	—	—	—	—	—	—	—
$\nu_1 - \nu_5 - \nu_6$	$A_1 + A_2 + E$	1996				—	—	—	—	—	—	—	—	—	—	—
$2\nu_5 + \nu_2$	$A_1 + E$	2188	2 187	0.60	28	36	—	—	—	—	—	—	—	—	—	—
$\nu_1 - \nu_5$	E	2 258				—	—	—	—	—	—	—	—	—	—	—
$3\nu_5$	$A_1 + A_2 + E$	2 283	} 2 250	1.5	83	50	—	—	—	—	—	—	—	—	—	—
$\nu_3 + \nu_2 + \nu_4$	E	2 250				—	—	—	—	—	—	—	—	—	—	—
$2\nu_4$	$A_1 + E$	2 431	2 410	58	1 300	15	2 410	—	—	—	—	—	—	—	—	—
?		—	2 442	19 (15) *	450	25	—	—	—	—	—	—	—	—	—	—
$\nu_1 - \nu_3$	A_1	2 653	} 2 630	0.32	—	—	—	—	—	—	—	—	—	—	—	—
$\nu_2 + \nu_5 + \nu_4$	$A_1 + A_2 + E$	2 645			—	—	—	—	—	—	—	—	—	—	—	—
$2\nu_4 + \nu_6$	$A_1 + A_2 + 2E$	2 672	} 2 698	0.56	—	—	—	—	—	—	—	—	—	—	—	—
$\nu_1 + \nu_3 - \nu_2$	A_1	2 717			—	—	—	—	—	—	—	—	—	—	—	—
$\nu_1 - \nu_6$	E	2 757	2 763	0.28	—	—	—	—	—	—	—	—	—	—	—	—
$2\nu_4 + \nu_3$	$A_1 + E$	2 776	2 795	0.21	—	—	—	—	—	—	—	—	—	—	—	—
$\nu_1 + \nu_6 - \nu_3$	E	2 915	2 896	3.0	—	—	—	—	—	—	—	—	—	—	—	—
$4\nu_5$	$A_1 + 2E$	3 044	2 980	12.0	—	—	—	—	—	—	—	—	—	—	—	—
ν_1	A_1	3 019	3 019	170	} 8 100	24	3 040	—	—	3 044	—	—	—	—	—	—
?		—	3 066	41		—	—	—	—	—	—	—	—	—	—	—
$\nu_1 + \nu_6$	E	3 281	3 287	1.2	—	—	—	—	—	—	—	—	—	—	—	—
$3\nu_4$	$A_1 + A_2 + E$	3 647	} 3 620	6.6	280	31	3 597	—	—	—	—	—	—	—	—	—
$\nu_1 + \nu_3 + \nu_6$	E	3 647				—	—	—	—	—	—	—	—	—	—	—
$\nu_1 + \nu_2$	A_1	3 687	3 697	9.0	440	37	3 663	—	—	3 846	3 877	—	—	—	—	—
$\nu_1 + \nu_5$	E	3 780	3 785	3.2	170	44	—	—	—	—	3 986	—	—	—	—	—
$\nu_1 + \nu_5 + \nu_6$	$A_1 + A_2 + E$	4 042	4 035	0.35	—	—	—	—	—	—	—	—	—	—	—	—
$\nu_1 + \nu_4$	E	4 234	4 205	53	2 000	33	4 202	—	—	4 484	4 294	4125	4 227	4211	—	—
?		—	4 240	16 (7.5) *	190	23	—	—	—	—	—	—	—	4 250	—	—
?		—	4 391	0.94	—	—	—	—	—	—	—	—	—	—	—	—
$(\nu_1 + \nu_4) + \nu_6$	$A_1 + A_2 + E$	4 496	4 465	0.43	—	—	—	—	—	—	—	—	4 468	4 476	—	—
$(\nu_1 + \nu_4) + \nu_3$	E	4 600	4 565	0.09	—	—	—	—	—	—	4 570	—	4 573	4 538	—	—
?		—	4 735	0.30	—	—	—	—	—	—	—	4 750	4 735	4 742	—	—
$4\nu_4$	$A_1 + 2E$	4 862	4 770	0.26	—	—	—	—	—	—	—	—	—	4 775	—	—
$(\nu_1 + \nu_4) + \nu_2$	E	4 902	4 863	0.32	—	—	—	—	—	—	4 855	4 870	4 869	4 873	—	—
$(\nu_1 + \nu_4) + \nu_5$	$A_1 + A_2 + E$	4 995	4 956	0.18	—	—	—	—	—	—	4 978	—	4 980	—	—	—
?		—	5 095	0.05	—	—	—	—	—	—	5 102	—	—	—	—	—
$2\nu_1 - \nu_2$	A_1	5 230	5 260	0.24	—	—	—	—	—	—	5 435	5 236	5 280	—	—	—
$(\nu_1 + \nu_4) + \nu_4$	$A_1 + A_2 + E$	5 425	5 381	2.0	210	74	—	—	—	5 587	5 556	5 440	5 382	5 376	—	—
$2\nu_1$	A_1	6 038	5 889	11.5	840	63	—	—	—	5 989	5 883	5 890	5 921	5 900	—	—
$2\nu_1 + \nu_6$	E	6 162	6 121	0.12	—	—	—	—	—	—	—	—	—	6 160	—	—
$2\nu_1 + \nu_3$	A_1	6 266	6 265	0.10	—	—	—	—	—	—	—	—	—	6 266	—	—
$2\nu_1 + \nu_2$	A_1	6 568	6 525	0.19	—	—	—	—	—	—	6 494	—	6 557	6 530	—	—
$2\nu_1 + \nu_5$	E	6 661	6 635	0.14	—	—	—	—	—	—	—	—	6 670	6 660	—	—
$2\nu_1 + \nu_4$	E	7 115	7 050	1.8	240	118	—	—	—	6 993	7 143	6 900	7 080	7 087	—	—
$(2\nu_1 + \nu_4) + \nu_3$	E	7 453	—	—	—	—	—	—	—	—	—	—	—	7 436	—	—
?		—	—	—	—	—	—	—	—	—	—	—	—	7 610	—	—
$(2\nu_1 + \nu_4) + \nu_5$	$A_1 + A_2 + E$	7 848	—	—	—	—	—	—	—	—	—	—	—	7 825	—	—
$(2\nu_1 + \nu_4) + \nu_4$	$A_1 + A_2 + E$	8 302	8 220	0.16	8	80	—	—	—	—	8 130	—	8 240	8 220	—	—
$3\nu_1$	A_1	9 057	8 670	0.24	22	104	—	—	—	8 404	8 696	8 690	8 703	8 665	—	—
$3\nu_1 + \nu_3$	A_1	9 036	—	—	—	—	—	—	—	—	—	—	—	9 049	9 049	—
$3\nu_1 + \nu_2$	A_1	9 338	9 420	—	—	—	—	—	—	—	9 346	—	9 381	9 376	9 376	—
$(3\nu_1 + \nu_2) + \nu_6$	E	9 640	—	—	—	—	—	—	—	—	—	—	—	9 645	9 658	—
$3\nu_1 + \nu_4$	E	9 885	9 790	0.12	6	88	—	—	—	9 707	—	9 780	9 850	9 830	9 840	—
$(3\nu_1 + \nu_4) + \nu_6$	$A_1 + A_2 + E$	10 100	—	—	—	—	—	—	—	—	—	—	—	—	10 115	—
?		—	—	—	—	—	—	—	—	—	10 417	—	10 357	—	—	—
$(3\nu_1 + \nu_4) + \nu_4$	$A_1 + A_2 + E$	11 045	11 035	0.08	5	72	—	—	—	11 235	—	11 040	10 990	—	—	—
$4\nu_1$	A_1	12 076	11 330	—	—	—	—	—	—	—	11 494	—	11 334	—	—	11 315
$4\nu_1 + \nu_5$	E	12 076	—	—	—	—	—	—	—	—	—	—	—	—	—	12 075
$4\nu_1 + \nu_4$	E	12 530	—	—	—	—	—	—	—	—	—	—	—	—	—	12 470
$5\nu_1$	A_1	15 095	—	—	—	—	—	—	—	—	—	13 870	—	—	—	13 860
$5\nu_1 + \nu_2$	A_1	14 528	—	—	—	—	—	—	—	—	—	14 490	—	—	—	—
$5\nu_1 + \nu_4$	E	15 075	—	—	—	—	—	—	—	—	—	15 040	—	—	—	—
$6\nu_1 - \nu_6$	E	16 025	—	—	—	—	—	—	—	—	—	16 077	—	—	—	—
$6\nu_1$	A_1	18 114	—	—	—	—	—	—	—	—	—	16 287	—	—	—	—

*In brackets (column K) are given values for K obtained after the division of overlapping bands.

THE DISPERSION OF CHLOROFORM IN THE REGION ν_5

Figure 8 shows the dispersion curve of $CHCl_3$ in the absorption region corresponding to the vibration ν_5, together with the curve of the refractive index κ ($\kappa = K/4\pi\nu$). The data obtained by the reflection method are marked with triangles, and those by the interference method by dark circles. The light circles represent the values of n obtained by the prism method [19]. Since the sensitivity of the reflection method is not sufficiently high in the regions of weak reflection, the behavior of the dispersion curve at the minimum could not be clarified and was here extrapolated with dotted lines. Even so, one can conclude that this curve shows considerable asymmetry. A similar asymmetry is observed for water close to $\lambda = 3\mu$ [29], for $CHCl_3$ and $CHCBr_3$ in the region of the fundamental vibration ν_4 [19], and for CCl_4 in the region of fundamental vibration ν_3 [26], i. e. practically in all well known cases (except for [30]) in which the abnormal dispersion of pure liquids was measured within infrared absorption bands.

It is worthwhile to mention the fact -- unusual from the viewpoint of the classic theory (developed, it is true, for gases) -- that the absorption maximum is shifted to the longwave side, beyond the maximum dispersion curve.

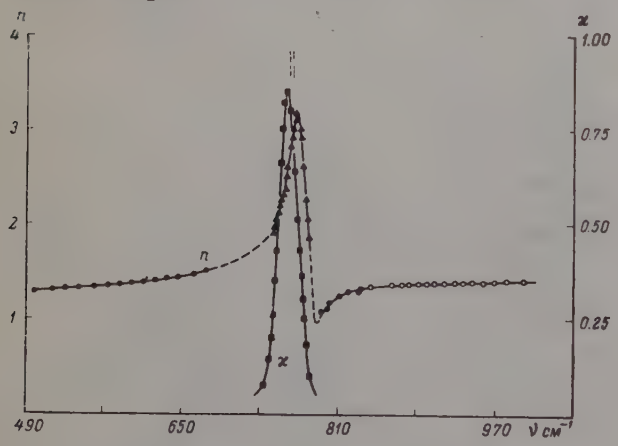

Figure 8. Dispersion of Chloroform in the region of the fundamental vibration ν_5.

In our case, the position of the latter coincides with a maximum in the reflectivity of the compound. A similar shift is also observed for dihalogenomethanes within the relatively weak fundamental bands [30] and also for CCl_4 in the region of the fundamental vibration ν_3.

May 8, 1958

References

1. C. SCHAEFER, F. MATOSSI: Das ultrarote Spektrum. Berlin, Springer, 1930 (ONTI, Leningrad-Moscow, 1935)
2. J. W. ELLIS: Phys. Rev., 23, 48 (1924)
3. C. CORIN: C.R., 202, 747 (1936)
4. C. CORIN: J. Chim. Phys., 32, 241 (1935)
5. YEOU TA: C.R., 206, 1371 (1938)
6. A. MAIONE: N. Cimento, 14, 361 (1937)
7. A. CARELLI, P. TULIPANO: N. Cimento, 15, 1 (1938)
8. R. MECKE, F. OSWALD: Zs. f. Phys., 130, 445 (1951)
9. H. KEMPTER, R. MECKE: Zs. f. Naturf., 2A 549 (1947)
10. J. W. ELLIS: Phys. Rev., 32, 906 (1928)
11. K. RUMPF, R. MECKE: Zs. f. phys. Chem., 44B, 299 (1939)
12. R. FREYMAN, A. NAHERNIAC: J. Phys. Rad., 5, 75 (1934)
13. G. EMSCHWILLER, J. LECOMTE: J. Phys. Rad., 8, 130 (1937)
14. P. BARSCHEWITZ, M. PARODI: J. Phys. Rad., 10, 143 (1939)
15. E. K. PLYLER, W. S. BENEDICT: J. Res. Nat. Bur. Stand., 47, 202 (1951)
16. V. M. CHULANOVSKII, M. P. BURGOVA: OiS, 2, 330 (1957)
17. U. LIDDEL, E. D. BECKER: J. Chem. Phys., 25, 173 (1956)
18. B. TIMM, R. MECKE: Zs. f. Phys., 98, 363 (1936)
19. M. A. PITTMAN: JOSA, 29, 358 (1939)
20. J. VINCENT-GEISSE, J. LECOMTE: C.R., 244, 577 (1957)
21. M. P. LISITSA: DAN USSR, 111, No. 4, 806 (1956)
22. M. YASUMI: Bull. Chem. Soc. Japan, 28, 489 - 492 (1955)
23. M. CZERNY: Zs. f. Phys., 65, 600 (1930)
24. M. P. LISITSA, V. N. MALINKO: PiTE, No. 3, 52 - 54 (1957)
25. V. M. CHULANOVSKII, N. P. PENKIN: IAN USSR, SF, 9, 206 (1945)
26. M. P. LISITSA, IU. P. TSIASHCHENKO: PiTE (In press)
27. M. V. VOL'KENSHTEIN, M. A. EL'IASHEVICH, B. I. STEPANOV: Kolebaniia molekul (Vibrations of molecules) 2. GITTL, Moscow-Leningrad, 1949
28. G. HERTZBERG: Vibrational and rotational spectra of polyatomic molecules. IL, Moscow, 1949
29. H. RUBENS, E. LADENBURG: Ber. physik. Gesell., No. 1, 16-27 (1909)
30. A. I. MAHAN: JOSA, 31, 248 (1941)

TOM VI, Vyp. 5 OPTIKA I SPEKTROSKOPIIA Mai, 1959
VOL. VI, No. 5 OPTICS AND SPECTROSCOPY May, 1959

Acoustic Birefringence of Phenylethyl Alchohol at Low Temperatures

V. E. ESKIN AND I. A. BARANOVSKAIA

Abstract: The viscosity and acoustic birefringence of phenylethyl alcohol were measured at temperatures from -30° to -40° C. The orientational relaxation time was determined for the molecules of this substance. The relaxation time is in agreement with that calculated from data on streaming birefringence and depolarization of scattered light.

In several publications [1-5] it has been shown that the measurement of birefringence of liquids in laminar flow (streaming birefringence) and in an ultrasonic field (acoustic birefringence) can be used for studying the process of molecular orientation in some liquids. The objects of investigation are limited to liquids with a considerable optical molecular anistropy and a relatively high viscosity. Therefore the investigations in the publications [1-5] covered mainly mineral and vegetable oils which were chemically not individual substances. Suitable subjects among chemically pure liquids are mainly those molecules which contain phenyl rings and which have consequently a high optical anistropy. However, the viscosity of such liquids is too low at normal temperatures and the magnitude of the acoustic birefringence remains beyond the limits of possible quantitative determination. Decreasing the temperature considerably makes it possible to increase the viscosity by a factor of several hundred and makes acoustic birefringence an accurately measurable quantity.

We have made the appropriate measurements on phenylethyl alcohol ($C_6H_5CH_2CH_2OH$) . Its viscosity was measured in the interval +20 to -37.5° with the falling ball method (Höppler Viscosimeter). In this temperature range it increases by a factor of 320 from 0.115 to 36.8 poise.

The acoustic birefringence was measured applying a method described earlier [3,5] at ultrasonic frequencies of 18.8 and 38.5 megacycles and at 5 different temperatures. In this method the measurable quantity in practice is the angle of rotation α of the analyzer of the polarimeter as a function of the voltage V supplied to the faces of the piezo-electric quartz plate.

We used gasoline as a working liquid to fill the large cell containing the piezo-electric quartz emitter and a small cell with a millimeter layer of the liquid being investigated. Butyl alcohol (supplied to the jacket of the large cell from a Höppler Thermostat) was employed as a thermostatic liquid. The large cell was enclosed on all sides by a centimeter layer of heat insulating material. To the outsides of two side walls were cemented pipes (70 mm long; 20 mm diameter), made from a plastic material with a very low heat conductivity, filled with calcium chloride. This prevented icing of the glass transmitting the light beam. The temperature was measured with a pentane thermometer inserted into the cell. The figure shows the dependence of the angle of analyzer rotation (a quantity directly proportional to the measured acoustic birefringence Δn) on the Voltage V applied to the quartz transducer for the temperature -37.5° .

The acoustic birefringence constant of the liquid K , in analogy to the streaming birefringence constant M , is defined [1, 5] as the ratio of the amplitude of birefringence Δn^* to the viscosity of the liquid η and the corresponding value g of the gradient of the ultrasonic wave velocity

$$K = \frac{\Delta n^*}{\eta g} . \qquad (1)$$

One can determine the gradient g by measuring the intensity of the ultrasound by any method, e. g. from pressure on a receiver [3, 5] . At low temperatures such a measurement is quite difficult. Therefore, we had to calculate g from the amplitude A of vibrations of the quartz, excited at the resonance frequency. One can calculate [6] the value of A from the relation

$$A = 6.4 \cdot 10^{-8} V \frac{m}{\pi}, \qquad (2)$$

where V is the voltage measured in absolute electrostatic units; m is the ratio of the acoustic resistances of the quartz and the medium in which it vibrates. (In our case m = 10)

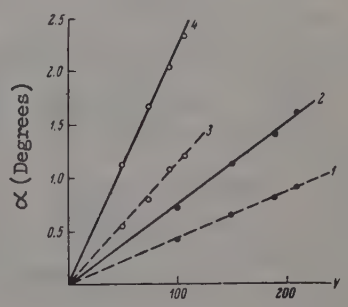

Dependence of the angle of analyzer rotation on the voltage supplied to the quartz transducer.

Frequency and temperature respectively : 1- 18.8 Mc, -29.5°; 2- 18.8 Mc, -37.5°; 3- 38.5 Mc, -29.5°; 4- 38.5 Mc, - 37.5° .

We know that

$$g = \frac{A\omega^2}{c}, \qquad (3)$$

where c is the sound velocity in the liquid in which the ultrasonic wave is propagated.

The birefringence Δn, when measured with a polarimeter, is calculated from the formula

$$\Delta n = \frac{\lambda \alpha}{\pi l}, \qquad (4)$$

where λ is the wave length of the light wave (in our case λ = 5500 Å); l is the path length of the light in the ultrasonic field (l = 1.6 cm) . The amplitude of birefringence Δn^* exceeds by a factor of 2-1/2 the measured value Δn averaged over time.

Thus one can calculate K from the relation

is given here in radians, V in electrostatic units.

$$(5) \qquad K \equiv \frac{\Delta n}{\eta g}^{*} = \frac{2}{6.4} 10^{8} \frac{c\lambda}{2\omega^{2}\eta m} \cdot \frac{\alpha}{V} .$$

The results of the calculation of the birefringence constant for phenylethyl alcohol at different temperatures are shown in Table 1. The relaxation (lag) of the molecular orientation in phenylethyl alcohol shows up as a decrease of K with increasing ultrasonic frequency.

References [1-5] show that the relaxation time τ of the molecular orientation in the liquid can be calculated, if one knows the constants K and M of its acoustical and streaming birefringences, from the relation

$$(6) \qquad \tau = \frac{1}{\omega}\left(\frac{M}{K}^{2} - 1\right)^{\frac{1}{2}} .$$

The relaxation time which we calculated in this manner for phenylethyl alcohol is shown in Table 2. As M_{20° we took the value $1.22 \cdot 10^{-10}$ (measured in the polymer solutions laboratory of the Institute of Macromolecular Compounds of the Academy of Sciences of the U. S. S. R.)

Table 1

T (in °C)	η (in poise)	$\omega = 18.8$ megacycles	$\omega = 38.5$ megacycles
		$K \cdot 10^{12}$	
−29.5	16.0	50.6	31.2
−33.0	22.5	44.9	36.3
−34.0	25.2	42.8	37.2
−36.0	30.0	40.7	30.6
−37.5	36.8	38.1	27.8

Table 2

T(in °C)	η (in poise)	$\omega = 18.8$ megacycles	$\omega = 38.5$ megacycles
		$\tau \cdot 10^{7}$ sec.	
−29.5	16.0	1.5	1.2
−33.0	22.5	1.7	1.1
−34.0	25.2	1.8	1.0
−36.0	30.0	1.9	1.3
−37.5	36.8	2.1	1.4

Since the theory of streaming birefringence of pure liquids [7] leads to the relation $M\tau$ = const., we multiplied the value of M_{20° by a factor equal to 293/T.

As one can see from table 2, the values of τ obtained for different ultrasonic frequencies ω, are in agreement and increase slightly with decreasing temperature (increasing viscosity). However we did not observe a full correspondence of the variation of the orientational relaxation time τ and viscosity η, as was found in reference [4]. The reason for this is the high sensitivity of the vibration amplitude of the quartz to the tuning of the generator to the exact resonance frequency. The adjustment was done by visually observing the maximum of the acoustic birefringence. Therefore, the value of the velocity gradient g which we calculated with the aid of formulae (2) and (3) was approximate and too large. In order to estimate the error, applying the same method, we calculated τ for castor and vacuum oil taking the data on α (V) from reference [3] where τ had been determined by a much more exact method. It turned out that when the gradient g is calculated from the resonance amplitude of the quartz for viscous oils, the value of τ is too large by a factor of 2-4.

Thus one has to take the more correct value $\tau = 5 \cdot 10^{-8}$ sec. instead of the average value $\tau = 1.7 \cdot 10^{-7}$ sec. at the temperature −37.5°. This value of τ can be compared with the orientational relaxation time of phenylethyl alcohol calculated from the depolarization of scattered light.

As Leontovich [8] has shown

$$(7) \qquad M \equiv \frac{\Delta n}{g\eta} = \frac{(n^{2}-1)(n^{2}+2)}{12n}\left[\frac{\tau\beta}{\eta}\left(\frac{12\,\Delta}{6-7\Delta}\right)\right]^{\frac{1}{2}} ,$$

where Δ is the degree of depolarization of scattered light, β is the isothermal compressibility, and η is the index of refraction.

The degree of depolarization Δ of the light scattered by phenylethyl alcohol which we measured at 20°, turned out to be 0.71. Using the value $M_{20^\circ} = 1.22 \cdot 10^{-10}$ given above, we calculated the orientational relaxation time $\tau_{20^\circ} = 4.10^{-11}$ from formula (7). According to conventional concept [9]

$$(8) \qquad \tau = \frac{1}{6D} = \frac{W\eta}{6kT} ,$$

where D is the coefficient of rotational molecular diffusion; W is the coefficient of rotational molecular friction, determined only by molecular structure.

If we extrapolate the value of τ_{20° from 20° to −37.5° and to the corresponding viscosity we obtain $\tau = 1.6 \cdot 10^{-8}$. This value agrees in order of magnitude with that which we obtained from acoustic birefringence $\tau = 5 \cdot 10^{-8}$. One can not expect a better agreement considering the range of the values of τ obtained from the two methods of extrapolation from M_{20° and τ_{20°.

One can assume that continuing this experiment at low temperatures would allow us to determine τ by this method for several other liquids: diacetone alcohol, propylene glycol, hexahydrocreosol and glycerol tributyrate, in which we observed a noticeable acoustic birefringence below −50°.

May 23, 1958

References

1. V. N. TSVETKOV, A. A. MINDLINA, G. I. MAKAROV: ZETF, 16, 891 (1946)
2. V. N. TSVETKOV, V. E. ESKIN: DAN USSR, 59, 1089 (1948)
3. V. N. TSVETKOV, V. E. ESKIN: ZETF, 18, 614 (1948)
4. V. N. TSVETKOV, V. E. ESKIN: DAN USSR, 67, 263 (1949)
5. V. E. ESKIN: Kand. Diss., Leningrad Univ., 1953
6. B. B. KUDRIAVTSEV: Primenenie ultraakustich-eskikh metodov v praktike fiziko-khimich-eskikh issledovanii (Use of ultrasonic methods in physical chemical investigations) GITTL, Moscow-Leningrad, 1952 (German translation available, Akad. Verlag, Berlin)
7. S. BHAGAVANTAM: Scattering of light and the Raman effect, New York, 1942
   C. V. RAMAN, K. S. KRISHNAN: Phil. Mag. 5, 769 (1928)
8. M. A. LEONTOVICH: J. of Phys. URSS, 4, 499 (1941) (In English)
9. IA. I. FRENKEL': Kineticheskaia teoriia zhidkostei (Kinetic theory of liquids). Akad. Nauk Press, 1945. English version available from Dover Publ., N.Y., 1957

TOM VI, Vyp. 5
VOL. VI, No. 5

OPTIKA I SPEKTROSKOPIIA
OPTICS AND SPECTROSCOPY

Mai, 1959
May, 1959

The Influence of Concentration and Type of Solvent on the Raman Line Intensity of Totally Symmetric Vibrations of the Nitro Group and on the Electronic Absorption Spectra of Aromatic Nitro Compounds

V. M. PIVOVAROV AND N. D. ORDYNTSEVA

Abstract: The dependence on concentration and solvent type of the integrated intensities of the Raman lines of the totally symmetric vibration of the nitro group was measured in a series of aromatic nitro compounds. The long wavelength bands in the electronic spectra of these same materials was investigated. A correspondence in the character of the measured values was established.

INTRODUCTION

In earlier published works Bobovich and Pivovarov [1-3] investigated the concentration dependence of the Raman line intensity of the totally symmetric vibration at 1340 cm^{-1} of the nitro group in solutions of some aromatic nitro compounds, and expressed the opinion that the anomalies found might be connected with parameters of the electronic absorption band, [relevant for Raman excitation] . These parameters determine the intensity of the Raman spectrum in the following way [4] :

$$I \sim \left[\frac{\nu_{0e}^2 + \nu^2}{\left(\nu_{0e}^2 - \nu^2\right)^2} P_{0e}^2 k' q' \right]^2 ,$$

where ν = the frequency of the exciting light, P_{0e} = matrix element, ν_{0e} = the frequency of the electronic transition, k' = the quasi-elastic constant for vibration in the excited electronic state, q' = the difference between equivalent distances of the molecule in the ground and excited electronic states.

In order to elucidate the role of each of the enumerated parameters, this paper presents an investigation of the influence of concentration and type of solvent on the intensity of the Raman lines and, at the same time, on the character of the absorption spectra of the following aromatic nitro compounds: p-nitroaniline, p-nitrophenol, p-nitrophenetole and p-nitrotoluene.

1. EXPERIMENTAL

The Raman spectra were obtained using the photoelectric apparatus described in references [3 and 5]. The entrance and exit slits of the monochromator had equal widths of 0.5 mm (approximately 20 cm^{-1} in the blue-green part of the spectrum) the 1380 cm^{-1} line of the naphthalene served as the internal standard necessary for calculation of the absorption of the solvents in the region of the 1340 cm^{-1} line being investigated. By comparison of the integrated intensity of the 1340 cm^{-1} line in the spectra of some pure solutions and in the spectra of solutions containing an addition of naphthalene it was established that the influence of the latter could be disregarded. The results of the measurement of the Raman spectra are assembled in table 1, where, by intensity coefficient is understood the value of the ratio of intensity of 1340 cm^{-1} line to the intensity of the 1380 cm^{-1} line, referred to unit concentration of nitro compound and naphthalene.

The absorption spectra in the 230-400 mμ region were taken on a SF-4 spectrophotometer. For the investigation of concentrated solutions a cell was used with a specially manufactured ring, which, coupled with a standard quartz insert, permitted us to obtain a thickness of the absorption layer of the order of 4-5μ . The absolute thickness was determined spectrophotometrically by comparison with the absorption in a 50μ thick cell

Table 1

Material	Concentration (moles)	Solvent	Intensity coefficient	Wavelength of exciting light (Å)
p-nitroaniline	0.164	acetone	17±1	5461
	0.0754	"	24±1	
	0.0754	50% acetone+50% CCl_4	31.5±0.8	
	0.0047	acetone	108±4	
	0.00485	90% CCl_4 + 10% acetone	49±2	
p-nitrophenol	0.804	acetone	9.0±0.2	
	0.380	"	9.7±0.15	
	0.380	50% acetone+50% CCl_4	9.15±0.2	
	0.0485	acetone	9.2±0.1	
	0.0485	91% CCl_4 + 9% acetone	8.5±0.15	
p-nitrophenetole	0.79	acetone	7.5±0.1	4358
	0.365	"	8.4±0.1	
	0.365	50% acetone+50% CCl_4	7.6±0.1	
	0.048	acetone	8.5±0.15	
	0.048	CCl_4	5.9±0.2	
p-nitrotoluene	0.91	acetone	2.50±0.05	
	0.435	"	2.75±0.05	
	0.435	50% acetone+50% CCl_4	2.65±0.04	
	0.2	acetone	3.6±0.1	
	0.19	CCl_4	2.45±0.06	

Table 2

Material	Solvent and concentration of the material (moles)	ν_{max} (cm^{-1})	f	ε_{max}	Half-width (cm^{-1})
p-nitroaniline	acetone, 0.005 and 0.0033	27000±100	1.1±0.09	17800±900	4400±150
	acetone, 0.164	27350±300	1.15±0.15	17800±2000	4700±300
	acetone, 0.082	27200±200		19100±1500	4500±250
	acetone (14%) + + hexane (86%), 0.003	29000±100	1.05±0.09	15000±750	4900±150
p-nitrophenol	acetone, 0.01	32300±100	1.05±0.09	12200±600	6200±150
	acetone, 0.30	32300±200	1.0±0.12	11600±800	6200±200
	hexane (93%) + + acetone (7%), 0.01	33300±100	0.85±0.09	11300±300	5900±150
p-nitrophenetole	acetone, 0.01	32300±100	1.25±0.12	15500±700	5900±150
	hexane, 0.01	33900±100	0.90±0.09	13200±700	5100±150
p-nitrotoluene	acetone, 0.01	36700±100	0.75±0.06	8800±400	6200±150
	acetone, 0.45	37000±400	0.72±0.08	9000±1000	6400±300
	hexane, 0.01	37700±100	0.81±0.09	10400±500	6100±150

The spectral slit width is approximately 70 cm^{-1}. The results of these measurements are assembled in table 2, where the frequency of the absorption maximum ν_{max} was taken as an average of several measurements. The energy of the oscillator was determined by the formula $f = 1.29 \cdot 10^{-8} \int \epsilon d\nu$ [6], where the integral $\int \epsilon d\nu$ is calculated by changes of the area bound by the average curve $\epsilon(\nu)$ and the frequency axis *. In figure 1 are shown the spectral shifts of the extinction coefficients of the materials investigated depending on solvent and concentration of the materials. For elucidation of the character of the change of form of the bands the spectral curves were reduced in figure 2 to a single height and combined according to absorption maximum.

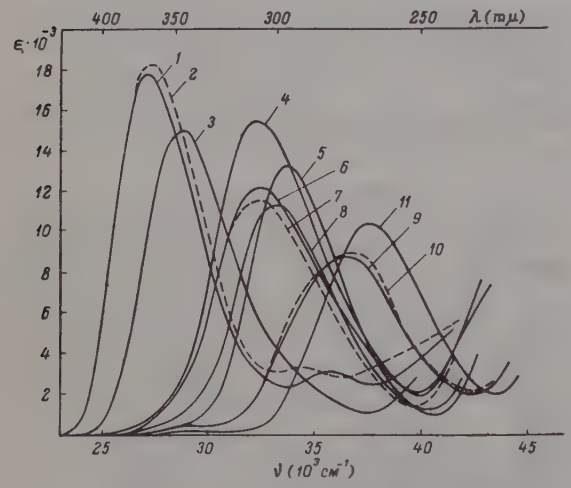

Figure 1. Absorption spectra of aromatic nitro compounds.

1- p-nitroaniline in acetone; 2- p-nitroaniline in acetone; 3- p-nitroaniline in hexane (86%) and acetone (14%); 4- p-nitrophenetole in acetone; 5- p-nitrophenetol in hexane; 6- p-nitrophenol in acetone; 7- p-nitrophenol in acetone; 8- p-nitrophenol in hexane (93%) and acetone 7%; 9-p-nitrotoluene in acetone; 10- p-nitrotoluene in acetone; 11- p-nitrotoluene in hexane.

Concentration (moles): 1 = 0.005, 0.003; 2 = 0.164, 0.082; 3 = 0.003; 4 = 0.01; 5 = 0.01; 6 = 0.01; 7 = 0.30; 8 = 0.01; 9 = 0.01; 10 = 0.45; 11 = 0.01 .

Absorption and Raman spectra were studied of solutions of p-nitroaniline and p-nitrophenol in acetone and in a mixture of hexane or carbon tetrachloride with a small amount of acetone, added to increase their solubility. Such addition of acetone as measurements showed, had practically no effect on the absorption spectrum.

Choice of one or another non-polar solvent was of no importance for the absorption spectrum, as shown in figure 3, in which are presented the absorption spectra of p-nitroaniline in acetone, hexane, CCl_4 and benzene. However, in investigating absorption spectra it is advantageous to take hexane as the solvent, since it is transparent throughout the whole spectral region in which the bands of nitro compounds are found. At the same time, in investigating the Raman spectra it is expedient to use carbon tetrachloride as solvent, since it does not have lines in the 1400 cm^{-1} region.

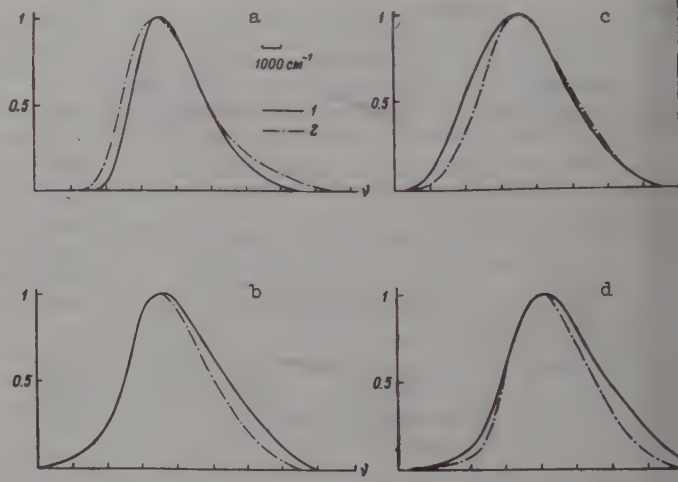

Figure 2. Change of form of absorption curves of aromatic nitro compounds.

1- Solution in acetone; 2- Solution in hexane;

a- NO_2-C_6H_4-NH_2; b- NO_2-C_6H_4-OH; c- NO_2-C_6H_4-CH_3; d- $NO_2C_6H_4$-OC_2H_5.

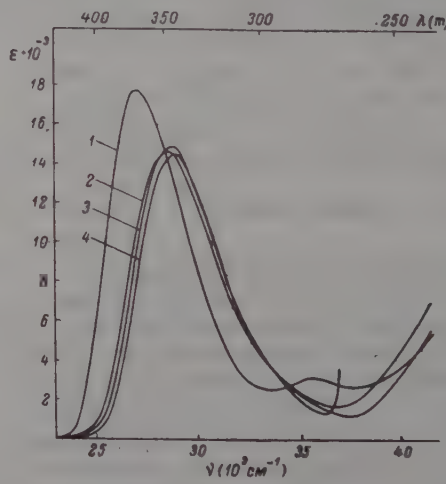

Figure 3. Spectra of p-nitroaniline in different solvents.

1- Acetone 2-CCl_4; 3- Hexane; 4- Benzene.

---

* We did not correct the spectra for the internal field in the solution (see [6]), since the differences for the solvents employed do not exceed the experimental errors.

2. RESULTS AND DISCUSSION

We shall first consider the Raman data. In acetone solution all the materials investigated (in agreement with references [1-3]) showed an increase in the intensity coefficient upon decreasing the concentration of the solution. Transition from solution in acetone to solution in a mixture of acetone and CCl_4 or to solution in CCl_4 was accompanied by a decrease in the intensity coefficient. The last rule is violated in the case of p-nitroaniline upon excitation by the 5461 Å line.

Turning to the results of the investigation of the absorption spectrum, we can note that the bands studied, which, as is well known [1-3], are relevant for the investigations of the Raman line ν_{NO_2} are displaced in the direction of short wavelength upon transition from polar to non-polar solvents. Absolute values for the shift of the absorption maxima are for p-nitroaniline 2000 ± 200 cm^{-1}, for p-nitrophenol 1000 ± 200 cm^{-1}, for p-nitrophenetole 1600 ± 200 cm^{-1} and for p-nitrotoluene 1300 ± 200 cm^{-1}. If the absorption band shift shows direct relationship to the type of solvent, then it is not possible to speak of another quantity, the energy of oscillation. It does not change at all in p-nitroaniline and p-nitrotoluene. However the energy of oscillation of the two other materials diminishes somewhat in the transition from solution in acetone to solution of hexane. The data presented in figure 2 show that simultaneously with the shifting of the absorption maximum some change of its form takes place. We are not able at this time to establish any kind of correspondence between the character of the change of contour and the nature of the solvent. Therefore, the question of the influence of the band form on the intensity of the Raman line remains open.

The influence of the concentration of the dissolved material on the parameters of the absorption spectrum is evidently small, and does not exceed the experimental errors, which in our case, are as high as 10-15% owing to the inexactness of the measurement of the thickness of the samples.

Comparison of the results presented in tables 1 and 2 shows that the dependence of the intensity, I, of the Raman lines on the nature of the solvent can be explained qualitatively by the change of the value of ν_{0e}. We note that Minc and Kurowsky [7] came to an analogous conclusion in the recently published paper devoted to the study of p-nitroaniline alone. At the same time it is not possible at present to connect concentration dependence of the intensity of the Raman lines with changes of the absorption spectra; the position and intensity of the absorption spectra, as indicated, do not depend on concentration, within the limits of accessible accuracy of practical measurement. We shall note that the increase in the intensity coefficient of p-nitroaniline in the mixed solvent acetone-CCl_4 may possibly be caused by the appearance of hydrogen bonding [8].

The authors express their gratitude to A. S. Bobovich for his kind interest in this work.

July 7, 1958

References

1. IA. S. BOBOVICH, V. M. PIVOVAROV: DAN USSR, 108, 607 (1956) (See Sov. Physics, Doklady 1, 341-344 (1956))
2. IA. S. BOBOVICH, V. M. PIVOVAROV: Materialy X Vsesoiuz. Soveshch. po Spektroskopiia (Proceedings of the X Conf. on Spectr.) 1, 1957, L'vov Univ. Press
3. IA. S. BOBOVICH, V. M. PIVOVAROV: OiS, 3, 227 (1957)
4. M. V. VOL'KENSHTEIN, M. A. EL'IASHEVICH, B. I. STEPANOV: Kolebaniia molekul (Vibrations of molecules), 2, GITTL, Moscow, 1949
5. IA. S. BOBOVICH, D. B. GUREVICH: ZETF, 27, 318 (1954)
6. N. G. BAKHSHIEV: OiS, 5, 646 (1958)
7. S. MINC, S. KUROWSKI: Z. Elektrochem., 61 833 (1957)
8. IA. S. BOBOVICH, V. M. PIVOVAROV: OiS, 3, 387 (1957)

TOM VI, Vyp. 5
VOL. VI, No. 5

OPTIKA I SPEKTROSKOPIIA
OPTICS AND SPECTROSCOPY

Mai, 1959
May, 1959

Difference in Energy of Rotational Isomers in Liquid and Gaseous 1, 2-Chlorofluoroethane

P. A. BAZHULIN AND L. P. OSIPOVA

Abstract: The Raman and infrared absorption spectra of 1, 2-Chlorofluoroethane were investigated. On the basis of a comparison of the infrared absorption spectra of liquid and crystalline 1, 2-Chlorofluoroethane a conclusion was drawn concerning the existence of rotational isomers in this compound. The difference of energy of the rotational isomers was measured in liquid and gaseous phases.

The study of internal rotation, observed in a series of compounds [1-4] , gives valuable information about the structure of molecules and of the energy properties of rotational isomers. The simplest compounds with rotational isomers are the dihalogenoethanes. It is very important to obtain reliable experimental data for them in order to devise a theory of the phenomenon of rational isomerism.

At the present time there is a great number of experimental and theoretical papers which show reliably the existence of two isomeric forms, trans and gauche, in gaseous and liquid dihalogenoethanes, and one isomer in the solid phase [1-3]. However the determination of the difference of energy of the rotational isomers has been given significantly less attention. Evidently this fact is connected with the experimental difficulty of carrying out quantitative measurements on the temperature dependence of the ratio of the intensities of two lines which belong to the different isomers.

The purpose of this paper is the elucidation of the question of the existence and configurations of the stable forms of 1, 2-Chlorofluoroethane, and the determination of the difference in energy of the rotational isomers in the gaseous and liquid phases.

EXPERIMENTAL RESULTS AND DISCUSSION

The Raman spectrum of 1, 2-Chlorofluoroethane was obtained photographically on an ISP-51 spectrograph with a camera of focal length 270 mm. A low pressure lamp with cooled electrodes served as the light source. Measurements of the frequencies of Raman lines, their intensities and degrees of depolarization are presented in table 1.

Calibration of the spectrum was carried out by comparison with the spectrum of iron. The values of the Raman shifts $\Delta\nu$ were obtained as averages over three spectra. The accuracy of the frequencies was 1-3 cm^{-1} , depending on the character of the lines. Estimation of the intensities was carried out by a visual method on a ten-step scale. The following designations were introduced to characterize the Raman lines: w. = wide, sh. = sharp, bg. = a line located on a background of significant intensity. Degree of depolarization of the lines was determined photographically. Accuracy of the measurements is of the order of 15-20% .

As is well known, in the most general case the vibration spectrum of a non-linear eight-atom molecule may exhibit eighteen frequencies. In our measurements in the Raman spectrum 23 frequencies are found (table 1) . Such a departure from the expected number of vibration frequencies can be explained by assuming the presence of two isomeric forms in the molecule of 1, 2-Chlorofluoroethane. A definite conclusion about the presence of two isomeric forms can be made only on the basis of temperature studies. Of course, on lowering the temperature, the number of molecules of the less stable isomer gradually diminishes, until in the solid phase only the one stable form ought to be present [1, 2] . Therefore it was to be expected that the spectrum of crystalline 1, 2-Chlorofluoroethane would be simplified on account of the disappearance of frequencies corresponding to vibrations of the less stable isomeric form.

Preliminary investigations [5] of the influence of temperature on the intensity of the Raman lines showed that the intensity of the 759 cm^{-1} line diminishes with a drop in temperature, while the intensity of the 672 and 840 cm^{-1} lines increases. On this basis it is assumed that the 759 cm^{-1} line belongs to the spectrum of the isomer which is unstable in the solid state. We were prevented by the interference of a strong background from obtaining the Raman spectrum of crystalline 1, 2-Chlorofluoroethane. Therefore we decided to carry the investigation further by the infrared method. This work was done on a double-beam IKS-2 spectrophotometer. The infrared absorption spectrum of the compound being investigated was obtained in the range from 600 to 1500 cm^{-1} .

Table 1

Raman Spectrum			Infrared Absorption Spectrum ν (in cm^{-1})		
$\Delta\nu$ (in cm^{-1})	Intensity	Degree of Depolarization	Gas	Liquid	Crystal
146 w.bg	4	0.65	—	—	—
286 w.	8	0.45	—	—	—
384 sh	8	0.29	—	—	—
470	5	0.62	—	—	—
—	—	—		625 v.w.	625 w.
—	—	—	660 m.	657 m.	657 m.
672 w.	10	0.19	679 m.	670 m.	676 m.
—	—	—		710 w.	—
759 w.	5	0.32	756 w.	754 m.	—
840 sh	8	0.36	837 m.	830 v.s.	830 v.s.
—	—	—	876	871 w.	870 w.
957 w.	5	0.95	961 w.	953 s.	954 s.
1010	2	—	1015 v.s.	1012 v.s.	1012 v.s.
1028	6	0.41		1039 v.s.	1039 v.s.
1075	5	0.75	1070 v.s.	1073 v.s.	1070 v.s.
—	—	—	1159 v.w.	—	—
1192	6	0.56	1194 w.	1198 m.	1195 m.
—	—	—	—	1225 v.w.	1230 w.
1254	7	1.0	1250 w.	1258 w.	—
1302	5	0.18	1300 s.	1295 s.	1300 s.
—	—	—	—	1331 w.	1343 m.
1387	2	0.85	1390 s.	1380 s.	1391 s.
1426	7	0.85	1420 s.	1420 s.	1425 s.
1458	7	0.94	1452 s.	1456 s.	1440 s.
2760	4	—	—	—	—
2844	3	—	—	—	—
2899	7	—	—	—	—
2962	10	—	—	—	—
3020 bg	3	—	—	—	—
3046 bg	1	—	—	—	—

For investigation of the influence of temperature on the intensity of the infrared absorption bands special cells were used, analogous to those described in references [2, 6 and 7]. The spectrum of crystalline 1, 2-Chlorofluoroethane was taken at -186° C. The frequencies of the infrared absorption bands measured for the gaseous, liquid, and crystalline states are presented in Table 1. The value of $\nu(cm^{-1})$ is obtained as an average over three to five spectra. The accuracy of determination of the frequencies is of the order of 3 to 5 cm^{-1}, depending on the character of the absorption band. We point out that the bands at 625, 657, 676 cm^{-1}, as well as those at 1015, 1039 and 1073 are poorly resolved. The following designations were introduced to characterize the infrared absorption bands: v. s. = very strong, s. = strong, m. = medium, w. = weak, v. w. = very weak.

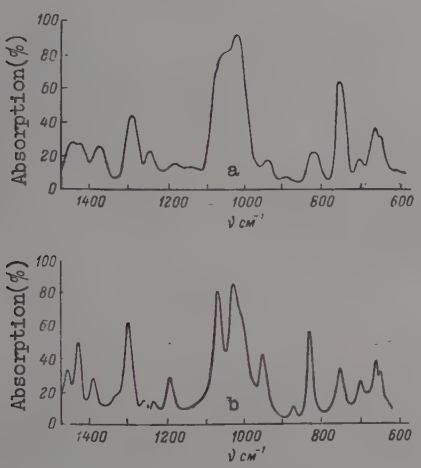

Fig. 1

Figure 1 shows the form of the absorption curves in gas (a) and liquid (b) phases. From this figure it is evident that the absorption bands in the gas phase are broader than the corresponding bands in the liquid. Broadening of the absorption bands in the spectrum of the gas may be explained by the superposition of P and R branches, which, in the cases we investigated, were of comparable intensity. Figure 2 a shows the portion of the spectrum of the liquid in the region of 850-700 cm^{-1} at temperatures of +25° and -50° C (dotted line). Figure 2 b shows the portion of the spectrum of the crystal in the 850-700 cm^{-1} region at -186° C. From Table 1 and figure 2 it is seen that the infrared absorption spectrum of crystalline 1, 2-Chlorofluoroethane differs from the spectrum of the liquid or gas by the disappearance of the bands at 759 and 1252 cm^{-1}. This decrease in the number of bands in the spectrum of crystalline 1, 2-Chlorofluoroethane, and the total number of vibration frequencies found, indicate the existence of two isomeric forms in the gas or liquid, and one form in the solid phase.

To measure the difference of energy of the rotational isomers it was necessary to choose a pair of lines which clearly belong to the different isomers. Comparison of the spectra in different states of aggregation allows this to be done. As is seen from the absorption curves the line at 759 cm^{-1} (ν_1), which belongs to the isomer which is unstable in the solid state, and the line at 840 cm^{-1} (ν_2), which belongs to the isomer which is stable in the solid state, form a convenient pair for this purpose.

Calculation of the difference in energy of the rotational isomers, ΔU, is carried out according to the formula

$$\Delta U = \frac{R \ln \frac{K_{T_1}}{K_{T_2}}}{\frac{1}{T_2} - \frac{1}{T_1}}$$

where

where $K_T = \frac{D_{\nu_1}}{D_{\nu_2}}$, D_{ν_1} and D_{ν_2} are the optical densities of the absorption bands being compared.

Several authors [2, 6, 8-10] have studied the influence of temperature on the ratio of optical densities at the maxima of absorption bands. Use of the optical densities at the maxima, instead of integrated absorption in calculating the difference of energy of rotational isomers, is evidently possible when the widths of the bands being compared are equal [8-10], and do not change (or change equally) with change of temperature.

Our findings showed that the widths of the 759 and 840 cm^{-1} absorption bands are approximately equal in the liquid at +25° C, but with lowering of the temperature to -50 ° C, the width of the 759 cm^{-1} band changes, while that of the 840 cm^{-1} band remains practically unaltered. In the gas the widths of the 840 and 759 cm^{-1} bands at +35° C. differ somewhat, but on raising the temperature to 90° C. they are practically unchanged. The different influence of the temperature on the width

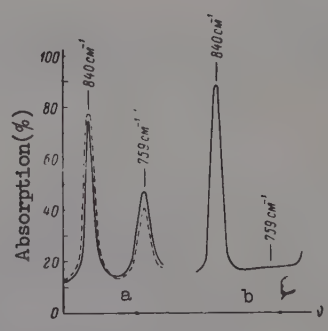

Fig. 2

of the 759 and 840 cm^{-1} bands might be explained by the fact that these bands, as shown below, correspond to different modes of vibration. Therefore we carried out the calculation of the energy difference by integrating the values of the optical densities (D_ω) of the absorption bands being compared. Measurements of the optical densities of

these bands were carried out 5-6 times at four temperatures (+25, -25, -50, -100° C.) on liquid samples. Measurement of the optical densities of the absorption bands in the gas phase were carried out 5-6 times at +35 and +90° C.

The following values and experimental errors were obtained for the energy difference of the rotational isomers of 1, 2-Chlorofluoroethane:

$$\Delta U_{liquid} = 470 \pm 60 \text{ cal./mole}$$

$$\Delta U_{gas} = 60 \pm 40 \text{ cal./mole}$$

We should state that, for comparison, a calculation of ΔU was also carried out according to the values of the optical densities at the maxima of the bands. The values obtained were

$$\Delta U_{liquid} = 600 \pm 50 \text{ cal./mole}$$

$$\Delta U_{gas} = 90 \pm 30 \text{ cal./mole}$$

which differ little from the values of ΔU calculated using integrated optical densities.

Usually, in measuring the difference of energy of rotational isomers, the temperature dependence of the intensity of the two lines arising from the same type of vibration is studied. The reason for this is connected with a series of circumstances which influence the size of the error - in particular with the fact that the intensities of the lines can change anomalously with a change of temperature, and the size of the anomaly can depend considerably on the type of vibration [11].

In this case these considerations do not have great importance, since calculation using another pair of lines, 1252 and 1195 cm^{-1}, arising from like vibrations, leads to the value

$$\Delta U_{liquid} = 400 \pm 100 \text{ cal/mole}$$

which is practically coincident with the former value. Choice of the pair of lines at 759 and 840 cm^{-1} was dictated by considerations of practical convenience.

To verify the method of measuring intensities on the double-beam IKS-2 spectrophotometer we determined the energy difference of rotational isomers in gaseous dichloroethane. The value obtained

$$\Delta U_{gas} = 1200 \pm 100 \text{ cal/mole}$$

agrees well with literature data [2, 8] which vary between 1000 and 1400 cal/mole.

On the basis of the experimental data obtained it was found possible to make an assumption about the form of the stable isomer in the solid state, and to determine which isomer, trans or gauche, is relatively more stable in the gas and liquid phase.

A complete interpretation of the vibrational spectrum of the 1, 2-Chlorofluoroethane molecule without theoretical calculation is difficult. Since, however, there is in the literature [1, 2] detailed analysis and interpretation of the vibrational spectra of 16 halogenoethanes, we carried out, by comparison, an examination of some vibration frequencies of the spectrum of the molecule we studied. Since the bands at 759 and 1252 cm^{-1} are missing in the spectrum of crystalline 1, 2-Chlorofluoroethane, a determination of the stable isomeric form in the solid state requires a reliable assignment of just these two frequencies. In the spectra of liquid dihalogenoethanes analogous to the compound studied, two bands are found in the 750-600 cm^{-1} region corresponding to the C-Cl stretching vibration [1]. The higher frequency band (at ~ 750 cm^{-1}) corresponds to the trans isomer, while the lower frequency band (~ 650 cm^{-1}) belongs to the gauche isomer. Table 2, based on literature data, illustrates this assignment. In the solid state one of the bands is retained. In the case of dichloroethane and bromochloroethane the higher frequency band , the band belonging to the trans isomer [1, 2], is retained in the solid state. However in the case of the halopropanes [8], the lower frequency band is retained in the solid state, and, consequently, the gauche form is stable.

Table 2

Material	$\Delta\nu$ cm^{-1}			
	Cl		Br	
	Trans-form	Gauche form	Trans-form	Gauche form
1,2-dichloroethane [1]	753	653	-	-
1,2-bromochloroethane [1]	724	665	631	567
1,2-dibromoethane [1]	-	-	660	551
1,2-bromofluoroethane [1]	-	-	679	574
1,2-chlorofluoroethane [1]	759	672	-	-

Comparison of the spectra of a large number of chloro-substituted paraffins [1, 2, 8] shows that the C-Cl frequencies of trans and gauche isomers are retained on going from compound to compound.

In view of the foregoing it is possible to interpret the 672 cm^{-1} frequency found in the spectrum of 1, 2-Chlorofluoroethane as ν_{C-Cl} of the gauche isomer, and the 759 cm^{-1} as ν_{C-Cl} of the trans isomer. Thus, in the solid state, the stable isomer of 1, 2-Chlorofluoroethane is the gauche form, since the 759 cm^{-1} band is completely absent in the solid state spectrum (Fig. 2 b). This assignment is confirmed by assignment of the 1195 and 1252 cm^{-1} bands. By comparison of these frequencies with spectra of dichloroethane [2], bromochloroethane [2], and bromofluoroethane [12] it is evident that the 1195 cm^{-1} band must be interpreted as a CH_2 deformation vibration belonging to the gauche isomer, and the 1252 cm^{-1} band as the CH_2 deformational vibration of the trans isomer. In our case the disappearance of the 1252 cm^{-1} band was observed, which also confirms the stability of the gauche isomer in the solid phase. In the liquid the gauche form is relatively more stable since the intensity of the 759 and 1252 cm^{-1} bands diminishes with lowering of the temperature. In the gas phase the trans form is relatively more stable, since with increasing temperature a decrease of the intensities of the 759 and 1252

cm^{-1} bands is found.

We can assume that the strong stabilization of the gauche isomer on going from gas to liquid occurs as a result of dipolar orientation interaction, since it is well known that a more polar form is strongly stabilized in a liquid [1, 2].

The existence of the gauche isomer in the 1,2-Chlorofluoroethane molecule is demonstrated also by radio frequency investigations. In a paper [13] on the analysis of the microwave spectrum it was established that there is a stable configuration for the 1, 2-Chlorofluoroethane molecule with an angle (α) of 70° between projections of the C-F and C-Cl bonds on a plane perpendicular to the C-C axis.

Thus, we can consider it definite that the molecule $FH_2C\text{-}CH_2Cl$ exists in gas and liquid phases in two isomeric forms. In solid and liquid states the gauche forms are stable, while the trans form is stable in the gas phase.

In conclusion we take the opportunity to express our thanks to A. M. Prokhorov and I. A. Mukhtarov for their valuable advice both on carrying out the work, and on discussion of the results obtained.

June 9, 1958

References

1. M. V. VOL'KENSHTEIN, M. A. EL'IASHEVICH, B. I. STEPANOV: Kolebaniia molekul (Vibrations of molecules), GTTL, 1949
2. S. MIDZUSHIMA: Structure of molecules and internal rotation. Academic Press, N.Y., 1954 (IL, Moscow, 1957)
3. W. F. EDGELL, G. GLOCKLER: J. Chem. Phys., 9, 375 (1941)
4. K. W. F. KOHLRAUSCH: Ramanspektren, Leipzig, 1943, Akad. Verlagsgesell. (IL, Moscow, 1952)
5. ARKHIPOV: Dipl. Thesis, Moscow Univ., 1956
6. I. I. NOVAK, E. S. SOLOV'EV: OiS, 2, 62 (1957)
7. V. A. POZDYSHEV, IU. A. PENTIN, V. M. TATEVSKII: OiS, 3, 211 (1957)
8. IU. A. PENTIN, V. M. TATEVSKII: Vestnik, Moscow Univ., No. 3, 63, 73 (1955)
9. H. J. BERNSTEIN: J. Chem. Phys., 17, 258 (1949)
10. H. J. BERNSTEIN: J. Chem. Phys., 18, 897 (1950)
11. P. A. BAZHULIN, A. V. RAKOV: DAN USSR, 105(1), 54-56 (1955)
12. D. SIMPSON, E. K. PLYLER: J. Res. Nat. Bur. Stand., 50, No. 5, 223 (1953)
13. I. A. MUKHTAROV: DAN USSR, 115(3), 486 (1957) (See Sov. Phys. Doklady, 2, 357-358)

TOM VI, Vyp 5
VOL. VI, No. 5

OPTIKA I SPEKTROSKOPIIA
OPTICS AND SPECTROSCOPY

Mai, 1959
May, 1959

Absorption Spectra of Carbanions

I. V. ASTAF'EV AND A. I. SHATENSHTEIN

Abstract: For the first time a systematic investigation has been made of the electronic spectra of carbanions formed by acidic ionization of aliphatic-aromatic hydrocarbons and their derivatives. Measurements were made of twenty carbanions of the type $ArCH_2^-$, Ar_2CH^-, Ar_3C^- and others, obtained by the action of potassium amide or potassium hydroxide on the corresponding hydrocarbons and their derivatives in liquid ammonia. Some regularities were discovered in the spectra of carbanions. The spectra of carbanions were compared with the spectra of carbonium ions (carbcations) of similar structure.

This work* was carried out in connection with a study of the mechanism of isotopic exchange of hydrogen in hydrocarbons catalyzed by a solution of potassium amide in liquid ammonia. Under these circumstances hydrocarbons react as acids [2] and conditions are created which favor the formation of ions with trivalent, negatively charged carbon—carbanions. Aliphatic-aromatic hydrocarbons form colored carbanions. There is little information in the literature concerning their electronic spectra. Bridging this gap is a matter of interest for spectroscopy, particularly the comparison with spectra of carbonium ions of similar structure. A similar comparison was made by Anderson [3], who measured the spectra of triphenylmethyl as anion, radical and cation. He determined that the absorption spectra, irrespective of charge, have maxima in the visible region in the 400-500 mμ region. To obtain the anion he used the reaction of triphenylmethyl bromide with sodium amalgam in ether. This reaction does not go to completion [4], which accounts for the qualitative character of his absorption curve. Two further attempts to measure the spectrum of the triphenylmethyl anion are known [5, 6].

Methods for the quantitative measurement of the spectra of solutions in liquid ammonia at room temperature were worked out by Shatenshtein and Izrailevich [7, 8]. We have basically confined ourselves to the methods described in reference [8], (for more detail concerning the methods see reference [9]). A solution of potassium amide in liquid ammonia absorbs light in the near ultraviolet ($\lambda_{max.} = 345$ mμ), see also [10]. We used this base for obtaining carbanions (for example, α-naphthylmethyl anions $\alpha\text{-}C_{10}H_7CH_3 + NH_2^- \rightleftarrows \alpha\text{-}C_{10}H_7CH_2^- + NH_3$) only for measurements in the visible region. Potassium amide (0.01-0.1 N.) was employed, as a rule, in considerable excess. Completeness of the transformation of the material into the carbanion under the influence of the NH_2^- ion was verified by obedience of absorption to Beer's law.

For measurements in the ultraviolet region we took advantage of the observation that in liquid ammonia potassium hydroxide partially converts quinaldine [11] and triphenylmethane [12] into carbanions. We obtained potassium derivatives of fluorene, diphenylmethane ($(C_6H_5)_2CH_2 + OH^- \rightleftarrows (C_6H_5)_2CH^- + H_2O$), and also diphenylamine. For calculation of log ε data from the visible region of the spectrum were used. Judging from spectrophotometric measurement in the ultraviolet region, the reaction $KOH + NH_3 \rightarrow KNH_2 + H_2O$ does not go to a noticeable extent.

The reaction vessel consisted of a quartz cell of 5-8 ml. volume with plane parallel optical windows spaced about 1 mm. apart. The cell was soldered with Wood's metal alloy to a piece of steel which was screwed to a mounting [8, 9] assembled from standard metal parts [13]. Hermetic gaskets were made of cadmium. With the aid of the mounting mentioned the system was evacuated, carefully dried with gaseous ammonia, and the cell (into which the sample had been introduced beforehand) was filled with a solution of potassium amide in liquid ammonia. The sample was introduced in the form of a solution of known concentration (the amount of the solution was measured) in a volatile solvent which was subsequently removed.

For the measurements the cell, with a valve, was placed in a special protective case in which it could be moved. The case was mounted in place of the cell compartment of the Beckman spectrophotometer (model DU). In view of the errors of measurement, the values of log ε were rounded off to the first decimal place.

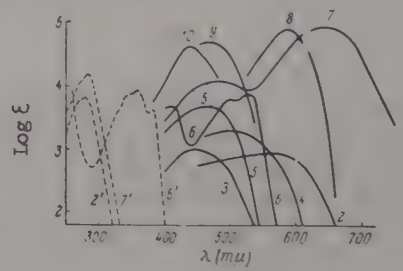

Figure 1

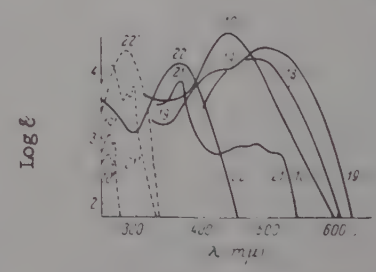

Figure 2

Liquid ammonia does not significantly change the spectra of the hydrocarbons we used, and these correspond to literature values obtained with ordinary solvents. Addition of a strong base (NH_2^- or OH^- ions) causes significant displacement of absorption in the direction of long wavelengths. As could be inferred from measurements of the infrared spectra [1] carried out earlier in our

* A preliminary report was published in 1956 [1].

laboratory, this effect was due to the formation of carbanions as a result of the acid ionization of an aliphatic C-H bond, the carbon atom of which is joined to the aromatic ring. In figures 1 and 2 the spectra of unionized material in liquid ammonia solutions are compared with spectra of the anions. (Numbering of the curves corresponds to numbering of the anions in the tables, the spectra of solutions of unionized materials are noted by dashed curves.)

Table 1

Absorption of light by carbanions of the type $ArCH_2^-$

No. Anion	Anion	$\lambda_{max.}$ (mμ)	Log $\varepsilon_{max.}$
1	$C_6H_5CH_2^-$	408[14], 430[15], 462[16]	—
2	α-$C_{10}H_7CH_2^-$	560	2.9
3	α-$(C_5H_4N)CH_2^-$	445	3.0
4	α-$(C_9H_6N)CH_2^-$	495	3.3
5	γ-$(C_9H_6N)CH_2^-$	465	3.7
6	9-$(C_{13}H_8N)CH_2^-$	530	3.8

Table 2

Absorption of light by carbanions of the type Ar_2CH^-

No. Anion	Anion	$\lambda_{max.}$ (mμ)	Log $\varepsilon_{max.}$
7	α, α'-$(C_{10}H_7)_2CH^-$	645	4.9
8	$(C_6H_5C_6H_4)_2CH^-$	590	4.9
9	$(C_6H_5CH_2C_6H_4)_2CH^-$	470	4.7
10	$(C_6H_5)_2CH^-$	440	4.6
11	$(C_6H_5OC_6H_4)_2CH^-$	450	4.5
12	$[(H_3C)_3CC_6H_4]_2CH^-$	440	4.5
13	$(H_3CC_6H_4)_2CH^-$	445	4.4
14	$(H_3COC_6H_4)_2CH^-$	430	4.1
15	$[(H_3C)_2NC_6H_4]_2CH^-$	445	3.5
16	$[(H_5C_2)_2NC_6H_4]_2CH^-$	450	3.3
17	$C_6H_5CHCH{=}CH_2$	420	4.2

Under the conditions of our experiments with solutions of potassium amide, toluene is not converted into carbanions to a noticeable extent. The red-orange color characteristic of its potassium organic compound was not found. However the hydrogen of the methyl group is easily ionized if this group is bonded with a pyridine or naphthalene nucleus instead of a benzene ring. Lengthening of the chain of the conjugated aromatic system is accompanied by a bathochromic shift. This is seen, in particular, from a comparison of $\lambda_{max.}$ in the group of $ArCH_2$ anions (table 1, fig. 1): benzyl and α-naphthylmethyl anions (for benzyl anions results of quantum-mechanical calculations are taken [14-16]), and also the anions α-methylpyridine, α- and γ-methylquinoline and 9-methylacridine.

In table 2 are presented data on the characteristic absorption of light by carbanions of the type Ar_2CH^- (see also fig. 1 and 3). On the whole these anions are colored more intensely than anions of the type $ArCH_2^-$ (for example, fig. 1, spectra 7 and 2 of solutions of α, α'-dinaphthylmethyl anions and α-naphthylmethyl anions).

Comparing the positions of the maxima in the absorption curves of the carbanions of diphenylmethane and its para-substituents (anions 8-16) it can be seen that carbanions of para-phenyl and para-benzyl derivatives differ both by a much deeper color (bathochromic shift) and also by a greater intensity. This phenomenon is apparently connected with the production of electrophilic characteristics by these substituents. Carbanions of other para-derivatives are characterized by absorption in the very same region of long wavelength as the diphenylmethyl anion ($\lambda_{max.} = 440 \pm 10$ mμ), but are distinguished by the intensity of the color. The least intense absorption is found in the case of the substituents with the most pronounced nucleophilicity, $(H_5C_2)_2N(H_3C)_2N$.

Closing the carbon-carbon bond between ortho atoms of the benzene rings of the diphenylmethyl anion completely alters the conditions of conjugation of the electrons in the anion. On going from the $(C_6H_5)_2CH^-$ anion to the fluorenyl anion the intensity of absorption in the visible region is sharply reduced, and the absorption in the ultraviolet is reinforced (table 3, fig 2) .

Table 3

Comparison of data on the absorption spectra of carbanions and carbonium ions

No. Anion	Ions	Anions		Cations	
		$\lambda_{max.}$	log $\varepsilon_{max.}$	$\lambda_{max.}$	log $\varepsilon_{max.}$
10	$(C_6H_5)_2\overset{\pm}{C}H$	440	4.6	440	4.6
15	π, π'-$[(H_3C)_2NC_6H_4]_2\overset{\pm}{C}H$	445	3.5	610	—
18	$(C_6H_5)_2\overset{+}{C}CH_3$	480	4.3	429	4.5
19	$(C_6H_5)_2\overset{+}{C}C_6H_5$	495	4.4	431	4.6
20	π, π'-$(H_3COC_6H_4)_2\overset{\pm}{C}C_6H_5$	480	4.2	500	4.8
21	Флуоренил$^{\pm}$	480 367	2.9 3.9	655 484	3.1 2.9

The type Ar_3C^- was represented by anions of triphenylmethyl $(C_6H_5)_3C^-$ and its p, p'-dimethoxy derivative $(H_3COC_6H_4)_2\overset{-}{C}C_6H_5$ (see table 3 and fig. 2, 3).

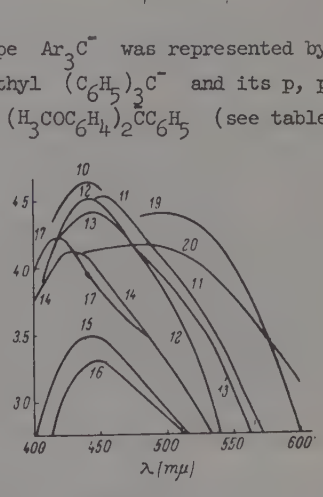

Figure 3

By comparison of the absorption curves of the anions $(C_6H_5)_2CH^-$ and $H_3COC_6H_4)_2CH^-$ it is obvious that introduction of a third benzene ring shifts the

absorption maximum in the direction of long wavelength. This cannot be ascribed solely to the presence of a third benzene ring, since the anion 1, 1-diphenylethane $(C_6H_5)_2\bar{C}CH_3$ also absorbs light in a longer wavelength region ($\Delta\lambda_{max.} = 40$ mμ). Lately the planarity of the triphenylmethyl has been frequently questioned, primarily because of geometric considerations [17].

It has been speculated that only two benzene rings participate in conjugation [18]. This can be used to explain the resemblance of spectral effects which accompanies the transition from the $(C_6H_5)_2CH^-$ ions to $(C_6H_5)_2\bar{C}CH_3$ and $(C_6H_5)_2\bar{C}C_6C_5$ (table 3, fig. 2).

We must note that the unionized molecules $(C_6H_5)_2CH_2$ and $(C_6H_5)_3CH$ absorb light in the ultraviolet region in the same interval, 250-280 mμ (fig. 2). Their acidic ionization simultaneously with a strong shift of absorption in the direction of long wavelength leads to significant discrepancy in the spectra. An analogous result is found on comparing spectra of unionized molecules and carbanions of α-methylnaphthalene and α, α-dinaphthylmethane, (fig. 1). Thus, the mechanism of light absorption of molecules and ions is not identical.

In contrast to toluene, allylbenzene $C_6H_5CH_2CH=CH_2$ is easily transformed into an anion under the action of a solution of potassium amide. This may be explained by the higher mobility of the hydrogen atoms of the α-C-H bonds as a result of conjugation with the π electrons of the benzene ring system and, simultaneously, the π electrons of the double bond. The spectrum of the anion of allylbenzene $C_6H_5\bar{C}HCH=CH_2$ is similar to the corresponding curves of anions of the Ar_2CH^- group with nucleophilic substituents in the para-positions (see table 2 and fig. 3). Anions of allylbenzene differ most markedly in their capacity for secondary reactions [19]. In particular, upon neutralizing the solution with ammonium chloride, which is an acid in liquid ammonia, a mixture of allylbenzene and its isomer, β-methylstyrene, $C_6H_5CH=CHCH_3$, is formed [20]. This very graphically confirms the hypothesis concerning the mechanism of carbanion isomerization (with shift of the double bond) of olefinic hydrocarbons by amides, proposed by Kazanskii and Gostunskaia [21], (see also [22]).

At the same time as the acid ionization of the C-H bond, whose carbon atom is adjacent to the aromatic system, causes a shift of the absorption maximum in the visible region, we found the N-H bonds of the molecules of ammonia and diphenylamine undergo a shift under conditions of acid ionization of the absorption maxima in the near ultraviolet part of the spectrum: NH_2^-: $\lambda_{max.} = 345$ mμ; $(C_6H_5)_2N^-$: $\lambda_{max.} = 365$ mμ; $\log\epsilon = 4.2$ (fig. 2, curve 22).

When a carbon atom passes from a state of tetrahedral hybridization to a state of trigonal hybridization, the possibility arises of conjugation of the π - electrons of the aromatic rings with the unhybridized p-orbital which is formed. With this, evidently, is connected the appearance of color, which takes place irrespective of the extent of filling of the p-orbital, i.e. irrespective of the charge of the species (see, for example, the work of Anderson [3]). For spectra of simple species of this kind (benzyl anion, $C_6H_5\dot{C}H_2^-$, $C_6H_5CH_2^{\cdot}$ radical and $C_6H_5CH_2^+$ + cation), in recent years three independent quantum-mechanical calculations by the method of molecular orbitals have been made [14-16]. These calculations predict the visible absorption and similarity of the spectra of anions and cations. The similarity of the spectra of more complicated ions determined experimentally in this work can be compared with the theoretical prediction concerning the similarity of spectra of benzyl ions: the more complicated ions are the anions and cations of diphenylmethyl $(C_6H_5)_2\dot{C}H^{\pm}$.

In table 3 our results on the carbanions are compared with the data of Deno and co-workers [18] of the spectra of carbonium ions of similar structure. From the table it is obvious that further complication of the structure of the ions, in particular introduction of a third phenyl group, leads to divergence in the spectra: one and the same substituent shows a different influence on the spectra of anions and cations.

We intend to continue our investigation of the spectra of carbanions, extending it to other classes of hydrocarbons. We are also interested in the determination of acid ionization constants of hydrocarbons by means of spectrophotometric measurements.

We are grateful to D. A. Drapkina and V. F. Lavrushin for placing a number of compounds at our disposal.

June 16, 1958

References

1. E. A IZRAILEVICH, D. N. SHIGORIN, I. V. ASTAF'EV, A. I. SHATENSHTEIN: DAN USSR, 111, 617 (1956)
2. A. I. SHATENSHTEIN: Usp. Khim., 24, 377 (1955)
3. L. C. ANDERSON: J. Amer. Chem. Soc., 57, 1673 (1935)
4. H. E. BENT: J. AMer. Chem. Soc., 52, 1498 (1930)
5. A. HANTZSCH: Ber., 54, 2613 (1921)
6. H. LINSCHITZ, M. G. BERRY, D. SCHWEITZER: J. Amer. Chem. Soc., 76, 5833 (1954)
7. A. I. SHATENSHTEIN, E. A. IZRAILEVICH: ZFKh, 13, 1791 (1939)
8. A. I. SHATENSHTEIN, E. A. IZRAILEVICH: ZFKh, 26, 377 (1952)
9. I. V. ASTAF'EV: Cand. Diss., Karpov Phys.-Chem. Inst., Moscow, 1958
10. R. A. OGG, Jr., P. A. LEIGHTON, F. W. BERGSTROM: J. Amer. Chem. Soc., 55, 1754 (1933)
11. A. I. SHATENSHTEIN, E. N. ZVIAGINTSEVA: DAN USSR, 117, 852 (1957)
12. C. A. KRAUS, R. ROSEN: J. Amer. Chem. Soc., 47, 2739 - 2748 (1925)
13. A. I. SHATENSHTEIN: ZFKh, 15, 246 (1941)
14. W. BINGEL: Zs. Naturforschg., 10a, 462 (1955)

References (continued)

15. F. A. MATSEN: Chemical application of spectroscopy. Ed. W. West, N.Y., 1956, p. 690 Vol. 9 of "Techniques of Org. Chem." edited by A. Weissberger
16. H. C. LONGUET-HIGGINS, J. A. POPLE: Proc. Phys. Soc., 68A, 591 (1955)
17. G. N. LEWIS, T. T. MAGEL, D. LIPKIN: J. Amer. Chem. Soc., 64, 1774 (1942)
18. N. C. DENO, J. J. JARUZELSKI, A. SCHRIESHEIM: J. Org.Chem., 19, 155 (1954)
19. R. H. DEWOLFE, D. E. JOHNSON, R. I. WAGNER, W. G. YOUNG: J. Am. Chem. Soc., 79, 4798 (1957)
20. T. W. CAMPBELL, W. G. YOUNG: J. Am. Chem. Soc., 69, 688 (1947)
21. I. V. GOSTUNSKAIA, N. I. TIUN'KINA, B. A. KAZANSKII: DAN USSR, 108, 473 (1956)
22. A. I. SHATENSHTEIN, L. N. VASIL'EVA, N. M. DYKHNO, E. A. IZRAILEVICH: DAN USSR, 85, 381-384 (1952) (See CB P-11 , $11.00); ZFKh, 28, 193, (1954)

TOM VI, Vyp. 5 OPTIKA I SPEKTROSKOPIIA Mai, 1959
VOL. VI, No. 5 OPTICS AND SPECTROSCOPY May, 1959

Optical Investigation of the Molecular Structure of Cyanamide and its Derivatives
I. Molecular Structure of Dicyanamide

B. I. SUKHORUKOV AND A. I. FINKEL'SHTEIN

Abstract: An investigation of the infrared absorption spectra of crystals of dicyanamide, deuterodicyanamide and their silver salts, and a study of the Raman spectra of dicyanamide solutions has shown that the structure of dicyanamide corresponds to the structural formula

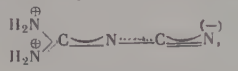

while that of the silver salt corresponds to the formula

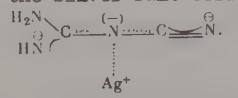

In spite of the large number of papers (see reviews [1,2] devoted to the elucidation of the molecular structure of dicyanamide (a dimer of cyanamide), until the present time there has not been a simple solution to this problem. Of the structural formulae proposed for dicyanamide by various authors, only the following three deserve attention:

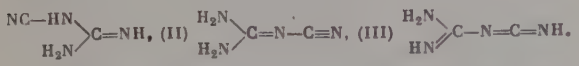

Structure I was proposed by Bamberger [3] in 1880, II by Pohl in 1906 [4], and III by Ratke (see [1]) in 1888, and recently advanced anew by Dangian [5].

The physico-chemical investigations which have been made give rather ambiguous results. Thus, Kohlrausch and coworkers [6,7] interpret the Raman spectra in terms of formula I. However Hughes [8], in a discussion of the results of an X-ray investigation, uses formula II, including the delocalization of the π-electrons.

The present work is devoted to an investigation of the molecular structure of dicyanamide by means of vibration spectra.

The infrared spectra of crystalline dicyanamide and deuterodicyanamide were obtained by a KBr pellet method to be described elsewhere.

Deuterodicyanamide was obtained by a single exchange with heavy water in which 5% dicyanamide was dissolved. The duration of the isotope exchange was 3-5 days.

The silver salts of dicyanamide and deuterodicyanamide were obtained by the reaction with silver nitrate in solutions in light and heavy water. The KBr pellet method was unsuited to investigation of the spectra of the silver salts owing to the gradual change of the spectra with time. Therefore the spectra of these salts were obtained from a paste of material in Vaseline (7-15 μ) and fluorocarbon oil (2-7 μ).

The Raman spectrum was obtained with an ISP-51 spectrograph with illumination by a single source. A filter made either of a saturated solution of sodium nitrite (which singles out radiation of $\lambda = 4358$ Å) or of glass selective of the mercury line at $\lambda = 4047$ Å was employed. Liquid ammonia was used as a solvent, since dicyanamide is more soluble in it than in water.

The absorption spectra of crystals of dicyanamide* and deuterodicyanamide are presented in figure 1.

*The IR spectrum of dicyanamide, carried out in hydrocarbon oil medium, has been reported by Bellamy [9].

The Raman spectrum of dicyanamide in ammonia is given in the table. As is seen from figure 1, the spectrum of dicyanamide in the 2200 cm^{-1} region shows an absorption band split into two components.

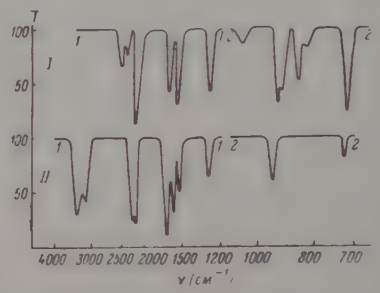

Figure 1 Infrared absorption spectra of crystals of deuterodicyanamide (I) and dicyanamide (II) 1-0.33% and 2-1% in a mixture with KBr.

Since the splitting vanishes, the splitting can only be caused by Fermi resonance. If the splitting of the C≡N band were connected with intermolecular interaction or the presence of tautomers, then in deuterodicyanamide the splitting ought to remain. The band maximum is at 2125 cm^{-1}. This value is noticeably lower than the average of the two split frequencies of undeuterated dicyanamide at 2175 $\pm$7 cm^{-1} (an average of our measurements and literature data).

In the N-H region of the IR spectrum two wide bands are found, which correspond to the symmetrical and antisymmetrical stretching vibrations of the NH_2 group. The corresponding N-D bands are found in the spectrum of deuterodicyanamide.

In the double bond region of the IR spectrum of dicyanamide three bands are found, with maxima at 1670, 1575, and 1517 cm^{-1}. Deuteration causes the 1517 cm^{-1} band to disappear. This band is consequently attributed to the deformation vibration of the NH_2 group, while the others are ascribed to multiple bonds. In this region of the Raman spectrum, only the deformation vibration band of the N-H bond at 1527 +5 cm^{-1} (average of literature and our data) is distinctly found. Two other bands are so weak that their determination is difficult.

The bands in the 2150-2200 cm^{-1} region of the Raman spectrum are most intense, while in the infrared their intensity is close to the intensity of the bands in the 1700-1500 cm^{-1} region.

We shall now compare the results with the structural formulae I, II and III. If the molecular structure of dicyanamide were given by I or III, then in the N-H region we should anticipate three (or four) bands, corresponding to the groups $-NH_2$, $>NH$, and $=NH$. In reality only two bands are found under our experimental conditons, which argues for formula II, where there is only the NH_2 group.

Crystalline dicyanamide [8]	Aqueous solution of dicyanamide [7]	Solution of dicyanamide in liquid NH_3 (our data)
—	—	259 (0)
—	—	380 (0)
500 (3)	—	505 (1/2)
516 (3)	—	530 (1/2)
582 (1)	—	624 (1/2)
669 (8)	655 (1)	671 (1)
—	—	808 (1/2)
936 (10)	927 (2)	920 (2)
1097 (4)	1111 (1)	1085 (1/2)
1171 (1)	—	—
1411 (1/2)	—	—
1528 (1)	—	1526 (1)
1649 (0)	1648 (1)	—
2158 (12)	2156 (3)	2147 (4)
2202 (6)	2195 (3)	2194 (4)
3138 (1в)	—	—
3330 (2в)	—	3359 (0)
3449 (1/2)	—	3408 (1/2)

The presence of two bands, at 1670 and 1575 cm^{-1}, which are attributed to skeletal vibrations, cannot be explained on the basis of formula I in which the isolated double bond can give only one band.

The frequency of the C ≡ N bond in this case ought to be close to the frequency of the corresponding bands in cyanamide (2232 cm^{-1}) or dimethylcyanamide (2206 cm^{-1}), while the found value was much lower, at 2175 ±7 cm^{-1}.

Structural formula III cannot explain the presence of intense bands in the 1500-1700 cm^{-1} region. All compounds containing the allene group show [10] an intense band in the Raman spectrum with frequency less than 1400 cm^{-1}.

An antisymmetrical band in the Raman spectra of symmetrical molecules with "accumulated" double bonds, found in the 1900-2200 cm^{-1} region, generally are significantly less intense than the band corresponding to symmetrical vibration. In the Raman spectrum of dicyanamide the bands in the region 1900-2200 cm^{-1} are most intense.

Thus examination of the absorption bands and Raman bands of the multiple bonds, as well as study of the N-H bond bands, militates against the assigment of structural formulas I or III to dicyanamide.

To investigate the applicability of formula II to the spectroscopic properties of dicyanamide, we studied compounds of the formula $R_2C{=}N{-}CN$, where R is an alkyl radical. These compounds were obtained in our laboratory by Gol'dberg and Golov [11]. In all the compounds investigated (detailed description to be given elsewhere) two bands were found in the 1500-1700 cm^{-1} region of the infrared spectrum -- a feature characteristic of the cyanimide grouping. Thus, the presence in the spectrum of dicyanamide of two absorption bands at 1670 and 1515 cm^{-1} confirms the presence in it of the cyanimide grouping, corresponding to formula II.

The C≡N frequency in the spectrum of dicyanamide is also in agreement with formula II. In reality, the average position of the Fermi resonance components, 2175 ±7 cm^{-1}, is lower than the C ≡ N frequency in cyanamide (2232 cm^{-1}) and dimethylcyanamide (2206 cm^{-1} [10]) - a fact which is explained by the conjugation of the bonds.

The high intensity of the C≡N band in the Raman spectrum corresponds to the increase in intensity noted by Shigorin [12] with increase in the multiplicity of bonds, and is also connected with the presence of conjugation. The weakening of the C= N band in the Raman spectrum can be attributed to the influence of the amino group analogous to the influence established by one of the authors [13] of the amino group on the intensity of the C=O band in the case of aminocarbonyl compounds.

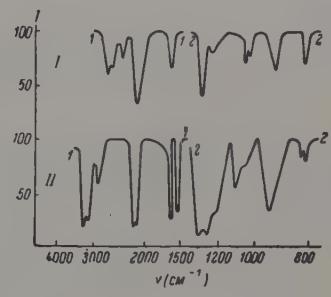

Figure 2 Infrared absorption spectra of crystals of the silver salts of deuterodicyanamide (I) and dicyanamide (II).

Thus the only structural formula possible for dicyanamide is II. Using conventional designations [14], we can represent the molecular structure of dicyanamide by the formula

(IV)

The conjugation of multiple bonds and influence of the amino group leads to the equalizing of the orders of double and single bonds. Under this circumstance the C ····· N distance may be equal to or even less than the C ═ N distance, since the carbon atom giving rise to the first bond is in the sp valence state, and thus produces a shorter bond than the sp^2 carbon atom which gives rise to the C ═ N bond [15]. These considerations explain the results of the X-ray study, in which a lower value was obtained for the N----C≡ distance than for the >C=N distance.

In order to study the transformation of dicyanamide on salt formation we investigated the infrared absorption spectra of silver salts of dicyanamide and deuterodicyanamide (fig. 2).

Three bands are found in the spectra of the salts in the N-H and N-D region. This shows that, besides the amino group, there is also an N-H bond in the salt molecule.

The C≡N band in the spectrum of the silver salt of dicyanamide is split into two components with ν_{max} at 2200 and 2175 cm^{-1} and $\nu_{av.}$ at 2187 cm^{-1}. Here also we find a lowering of the C≡N frequency in comparison with cyanamide and dimethylcyanamide, showing a reduction of the order of this bond.

In the 1500-1700 cm^{-1} region of the IR spectrum of the silver salt of dicyanamide two absorption bands are found at 1615 and 1550 cm^{-1}. On deuteration the 1550 cm^{-1} band disappears, which indicates its origin in the N-H deformation vibration. The 1615 cm^{-1} band shows that the C= N double bond is present in the silver salt of dicyanamide. All the aforementioned correspond to the structural formula

Ag^+

June 24, 1958

References

1. F. CHASTELLAIN: Helv. Chim. Acta, 18, 1287 (1935)
2. A. E. KRETOV: Usp. Khim., 23, 105 (1954)
3. E. BAMBERGER: Ber., 16, 1074 (1883)
4. F. POHL: J. Prakt. Chem. (2), 77, 533 (1908)
5. M. T. DANGIAN: DAN Arm. SSR, 1, 22 (1944)
6. A. DADIEU, K. W. F. KOHLRAUSCH: Monatsh. f. Chem., 57, 225 (1931)
7. L. KAHOVEC, K. W. F. KOHLRAUSCH: Z. phys. Chem. 193, 188 (1944)
8. E. W. HUGHES: JACS, 62, 1258 (1940)
9. L. J. BELLAMY: Infrared Spectra of Complex Molecules, Wiley & Sons, N. Y., 1954 (IL, 1957)
10. K. W. F. KOHLRAUSCH: Ramanspektren, Akad. Verlagsgesell., Leipzig, 1943 (IL, 1952)
11. N. A. GOL'DBERG, V. G. GOLOV: Khim. Nauka i Promyshl., (In press)
12. P. P. SHORYGIN: ZFKh, 21, 1125 (1947)
13. A. I. FINKEL'SHTEIN: ZFKh, 30, 2061 (1956)
14. A. I. FINKEL'SHTEIN: ZFKh, 31, 1659 (1957)
15. A. I. FINKEL'SHTEIN: ZFKh, 32, 1817 (1958)

TOM VI, Vyp. 5
VOL. VI, No. 5

OPTIKA I SPEKTROSKOPIIA
OPTICS AND SPECTROSCOPY

Mai, 1959
May, 1959

Dependence of the Probability of Energy Transport in Sensitized Phosphorescence on the Oscillator Strength of a Triplet-Singlet Transition in an Energy Acceptor Molecule*

V. L. ERMOLAEV

Abstract: The quenching of luminescence from an energy donor in the presence of an equal concentration of acceptors in the phenomenon of sensitized phosphorescence does not change appreciably when napthalene is replaced by 1-chloro, 1-bromo or 1-iodonaphthalene in the role of acceptor. From the theory of non-radiative energy transfer (Galanin, Förster, Dexter) it follows that for an inductive interaction of the electromagnetic fields of the molecules taking part in the transfer, the magnitude of the quenching of the donor luminescence depends strongly on the probability of a radiative transition in the acceptor. To the extent that the probability of quenching in sensitized phosphorescence does not depend on the oscillator strength of the triplet-singlet transitions in the acceptor(in the series of the halogen derivatives of napthalene the probability of the triplet-singlet transition changes by three orders of magnitude), it follows that the phenomenon of sensitized phosphorescence is governed by exchange-resonance effects and not by the interaction of the electromagnetic fields of the energy donor and acceptor molecules.

In 1952 Terenin and the author [1, 2] discovered the phenomenon of sensitized phosphorescence in aromatic compounds. Furthermore, we studied the properties of this phenomenon [3-5] and showed that during sensitized phosphorescence a resonance transfer of electron energy takes place with the direct excitation of the triplet level of the acceptor. The present work is an investigation of the way in which the energy transfer process between triplet levels is affected by the oscillator strengths of the triplet-singlet transition in the energy acceptor, with the aim of answering the question of the nature of the interaction responsible for the resonance transfer of energy during sensitized phosphorescence.

In a large number of previous papers (cf. references [6-8])the phenomena of sensitized fluorescence, concentration depolarization and concentration quenching of the fluorescence of solutions of organic compounds have been investigated. In this case we consider an interaction between singlet excited and unexcited (also singlet) molecules, i.e. with the dipole-dipole interactions of allowed transitions. The theoretical concept of the interaction of the electromagnetic fields of molecules, leading in the cases mentioned to a non-radiative transfer of electronic excitation energy, was developed in the works of Jean and Francis Perrin [9-11], Vavilov [12-14], Galanin [8,15], Galanin and Frank [16], Förster [17-19] and Dexter [20]. As was shown in these papers, the strength of the interaction between excited and unexcited molecules leading to the energy transfer and, hence, the critical concentration for quenching** depend on the overlap of the acceptor absorption spectrum with the donor emission spectrum. The transfer probability increases with increasing overlap of the spectra (normalized to unit area). Experimental confirmation of this was found in the work of Vavilov, Galanin and Pekerman [14], and also of Förster [17,20], and Galanin and Levshin [22], in which they showed that the magnitude of the reduction in τ for the quenching of the fluorescence by foreign absorbing substances is approximately proportional to the average absorption coefficient of quenching, averaged over the fluorescence spectrum, and is almost independent of the τ_0 of the fluorescing substance.

According to the theory of Förster [19] for the dipole-dipole interaction (for a given acceptor concentration), the energy transfer should be directly proportional to the oscillator strength of the transition in the acceptor if the magnitude of the overlap of the spectra remains constant. The critical acceptor concentration is inversely proportional to the square root of the oscillator strength of the appropriate transition in the acceptor, or directly proportional to the square root of the relaxation time of the corresponding luminescence.

We studied the applicability of these concepts to the phenomenon of sensitized phosphorescence, since it was shown by the experiments of Weissman and Lipkin with the interference of dispersed rays that the phosphorescent radiation (in the case of dyes) has a dipole character. One would expect a strong dependence of the transport probability in sensitized phosphorescence on the oscillator strength of the triplet-singlet transition in the acceptor for a given donor and for an approximately equal overlap of the spectra of donor emission and acceptor absorption. In the case of sensitized phosphorescence we cannot measure directly the spectrum of the triplet-singlet absorption in the acceptor; however one may expect that it will be approximately the mirror image of the emission spectrum of the phosphorescence. Hence in order to check the dependence of the transport probability in sensitized phosphorescence on the oscillator strength of the acceptor transition, we need a series of acceptors having identical phosphorescence spectra and differing sharply in their relaxation times. In our case these requirements are met by the series of halogen derivatives of napthalene, (napthalene, 1-chloro, 1-bromo and 1-iodonapthalene). In table 1 are listed the spectroscopic characteristics of the above napthalene derivatives.

However our experiments on the quenching of the phosphorescence of benzophene or benzaldehyde by various napthalene derivatives showed that the magnitude of the quenching of the donor emission by an identical acceptor concentration was the same for the whole series, beginning with napthalene and ending with 1-iodonaphthalene. (See Table 2).

---

* This work was reported on at the VI Conference on Luminescence (Leningrad Feb. 1958).

** The critical quenching concentration is defined as the acceptor concentration for which the transport probability is equal to the emission probability of the energy donor molecule, i.e. when the intensity of the donor luminescence has fallen by one half.

Table 1

Compound	$\nu^*_{Phosp.}$ (in cm^{-1})	$\tau^*_{Phosp.}$ (in sec.)	$\eta^*_{Phosp.}$ Quant.
Napththalene	21250	2.3	0.095***
1-Chloronapthalene	20700	0.29	0.54 ± 0.04
1-Bromonapthalene	20650	0.018**	0.55 ± 0.09
1-Iodonaphthalene	20500	0.002	0.70 ± 0.09

Notes: $\nu^*_{Phosp.}$ is the height of the triplet level in cm^{-1}, determined from the position of the first band in the phosphorescence spectrum; $\tau_{Phosp.}$ is the relaxation time of the phosphorescence; $\eta_{Phosp.\ Quant.}$ is the quantum yield of the phosphorescence. All measurements were made in a mixture of alcohol and ether (2:1) at -195° C.

** From the data of McClure [24].
*** From the data of McClure and co-workers [25].

Table 2

Quenching of the donor phosphorescence I/I_0 (excited at $\lambda = 3650$ Å) in the presence of various energy acceptors in a concentration of $3.2 \cdot 10^{-1}$ mol/l. in a mixture of alcohol and ether at -195° C.

Acceptor	I/I_0 Donor: Benzophene C = 2.10^{-2} m/l.	I/I_0 Donor: Benzaldehyde C = 2.10^{-2} m/l.
Napthalene	0.19 ± 0.03	0.27 ± 0.04
1-Chloronapthalene	0.16 ± 0.03	0.26 ± 0.04
1-Bromonapthalene	0.19 ± 0.03	0.25 ± 0.04
1-Iodonapthalene	0.19 ± 0.03	–

The amount of quenching was the same for all acceptor concentrations investigated. In figure 1 are plotted the curves of the quenching of the benzophene luminescence by napthalene (circles) and by 1-bromonapthalene (crosses); the horizontal axis gives the molar concentration of the acceptors, and the vertical axis the amount of quenching $\frac{I_0 - I}{I}$. Regardless of the fact that the oscillator strengths of napthalene and 1-bromonapthalene differ by a factor of a hundred, they quench the luminescence of benzophene equivalently. Also in figure 1 is shown the reduction of the relaxation time of the benzophene luminescence in the presence of napthalene (solid circles) and 1-bromonapthalene (triangles); as in the case of the quenching, the change in the relaxation time is the same in both cases. As has already been pointed out in a paper by the author [3], the quenching during sensitized phosphorescence increases considerably faster than the decrease in relaxation time.

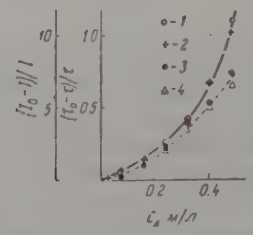

Figure 1. Quenching of the phosphorescence of benzophene. The napthalene concentration in mol/l. is plotted on the horizontal axis; the solution was alcohol and ether at -195°C., ($\lambda_{exc.}$ = 3650 Å.)

The slope of the tangent to the quenching curve is approximately ten times larger than the slope for the curve of $\frac{\tau_0 - \tau}{\tau}$ near the origin. In the case of sensitized fluorescence and the concentration quenching of fluorescence, the slopes of the curves differ only by a factor of two (see the papers of Galanin [26] and Sveshnikov [27]). The quenching curves for sensitized phosphorescence can be well described by the formula $(I_0 - I)/I = e^{\alpha C} - 1$, where α is a constant, contrary to the case of concentration quenching of dyes (see reference [28]). Hence the energy transfer mechanism in sensitized phosphorescence differs in a number of important ways from the usual energy transfer mechanism for concentration effects in solutions of dyes. Although the quenching of donor luminescence in sensitized phosphorescence does not change for the above series of napthalene derivatives, the relative emission of sensitized phosphorescence, defined as the ratio of the number of quanta I_A emitted by the acceptor to the number of quanta I_D emitted by the donor, increases rapidly during the transition from napthalene to chloro, bromo, and iodonapthalene. Hence as the oscillator strength of the triplet-singlet transition in the acceptor increases (i.e. with a decrease in the relaxation time of the donor phosphorescence) the relative emission of sensitized phosphorescence increases. Data on the relative emissions of sensitized phosphorescence are given in figure 2. However even the increase of the emission takes place much more slowly with increasing oscillator strength of the acceptor transition than would be expected for an interaction of two electric dipoles (allowed transitions). Since the amount of quenching of the benzophene and benzaldehyde luminescence remains nearly constant during the change from napthalene to its halogen derivatives, whereas the relative emission of sensitized luminescence increases, there should be a corresponding increase in the ratio of the number of energy quanta emitted by the acceptors to the number of quenched energy acceptor molecules i. e. the quantity $\frac{I_A}{I_{0D} - I_D}$. should increase. In Table 3 the values of these ratios are given. During the change from napthalene

to its chloro, bromo, iodo derivatives there is an increase in the share of the energy, absorbed by the donor, which goes into the sensitized phosphorescence and there is a decrease in the share which is simply dissipated by the molecule. It is possible that this is related to a different probability of phosphorescent emission (i. e. triplet-singlet transition), which is rapidly increasing in the series used, and to a related change in the usual phosphorescent emission of the napthalene derivatives (cf. Table 1). On the other hand an increase in the triplet-singlet probability in the acceptor might influence the transfer mechanism itself, increasing the interaction and leading to an energy transfer without dissipating all the electron energy as heat.

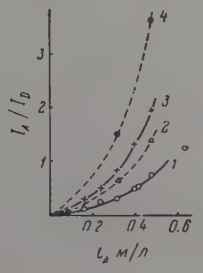

Figure 2 Relative emission of sensitized phosphorescence of the 1-halogen derivatives of napthalene I_A/I_D (the donor was benzophene, λ_{exc} = 3650 Å) 1. napthalene. 2. 1-chloronapthalene 3. 1-bromo napthalene 4. 1-iodonapthalene. The molar concentration of the acceptor in a mixture of alcohol and ether at -195° is plotted on the horizontal axis. (The Curves for 1-chloro and 1-bromonapthalene are given only for comparison and are not intended to give an accurate description of the dependence of emission on concen tration.).

Table 3

The emission of sensitized phosphorescence in relation to quenched energy-donor intensity for an acceptor concentration of 3.2 10^{-1} mol/l. in a mixture of alcohol and ether at -195° C.

Acceptor	$\frac{I_A}{I_{oD} - I_D}$ Donor		
	Benzophene C=2.10^{-2} m/l	Benzaldehyde C=2.10^{-2} m/l	Xanthone C = 1.10^{-2} m/l
Napthalene	0.07	0.13	0.11
1-Chloronapthalene	0.12	0.22	–
1-Bromonapthalene	0.20	0.27	–
1-Iodonapthalene	0.35	–	–

The sum total of the experimental facts described above does not agree with the idea that the interaction of the electromagnetic fields of the molecules provides the mechanism for energy transport in sensitized phosphorescence. As a further test of this difficulty the average separation between the energy donor and acceptor molecules for the critical concentration of the latter $C_{\frac{1}{2}}$ (i.e. for quenching of the donor luminescence by a factor of one half) for the pair benzophene + napthalene, calculated from the

formula $\bar{R}_{\frac{1}{2}} = \frac{7.35}{\sqrt[3]{C_{\frac{1}{2}}}} \cong 14$ Å was compared with

the separation as found from Förster's formula [19], which was derived under the assumption of an electric dipole-dipole interaction. A rough estimate of this separation for the same pair benzophene + napthalene gives the quantity 1.1 Å , which differs by an order of magnitude from a separation for the given pair found from experiment (about 14Å) and which is also considerably smaller than the size of the interacting molecules themselves. This is further demonstration that the theory developed on the assumption of the interaction of excited and non-excited atoms via the electromagnetic fields is not applicable to the phenomenon of sensitized phosphorescence.

In the theoretical papers [8,15,16,19,20,29] the following cases of intermolecular interaction of an excited donor molecule and an unexcited acceptor molecule have been treated, leading in all cases to a non-radiative transfer of energy: 1) the interaction of two electric dipoles, 2) the interaction of an electric quadrupole with a dipole, 3) the interaction of electric dipoles and quadrupoles, 4) the interaction of an electric and a magnetic dipole and finally, 5) the exchange interaction arising from an overlap of the electron clouds of the interacting molecules. According to an estimate of Dexter, [20], in going from the first case to the third the efficiency of the transfer falls by approximately a factor of thirty, and in the fourth case by a factor of 10^8 . Exchange effects lead to a transport efficiency of the same order as the dipole-quadrupole interaction (case 3). Interactions of types 1-4 (and also interactions of electric and magnetic multipoles of higher order) should lead to a strong dependence of the probability of energy transfer on the oscillator strength of the excited electron transition in the acceptor (for an equal overlap of the spectra, normalized to unit area). The natural type of transport, for which the above dependence would not hold, would be an exchange interaction. This sort of interaction occurs when there is an overlap of the outer parts of the electron clouds of the interacting energy donor and acceptor molecules. According to Dexter the matrix element of the exchange interaction of an excited donor molecule and an unexcited acceptor has the form

$$\langle H \rangle = \int \varphi'^{*}_{D}(\vec{r}_1) \cdot \varphi^{*}_{A}(\vec{r}_2) \cdot H \cdot \varphi'_{A}(\vec{r}_1) \cdot \varphi_{D}(\vec{r}_2) \times$$

$$\times \chi'^{*}_{D}(\vec{\sigma}_1) \cdot \chi^{*}_{A}(\vec{\sigma}_2) \cdot \chi'_{A}(\vec{\sigma}_1) \cdot \chi_{D}(\vec{\sigma}_2) d\tau .$$

Here the prime refers to an excited state and the asterisk to a complex conjugate quantity. The spin part $\chi(\vec{\sigma})$ may be factored out of the wave function $\psi(\vec{r},\vec{\sigma}) = \varphi(\vec{r}) \cdot \chi(\vec{\sigma})$. Since H does

not operate on $\chi(\vec{\sigma})$ the above integral is non-zero only in the case that its spin function is not equal to zero. From this fact we get a selection rule for these transitions; the exchange integral is non-zero only if $\chi'_D = \chi_A$, and $\chi_A = \chi_D$. At the same time however χ' is not necessarily equal to χ, i. e. the spin functions of both molecules may change in a similar fashion. This last rule is analogous to the selection rule of Wigner, which is satisfied in the case of sensitized phosphorescence, as has already been pointed out in previous papers by Terenin and the author [1, 2].

The probability of energy transfer by the exchange mechanism may be written in the form (cf. 20):

$$P_{DA}(ex) \cong (2\pi/\hbar)\, Y \exp\left(-\frac{2R}{L}\right) \int F_D(\nu)\, \epsilon_A(\nu)\, d\nu$$

where $F_D(\nu)$ is the donor emission spectrum and $\epsilon_A(\nu)$ is the corresponding acceptor absorption spectrum, (where both spectra are normalized to unit area). According to Galanin [8], the integral may be understood as an expression of the Franck-Condon principle for the non-radiative transfer of energy between two molecules. Y is a dimensionless quantity $\ll 1$, R is the separation between the energy donor and acceptor molecules, and L is the effective Bohr radius of the excited and unexcited molecules. The exponential factor $\exp[\frac{-2R}{L}]$ appears due to the fact that the electron cloud density of a molecule falls off exponentially with distance. Thus for exchange interactions the transfer probability falls exponentially with increasing separation, i.e. much faster than for the case of two interacting electric dipoles (R^{-6}). These concepts are in good agreement with the large divergence in the quenching rates $\frac{I_o - I}{I}$ and the reduction in the donor relaxation time $\frac{\tau_o - \tau}{\tau}$ in the presence of an acceptor, which we pointed out above; the concepts agree also with the exponential dependence of the amount of quenching on the acceptor concentration.

It should be pointed out at once that the overlapping of the electron clouds of the energy donor and acceptor molecules, which is necessary for energy transfer via the exchange mechanism, does not have any noticeable effect on the positions of the electron levels of the interacting molecules nor on the probability of transitions between them. As was shown in papers by Terenin and the author [2,5] the phosphorescence spectrum of the energy acceptor remains constant independently of whether the acceptor is excited in its own absorption band or by means of a non-radiative energy transfer from a donor, absorbing the excited radiation. The relaxation time of the acceptor afterglow is also constant in both cases considered (cf.[3]).

Thus the phenomenon of sensitized phosphorescence has opened up the possibility of studying a new type of resonance transfer during exchange interactions between organic molecules. There is a series of very important and interesting phenomena in which these exchange effects may play a very important role. Among these we must first of all point out photosynthesis in green plants. It is well known that the concentration of chlorophyll in the surface of leaves is 0.1 mole/l. and that this corresponds to precisely the separation between molecules for which exchange-resonance interactions are important. One must also mention the sensitization of photoconducting semiconductors and the sensitization of photographic emulsions by means of dyes. The dyes, in these cases, are firmly absorbed on the surface of the semiconductor and hence their electron clouds interact strongly with the electron cloud of the semiconductor.

The method applicable to treatment of these problems is analogous to that described by Terenin and the author [5].

In conclusion I consider it my pleasant duty to extend my deep thanks to Academician A. N. Terenin for suggesting this problem and guiding it to its conclusion.

July 20, 1958

References

1. A. N. TERENIN, V. L. ERMOLAEV: DAN USSR, 85(3), 547-550 (1952) (See NRC TT-529)
2. V. L. ERMOLAEV, A. N. TERENIN: Pamiati S. I. VAVILOVA (In memory of S. I. Vavilov), Moscow 1952, pp. 137-146 (See NRC TT-540)
3. V. L. ERMOLAEV: DAN USSR, 102, 925 (1955)
4. V. L. ERMOLAEV: IAN USSR FS, 20(5), 514 (1956) (See CTT Bulletin, p. 471)
5. A. N. TERENIN, V. L. ERMOLAEV: Trans. Faraday Soc., 52, 1042 (1956)
6. A. N. TERENIN: UFN, 43, 347-379 (1951)
7. A. N. TERENIN, V. L. ERMOLAEV: UFN, 58, 37-68, (1956) (See AEC-tr-3031 , 64 pp. for translation of references 6 and 7)
8. M. D. GALANIN: Rezonansnyi perenos energii vozbuzhdeniia v liuminestsiruiushchikh rastvorakh (Resonance transfer of excitation energy in luminescent solutions) Doct. Diss. FIAN USSR, Moscow, 1955
9. J. PERRIN: C.R., 184, 1097 (1927)
10. J. PERRIN: 2me Conseil de chim. Solvay, Paris 1925, p. 322
11. F. PERRIN: C.R., 192, 1727 (1932)
12. S. I. VAVILOV: Mikrostruktura sveta (Microstructure of light), Coll. Works, Akad. Nauk Press, 2, 383, 1952
13. S. I. VAVILOV: ZETF, 13, 13-32 (1943) (See AEC-tr-3185)
14. S. I. VAVILOV, F. M. PEKERMAN, M. D. GALANIN: IAN USSR FS, 13, 18-32 (1949) (See LC RT-896 28 pp.)
15. M. D. GALANIN: ZETF, 21, 126 (1951)
16. M. D. GALANIN, I. M. FRANK: ZETF, 21, 114 (1951)
17. T. FÖRSTER: Zs. Elektrochem., 53, 93 (1959)
18. T. FÖRSTER: Naturwiss., 33, 166 (1946)
19. T. FÖRSTER: Ann. Phys., Series 6, 2, 55-75 (1948) (See SLA 2996, 37 pp.)
20. D. L. DEXTER: J. Chem. Phys., 21, 836 (1953)
21. T. FÖRSTER: Zs. Naturforschung, 4a, 321 (1949)
22. M. D. GALANIN, L. V. LEVSHIN: ZETF, 21, 121 (1951)
23. S. I. WEISSMAN, D. LIPKIN: JACS, 64, 1916 (1942)
24. D. S. MC CLURE: J. Chem. Phys., 17, 905 (1949)
25. E. H. GILMORE, G. E. GIBSON, D. S. MC CLURE: J. Chem. Phys., 20, 829 (1952); 23, 399 (1955)
26. M. D. GALANIN: ZETF, 28, 485 (1955) (See Soviet Physics JETP)
27. B. IA. SVESHNIKOV: DAN USSR, 115, 274 (1957) (See Soviet Physics Doklady)
28. F. PERRIN: C.R., 178, 1978 (1924)

TOM VI, Vyp. 5 OPTIKA I SPEKTROSKOPIIA Mai, 1959
VOL. VI, No. 5 OPTICS AND SPECTROSCOPY May, 1959

Influence of Reabsorption on the Yield and Duration of Luminescence of Molecular Crystals. I

V. M. AGRANOVICH, IU. V. KONOBEEV

Abstract: A kinetic equation, which describes the exciton distribution in a molecular crystal by taking into account the reflection of luminescent light from the crystal surface is analyzed. For the case when the exciton diffusion coefficient is small enough, exact formulas are obtained which determine the quantum yield and the duration of the luminescence of crystals having the shape of plane-parallel plates of any thickness. The formulas for the quantum yield permit the spectral curve of the crystal luminescence to be calculated.

INTRODUCTION

In previous computations using the phenomenological theory of excitons in molecular crystals [1-3], it has been assumed implicitly that the reflection of the luminescent light from the crystal surface may be neglected. However, as shown by experiment [4], the reflection of the luminescent light from the crystal surface appears to be an essential factor which, in certain cases, affects the shape of the luminescence curve.

Let us assume that the crystal has the shape of a plane-parallel plate bounded by the planes $x = 0$ and $x = d$. In this case, the following integro-differential equation can be written for the exciton concentration $C_1(\vec{r},t)$, taking reflection of the luminescent light from the crystal surface into account *

$$\frac{\partial C_1}{\partial t} = D\Delta C_1 - PC_1 + \Phi_0 \exp[-kx] + \frac{P}{4\pi}\int_0^\infty d\nu E(\nu)\eta(\nu)k(\nu)\int_V C_1(\vec{r}_1,t)\frac{\exp\left[-k(\nu)|\vec{r}-\vec{r}_1|\right]}{|\vec{r}-\vec{r}_1|}dV_1 + \frac{P}{4\pi}\int_0^\infty d\nu E(\nu)\eta(\nu)k(\nu)\int_V C_1(\vec{r}_1,t)\left[\frac{\exp\left[-k(\nu)|\vec{r}-\vec{r}_2|\right]}{|\vec{r}-\vec{r}_2|}r_\nu(\cos\theta_1) + \frac{\exp[-k(\nu)|\vec{r}-\vec{r}_3|]}{|\vec{r}-\vec{r}_2|^2}r_\nu(\cos\theta_2)\right]dV_1, \quad (1)$$

where D is the exciton diffusion coefficient; P the total probability of an exciton disappearing each second; $\eta(\nu)$ the molecular quantum yield under excitation by light of frequency ν; $E(\nu) = \frac{\rho(\nu)}{\int_0^\infty \rho(\nu)\,d\nu}$ where $\rho(\nu)$ is the density of the total probability of the quantum $h\nu$ being emitted per second due to luminescence of the exciton in any direction; $k(\nu)$ is the absorption coefficient of light of frequency ν in the crystal; $k = \frac{\bar{k}}{\cos\theta_0}$, where $\bar{k}$ is the absorption coefficient for light incident on the crystal at the angle θ_0; $r_\nu(\cos\theta) = \sum_{n=0}^{\infty} a_n^{(\nu)}\cos^n\theta$ is the reflection coefficient of the luminescent light of frequency ν incident at the angle θ on the crystal surface from within. The vectors $\vec{r}_2$ and $\vec{r}_3$ are defined by the relations $\vec{r}_2 \equiv (-x_1, y_1, z_1)$, $\vec{r}_3 \equiv (2d-x_1, y_1, z_1)$, $\cos\theta_1 = \frac{x + x_1}{|\vec{r} - \vec{r}_2|}$, $\cos\theta_2 = \frac{2d - x_1 - x}{|\vec{r} - \vec{r}_3|}$.

*The anisotropy of the optical properties of the crystal has not been taken into account in (1).

A kinetic equation describing the energy migration in luminophors with a low exciton diffusion coefficient has been considered here. In this case, the diffusion component in (1) can be discarded.

Let us introduce the nondimensional quantities

$$z = k_0 x,\ \gamma = \frac{k}{k_0},\ C(z,\tau) = \frac{PC_1(\vec{r},t)}{\Phi_0},\ \tau = Pt, \quad (2)$$

$$b(\nu) = \frac{k(\nu)}{k_0},\ a(\nu) = \frac{1}{2}E(\nu)\eta(\nu),\ z_0 = k_0 d.$$

The quantity $k_0 \equiv k(\nu_0)$, where ν_0 is the frequency at which the function $a(\nu)$ has a maximum. Equation (1) has the following form in the usual notation

$$\frac{\partial C}{\partial \tau} = -C + \exp[-\gamma z] + \int_0^\infty a(\nu)\,b(\nu)d\nu \times \int_{z_0}^{z} C(z_1,\tau)E_1\left(b(\nu)|z-z_1|\right)dz_1 + \int_0^\infty a(\nu)b(\nu)d\nu \int_0^{z_0} C(z_1,\tau)\sum_{n=0}^{\infty} a_n^{(\nu)}\left\{E_{n+1}\left(b(\nu)(z+z_1)\right) + E_{n+1}\left(b(\nu)(2z_0 - z_1 - z)\right)\right\}dz_1. \quad (3)$$

Here

$$E_m(z) = \int_1^\infty \frac{\exp[-z\xi]}{\xi^m}\,d\xi. \quad (4)$$

Exact expressions are found in the next two paragraphs for the yield and the time of luminescence both with and without luminescent light reflection from the crystal surface taken into account.

1. DETERMINATION OF THE QUANTUM YIELD AND DURATION OF CRYSTAL LUMINESCENCE WITHOUT TAKING INTERNAL LIGHT REFLECTION FROM THE CRYSTAL SURFACE INTO ACCOUNT

In an experimental study of luminescence excited in plane-parallel samples, the determination of the intensity of light which emerges in different directions from the sample under investigation is possible. Let $J_0^{(\nu)}(\theta,t)d\nu$ denote the intensity

of the luminescent light in the frequency band $d\nu$, which emerges from the crystal at an angle θ to the external normal through 1 cm^2 of surface $x = 0$ per unit solid angle per second. Furthermore, let $J_d^{(\nu)}(\theta,t)d\nu$ define the similar magnitude of the intensity of light emerging through the crystal surface $x = d$. The quantities $J_o^{(\nu)}$ and $J_d^{(\nu)}$ are defined by the expressions

$$J_o^{(\nu)}(\theta,t) = \frac{\rho(\nu)}{4\pi}\int_0^d C_1(x,t)\exp[-k(\nu)x\sec\theta]\,dx; \tag{5}$$

$$J_d^{(\nu)}(\theta,t) = \frac{\rho(\nu)}{4\pi}\int_0^d C_1(x,t)\exp[-k(\nu)(d-x)\sec\theta]\,dx. \tag{6}$$

In place of (5) and (6), it is convenient to introduce the relative intensities by dividing these expressions by the total number of photons of the exciting radiation being absorbed per second, referred to 1 cm^2 of crystal surface. These relative intensities are expressed as follows in nondimensional variables.

$$B_o^{(\nu)}(\theta,t)k = \frac{J_o^{(\nu)}(\theta,t)k}{\Phi_o(1-\exp[-kd])} = \tag{7}$$

$$= \frac{\rho(\nu)\gamma}{4\pi P(1-\exp[-\gamma z_o])}\int_0^{z_o} C(z,\tau)\exp[-b(\nu)\sec\theta z]\,dz;$$

$$B_{z_o}^{(\nu)}(\theta,t) = \frac{J_d^{(\nu)}(\theta,t)k}{\Phi_o(1-\exp[-kd])} = \frac{\rho(\nu)\gamma}{4\pi P(1-\exp[-\gamma z_o])} \times \tag{8}$$

$$\times \int_0^{z_o} C(z,\tau)\exp[-b(\nu)\sec\theta\,(d-z)]\,dz.$$

The quantities (7) and (8) depend, through the integrals, on the function $C(z,\tau)$. These integrals can be obtained by using the Ambartsumian method [5] without looking for the function $C(z,\tau)$.

Let us first consider the stationary case without taking into account light reflection from the crystal surface; in this case, (3) is simplified considerably and becomes

$$C_o(z,\gamma) = \exp[-\gamma z] + \int_0^\infty a(\nu)b(\nu)\,d\nu \int_0^{z_o} C_o(z_1,\gamma)E_1(b(\nu)|z-z_1|)\,dz_1. \tag{9}$$

The solution of (9) depends on the quantity γ as a parameter. Taking the derivative with respect to z of both sides of (9), we find

$$C_o'(z,\gamma) = -\gamma\exp[-\gamma z] + C_o(0,\gamma)\int_0^\infty a(\nu)b(\nu)\,d\nu E_1(b(\nu)\,z) -$$

$$-C_o(z_o,\gamma)\int_0^\infty a(\nu)b(\nu)\,d\nu E_1[b(\nu)(z_o-z)] + \tag{10}$$

$$+\int_0^\infty a(\nu)b(\nu)\,d\nu \int_0^\infty C_o'(z_1,\gamma)E_1(b(\nu)|z-z_1|)\,dz_1.$$

Comparing (9) and (10) and using the integral representation of the functions $E_1[b(\nu)z]$ and $E_1[b(\nu)(z_o - z)]$ with the aid of (4), we conclude that

$$C_o'(z,\gamma) = -\gamma C_o(z,\gamma) + C_o(0,\gamma)\int_0^\infty a(\nu)b(\nu)\,d\nu\int_1^\infty \frac{C_o\left(z,b(\nu)\xi\right)}{\xi}\,d\xi - \tag{11}$$

$$-C_o(z_o,\gamma)\int_0^\infty a(\nu)b(\nu)\,d\nu\int_1^\infty \frac{\exp[-b(\nu)z_o\xi]C_o\left(z,-b(\nu)\xi\right)}{\xi}\,d\xi.$$

Let us introduce the function

$$R(\eta,\gamma) = \int_0^{z_o} \exp[-\eta z]C_o(z,\gamma)\,dz. \tag{12}$$

Multiplying (11) by $e^{-\eta z}$ and integrating with respect to z from 0 to z_o, we find

$$(\eta+\gamma)R(\eta,\gamma) = C_o(0,\gamma) - C_o(z_o,\gamma)\exp[-\eta z_o] +$$

$$+C_o(0,\gamma)\int_0^\infty a(\nu)b(\nu)\,d\nu\int_1^\infty \frac{R(\eta,b(\nu)\xi)}{\xi}\,d\xi - \tag{13}$$

$$-C_o(z_o,\gamma)\int_0^\infty a(\nu)b(\nu)\,d\nu\int_1^\infty \frac{\exp[-b(\nu)z_o\xi]\,R(\eta,-b(\nu)\xi)}{\xi}\,d\xi.$$

It follows from (9) that

$$C_o(0,\gamma) = 1 + \int_0^\infty a(\nu)b(\nu)\,d\nu\int_1^\infty \frac{R\left(b(\nu)\xi,\gamma\right)}{\xi}\,d\xi; \tag{14}$$

$$C_o(z_o,\gamma) = \exp[\gamma z_o] + \int_0^\infty a(\nu)b(\nu)\,d\nu\int_1^\infty \frac{R\left(-b(\nu)\xi,\gamma\right)}{\xi}\exp[-b(\nu)z_o\xi]\,d\xi.$$

Comparing (14) and (13), we finally find

$$R(\eta,\gamma) = \frac{C_o(0,\gamma)C_o(0,\eta) - C_o(z_o,\gamma)C_o(z_o,\eta)}{\eta+\gamma} \tag{15}$$

Now, if (15) is substituted into (14) and it is taken into account that, as follows from (9),

$$C_o(0,-\gamma) = \exp[\gamma z_o]C_o(z_o,\gamma)$$

$$C_o(z_o,-\gamma) = \exp[\gamma z_o]C_o(0,\gamma), \tag{16}$$

we obtain the following system of equations for $C_o(0,\gamma)\equiv\varphi(x)$ and $C_o(z_o,\gamma)\equiv\chi(x)$; $(x = 1/\gamma)$:

$$\varphi(x) = 1 + x\int_0^\infty a(\nu)b(\nu)\,d\nu\int_0^{\frac{1}{b(\nu)}} \frac{\varphi(x)\varphi(y)-\chi(x)\chi(y)}{x+y}\,dy.$$

$$\chi(x) = \exp[-\frac{z_o}{x}] + x\int_0^\infty a(\nu)b(\nu)\,d\nu\int_0^{\frac{1}{b(\nu)}} \frac{\varphi(x)\chi(y)-\varphi(y)\chi(x)}{y-x}\,dy. \tag{17}$$

When $a(\nu)$ has a sufficiently sharp maximum* at $\nu = \nu_0$, equations (17) are simplified

$$\varphi(x) = 1 + \frac{q}{2} x \int_0^1 \frac{\varphi(x)\varphi(y) - \chi(x)\chi(y)}{x + y} dy; \quad (18)$$

$$\chi(x) = \exp[-\frac{z_0}{x}] + \frac{q}{2} x \int_0^1 \frac{\varphi(x)\chi(y) - \varphi(y)\chi(x)}{y - x} dy,$$

where $q = 2\int_0^\infty a(\nu)d\nu$. Equations (18) in such form are in agreement with those obtained by Chandrasekhar [6] in investigations of light scattering in planetary atmospheres. If the nondimensional crystal thickness $z_0 \to \infty$, then $\chi(x) \to 0$. The systems of equations (17) and (18) are nonlinear; however, since $q < 1$, the solutions of these equations may be obtained, to any degree of accuracy, by iteration. Values of the functions $\varphi(x) \equiv \varphi_0(x)$ are presented for $z_0 = \infty$ in table 1 for different values of q. Knowledge of the functions $\varphi(x)$ and $\chi(x)$ permits $R(\eta,\gamma)$ to be found and, therefore, the quantities $B_0^{(\nu)}(\theta)$ and $B_{z_0}^{(\nu)}(\theta)$ also, since according to (7), (8), (12)

$$B_0^{(\nu)}(\theta) = \frac{\rho(\nu)\gamma}{4\pi P(1 - \exp[-\gamma z_0])} R(b(\nu)\sec\theta, \gamma), \quad (19)$$

$$B_{z_0}^{(\nu)}(\theta) \frac{\rho(\nu)\gamma}{4\pi P(1 - \exp[-\gamma z_0])} R(-b(\nu)\sec\theta, \gamma)\exp[-b(\nu)z_0\sec\theta].$$

Now, let us analyze the nonstationary region which occurs in a luminophor upon the instantaneous cessation of the illumination. The average decay time of the luminescence in the θ direction can be determined as follows:

$$\bar{\tau}_1(\theta) = \frac{P\int_0^\infty d\nu \int_0^\infty B_0^{(\nu)}(\theta,t)\,dt}{\int_0^\infty d\nu B_0^{(\nu)}(\theta,0)} = \quad (20)$$

$$= \frac{\int_0^\infty \rho(\nu)d\nu \int_0^\infty d\tau \int_0^{z_0} C(z,\tau)\exp[-b(\nu)\sec\theta\, z]dz}{\int_0^\infty \rho(\nu)d\nu \int_0^{z_0} C_0(z,\gamma)\exp[-b(\nu)\sec\theta\, z]dz};$$

$$\bar{\tau}_2(\theta) = \frac{P\int_0^\infty d\nu \int_0^\infty B_{z_0}^{(\nu)}(\theta,t)dt}{\int_0^\infty d\nu B_{z_0}^{(\nu)}(\theta,0)} \quad (21)$$

$$= \frac{\int_0^\infty \rho(\nu)d\nu \int_0^\infty d\tau \int_0^\infty C(z,\tau)\exp[-b(\nu)\sec\theta\,(d-z)]dz}{\int_0^\infty \rho(\nu)d\nu \int_0^\infty C_0(z,\gamma)\exp[-b(\nu)\sec\theta(d-z)]dz},$$

where the function $C(z,\tau)$ satisfies the equation

$$\frac{\partial C(z,\tau)}{\partial \tau} = -C + \int_0^\infty a(\nu)b(\nu)d\nu \int_0^{z_0} C(z,\tau)E_1\left(b(\nu)|z - z_1|\right)dz_1 \quad (22)$$

with the initial condition $C(z,0) = C_0(z,\gamma)$.

It follows from (21) that it is sufficient to know the following function in order to determine $\tau_{1,2}$:

$$\varphi(z,\gamma) = \int_0^\infty C(z,\tau)d\tau.$$

Table 1

The Function $\varphi(x)$

x	q						
	0.4	0.5	0.6	0.7	0.8	0.9	0.95
0	1.00	1.00	1.00	1.00	1.00	1.00	1.00
0.1	1.06	1.07	1.09	1.11	1.14	1.17	1.19
0.2	1.09	1.11	1.15	1.18	1.23	1.29	1.34
0.3	1.11	1.14	1.19	1.24	1.30	1.39	1.46
0.4	1.13	1.17	1.22	1.28	1.36	1.48	1.57
0.5	1.14	1.19	1.25	1.32	1.41	1.56	1.67
0.6	1.15	1.20	1.27	1.35	1.46	1.63	1.76
0.7	1.16	1.22	1.29	1.38	1.50	1.69	1.85
0.8	1.17	1.23	1.31	1.40	1.54	1.75	1.93
0.9	1.18	1.24	1.32	1.42	1.57	1.80	2.01
1.0	1.18	1.25	1.34	1.44	1.60	1.85	2.08
2.0	1.22	1.31	1.40	1.57	1.79	2.19	2.60
3.0	1.24	1.34	1.46	1.63	1.89	2.38	2.93
4.0	1.25	1.35	1.48	1.67	1.96	2.52	3.16
5.0	1.26	1.36	1.50	1.69	2.00	2.63	3.34
6.0	1.26	1.37	1.51	1.71	2.03	2.69	3.47
7.0	1.27	1.37	1.52	1.73	2.06	2.74	3.57
8.0	1.27	1.38	1.53	1.74	2.08	2.78	3.65
9.0	1.27	1.38	1.53	1.74	2.09	2.82	3.74
10.0	1.28	1.39	1.54	1.75	2.10	2.84	3.78
30.0	1.29	1.40	1.57	1.80	2.18	3.05	4.20
50.0	1.29	1.41	1.57	1.81	2.20	3.09	4.29
100.0	1.29	1.41	1.58	1.82	2.21	3.12	4.36
∞	1.29	1.41	1.58	1.83	2.24	3.16	4.46

Note. For $q < 0.4$, $\varphi(x) = 1 + \frac{q}{2} x \ln(1 + \frac{1}{x})$

*The function $a(\nu)$, which is always non-zero in a finite frequency range Δ, can have a complicated structure in certain important cases (for example, there are maxima for anthracene, etc.). The transformation from (7) to (18) corresponds to replacing the function $k(\nu)$ in the frequency range Δ by the constant $k(\nu_0)$. In the simplest case, when $a(\nu)$ has a single maximum at ν_0, the quantity ν_0 is selected equal to that frequency for which $a(\nu)$ has a maximum. If $a(\nu)$ has several comparable maxima in Δ, the quantity ν_0 should be selected equal to the frequency corresponding to the maximum of shortest wavelength, which range of frequencies is absorbed most by the substance. However, it should be kept in mind that, in those cases when the function $a(\nu)$ has a complicated shape, the q-approximation may appear to be inadequate. Using the functions $\varphi(x)$ and $\chi(x)$, obtained from (18) in a q-approximation, sufficiently exact solutions of (17) can be obtained by means of one or two successive iterations.

Integrating (22) with respect to τ from 0 to ∞, we find that the function $\varphi(z,\gamma)$ satisfies the following equation

$$\varphi(z,\gamma)=C_0(z,\gamma)+\int_0^\infty a(\nu)b(\nu)d\nu\int_0^{z_0}\varphi(z_1,\gamma)E_1\left(b(\nu)|z-z_1|\right)dz_1. \tag{23}$$

Let us introduce the function

$$\Phi(\eta,\gamma)=\int_0^{z_0}\exp[-\eta z]\varphi(z,\gamma)dz. \tag{24}$$

Using (12) and (24), the expression (21) may be written as follows

$$\bar\tau_1(\theta)=\frac{\int_0^\infty \rho(\nu)d\nu\Phi\left(b(\nu)\sec\theta,\gamma\right)}{\int_0^\infty \rho(\nu)d\nu R\left(b(\nu)\sec\theta,\gamma\right)};$$

$$\bar\tau_2(\theta)=\frac{\int_0^\infty \rho(\nu)d\nu\exp[-b(\nu)\sec\theta z_0]\Phi\left(-b(\nu)\sec\theta,\gamma\right)}{\int_0^\infty \rho(\nu)d\nu\exp[-b(\nu)\sec\theta z_0]R\left(-b(\nu)\sec\theta,\gamma\right)}. \tag{25}$$

It follows from (25) that it is sufficient to know $\Phi(\eta,\gamma)$ to determine $\bar\tau_{1,2}$. Despite the fact that the function $C_0(z,\gamma)$ in (23) is not only not an exponential (precisely this case was analyzed by Ambartsumian [5]), but is also not generally determined, the quantities $\Phi(\eta,\gamma)$ can be found. Actually, differentiating (23) with respect to z and using (11), and in addition comparing the equation for $\varphi'(z,\gamma)$ with the equations for $\varphi(z,\gamma)$ and $C_0(z,\gamma)$, we conclude that

$$\varphi'(z,\gamma)=-\gamma\varphi(z,\gamma)+C_0(0,\gamma)\int_0^\infty a(\nu)b(\nu)d\nu\int_1^\infty\frac{\varphi\left(z,b(\nu)\xi\right)}{\xi}d\xi-$$
$$-C_0(z_0,\gamma)\int_0^\infty a(\nu)b(\nu)d\nu\int_1^\infty\frac{\exp[-b(\nu)z_0\xi]\varphi\left(z,-b(\nu)\xi\right)}{\xi}d\xi+$$
$$+\varphi(0,\gamma)\int_0^\infty a(\nu)b(\nu)d\nu\int_1^\infty\frac{C_0\left(z,b(\nu)\xi\right)}{\xi}d\xi-$$
$$-\varphi(z_0,\gamma)\int_0^\infty a(\nu)b(\nu)d\nu\int_1^\infty\frac{\exp[-b(\nu)z_0\xi]C_0\left(z,-b(\nu)\xi\right)}{\xi}d\xi.$$

Multiplying both sides of this equality by $\exp[-\eta z]$ and integrating with respect to z from 0 to z_0, we find

$$\Phi(\eta,\gamma)=\frac{\varphi(0,\gamma)C_0(0,\eta)+\varphi(0,\eta)C_0(0,\gamma)-\varphi(z_0,\gamma)C_0(z_0,\eta)-\varphi(z_0,\eta)C_0(z_0,\gamma)}{\eta+\gamma}. \tag{26}$$

It can be shown similarly to the preceding that the functions $\varphi(0,\gamma)\equiv M(x)$ and $\varphi(z_0,\gamma)\equiv N(x)$, $(x=1/\gamma)$ satisfy the following system of equations

$$M(x)=1+x\int_0^\infty a(\nu)b(\nu)d\nu\int_0^{\frac{1}{b(\nu)}}\frac{\varphi(z)M(x)+\varphi(x)M(z)}{z+x}dz-$$
$$-x\int_0^\infty a(\nu)b(\nu)d\nu\int_0^{\frac{1}{b(\nu)}}\frac{\chi(x)N(z)+\chi(z)N(x)}{z+x}dz;$$

$$N(x)=\exp[-\frac{z_0}{x}]+x\int_0^\infty a(\nu)b(\nu)d\nu\int_0^{\frac{1}{b(\nu)}}\frac{M(x)\chi(z)-\chi(x)M(z)}{z-x}dz$$
$$+x\int_0^\infty a(\nu)b(\nu)d\nu\int_0^{\frac{1}{b(\nu)}}\frac{\varphi(x)N(z)-N(x)\varphi(z)}{z-x}dz. \tag{27}$$

In this case, when $z_0\to\infty$, $N(x)\to 0$. Using (15), (25) and (26), we find $(y_\nu=\cos\theta/b(\nu))$

$$\bar\tau_1(\theta,\gamma)=\frac{\int_0^\infty\rho(\nu)d\nu[M(x)\varphi(y_\nu)+\varphi(x)M(y_\nu)-\chi(x)N(y_\nu)-\chi(y_\nu)N(x)}{\int_0^\infty\rho(\nu)d\nu[\varphi(x)\varphi(y_\nu)-\chi(x)\chi(y_\nu)]} \tag{28}$$

$$\bar\tau_2(\theta,\gamma)=\frac{\int_0^\infty\rho(\nu)d\nu[M(x)\chi(y_\nu)+\varphi(x)N(y_\nu)-\chi(x)M(y_\nu)-\varphi(y_\nu)N(x)}{\int_0^\infty\rho(\nu)d\nu[\varphi(x)\chi(y_\nu)-\chi(x)\varphi(y_\nu)]} \tag{29}$$

In the frequency range where $\rho(\nu)$ is a maximum, the ratio $b(\nu)\ll 1$. Consequently, the integrands in (28) and (29), dependent on y_ν, can be taken out of the integral sign, to a good enough approximation, for $y_\nu=\infty$. In this case

$$\bar\tau_1(\gamma)=\bar\tau_2(\gamma)=\bar\tau(\gamma)=\frac{M(x)-N(x)}{\varphi(x)-\chi(x)}+\frac{M(\infty)}{\varphi(\infty)}-1, \tag{30}$$

since $\varphi(\infty)=\chi(\infty)$ and $M(\infty)=N(\infty)$ when $z_0=\infty$.

If the overlap of the emission and absorption spectra is slight $(q<0.4)$ then

$$\bar\tau(\gamma)=1+\int_0^\infty a(\nu)d\nu\left\{1+b(\nu)\frac{x}{1-\exp[-\frac{z_0}{x}]}\int_0^{\frac{1}{b(\nu)}}dy\left[\frac{1-\exp[-z_0\left(\frac{1}{x}+\frac{1}{y}\right)}{x+y}\right.\right.$$
$$\left.\left.+\frac{\exp[-\frac{z_0}{x}]-\exp[-\frac{z_0}{y}]}{y-x}\right]-b(\nu)\exp[-\frac{z_0}{x}]\int_0^{\frac{1}{b(\nu)}}\exp[-\frac{z_0}{y}]\,dy\right\}. \tag{31}$$

This expression agrees with the expression obtained earlier by Galanin [7] for $z_0\to\infty$.

If $z_0 = \infty$ (semi-infinite crystal, $\theta(x) = \frac{M_0(x)}{\varphi_0(x)}$)

$$\bar{\tau}(x) = \frac{M_0(x)}{\varphi_0(x)} + \frac{M_0(\infty)}{\varphi_0(\infty)} - 1 = \theta(x) + \theta(\infty) - 1, \quad (32)$$

where the functions $M_0(x)$ and $\varphi_0(x)$ are defined by the equations

$$\varphi_0(x) = 1 + x\int_0^\infty a(\nu)b(\nu)d\nu \int_0^{\frac{1}{b(\nu)}} \frac{\varphi_0(x)\varphi_0(y)dy}{x+y},$$

$$\frac{M_0(x)}{\varphi_0(x)} = 1 + x\int_0^\infty a(\nu)b(\nu)d\nu \int_0^{\frac{1}{b(\nu)}} \frac{M_0(y)\,\varphi_0(x)}{x+y}\,dy. \quad (33)$$

Equations (33) have the following form in the q - approximation

$$\varphi_0(x) = 1 + \frac{q}{2}\,x\int_0^1 \frac{\varphi_0(x)\varphi_0(y)}{x+y}\,dy, \quad (34)$$

$$\frac{M_0(x)}{\varphi_0(x)} = 1 + \frac{q}{2}\,x\int_0^1 \frac{M_0(y)\varphi_0(x)}{x+y}\,dy. \quad (35)$$

If the data of table 1 are used, the function $M_0(x)$ can be calculated by replacing the integral equation (35) by a system of linear algebraic equations. The results of computing the function $\theta(x)$ are presented in table 2 (for $q \geq 0.4$). Earlier, [3], one of the authors obtained an approximate formula for $\bar{\tau}(x)$. Comparison of the values of $\bar{\tau}(x)$, calculated using the approximate formula and formula (32), shows that the limiting values of $\bar{\tau}(x)$ for $x = 0$ and $x = \infty$ agree in both cases.

Table 2

The Function $\theta(x)$

x	q						
	0.4	0.5	0.6	0.7	0.8	0.9	0.95
0	1	1	1	1	1	1	1
0.1	1.07	1.09	1.12	1.15	1.21	1.32	1.47
0.2	1.10	1.13	1.18	1.24	1.34	1.54	1.78
0.3	1.12	1.17	1.23	1.32	1.45	1.74	2.10
0.4	1.14	1.20	1.27	1.38	1.55	1.92	2.39
0.5	1.16	1.22	1.31	1.43	1.63	2.07	2.65
0.6	1.17	1.24	1.34	1.48	1.71	2.22	2.90
0.7	1.19	1.26	1.36	1.52	1.77	2.35	3.14
0.8	1.19	1.28	1.38	1.55	1.83	2.47	3.35
0.9	1.20	1.29	1.40	1.58	1.88	2.61	3.55
1.0	1.21	1.30	1.42	1.61	1.94	2.73	3.76
2.0	1.25	1.35	1.53	1.76	2.25	3.45	5.21
3.0	1.28	1.40	1.59	1.85	2.43	3.86	6.13
4.0	1.28	1.42	1.62	1.94	2.54	4.13	6.74
5.0	1.30	1.43	1.64	1.97	2.61	4.35	7.25
6.0	1.30	1.44	1.66	2.00	2.67	4.49	7.62
7.0	1.31	1.45	1.67	2.03	2.71	4.60	7.92
8.0	1.31	1.46	1.68	2.04	2.73	4.68	8.12
9.0	1.31	1.46	1.69	2.05	2.76	4.74	8.37
10.0	1.31	1.46	1.69	2.06	2.78	4.82	8.51
30.0	1.33	1.49	1.73	2.08	2.91	5.26	9.67
50.0	1.33	1.49	1.74	2.14	2.94	5.35	9.92
100.0	1.33	1.49	1.74	2.15	2.96	5.43	10.13
∞	1.33	1.50	1.75	2.17	3.00	5.50	10.50

Note: For $q < 0.4$, $\theta(x) \approx \varphi(x)$.

Consequently, the method proposed in [3] to determine the magnitude of the quantum yield of a crystal Q not changed by reabsorption is retained. The approximate value of $\bar{\tau}(x)$, found in [3], differs in the range $0 < x < \infty$ from the value calculated using (32) in the q -approximation by not more than 10%. When the determination of $M_0(x)$ and $\varphi_0(x)$ in the q -approximation appear to be insufficiently exact, more exact values of these functions can be obtained from one or two iterations in (33), where the values of $M_0(x)$ and $\varphi_0(x)$ found in the q -approximation should be taken as the zero approximation functions.

2. REFLECTION OF THE LUMINESCENT LIGHT FROM THE CRYSTAL SURFACE TAKEN INTO ACCOUNT

Without neglecting light reflection from the crystal surface, let us find the stationary solution of (3). Let us use the notation

$$S(\eta) = \int_0^{z_0} \exp[-\eta z]C_0(z)dz, \quad (36)$$

where $C_0(z)$ is the desired solution. If (4) is used, (3) can be rewritten as follows for the stationary case

$$C_0(z) = \exp[-\gamma z] + \int_0^\infty a(\nu)b(\nu)d\nu \int_0^{z_0} C_0(z_1)E_1(b(\nu)|z-z_1|)dz_1 +$$

$$+ \int_0^\infty a(\nu)b(\nu)d\nu \int_1^\infty \frac{1}{\xi} r_\nu\left(\frac{b(\nu)}{\xi}\right)\Big[\exp[-b(\nu)\xi z]S(b(\nu)\xi) + \quad (37)$$

$$+ \exp[b(\nu)\xi(z-2z_0)]S(-b(\nu)\xi)\Big]\,d\xi.$$

Comparing (37) and (9), we conclude that

$$C_0(z) = C_0(z,\gamma) + \int_0^\infty a(\nu)b(\nu)d\nu \int_1^\infty \frac{1}{\xi} r_\nu\left(\frac{b(\nu)}{\xi}\right)\times \quad (38)$$

$$\times C_0\left(z, b(\nu)\xi\right)S\left(b(\nu)\xi\right) + \exp[-2z_0 b(\nu)\xi]C_0\left(z, -b(\nu)\xi\right)S\left(-b(\nu)\xi\right)\Big]d\xi.$$

Multiplying both sides of (38) by $\exp[\pm\eta z]$ and integrating over z from 0 to z_0, we find

$$S(\eta) = R(\eta,\gamma) + \int_0^\infty a(\nu)b(\nu)d\nu \int_{b(\nu)}^\infty \frac{d\xi}{\xi} r_\nu\left(\frac{b(\nu)}{\xi}\right)[R(\eta,\xi)S(\xi) +$$

$$+ \bar{R}(\eta,\xi)\bar{S}(\xi)]; \quad (39)$$

$$\bar{S}(\eta) = \bar{R}(\eta,\gamma) + \int_0^\infty a(\nu)b(\nu)d\nu \int_{b(\nu)}^\infty \frac{d\xi}{\xi} r_\nu\left(\frac{b(\nu)}{\xi}\right)[\bar{R}(\eta,\xi)S(\xi) +$$

$$+ R(\eta,\xi)\bar{S}(\xi)],$$

where

$$\bar{S}(\eta) = \exp[-\eta z_0]S(-\eta);$$

$$\bar{R}(\eta,\gamma) = \exp[-\eta z_0]R(-\eta,\gamma),$$

and the functions $R(\eta,\gamma)$ are defined by (15).

Hence, it is necessary to solve a system of two linear inhomogeneous integral equations for the functions $S(\eta)$ and $\bar{S}(\eta)$ to determine the function $C_0(z)$.

The quantities $B_0^{(\nu)}(\theta,x)$ and $B_{z_0}^{(\nu)}(\theta,x)$, defined earlier by (19), are now expressed (taking reflection into account) as follows:

$$B_0^{(\nu)}(\theta,x)=\frac{\rho(\nu)[1-r_\nu(\cos\theta)]}{4\pi P(1-\exp[-\gamma z_0])}S\big(b(\nu)\sec\theta\big);$$

$$B_{z_0}^{(\nu)}(\theta,x)=\frac{\rho(\nu)[1-r_\nu(\cos\theta)]}{4\pi P(1-\exp[-\gamma z_0])}S\big(b(\nu)\sec\theta\big).$$

Let us consider the nonstationary solution of equation (3). In this case, the equation for the function

$$\varphi(z)=\int_0^\infty C(z,\tau)d\tau \tag{40}$$

is

$$\varphi(z)=C_0(z)+\int_0^\infty a(\nu)b(\nu)d\nu\int_0^{z_0}\varphi(z_1)E_1\big(b(\nu)|z-z_1|\big)dz_1+$$

$$+\int_0^\infty a(\nu)b(\nu)d\nu\int_1^\infty\frac{1}{\xi}r_\nu\Big(\frac{b(\nu)}{\xi}\Big)\Big[\exp[-b(\nu)\xi z]K\big(b(\nu)\xi\big)+$$

$$+\exp[b(\nu)\xi(z-2z_0)]K\big(-b(\nu)\xi\big)\Big]d\xi, \tag{41}$$

where

$$K(\eta)=\int_0^{z_0}\exp[-\eta z]\varphi(z)dz. \tag{42}$$

Substituting (38) in place of $C_0(z)$, multiplying (41) by $\exp[\pm\eta z]$ and integrating over z from 0 to z_0, we obtain the following system of equations for $K(\eta)$ and $\bar{K}(\eta)=\exp[-\eta z_0]K(-\eta)$:

$$K(\eta)=\Phi(\eta,\gamma)+\int_0^\infty a(\nu)b(\nu)d\nu\int_{b(\nu)}^\infty\frac{d\xi}{\xi}r_\nu\Big(\frac{b(\nu)}{\xi}\Big)[\Phi(\eta,\xi)S(\xi)+$$

$$+\bar{\Phi}(\eta,\xi)\bar{S}(\xi)+R(\eta,\xi)K(\xi)+\bar{R}(\eta,\xi)\bar{K}(\xi)]; \tag{43}$$

$$\bar{K}(\eta)=\bar{\Phi}(\eta,\gamma)+\int_0^\infty a(\nu)b(\nu)d\nu\int_{b(\nu)}^\infty\frac{d\xi}{\xi}r_\nu\Big(\frac{b(\nu)}{\xi}\Big)[\bar{\Phi}(\eta,\xi)S(\xi)+$$

$$+\Phi(\eta,\xi)\bar{S}(\xi)+\bar{R}(\eta,\xi)K(\xi)+R(\eta,\xi)\bar{K}(\xi)],$$

where

$$\bar{\Phi}(\eta,\xi)=\exp[-\eta z_0]\Phi(-\eta,\xi).$$

The system of inhomogeneous linear integral equations (43) can be solved, at least numerically. Similar to the preceding, the average luminescent time $\bar{\tau}_r(\gamma)$, taking into account reflection of the luminescent light from the crystal surface, is determined as follows:

$$\bar{\tau}_r(\gamma)=\frac{K(\eta)}{S(\eta)}\Big|_{\eta=0}=\frac{\bar{K}(\eta)}{\bar{S}(\eta)}\Big|_{\eta=0} \tag{44}$$

If the overlap of the absorption and emission spectra is sufficiently slight ($q<0.4$) then

$$\bar{\tau}_r(\gamma)=\bar{\tau}(\gamma)+\frac{3}{1-\exp\big[-\frac{z_0}{x}\big]}\int_0^\infty a(\nu)b(\nu)d\nu\int_0^{\frac{1}{b(\nu)}}zdzr_\nu\big(b(\nu)z\big)\Big(1-\exp\big[-\frac{z}{x}\big]\Big)\times$$

$$\times\left[\frac{1-\exp\Big[-z_0\Big(\frac{1}{x}+\frac{1}{z}\Big)\Big]}{x+z}+\frac{\exp[-\frac{z_0}{x}]-\exp[-\frac{z_0}{z}]}{x-z}\right], \tag{45}$$

where $\bar{\tau}(\gamma)$ is defined by (31).

When $z_0=\infty$ (semi-infinite crystal)

$$\bar{\tau}_r(\gamma)=\bar{\tau}(\gamma)+3\int_0^\infty a(\nu)b(\nu)d\nu\int_0^{\frac{1}{b(\nu)}}\frac{zdzr_\nu\big(b(\nu)z\big)}{z+x}\quad\Big(x=\frac{1}{\gamma}\Big).$$

Formulas (20) and (21) lead to good agreement with experiment only when the luminescence intensity drops according to an almost exponential law. In the opposite case, it is necessary to use the following expressions instead of (20) and (21)

$$\tau_1(\theta)=\frac{P\int_0^\infty d\nu\int_0^\infty B_0^{(\nu)}(\theta,t)tdt}{\int_0^\infty d\nu\int_0^\infty B_0^{(\nu)}(\theta,t)dt};$$

$$\tau_2(\theta)=\frac{P\int_0^\infty d\nu\int_0^\infty B_z^{(\nu)}(\theta,t)tdt}{\int_0^\infty d\nu\int_0^\infty B_z^{(\nu)}(\theta,t)dt}.$$

The method explained above can be used even in this case. The results of computations as well as tables for a semi-infinite crystal are presented in [8].

This method of analyzing integro-differential equations such as (1) may be used to investigate problems of light scattering in materials.

May 12, 1958

References

1. V. M. AGRANOVICH, A. N. FAIDYSH: OiS, 1, 885 (1956)
2. V. M. AGRANOVICH: OiS, 3, 29 (1957)
3. V. M. AGRANOVICH: OiS, 3, 84 (1957)
4. I. IA. KUCHEROV, A. N. FAIDYSH, Z. N. FESENKO: OiS, 2, 462 (1957)
5. V. A. AMBARTSUMIAN: AZ, 19, 30 (1942)
6. S. CHANDRASEKHAR: Radiative transfer. Oxford, Clarendon, 1950 (IL, Moscow, 1953)
7. M. D. GALANIN: Tr, FIAN USSR, 5, 339 (1950) (See LC R-3741, 79 pp.)
8. V. M. AGRANOVICH: IAN USSR SF, 23, 40 (1959) (See CTT Bulletin)

TOM VI, Vyp. 5 OPTIKA I SPEKTROSKOPIIA Mai, 1959
VOL. VI, No. 5 OPTICS AND SPECTROSCOPY May, 1959

Investigation of the Spectral Distribution of the Luminescence Decay Time of Ruby by The Pulse Taumeter Method

N. A. TOLSTOI, A. M. TKACHUK

Abstract: The spectral dependences of the decay time τ have been investigated by the pulse taumeter method for a number of individual lines of the luminescence spectrum of synthetic ruby over a range of chromium content. It has been established that the ruby can have seven or eight different decay times simultaneously and that the chromium concentration exerts a substantial influence not only on the absolute value of the τ of individual lines but also on the behavior of the temperature dependences of τ in the 80 - 500°K temperature range.

INTRODUCTION

The luminescence of ruby ($Al_2O_3 \cdot Cr$) long ago attracted the attention of investigators who used the comparative simplicity of the luminescent characteristics of this material and its ease of study [1,2] (arising from brilliance of the luminescence and comparative slowness of its relaxation) for the construction of a complete optical model of the ruby as a monomolecular luminophor. More careful investigations of the luminescent properties of the ruby have shown, however, that they are very much more complex than had been considered heretofore. Thus, for example, the statement that the decay of the luminescence of the ruby as a whole is exponential [3,4] and independent of the temperature within very broad limits [4] can undoubtedly be traced to crudity of the experiments in which the luminescence damping was studied. As Tolstoi and Feofilov [5] have shown, the values of the decay time τ for the doublet 6927 - 6942 Å and for luminescence in the longer wavelength part of the spectrum are different. This obviously means that the decay of the total luminescence (i. e., the sum of the two different exponentials) does not follow an exponential law. It also appears that the values of τ depend substantially on the temperature and the chromium concentration. There may be maxima in the temperature dependences of the doublet. Hence, creation of a theoretical optical model of ruby must await a much more detailed phenomenological picture of the luminescence.

The distribution of τ values over the luminescence spectrum or, as it is natural to designate it, the relaxation spectrum , should be an integral part of this picture. The development of the pulse taumeter method [6] permits this problem to be solved. The results of preliminary investigations of the relaxation spectrum of ruby as a function of temperature and chromium concentration are presented herein.

1. METHOD

Let us recall that the shape of the exciting pulse is unimportant in the pulse taumeter method [6] only if a) the relaxation process being studied is exponential and b) the exciting pulse has at least one steep front. The linearization method [7] can be used if these conditions are satisfied. The time resolution of the method decreases (in comparison with measurements made by using rectangular pulses with two very steep sides) by approximately a half. This loss in time resolution is compensated by the huge growth in the sensitivity of the method, which results from using a pulse-tube source.

Since, as experiment shows, the relaxation processes of almost all the lines and bands of the ruby are exponential, and the IS-50 pulse tube has a steep enough rise, the investigations of the relaxation spectra of ruby are not particularly difficult.

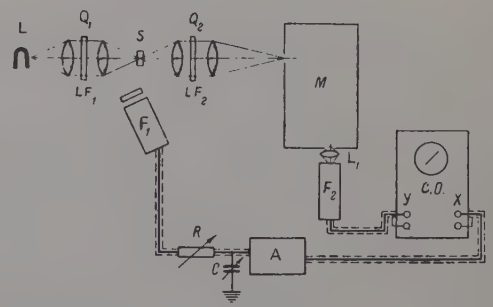

Figure 1. Pulse taumeter circuit. L-IS-50 impulse tube; Q_1-condenser; LF_1-SZS-10 light filter; S-sample; Q_2 - Condenser; LF_2 - ZhS-3 and KS-10 light filters, M-monochromator; L_1 - lens; R,C - taumeter; A-amplifier; C.O. - EO-7 cathode oscilloscope; F_1 - FEU-1 photo multiplier; F_2 - FEU-2 photo multiplier

The circuit of the pulse taumeter we used is shown in Figure 1. An IS-50 pulse lamp, with characteristics permitting the study of relaxation processes in the 10^{-2} - 2×10^{-5} sec. range, was used as the exciting light source. The exciting light from the lamp L is focussed by the quartz condenser Q_1 on the sample S . Part of this light, being dissipated by the condenser surface, falls on an FEU-1 photomultiplier (F_1), the signal from which is passed through the RC network (the τ-meter proper) is amplified by the amplifier A and fed to the X plates of the EO-7 cathode oscilloscope (C.O) which has a long persistence cathode ray tube. The luminescence of the sample is focussed by the quartz condenser Q_2 onto the input slit of a monochromator with a 150 x 150 mm, 600 line/mm diffraction grating. The large dispersion of the instrument (6.5 Å/mm) permitted operation with rather broad slits (0.2 - 0.5 mm). The luminescence, leaving the output slit of the monochromator, was focussed by lens L_1 on an FEU-2 signal photomultiplier (F_2) whose signal was fed through an amplifier to the Y plates of the oscilloscope.

The excitation was in the 340 - 600 mμ range [SZS-10 light filter (LF_1)]. In order to exclude

background noise from exciting light scattered into the measuring channel, ZhS-3 and KS-10 light filters (LF_2) were set up in front of the input slit of the monochromator.

The discharge tube could be fired every 5 or 10 sec. (depending on the power of the apparatus charging the 1600 μF discharge condenser). The adjustment of values in the RC network which "linearize" the loops on the oscilloscope screen, could be accomplished successfully, as experiment showed, after just a few trials. Hence, the measurement of τ occupied a time less than 1 min. (checking of the invariance of τ is of course accomplished more rapidly).

The apparatus described permitted τ to be measured with ±5% accuracy in the 10^{-2}–10^{-5} sec range.

2. RESULTS OF THE MEASUREMENTS

Six ruby samples whose chromium concentration varied from 0.05 to 2.89% were investigated. Two series of measurements were made.

1) The luminescence spectrum of ruby was recorded point by point (using a pulse tube and an oscilloscope) and then the value of τ was determined for all the lines or bands with sufficient intensity. These measurements were made for two fixed temperatures, -193° and + 20°. The data obtained are presented in the table.

Decay Time τ for Luminescence Lines of Synthetic Ruby Crystals with Different Chromium Concentrations

t = -193°C							t = 20°C							
λ, mμ	chromium concentration, %						λ, mμ	chromium concentration, %						No. of spectral region
	2.89	1.8	0.95	0.81	0.59	0.05		2.89	1.8	0.95	0.81	0.59	0.05	
—	—	—	—	—	—	—	690.0	0.75	—	2.0	—	—	—	I
691.7	0.35	0.85	2.5	3.0	4.0	5.6	692.7	0.8	2.0	2.9	2.9	3.0	2.5	II
693.2	0.35	0.85	2.5	3.0	4.0	5.6	694.2	0.8	2.0	2.9	2.9	3.0	2.5	
696.9	0.35	1.0	2.4	2.9	3.0	—	697.9	0.73	—	1.7	1.8	—	—	
697.7	0.35	1.0	2.4	2.9	3.0	—	698.6	0.72	1.4	1.6	1.8	—	—	
698.8	0.35	0.9	2.4	2.8	3.0	—	699.8	0.71	1.4	1.6	1.8	—	—	III
699.5	0.35	0.9	2.4	2.8	3.0	—	—	—	—	—	—	—	—	
700.3	0.35	0.9	2.4	2.7	3.0	—	—	—	—	—	—	—	—	
701.0	0.35	0.9	2.4	2.7	3.0	—	701.7	0.70	1.4	1.5	1.8	—	—	
704.2	0.55	1.6	3.0	3.3	3.0	—	704.9	0.75	1.4	1.7	1.8	—	—	IV
705.9	0.4	1.4	2.6	3.0	—	—	707.2	0.75	1.3	2.0	2.0	—	—	V
707.5	0.35	0.9	2.0	—	—	—	713.5	0.75	1.3	2.2	2.4	—	—	VI
715.8	0.35	0.8	2.0	2.8	3.0	—	716.7	0.75	1.4	2.2	2.4	—	—	
728.6	0.35	0.7	—	—	—	—	725.5	0.75	1.3	1.7	—	—	—	VII
745.5	0.35	0.6	0.6	—	—	—	745.5	0.7	—	0.75	—	—	—	
751.0	0.35	0.55	—	—	—	—	752	0.7	—	—	—	—	—	
754.3	0.35	0.55	—	—	—	—	755	0.7	1.0	—	—	—	—	
760.5	0.35	0.55	—	—	—	—	761.5	0.7	1.0	—	—	—	—	
768.5	0.35	0.55	—	—	—	—	773.3	0.7	1.0	—	—	—	—	VIII
773.3	0.35	0.55	0.6	0.6	0.5	—	776	0.7	1.0	—	—	—	—	
775.7	0.35	0.55	—	—	—	—	778	0.7	1.0	—	—	—	—	
781.3	0.35	0.55	—	—	—	—	782	0.7	—	—	—	—	—	
795.7	0.3	0.55	—	—	—	—	799	0.7	—	—	—	—	—	

2) Individual, intense lines or bands were selected and the temperature dependences of τ were measured in detail for them from -193° to 20°. At the same time, the temperature dependences of the luminescence intensity of these same lines were determined.

Shown in figure 2 are the luminescence and relaxation spectra for the -193 and 20° temperatures for three samples with chromium concentrations of 0.05, 0.95 and 2.89%. Note that the luminescence spectra presented in figure 2 are only semi-quantitative in nature: Although the positions of the maxima are sufficiently exact, the relative magnitudes of the maxima are somewhat reduced for larger values of τ since the "slow" lines of the spectra of ruby do not successfully "start to burn" until toward the end of the comparatively short time in which the impulse tube is lit. Nevertheless, the temperature and concentration deformations of the luminescence spectra are clearly seen in figure 2. These deformations were studied by Feofilov and Kuznetsova [8].

An analysis of the data of table 1 shows the following.

1) In contradiction to the statement in the literature that the decay time τ of ruby is a constant characterizing the exponential relaxation of this luminophore, it appears that τ can vary by at least a factor of 16 as the chromium concentration changes (from 0.05 to 2.89% for the doublet at -193°) and at least 5 times in the transition from one part of the spectrum to another (from 704.2 mμ to values of the wavelength larger than 745 mμ for a sample with a 0.95% chromium concentration at -193°).

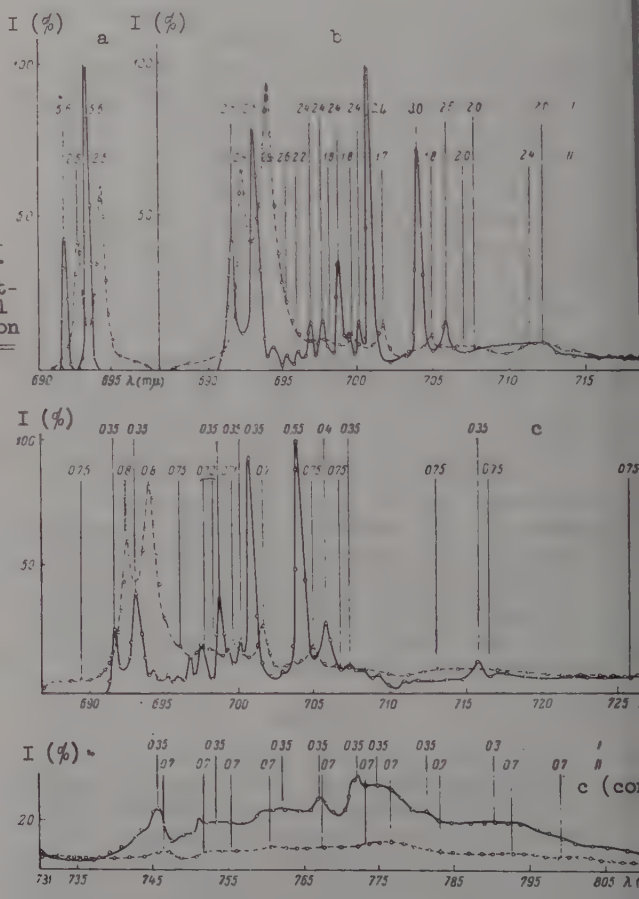

Figure 2. Luminescence and relaxation spectra of ruby for samples with different chromium concentrations. Chromium concentration (in %): a - 0.05, b - 0.59, c - 2.89.
The numbers in row I denote magnitudes of $\tau \cdot 10^3$ at -193°; those in row II, at 20°.

2) It appears possible to measure τ in the anti-Stokes region of the spectrum. Here τ is shorter than for the doublet.

3) Both lines of the resonance doublet (R_1 and R_2) always have the same value of τ.

4) The main secondary lines (N_1 and N_2) can have different τ.

5) The infrared tail of the luminescence, consisting of washed out bands ($\lambda > 750$ mμ), is all characterized by a single value of τ.

6) As the chromium concentration increases, the values of τ generally decrease significantly and equalize along the spectrum. For high chromium concentrations τ is almost constant over the spectrum

7) Approximately eight sections of the spectrum can be isolated which can be characterized either by different τ or by different temperature or concentration dependences of τ. These groups (I - VIII) are noted in the extreme right column of the table.

8) Since even at the temperature of liquid air the lines, and especially the luminescence bands, of ruby do not appear to be completely resolved, and since the values of τ of adjacent lines or bands can be distinguished, one should consider the possibility of appearance of impure exponentials at several points of the spectrum and of intermediate values of τ. (The sum of two exponentials with almost equal τ can be characterized in a first approximation by some average τ dependent on the weights of these exponentials.) From this viewpoint, the section of the spectrum denoted by the number VII (see table) may be a simple superposition of the edges of VI and VIII; in this case the spectrum of ruby has only seven different values of τ.

Let us return to figure 3 which shows smooth temperature dependences for certain lines of the luminescence spectrum of samples with different chromium concentrations. As is seen from figure 3, the character of the temperature dependences has a good deal of variety, and generally varies both with λ and with the change in the chromium concentration. Attention is called to the fact that not only does the τ decrease in samples with considerable chromium concentration at high enough temperatures but a drop in τ is observed as well when the samples are cooled. Hence, the statements in the literature about the independence of τ in ruby on temperature are not true; actually, the dependences $\tau(t^\circ)$ have a plateau on the order of 100° in extent in the best case in the room temperature range. The drop in τ with cooling occurs not only in ruby; we have encountered such a phenomenon in the study of the infrared luminescence of cuprous oxide [9], for example.

The temperature dependences of the separate lines in the spectrum of ruby appear to be unique also. We do not present them here since we hope to devote the next publication to this question in an equally or more detailed and exact analysis than we have applied to relaxation processes.

The facts explained are presented in the first place to illustrate the possibilities afforded by the new pulse taumeter method. As is seen, measurements of the τ of luminescence can now be realized with details completely unmeasurable up to this time.

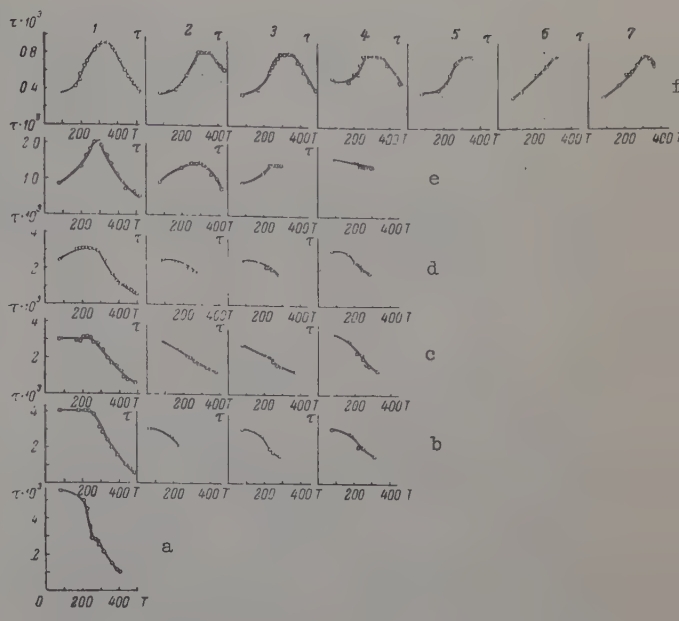

Figure 3. Temperature dependences of the spectral lines of synthetic ruby.
Chromium concentration (in %): a - 0.05; b - 0.59; c - 0.81; d - 0.95; e - 1.80; f - 2.89. Wavelength (in mμ): 1--692.7, 694.2; 2--699.8; 3--701.7; 4--704.9; 5--707.2; 6--region near 745; 7--region near 773.

Also we wanted to turn attention to the interesting spectral-kinetic regularities of the luminescence of ruby in which a certain, albeit poorly explained, mechanism of energy exchange between luminescence centers is clearly evident.

T. V. Kreitser participated in the measurements.

May 26, 1958

References

1. O. DEUTSCHBEIN: Ann. Phys., 14, 712 (1932); Z. Phys., 77, 489 (1932)
2. B. V. THOSAR: Phil. Mag., 26, 380, 878 (1938)
3. G. F. J. GARLICK, M. H. F. WILKINS: Proc. Roy. Soc. A184, 408 (1945)
4. V. I. ALIAVDIN, V. V. FEDOROV, V. L. LEVSHIN: DAN USSR, 25, 106-110 (1939) (In English); IAN USSR FS, 4, 173 (1940)
5. N. A. TOLSTOI, P. P. FEOFILOV: DAN USSR, 85, 551 (1952)
6. N. A. TOLSTOI: OiS, 4, 279-281 (1958) (See LC 59-10911, $1.80)
7. N. A. TOLSTOI, P. P. FEOFILOV: ZETF, 19, 421 (1949)
8. P. P. FEOFILOV, L. A. KUZNETSOVA: IAN USSR FS, 18, 297 (1954); Inzh.-Fiz. Zh., No. 4, 46 (1958)
9. N. A. TOLSTOI, N. N. TKACHUK: DAN USSR, 95, 65 (1954)

TOM VI, Vyp. 5
VOL. VI, No. 5

O P T I K A I S P E K T R O S K O P I I A
O P T I C S A N D S P E C T R O S C O P Y

Mai, 1959
May, 1959

Formal Analysis of the Theory of Two-Step Excitation of Phosphorescence and Photo Conduction

III. Comparison of Theory and Experiment (ZnS-Cu Luminescence)

N. A. TOLSTOI

Abstract: The theory of two-step excitation, developed in previous works, is compared with experimental results. The assumptions on the relations between the parameters of the scheme required for agreement between theory and experiment appear to be the same for both the stationary and the relaxation dependences of the luminescence. It is shown that stationary luminescence and the initial stages of the decay of phosphors of the ZnS-Cu type should be recognized as basically "pseudo-monomolecular".

INTRODUCTION

In previous papers, the question was analyzed on the possibility of two-step excitation of luminescence of sulfide type phosphors [1] and a formal analysis was given of the stationary [2] and relaxation [3] dependences in two-step theory. A number of examples of the comparison of theory with experiment has already been given in [1, 2, 4, 5]. In this paper, we shall compare the results of a formal analysis of the theory [2, 3] with certain typical stationary and relaxational properties of the well-known phosphor ZnS-Cu. We will cite the formulas of reference [1] by prefixing their number with the Roman numeral I and the formulas of reference [3] by prefixing the Roman numeral II.

STATIONARY DEPENDENCES

It is known that the luminescence yield excited by a purely two-step mechanism (optical excitation on both steps) cannot exceed 0.5 [see I(52) and subsequent]. However, it is also known [6] that the quantum yield of the green band in ZnS-Cu exceeds 0.5 in a number of cases and, therefore, the yield of the blue band is less than 0.5. Consequently, it can be assumed that both luminescences (green and blue) are excited in a two-step manner except that the blue luminescence is excited purely optically in both steps while the green luminescence is excited in both an optical and thermal manner in the second step. This means that $\xi_{12} < \gamma E$ and $\xi_{12} < \beta_{10}$, for blue luminescence and $\xi_{12} \approx \gamma E$ or $\xi_{12} \geqslant \gamma E$ and $\xi_{12} > \beta_{10}$ for green (see the notation in [2]). Then, in agreement with experiment, blue luminescence is super-linear and green is sub-linear. It is known that green luminescence transforms from sub to superlinear at elevated temperature (when its yield drops and becomes certainly less than 0.5). It is natural to explain this thus: β_{10} grows more rapidly with temperature than does ξ_{12} so that $\xi_{12} < \beta_{10}$ in the heated phosphor for the green (already superlinear) band. If it is considered that

$$(1) \qquad \beta_{10} = a \exp\left[-\frac{u_{10}}{kT}\right],$$

$$(2) \qquad \xi_{12} = b \exp\left[-\frac{u_{12}}{kT}\right],$$

then

$$(3) \qquad \frac{\xi_{12}}{\beta_{10}} = \frac{b}{a} \exp\left[\frac{\Delta u}{kT}\right],$$

where

$$(4) \qquad \Delta u = -(u_{12} - u_{10}).$$

In order for $\frac{\xi_{12}}{\beta_{10}}$ to diminish with heating, it is necessary to consider that $\Delta u > 0$, i. e., that

$$(5) \qquad u_{10} > u_{12}$$

Choosing the coefficients a and b in equation (3) permits the transition to be obtained from $\xi_{12} > \beta_{10}$ to $\xi_{12} \leq \beta_{10}$ at the required temperature.

Apparently the difference in the magnitude of the ratio $\frac{\xi_{12}}{\beta_{10}}$ for the blue and green bands must be explained by the levels of the first or second steps being different for green and blue luminescence. On the other hand, it could be possible that the method by which the electron is excited (optically or thermally) from the first step to the second step predetermines, to some degree, its predominant participation in the blue or green luminescence.

We carried out the whole formal analysis of the two-step theory [2, 3] under the assumption that the departure of electrons from levels of both the first and second steps has a pseudo-monomolecular nature. This was related to the necessity to explain the square of the photo conductivity and besides, this facilitated the mathematics of taking screening into account which is complicated otherwise. However, we do not intend to state that because some circumstances, in principle, exist, pseudo-monomolecularity must always take place. It is completely possible that the electron drift from the first stage ($1 \rightarrow 0$) is of bimolecular character in ZnS-Cu type phosphors under definite conditions. Unfortunately, the mathematical computation referred to here can hardly be performed in general form (without considering simple particular cases). It can only be stated that for "bimolecularity" in the first step and "pseudo-monomolecularity" in the second under intense quenching conditions, the stationary dependence of the luminescence on E will be

$$(6) \qquad I_\infty \sim E^{3/2},$$

which has repeatedly been observed in experiment.

RELAXATION DEPENDENCES

Let us compare the theoretical decay curves obtained by a formal analysis of the two-step theory with experimental decay curves by taking the decay

of ZnS-Cu luminescence (green band) as an example. Let us stress that we will speak of the initial stages of decay (the region enclosed by a taumeter [7];) the long "tails" in the decay are not considered here.

a) In what way do the hyperbolic character of the decay established by experiment [7] and the biexponential decay established by theory [3] agree?

First, let us note that experiment establishes intrinsically a linear growth with time of the instantaneous relaxation time θ [7, 3]:

$$\theta = \frac{1}{a\alpha} + \frac{1}{\alpha}\cdot t, \tag{7}$$

where $\theta = -\frac{I}{I'}$, and I is the luminescence intensity which drops according to the fractional hyperbolic law

$$I = \frac{I_\infty}{(1 + at)^\alpha}.$$

in case equation (7) is fulfilled. Here, the initial stages of decay themselves do not obey this formula, as experiment shows. On the other hand, the later stages (decay "tails") also do not follow this law since usually $\alpha < 1$ for the initial stages, which would lead to an infinite light sum if equation (8) were correct to $t = \infty$). Hence, the decay process, following equation (7), is only part of the total process and the linear growth of θ with time is just a linearly-approximated interpolation.

Now let us turn to the dependence $\theta(t)$, derived theoretically in [3] for the biexponential function. The comparatively large luminescence yield in ZnS-Cu (see above) permits us to consider that in practice there is no secondary binding ($R = 1$). On the other hand, the thermal excursion ξ_{12}, as mentioned above, exists. If the condition

$$b_{11} > b_{22} \quad (\beta_{20} > \beta_{10} + \xi_{12}) \tag{8}$$

is added [see II (35-38)], then we at once establish a set of formulas which must be compared with equation (7). These are equations [II(47)], [II(50-51)], and [II(53-60)]. As we have seen, the decay curve is the sum of two exponentials for the region of not too small excitation intensities (and experimental results exist for just this region also) and the quantity $\theta(t)$ is expressed by functions which increase with time. It is clear that this increase can be approximated by an oblique line in a definite interval, i. e., equation (7) can be satisfied. The difference in the behavior of the theoretical and experimental $\theta(t)$ is that the theoretical curve of $\theta(t)$ has a slope diminishing to zero with time ($\theta \to$ const) and the experimental curve of $\theta(t)$ has a slope diminishing to a finite quantity corresponding to $\alpha > 1$ in the Becquerel law [7] for the later stages. However, it is very probable that the recombination in the later stages of decay is not pseudo-monomolecular (as our variation of the two-step scheme hypothesizes) but is bimolecular. A corresponding change in the theoretical scheme would undoubtedly lead to agreement between theory and experiment in the respects mentioned. The question of the later stages ("tails") of decay are beyond the scope of our interests, as already mentioned.

b) How does theory agree with the differential regularities of luminescence relaxation ?

Experiment shows that the initial instantaneous relaxation time, i. e., $\theta(0)$ drops as E increases but tends to saturation. Theory leads to the same result. Actually, $\theta(0)$ is expressed by the equation

$$\theta(0) = \frac{1}{\beta_{20} - \xi_{12}\,\frac{n_{1\infty}}{n_{2\infty}}}. \tag{9}$$

$\theta(0)$ drops as E grows and approaches the saturation value

$$\theta(0) = \frac{1}{\beta_{20}}. \tag{I, 52}$$

Furthermore, experiment shows that the dependence of $\theta(0)$ on E is much weaker than the dependence on E of the decay curve itself which is characterized, say, by the half-life. At definite temperatures, the quantity $\theta(0)$ can cease to depend on E while the half-life must still vary as E changes. Theory yields the same result. As is seen from figure 1, and also from a comparison of equations [II(57)] and [II(60)], which are valid for $E \to \infty$, as $\theta(0)$ approaches saturation, the quantity $\theta'(0)$ and, hence, the shape of the decay curve as well, continue to depend on E

$$\theta'(0) \sim \frac{1}{E}. \tag{I.60}$$

c) How is the independence of α from E explained?

Experiment shows that the slope of the line $\theta(t)$ remains constant within certain limits. Although this result does not follow directly from any of the formulas of our theory, it is not however difficult to see that the $\theta(t)$ "lines" in the interval of E variation in which the decay is expressed as the sum of exponentials (see curves 4 - 10 on figure 1) first have an increasing slope and then a diminishing one; it is natural that the slope should be independent of E in a first approximation at its highest value.

d) How is the increase in the index α with temperature explained?

Experiment shows that the slope of the $\theta(t)$ "lines" diminishes as the temperature rises, in other words, α increases.

In the limit, at high temperatures, the decay curves approximate exponentials. Formally, an exponential is equivalent to a hyperbola with $\alpha \to \infty$ under the condition that $\frac{1}{a\alpha} \neq 0$, i.e., for a tending to zero according to such a law as would compensate for the tendency of α to ∞.

At first glance, the decrease in the slope of $\theta(t)$ with rise in temperature is explained very simply and graphically. Actually, $\xi_{12} + \beta_{10}$ grows and $\theta(\infty) = \frac{1}{(\xi_{12} + \beta_{10})}$ drops. The whole $\theta(t)$ curve "hugs" the horizontal axis. Hence, that $\theta(0) = \frac{1}{\beta_{20}}$ also drops plays no special role because $\theta(\infty) \gg \theta(0)$ and the change in the slope is determined almost exclusively by the quantity $\theta(\infty)$

(see Fig. 1). However, it is impossible to discuss this because the quantities $n_{1\infty}$ and $n_{2\infty}$, themselves, which determine the amplitude of the exponential in conjunction with the parameters of the scheme β_{10}, β_{20}, ξ_{12}, γE, depend on the temperature as do the parameters also and, consequently, such a discussion is not correct.

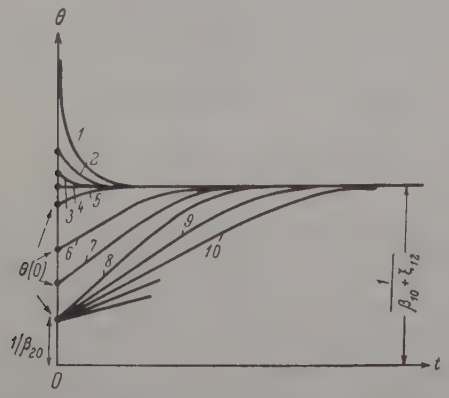

Figure 1. Curves numbered in order of increasing E.

In order to show in what manner and under what assumptions a drop in the slope of $\theta(t)$ with heating follows from the theory [i.e., a decrease in $\theta'(0)$], let us consider the region in which $n_{2\infty} \sim E^2$ and $n_{1\infty} \sim E$. This is the strong quenching region for which the transformation of the decay curve into an exponential almost independent of E is again typical. Then

$$n_{1\infty} = \frac{E}{\beta_{10}} \tag{I.28}$$

and

$$n_{2\infty} = \frac{\gamma E^2}{\beta_{10}\beta_{20}} \tag{I.47}$$

Here, as ever, it is assumed $R = 1$ (secondary binding absent) and it is moreover considered that

$$\xi_{12} \ll \beta_{10}. \tag{10}$$

The last assumption has already been made above: The rise in β_{10} outstrips the rise in ξ_{12} [see equations (1), (2) and subsequent] in heating ZnS-Cu. Now, let us form the expression for $\theta'(0)$:

$$\theta'(0) = \frac{n_{1\infty}b_{21}[n_{2\infty}(b_{11} - b_{22}) - n_{1\infty}b_{21}]}{(n_{2\infty}b_{22} + n_{1\infty}b_{21})^2}. \tag{11}$$

Substituting (I, 28) and (I, 47) here and assuming

$$b_{11} \gg b_{22}, \text{ i.e. } \beta_{20} \gg \beta_{10} + \xi_{12}, \tag{12}$$

we will have

$$\theta'(0) \approx \frac{\xi_{12}}{\gamma E - \xi_{12}}. \tag{13}$$

In order to obtain the desired result, it is necessary to consider that the quantity γE (or, rather, γ itself) grows with temperature more rapidly than does ξ_{12}. Then, for sufficient heating

$$\xi_{12} \ll \gamma E$$

and

$$\theta'(0) \approx \frac{\xi_{12}}{\gamma E}. \tag{14}$$

This formula shows that the slope of the curve $\theta(t)$ can become as close to zero as desired as the temperature rises. The dependence on E plays no part for such a slope. Thus, that it could be felt in the behavior of the $\theta(t)$ curve for very large t is also not essential since the luminescence itself drops to immeasurably small quantities (under intense quenching conditions) for very large t, without speaking of the fact that this luminescence refers to the decay "tail" region which we did not consider.

The theoretical result obtained above, the tendency of the decay curve to become an exponential during heating, can also be conceived if it is recalled that the decay curve, in the absence of a thermal excursion ξ_{12}, is expressed by a single exponential [equation (II. 64)] under all conditions. It is evident that if ξ_{12} is not zero but is small in comparison with other parameters of the scheme, then the results will be almost exactly the same as in the case $\xi_{12} = 0$.

It should be noted that use of equations (I.28) and (I.47) presumes the unscreened case. One of the conditions for the absence of screening $\xi_{12} \gg \gamma E$ (I.19) has been violated. Consequently, it should be required that the other condition $\beta_{10} \gg \gamma E$ (I.18) should be satisfied. This means that the above mentioned reasonings are appropriate if the following conditions are satisfied

$$\beta_{20} > \beta_{10} > \gamma E > \xi_{12} \tag{15}$$

[compare with (II.78)]

e) How does theory agree with the integrated relaxation laws, i. e., with the behavior of the quantity $\frac{L_i}{L_d}$?

Since a calculation of $\frac{L_i}{L_d}$ would only be possible for the unscreened case, comparison with experiment should be limited to the intense quenching region. The experimental results are: $\frac{L_i}{L_d} > 1$; values of $\frac{L_i}{L_d}$ can exceed unity considerably; $\frac{L_i}{L_d}$ drops as E increases; $\frac{L_i}{L_d}$ grows with rising temperature.

Theory establishes that $\frac{L_{i_1}}{L_{d_1}}$ is always less than unity. Therefore, $\frac{L_i}{L_d} = \frac{L_{i_2}}{L_{d_2}}$ for the green luminescence of ZnS-Cu. This is in agreement with our consideration of the green luminescence to be related to the second light sum (see above).

Theory shows that $\frac{L_{i_1}}{L_{d_1}}$ can exceed unity as much as desired. For example, in the absence of a thermal excursion and the absence of secondary sticking, we have

$$\frac{L_{i_2}}{L_{d_2}} = 1 + \frac{\beta_{20}}{\beta_{10}}. \tag{II.74}$$

If

$$\beta_{20} \gg \beta_{10},$$

then this quantity can be as large as desired. The presence of ξ_{12} diminishes it, however, if ξ_{12} is small compared to the other parameters of the scheme this does not change matters (see below).

Theory shows that $\frac{L_{i_2}}{L_{d_2}}$ drops as E grows if only condition (II.78) is satisfied. This again means that ξ_{12} must be small in comparison with γE. This result is sufficiently instructive: We explain the well-known fact of the drop in the ratio $\frac{L_i}{L_d}$ as E grows only to the degree to which the two-step optical mechanism prevails over the mechanism in which the "second step" of excitation is replaced by a thermal "excursion" of the localized electron.

Finally, theory establishes that the rise in $\frac{L_{i_2}}{L_{d_2}}$ with temperature can be obtained from the hypothesis that β_{20} is not only larger than β_{10} but, in addition, increases more rapidly with heating than does β_{10}.

Thus, we have proved the possibility of an agreement between theory and experiment both with respect to stationary and relaxation dependences of the luminescence. Here, we had to make definite assumptions on the relations of the parameters of the scheme for each kind of dependence. The most substantial result is that these assumption appear to be identical for all cases. Actually, the relation

$$\beta_{20} > \beta_{10} > \gamma E > \xi_{12}, \tag{15}$$

being referred to elevated temperatures, combines equations (16), (10), (8) which we indeed used in all the reasoning. As we have seen, in addition to compliance with equation (15), there should be required that all the quantities in this inequality should increase with temperature and in such a way that the large parameters would increase more rapidly; in other words, all parts of the inequality must be strengthened. On the other hand, the requirement of a different growth rate for a temperature reduction leads to reversal of the signs of the inequality for the last three parameters in equation (15) and we obtain the relation

$$\xi_{12} \geqslant \gamma E > \beta_{10}, \tag{16}$$

which has already been used to interpret the stationary green luminescence of ZnS-Cu at room temperatures. The growth of the parameters β_{10}, ξ_{12} and β_{20} with temperature is greater than is natural; an essential requirement of the two-step theory is the growth of γE, more exactly, an increase in the absorptive capacity of electrons at the first levels of γ with heating.

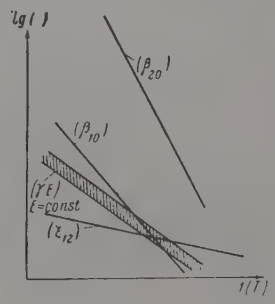

Figure 2

Presented for clarity on figure 2 are rough qualitative forms of the temperature dependences of the scheme parameters illustrating the above mentioned reasoning.

The explanation we have given of the regularities of luminescence decay of a crystal phosphor in the initial ("taumetric") stages is related to the two-step excitation hypothesis rather indirectly, in substance. Actually, the decay process proceeds with excitation disconnected and, consequently, the "two-stage" nature is felt only in the character of the dependences of the first and second light-sums ($n_{1\infty}$ and $n_{2\infty}$) on the intensity of the preceding excitation. Certainly this highly-important circumstance and that specific character which the relaxation regularities we derived acquire, is understandably related to the "two-step" character directly. However, the very idea that "hyperbolic" decay in the initial stages is actually bi-exponential decay dependent on the simultaneous expenditure of the second light-sum (conduction band and fine trapping levels) and its "sustaining" expenditure of the first light-sum (deeper local levels "1") is an idea which can be proposed and defended outside the span of the two-step mechanism hypothesis.

In conclusion, let us express certain reasoning apropos whether the luminescence of such a phosphor as ZnS-Cu (or those similar to it) should be considered as "bi-" or "monomolecular". This question raised a great deal of discussion in the past.

No one has ever apparently doubted that the luminescence mechanism is a recombination mechanism. Properly, we speak of whether recombination is a second order reaction ("bimolecularity") or a first order reaction ("monomolecularity" or, more accurately, "pseudo-monomolecularity"). Experiments with instantaneous excitation [8,9] ($I_{inst} \sim E^2$) and experiments studying decay in the later stages [10] were very serious proofs of "bimolecularity". As regards experiments with instantaneous excitation, they have an alternative interpretation: According to the two-step excitation theory $I_{inst} \sim E^2$ for pseudo-monomolecular recombination. As regards experiments studying the decay in later stages, they prove the bimolecular character of the luminescence in these later stages. We assume that the latter is completely valid. But this by no means proves that the luminescence under stationary excitation, i. e., intrinsic luminescence, has bimolecular character also. It is sometimes said that in the later stages of decay, the overwhelming part of the light sum is quenched and, consequently, the overwhelming part of the luminescence depends on that mechanism which has been established for this overwhelming part of the light-sum. Understandably, this is untrue. The greatest intensity in the last stages of the afterglow is, as a rule, not more than several percent of the stationary intensity. Consequently, we apply that mechanism which acts in the later stages of the afterglow to the description of just several percent of the stationary luminescence (characterized by brilliance), in other words, its negligibly small part. In order to discuss the stationary luminescence mechanism, we must rely on kinetic data referring to the time interval during which the basic drop in brilliance occurs, in other words, to the kinetics of the initial stages of the afterglow. From the tests and their explanations, it follows that the recombination in the initial stages should be considered pseudomonomolecular, at least in a first approximation. Therefore, the recombination mechanism effective during stationary excitation is also basically pseudo-monomolecular.

Thus, the stationary luminescence of phosphors of ZnS-Cu type should be acknowledged as basically "pseudo-monomolecular" and their afterglow in the later stages as "bimolecular".

May 9, 1958

References

1. N. A. TOLSTOI: ZETF, 30, 171 (1956) (See Soviet Physics, JETP)
2. N. A. TOLSTOI, A. V. SHATILOV: OiS, 1, 215 (1956)
3. N. A. TOLSTOI, A. V. SHATILOV: OiS, 5, 590 (1958)
4. N. A. TOLSTOI: J. de Phys. et le Rad., 17, 801 (1956)
5. N. A. TOLSTOI: RTiE, 1, 1135 (1956) (See MDF T-131 , 12 pp, $6.00)
6. M. N. ALENTSEV, V. V. ANTONOV-ROMANOVSKII, L. A. VINOKUROV: DAN USSR, 96, 1133 (1954)
7. N. A. TOLSTOI, P. P. FEOFILOV: UFN, 41, 44 (1950)
8. V. V. ANTONOV-ROMANOVSKII: DAN USSR, 2, 93 (1936) (In German)
9. V. L. LEVSHIN: Acta Phys. Polon., 5, 301-317 (193 (In French)
10. V. L. LEVSHIN, V. V. ANTONOV-ROMANOVSKII: DAN USSR, 5, 205-6 (1933) (In French); ZETF, 4, 1022 (1939)

TOM VI, Vyp. 5
VOL. VI, No. 5

OPTIKA I SPEKTROSKOPIIA
OPTICS AND SPECTROSCOPY

Mai, 1959
May, 1959

Electro-luminophors on a Sulphide-Selenide Base

O. N. KAZANKIN, F. M. PEKERMAN, L. N. PETOSHINA

Abstract: Electro-luminophors on a ZnS·ZnSe base, activated by Cu, were obtained in a static H_2S + HCl atmosphere. This made it possible to get the hosts with greater ZnSe content, and thus, to prepare effective electro-luminophors with radiating capabilities in the long-wavelength region of the spectrum.

Investigation of the dependence of the brightness of this type of electro-luminophors on the voltage, frequency, and temperature, revealed some peculiarities, which are explained by the decreasing depth of the trapping levels as Se is added.

INTRODUCTION

Electro-luminophors on a mixed sulphide-selenide base are almost untouched by studies, yet investigation of this type of luminophors presents considerable interest. The addition of Se, on the one hand, permits one to get electro-luminophors of various colors, in particular, with a red glow. On the other hand, it is known that addition of Se leads to a decrease in depth of trapping levels [1], and thus, the investigation of electro-luminophors of this type may give a number of experimental facts about the influence of the depth of local levels on the brightness of electroluminescence. This question is very essential to the solution of the general problem of an increase in electroluminescence brightness, and, consequently, an increase in the stimulation quantum efficiency of electro-luminescent condensers. It is known, for instance, that several investigators, including ZALM [2], think that only those luminophors can be effective, that do not have deep local levels.

Electro-luminophors on a ZnS·ZnSe base were first mentioned by Roberts [3], however the method of preparation was not mentioned; it was merely mentioned that they were prepared according to Prener's patent, and radiated in the green region of the spectrum. The content of Se, introduced into the charge, did not exceed 20%.

Orlov [4] prepared electro-luminophors on a ZnS·ZnSe-Cu base, using the method of Homer, that is $Pb(NO_3)_2$ was added to the charge, and the firing was done in a nitrogen stream.

As follows from our experimental data [5], electro-luminophors obtained by Homer's method, are much weaker than electro-luminophors prepared in at atmosphere of H_2S + HCl. Therefore, this work includes the continuation of experiments on synthesis and investigation of effective electro-luminophors on a sulphide-selenide base, obtained by this method.

METHOD OF PREPARING ELECTRO-LUMINOPHORS

A detailed analysis of the technology of electro-luminophors on a ZnS·ZnSe base showed, that effective electro-luminophors can not be obtained with various luminescent colors by using the method of firing in a H_2S + HCl stream as occurs with the ZnS-Cu luminophor [5]. The reason is that under the conditions of H_2S + HCl flow, it was impossible to get the content of ZnSe in the luminophor to be greater than 40%, even if its content in the original charge was 100%.

The reason, apparently, is that selenium is displaced by the sulfur in the H_2S + HCl stream.

Therefore, under given conditions, it would be possible to get electro-luminophors with a radiation maximum not greater than 530 - 540 millicrons, and their brightness was much lower than the brightness of a usual green electro-luminophor on a ZnS-Cu base. To obtain effective electro-luminophors with a controlled ZnSe content, and mainly to obtain electro-luminophors with a large ZnSe content, whose radiation maximum is shifted into the red region, firing under quasi-stationary conditions was used.

For this purpose the charge was placed in a horizontal quartz tube, and a 50% H_2S + 50% HCl gas stream was blown through it for 30 minutes. Then, the tube was carefully pushed into a furnace, and 1-2 minutes later (the time sufficient for removal of moisture), the valve at the output of the tube was closed while the valve at the input of the tube was left open throughout the firing. Thus, the gases were consumed as they went into reaction. Firing under these conditon led to getting electro-luminophors radiating in the region from 510 to 630 millimicrons. However, under these conditions too, as follows from Table 1, the amount of ZnSe found in the luminophor differed from the amount introduced into the charge.

It follows from the aforementioned data, that even in the case of firing pure ZnSe under quasi-stationary conditions in a H_2S + HCl atmosphere, up to 5% ZnS is formed and therefore the radiation spectrum can not be displaced into the long-wavelength region further than 630 millimicrons. Later on, the amount of ZnSe put in the charge before firing will always be indicated.

Table 1

ZnSe Content in Electroluminophors

Quantity of ZnSe introduced into the charge (in %)	Quantity of ZnSe found in luminophor after firing (in %)
100	95
90	86
80	68
70	21
50	22
30	17
10	7

EXPERIMENTAL RESULTS

a) Radiation spectrum. The measurement of the electroluminescence radiation spectra showed that increasing the ZnSe content in the luminophors, shifts the radiation spectrum into the long-wavelength region. (Fig. 1). By varying the amount of ZnSe from 10 to 100%, one can obtain electroluminophors, whose rediation -spectra maxima, when excited by an alternating electric field (ν= 5000 cps, U = 400 V), lie in the region from 510 to 630 mμ.

The position of the radiation spectrum for the same luminophor depends on the frequency and voltage of the exciting field, and on the temperature of the luminophor.

As the frequency is increased the radiation spectrum shifts to short wavelengths, and the shift is more pronounced in the case of electro-luminophors with a low ZnSe content (Fig.2).

It is known [6] , that an increase in frequency leads to prevalence of short-wave over long-wave luminescence centers. This phenomenon is especially distinct in luminophors having pronounced blue and green bands. As the ZnSe content is increased the short-wave length radiation decreases, and, consequently, the change in the radiation spectrum, as the frequency is increased, appears weaker.

Changing the voltage of the exciting field from 350 to 700 volts has little effect on the radiation spectrum. It is noticed that increasing the voltage shifts the radiation spectrum into the short-wave region, but the shift is very small and for the given change in voltage does not exceed 5 millimicrons.

Heating the sample shifts its radiation spectrum into the long-wave region. For an increase in temperature from -10°C to +50°C this shift was approximately 20 millimicrons.

b) Brightness. The relative brightness of samples with various ZnSe contents is given in Table 2.

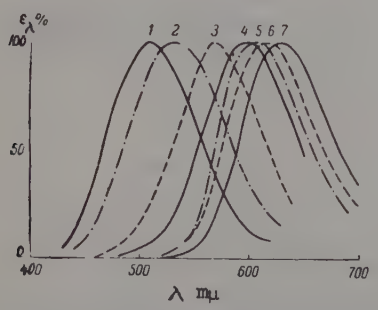

Figure 1. Radiation spectra of ZnS·ZnSe-Cu electroluminophors with various ZnSe contents. (Excitation conditions: U = 400 V, ν = 5000 cps) 1- 10%; 2- 30%; 3- 50%; 4- 70%; 5- 80%; 6- 90%; 7- 100%.

Since the color of electroluminescence varies from green to red as the ZnSe content is increased, the area under the radiation spectrum curve was used as a measure of brightness. It

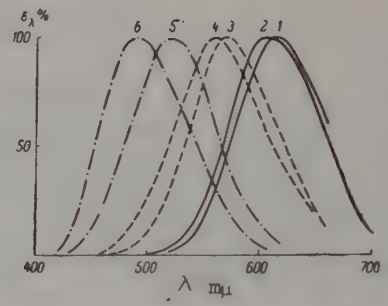

Figure 2. Radiation spectra of ZnS ZnSe-Cu electroluminophors at various frequencies.

1 - ZnSe - 90%, ν = 1000 cps, U =350 v;
2 - ZnSe - 90%, ν =20,000 cps, U =350 v;
3 - ZnSe - 50%, ν = 1000 cps, U =350 v;
4 - ZnSe - 50%, ν =20,000 cps, U =350 v;
5 - ZnSe - 10%, ν = 1,000 cps, U =350 v;
6 - ZnSe - 10%, ν =20,000 cps, U =350 v;

can be seen from the table that as ZnSe is introduced the electroluminescence brightness drops sharply. The samples containing 50 - 70% ZnSe have minimum brightness. As the ZnSe is further increased the brightness of electroluminescence increases sharply. From the same table, it can be seen that the brightness of even the better sulphide-selenide samples is only 20-30% of the brightness of the SnS-Cu luminophor.

Table 2*

Composition of the luminophor	Relative brightness
ZnS-Cu	100
ZnS (90%), ZnSe (10%)-Cu	29
ZnS (70%), ZnSe (30%)-Cu	19
ZnS (50%), ZnSe (50%)-Cu	4
ZnS (30%), ZnSe (70%)-Cu	1
ZnS (20%), ZnSe (80%)-Cu	17
ZnS (10%), ZnSe (90%)-Cu	25
ZnSe-Cu . . .	20

The results we obtained clearly contradict the previously expressed theoretical suppositions, which state that an addition of Se should lead to an increase in brightness. It is possible that a more thorough investigation of the technology of selenide electroluminophors is needed for final proofs; in particular, an investigation of the effect of oxygen, which will be carried out later. The addition of Se appeared, however, more characteristically in the frequency and voltage dependence of the brightness.

The voltage dependence of the brightness even for high Se contents follows the usual law, given in the Zalm work [2] ,

$$B = A \exp\left(-\frac{\alpha}{\nu U}\right)$$

where B is the brightness of electroluminescence, U is the applied voltage, ν is frequency, and A, α are constants.

*The data of the table 2. were obtained under the following conditions: V = 400 V, ν = 5000 cps, t = 20°C.

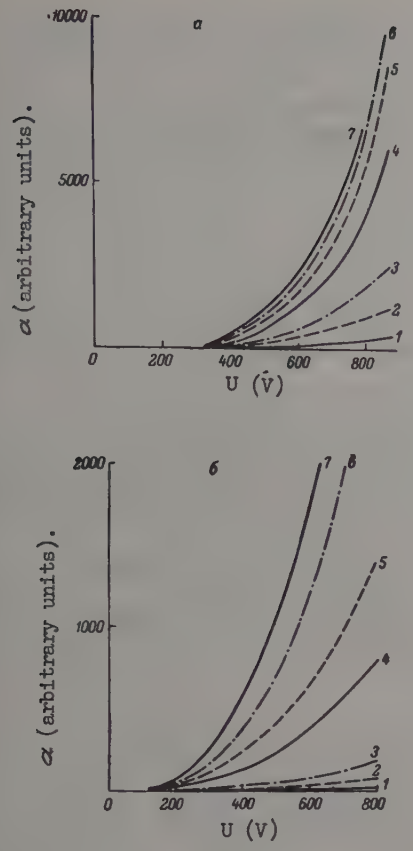

Figure 3. Dependence of electroluminescence brightness on the applied voltage field.

From Figure 3, which gives the curves of electroluminescence brightness vs voltage, it follows that luminophors with a high ZnSe content begin to glow at lower voltages, and have a steeper slope at the linear portion of the curve

$$B = f(U).$$

The curves $B = f(\nu)$ have a characteristic form for these luminophors (Fig.4). Saturation at high frequencies, which occurs for the luminophors ZnS-Cu and ZnS.ZnSe-Cu with a low ZnSe content, does not take place for luminophors containing a large amount of ZnSe.

All these peculiarities of luminophors with a high ZnSe content are explained by the low depth of local levels, created by selenium in the ZnS.ZnSe luminophors. From this point of view it was interesting to investigate the dependence of the electroluminescence brightness B on the temperature t.

On heating, the electroluminescence brightness, starting at some temperature, rises rapidly and reaches a maximum, which occurs at different temperatures for various luminophors. [7].

The curve $B = f(t)$ for the sulphide-selenide luminophors, investigated in the temperature range from -140 to +80°C, is given in Figure 5. As the

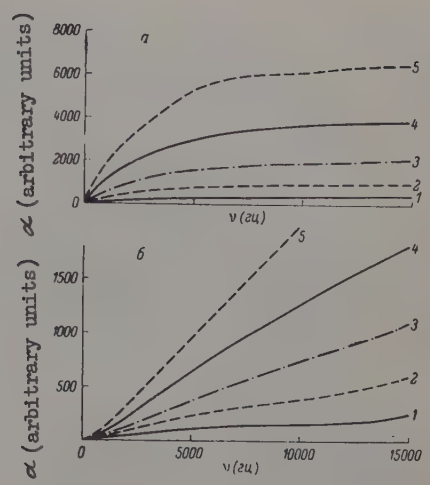

Figure 4. Dependence of electroluminescence brightness on the frequency of the exciting field. a - luminophor ZnS (90%), ZnSe (10%), b - luminophor ZnS (10%), ZnSe (90%). Voltages U (in volts): 1 - 1 - 400; 2 - 500; 3 - 600; 4 - 700; 5 - 800.

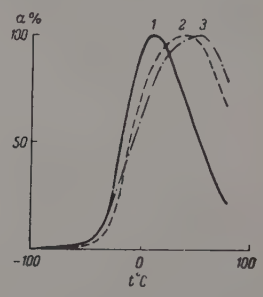

Figure 5. Temperature of electroluminescence (Excitation conditions: U = 500 v, ν = 5000 cps). 1 - ZnS (10%); ZnSe (90%); 2 - ZnS (50%) ZnSe (50%); 3 - ZnS (90%); ZnSe (10%).

temperature increases, the electroluminescence brightness begins to rise, reaches a maximum, and then drops. It is seen from Figure 5, that as the ZnSe content in the luminophor is increased, a reduction in brightness starts at lower temperatures. The maximum of electroluminescence brightness for the luminophor ZnS-Cu, is located at +55° C, while an addition of 90% of ZnSe in this luminophor shifts the maximum to +10°C. If it is assumed that the slope of the curve $B = f(t)$ is due to an increase in the number of electrons leaving the local levels, it becomes clear that the probability of this phenomenon increases as Se is added because the levels become more shallow and consequently, the maximum is reached at a lower temperature than in the case of ZnS-Cu luminophors. The region of drop in the $B = f(t)$ curve is explained, apparently, by quenching processes, whose probability increases as the temperature is increased. If it is assumed that the mechanism of the quenching process consists of holes leaving the levels of the ionized activator as the temperature is increased, then it should be expected that the farther the activator level is

from the valence band the weaker would the quenching be. However, in spite of the fact that the activator level in the ZnS.ZnSe-Cu luminophors is located farther from the valence band than in ZnS-Cu, the quenching process in selenides developes faster than in sulphides.

CONCLUSIONS

It follows from the data obtained that effective electroluminophors on a ZnS.ZnSe base can be obtained by firing in an atmosphere of H_2S + HCl under static conditions. On adding ZnSe into the ZnS lattice, shallower localization levels are formed and a number of specific peculiarities appear in the behavior of the luminophors:

1) electroluminophors on a ZnS.ZnSe base can be excited at lower voltages than luminophors on a sulphide base;
2) the larger the amount of ZnSe added to the luminophor, the higher the frequency at which brightness saturation occurs;
3) the location of the maximum on the curve of the temperature dependence of electroluminescence brightness depends on the ZnSe content in the luminophor; luminophors with a higher ZnSe content have their maximum at a lower temperature;
4) on adding Se, the expected increase in the brightness of electroluminophors was not observed, and further investigation will be carried out. In particular, the effect of oxygen in forming the luminophors on a sulphide-selenide base must be studied.

June 9, 1958

References

1. W. HOOGENSTRAATEN: J. Electrochem. Soc., 100, 365 (1953)
2. P. ZALM: Philips Res. Rep., 11, 353 (1956)
3. S. ROBERTS: JOSA, 42, 850 (1952)
4. I. N. ORLOV: IAN USSR, SF, 21, 731 (1957) (See CTT BULLETIN, p. 728)
5. O. N. KAZANKIN, F. M. PEKERMAN, L. N. PETOSHINA: IAN USSR, SF, 21, 721 (1957) (See CTT BULLETIN, p. 719)
6. P. ZALM, G. DIEMER, H. A. KLASENS: Philips Res. Rep., 9, 81 (1954)
7. O. N. KAZANKIN, L. N. PETOSHINA: OiS, 4(1), 76, (1958)

TOM VI, Vyp. 5 OPTIKA I SPEKTROSKOPIIA Mai, 1959
VOL. VI, No. 5 OPTICS AND SPECTROSCOPY May, 1959

Increasing the Transparency of Metallic Coatings

I. N. SHKLIAREVSKII, A. A. AVDEENKO

Abstract: A method is proposed for clarifying ("increasing the transparency") of aluminum and silver coatings from the glass side in the 0.6 - 1.1 μ range.* It is shown that the transmittance of treated coatings in this region is 2 or more times greater than that of the untreated coatings. If the transmittance of the treated coatings is such that the wave reflected by the metal-glass interface introduces no substantial contribution to the reflection coefficient from the air side, then an increase in the transmission of the clarified coverings is achieved because of the decrease in absorption. Treated coatings can be used for Fabry-Perot interferometers, etc.

Interference lines are reversed by applying this treatment to interferometer coatings. Their intensity is higher than the intensity of lines reversed by truncation of the zero ray. This affords the possibility of using reflecting interferometers with an opaque second coating to investigate the hyperfine structure of lines.

INTRODUCTION

The transparency of an optical glass surface is increased by coating it with a thin transparent film whose refractive index μ_2 satisfies the equation

$$\mu_2 = \sqrt{\mu_1 \mu_3}, \qquad (1)$$

where $\mu_1 = 1$ is the refractive index of air, and μ_3 is the refractive index of glass. The optical thickness of the film is

$$d = \frac{\lambda}{4}. \qquad (2)$$

No attention seems to have been devoted so far to increasing the transparency of metallic surfaces. At first glance there would seem to be little probability of finding a film satisfying conditions similar to (1) and (2), especially in view of the fact that the reflection coefficient of metal surfaces is 80 - 95%. However, it is difficult to overestimate the importance of being able to increase the transparency of partially transparent metallic coverings. The reduction of reflection at the glass-metal interface while keeping the reflection coefficient at the air-metal interface practically unchanged affords the possibility of significantly increasing the speed, contrast and resolving power of Fabry-Perot interferometers, etc. if the absorption of the film is not too great.

The following phenomenon had been detected in 1948 [1,2] and was later investigated in detail [3,4]. If a very thin (100 - 150 Å) silver film is deposited on a glass substrate heated to 300 - 400° and an opaque layer of aluminum or some other metal with a high reflection coefficient superposed on the first film at room temperature, a very intense interference coloring can be observed from the glass side. As the thickness of the silver film is increased, the coloring changes from a light yellow to blue, similar to the Newton interference colors in the first order. In contrast to the Newtonian colors, however, these colors appear to the eye to be independent of the angle of incidence of the light. Curves of the reflection coefficient of the colored films as a function of the wavelength have a sharp minimum. In this case, the film coloring always is complementary to the color of the wavelength for which the reflection coefficient is a minimum. It has been shown in [4] that for such small geometric film thicknesses, the required path difference $\lambda/2$ between the interfering beams is achieved because of phase shifts. Similarly, because of phase shifts, the first interference band in a wedge-shaped zinc-sulfide film deposited on a silver layer appears at an optical thickness of $\lambda/6$ and not $\lambda/2$, as in the case of films deposited on glass [5].

The foregoing was the starting point of the present investigation. Actually, if the opaque layer of aluminum is replaced by a partially transparent aluminum coating the latter becomes transparent. In this case, the wavelengths which have a maximum in transmittance are those which have a minimum in reflectance.

In contrast to treated glass, whose reflection coefficient R is 4 - 5%, the metallic coatings have an R of 80 - 95% at the glass boundary. Naturally, cancellation of this reflection would yield a high gain in transmittance. Even when the ray reflected from this boundary is not completely cancelled, a gain in the transmittance can be obtained even in spite of some light absorption by film.

A theoretical analysis of the transmittance of metallic films will be expedited best by detailed experimental investigation. Both metallic films and transmittance-increasing films are characterized by complex refractive indices. Even though the optical constants of fairly thick metallic coatings are known, the effective optical constants of thin films deposited on a heated substrate have not been studied at all. Working with hypothetical constants would hardly yield any quantitative relationships. Apparently, the formalism of classical electrodynamics permits the Vlasov theory [6] to be used even in this case.

CERTAIN OPTICAL PROPERTIES OF THIN SILVER FILMS

The transmittance-increasing films must not be highly absorbent. If they were, it would be impossible to expect any considerable gain in intensity of the light transmitted by the treated film as compared with the opaque one. Hence, it is necessary to investigate the dependence of the transmittance of thin silver films on the thickness and temperature of the substrate. Since the optical properties of the films can depend to a considerable degree on other factors also (degree of vacuum, evaporation rate), sections of the film were built up to different thicknesses by simultaneous evaporation at a given substrate temperature. Small glass plates cut from the same sheet were placed at different distances from the evaporator and were heated by reflector furnaces. The substrate temperature was checked by a thermocouple. The

* The idea of making metallic coatings transparent was originated by I. N. Shkliarevskii.

large dimensions of the dome permitted a sufficiently uniform coating to be obtained upon each plate.

The transmittance of the film was measured relative to clear glass with an SF-4 spectrophotometer for every 25 mμ within the band from 0.4 - 1 μ. The film thickness was measured by interferometer [7].

The transmissivity of several batches of silver films of different thicknesses, deposited on a substrate at temperatures of 100, 200, 300 and 400° has been investigated. In all cases, a deep minimum in the transmittance was observed in the 475 - 500 μ region. This minimum was displaced toward the red as the film thickness increased. The transparency of the film increased sharply in the long wave length part of the spectrum. Figure 1 shows $T = f(\lambda)$ for a batch of films deposited on the substrate at a temperature of 300°. It was noted that the higher the substrate temperature, the more transparent a film of given thickness was in the red part of the spectrum.

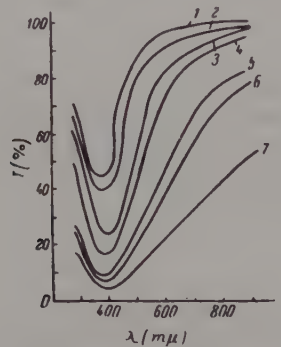

Figure 1. Transmittance of silver films deposited at 300°.
Film thickness in Å: 1 - 100, 2 - 130, 3 - 170, 4 - 180, 5 - 220, 6 - 250, 7 - 280.

Silver films deposited on glass heated to 300 - 400° have a yellow-brown color in transmitted light. In transmitted light, the color of silver films deposited on glass at 100° depends on the thickness and can be blue, dark-blue, violet or reddish, which is in complete agreement with the results of Krautkrämer [8].

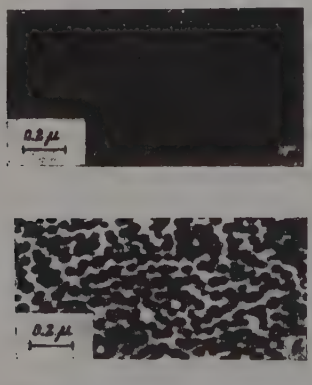

Figure 2. Microphotographs of silver films deposited on glass at 400°.
Film thickness in Å: a - 100 ± 25, b - 135 ± 25.

Silver films deposited on a heated substrate have clearly evident granular structure [9, 4]. As an illustration Figure 2 shows microphotographs of silver films deposited on glass at 400°, which were kindly made at our request by V. R. Golik on the EM-3 electron microscope. The microphotograph in Figure 2a corresponds to a film 100 ± 25 thick, which was colored purple after the deposition of aluminum; the microphotograph in Figure 2b is of a film 135 ± 25 Å thick colored blue. The electron-optical magnification is 5000, the total magnification 50,000.

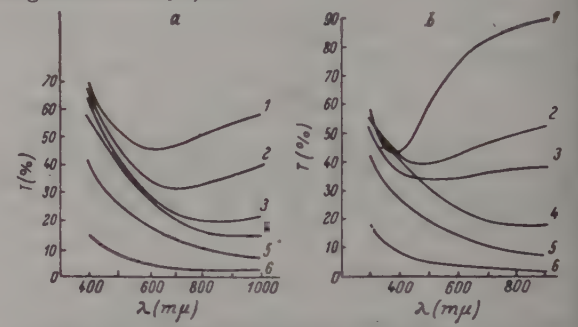

Figure 3. Transmissivity of silver films deposited at room temperature before (a) and after (b) annealing.
Film thickness in Å: 1 - 100, 2 - 160, 3 - 210, 4 - 260, 5 - 340, 6 - 470.

Figure 3 shows the function $T = f(\omega)$ for a batch of silver films deposited at room temperature. The behavior of the curves in this case is completely different from the similar curves of Figure 1; however, it is in good agreement with data in the literature [9]. These films were annealed for three hours at 100°. Longer annealing caused practically no change. Annealing in air or in vacuum led to the same results. Figure 3b shows the transmission curves of the same films as in Figure 3a, but recorded after annealing. The transmittance of films thicker than 200 Å was practically unchanged after annealing. A sharp minimum in the transmittance appeared for 100 Å films in the 475 mμ region; the transmittance grew sharply in the redder regions of the spectrum. The transmittance of films 160 and 210 Å thick increased somewhat in the same region.

It should be noted that the behavior of the $T = f(\lambda)$ curves for 50 - 70 Å films deposited at room temperature is similar to the behavior of the transmittance curves of thicker films deposited on heated glass. Thus, for example, the 50 Å silver film deposited at room temperature has a transmittance minimum of 70% in the 480 mμ region. The transmittance for $\lambda = 600$ mμ is 90%. After annealing the minimum of the transmittance, having been reduced by 2%, shifted to 400 mμ, but the transmittance in the long wavelength region increased to 98% for $\lambda = 600$ mμ and to almost 100% for longer waves. Apparently, thin silver films acquire a more clear-cut granular structure during annealing. This structure is not quite as evident in this case, however, as when the film is deposited on heated glass. Annealed silver films are not colored after being covered by aluminum. These experiments convincingly show that the deposition of films on a heated substrate cannot possibly be explained as an anneal of the films.

For theoretical computations, it is necessary to know the effective optical constants of films deposited on heated glass. We will make such measurements and they will be the subject of a separate report. The dependence of the effective optical constants of silver films deposited at room temperature on their thickness has already been determined [9,10]. We also made analogous measurements for $\lambda = 546$ mμ. The measurements of the transmissivity T and the reflection coefficients from the air side R and from the glass side R′ were made in an apparatus proposed by Dufor [11]. An exit collimator PS-381 was the radiation detector. The film thickness was measured by interferometer [7]. The effective values of the refractive, μ, and absorptive μχ, indices were computed by the graphical method of Male [12]. The dependence obtained for R, R′, T and the absorption A as a function of thickness is similar to that given by Fost [9] if a certain displacement in the minimum of T (and the maximum of A) toward greater thicknesses is not taken into account. The dependence of μ and μχ on the film thickness is also in agreement with results given in the literature [9,10]. Consequently, there is no necessity to present our measurements. As the thickness decreases, the effective values of μ increase and μχ values drop in comparison with the bulk silver constants. For films on the order of 50 A thick, $\mu > \mu\chi$. Since the optical properties of very thin silver films are, to a certain degree, similar to the optical properties of thicker films deposited on a heated substrate, it must be considered that the effective refractive indices of such films are greater than the effective absorption coefficients.

OPTICAL CHARACTERISTICS OF CLARIFIED ALUMINUM AND SILVER COATINGS

A 100 - 170 Å silver film in the form of a very flat wedge was deposited on a heated 4 x 8 cm glass plate. The plate was placed relative to the molybdenum boat of the evaporator in such a position that the thickness of the film was sufficiently uniform parallel to its short side. The calculated quantity of silver was loaded into the evaporator; the evaporation proceeded rapidly. A narrow strip of aluminum was deposited on the silver film at room temperature along the long side of the plate. The required sections of the silver film were selected according to the resulting color. Their transmittance relative to clear glass in the 0.35 - 1.1μ range was measured on an SF-4 spectrophotometer. A partially transparent aluminum coating was also deposited on the film (and on the clear glass sections of the same plate). Special attention was paid to the uniformity of the thickness of this coating. Then the transmittance T of the clarified aluminum coatings was measured relative to the transmittance T_0 of the aluminum coating deposited on the clear glass.

Figure 4 shows transmittance curves of silver films which, after superposition of aluminum films, were colored respectively, purple, dark-blue and blue. Figure 5 shows transmittance curves of the clarified aluminum films relative to the opaque films. As should have been expected, the transmissivity of the clarified coverings dropped sharply in the blue section of the spectrum because of the intense absorption by the silver films, but it increased a maximum of 2.3 fold (at 650 mμ) for the "purple" coating, 2.4 fold (at 725 mμ) in the "dark-blue" coating, and 3.6 fold (at 1050 mμ) for the "blue" coating. Similar results were also obtained in several other samples. The largest increase in the transmittance of the "blue" coating apparently is due to the fact that the silver film is almost completely transparent in this region.

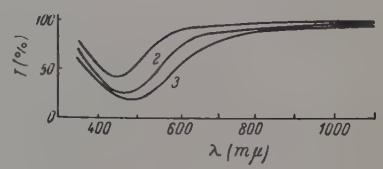

Figure 4. Transmittance of silver films which were colored after aluminum had been deposited thereon. 1 - purple; 2 - dark blue; 3 - blue.

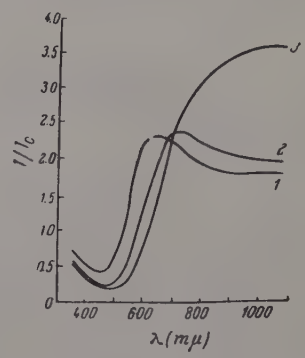

Figure 5. Transmittance of clarified aluminum layers relative to the transmittance of an aluminum coating deposited on clear glass. The curve numbers correspond to those in figure 4.

If the transmittance of the aluminum coatings deposited on clear glass is 1 - 3% in the red region of the spectrum, then as the measurements showed, the reflection coefficients from the air side of the clarified and opaque sections are identical to within 0.5%; it is completely impossible to differentiate them visually. Hence, the transmittance T of the clarified coatings increases considerably for an unchanged value of the reflection coefficient R from the air side, the reflection coefficient of the clarified sections drops in comparison to the opaque sections. Now the transmittance grows because of the decrease in R as well as in A. However, it is not difficult to see that the optical characteristics of such a coating appear to be better than those of an opaque coating with the same reflection coefficient R.

Unfortunately, a silver film makes an aluminum coating more transparent only in the red part of the spectrum. Aluminum coatings are not best for interferometer purposes in this region of the spectrum. If multilayer dielectric coatings are excluded from consideration, silver remains irreplaceable for this purpose.

Thin silver films deposited on heated glass after a silver coating had been superposed at room temperature do not yield a bright color. However, if an extremely thin film of aluminum is first covered by a silver film deposited in such a manner, then this appears to be sufficient to produce a bright color by the subsequent deposition of a silver coating, which does not reduce the intensity of the color arising upon the deposition of aluminum on a silver film.

Figure 6 shows transmittance curves of silver films deposited on heated glass, and covered by a thin aluminum film at room temperature. Figure 7 illustrates the effect of clarification. The transmittance of a silver coating deposited on clear glass is 1.5% in the red portion of the spectrum. The transmittance increased twofold or more in the 650 - 1000 mμ range for the "blue" clarified coating. Similar results have also been obtained in the other samples. In one of the samples where the thickness of the aluminum film was less, the magnitude of the transmittance increased 2.4 times at the maximum (λ = 725 mμ) for the "dark-blue" clarified coating.

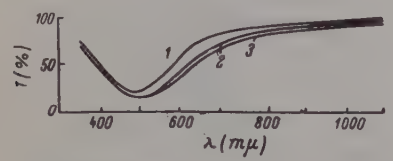

Figure 6. Transmittance of silver films deposited on heated glass, which have been covered by a thin aluminum film at room temperature. After the deposition of a partially transparent silver covering the films were colored:
1 - purple; 2 - dark-blue; 3 - blue

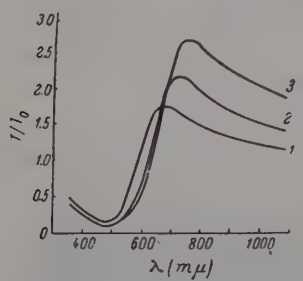

Figure 7 Transmittance of clarified silver layers with respect to the transmittance of a silver coating deposited on clear glass. Curve numbers correspond to those on figure 6.

Clarification of aluminum and silver coatings has been accomplished fully only in the red part of the spectrum so far. A rich color can be obtained if copper or gold [3] is deposited on the heated glass instead of silver. Possibly these or other clarifying films will give a good effect in the middle and blue regions of the spectrum.

In the next section, the optical characteristics of interferometers with clarified coatings will be investigated. A considerable increase in the luminosity in the red portion of the spectrum has qualitatively been observed in lines of even orders.

REVERSAL OF INTERFERENCE LINES BY CLARIFICATION OF INTERFEROMETRIC COATINGS

Interference lines in transmitted light have a number of advantages over interference fringes in reflected light. This question has been investigated in detail in [9] . If the "zero" ray is removed by a diaphragming during observation of an interference pattern in reflected light, then the dark lines against a bright background are converted into bright lines against a dark background. The interference pattern becomes completely identical to that which is observed in transmitted light. Bruce [13] postulated precisely this. The very same can be obtained considerably more simply and with better results by clarifying the interferometric coating which is facing the observer. It is useful here to use the "zero" ray, which is destroyed.

Figure 8 shows a photograph of lines of even order obtained in reflected light. Half of the interferometric aluminum coating turned to the spectrograph was first clarified by a dark-blue film. In conformance with this, the interference lines are reversed in the upper part of the photograph. The broadening of the reversed lines is a photographic effect. Having considerably greater intensity than the bright field of the lower part of the photograph, they light up the dark field. In order to emphasize the contrast between the two parts of the photograph, a narrow transition strip, caused by the diffuseness of the boundaries of the clarifying film has been cut out. The line reversal is observed not only in the red part of the spectrum but also in the blue-green. However, if a gain in intensity is obtained in the red part of the spectrum, the intensity drops in the blue portion.

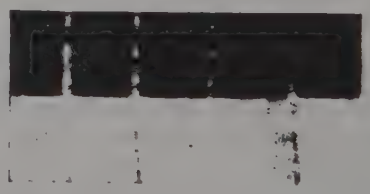

Figure 8. Photograph of lines of even order obtained in reflected light.

If the interference fringes consist of two or more components with sharply different intensities, they can be observed only in transmitted light. In the contrary case, the minimum of the weaker component falls on the broad maximum of the strong component and is overshadowed by the latter.

With a clarified interferometer coating when interference lines are reversed, complex lines can also be observed in reflected light. Moreover, lines in reflected light can advantageously be distinguished from lines in transmitted light if the second interferometric coating is also made opaque. In this connection, an investigation of reflecting interferometers (Fabry-Perot etc.) produced in the manner mentioned would be of interest. Such investigations will be made in our laboratory.

In conclusion, the authors take this opportunity to express their gratitude to K. D. Sinel'nikov for his interest in the research.

November 10, 1958

References

1. I. N. SHKLIAREVSKII: Cand. diss. Khar'kov Univ., 1949
2. I. N. SHKLIAREVSKII: Uch. Zap. Khar'kov Univ., Trudy fiz. otd. (Transactions of the physics section), 2, 83 (1950)
3. K. D. SINEL'NIKOV: I. N. SHKLIAREVSKII: Uch. Zap. Khar'kov Univ., Trudy fiz. otd., 3, 43 (1952)
4. K. D. SINEL'NIKOV, I. N. SHKLIAREVSKII, E.A.KANER: Uch. Zap., Khar'kov Univ., Trudy fiz. otd., 6, 127 (1955)
5. I. N. SHKLIAREVSKII: ZTF, 26, 333 (1956) (See Soviet Physics, Technical Physics)
6. I. V. GREBENSHCHIKOV, A. G. VLASOV, B.S. NEPORENT, N. V. SUIKOVSKAIA: Prosvetleni optiki (Elucidation of optics). GITTL, Moscow-Leningrad, 1946
7. N. V. RAPP: Uch. Zap. Khar'kov Univ., Trudy fiz. otd. 2, 55 (1950)
8. J. KRAUTKRAMER: Ann. d. Phys., 32, 537 (1938)
9. G. V. ROZENBERG: Optika tonkosloinykh pokrytii (Optics of fine layered coverings) GIFML, Moscow, 1958
10. S. METHFESSEL: Dunne Schichten. VEB Wilhelm Knapp Verlag, Halle, 1953
11. S. TOLANSKY: High resolution spectroscopy (IL, Moscow, 1955, Appendix 2)
12. D. MALE: ANN. de Phys., 9, 10, (1954)
13. C. F. BRUCE: Austral. J. Sci. Res., 4A, 1, 117 (1951)

TOM VI, Vyp. 5
VOL. VI, No. 5

OPTIKA I SPEKTROSKOPIIA
OPTICS AND SPECTROSCOPY

Mai, 1959
May, 1959

Determination of the Absolute Sensitivity of Certain Photographic Materials to Ultra-Soft X-Radiation

A. P. LUKIRSKII AND I. A. KARPOVICH

Abstract: This paper describes the method used to obtain curves of blackening of certain photographic emulsions under the action of ultra-soft x-radiation with wavelengths of 23.6, 44, 67, and 113 Å and the evaluation of the absolute sensitivity of the photographic materials studied.

Ultra-soft x-radiation is very strongly absorbed by materials, and therefore special equipment is required for the reception of this radiation and for short wave ultra-violet radiation, and in particular special photographic materials are required. In this paper are presented the data obtained relative to the absolute sensitivity of certain photographic materials to ultra-soft x-radiation.

The shape of the blackening curves characteristic of the x-ray lines $O_{K\alpha}$, $C_{K\alpha}$, $B_{K\alpha}$, and $Be_{K\alpha}$ as produced with the help of a vacuum-ray monochromator with a diffraction grating is described in the article [1]. A photographic plate was placed in a special cassette behind a Geiger Counter. The front cover of the cassette, on which was a window approximately 248 mm in size for the transmission of the radiation, was mounted in a monochromator in such a manner that the radiation was permitted to enter through the window and fall on the plate only when the counter was removed from the path of the radiation beam. It was possible to remove the back cover of the cassette together with the photographic plate in the antechamber back of the cassette, away from the window, without breaking the vacuum in the apparatus. At each insertion of the counter into the beam the irradiation of the photographic plate ceased, and the plate was then moved a fixed distance so that a new part of it appeared in front of the window; upon removal of the counter from the beam, this part was then exposed to the irradiation, etc. A single photographic plate was permitted to receive 9 blackening "marks". In order to obtain an appreciable blackening for the admissable duration of the irradiation, which in our experiments ranged from 10 seconds to 2 hours, a considerable radiation intensity was required. The monochromator allowed us to obtain an intensity of up to 10^6 quanta per second. Inasmuch as a Geiger Counter is not able in practice to count more than 1,000 quanta per second, an attenuator was placed in front of the counter window. The attenuator consisted of seven superimposed meshed grids. It was adjusted so that it provided a beam attenuation of 490. Hence for a counting rate of up to 500 pulses per second we could measure intensities up to 2.5×10^5 quanta per second. In determining the intensity, there was introduced, in addition to the attenuator correction, also an absorption correction of the radiation on the film covering the window of the counter, and a correction for the "dead time" of the counter. Details are given in [1]. Measurements of the intensities were plotted before and after the photograph of each blackening "mark" and the average value was taken. The slow change in the radiation intensity for long exposures which are related to irreversible processes on the anode of the x-ray tube was thus taken into account.

Blackening curves were plotted for Schumann plates, a special film NIKFI, and Spectral plate No. 3. The Schumann plates and the special film NIKFI were developed in developer Agfa-12 (composition: metol 8 grams, sodium sulfite (anhydrous) 12 grams, sodium carbonate (anhydrous) 6.75 grams, potassium bromide 2.5 grams, and water to make 1 liter) and Spectral plates No. 3 were developed in a developer having the following composition: metol 2.2 grams, sodium sulfite (anhydrous) 96 grams, hydroquinone 9 grams, sodium carbonate (anhydrous) 48 grams, and water to make 1 liter. The developing time was 5 minutes and the temperature 20 degre

The blackening "marks" obtained had the appearance of bands, the dimensions of which were approximately 0.4 x 4 mm. Inasmuch as the "marks" had an unequal blackening density, in order to determine the number of quanta falling on 1 mm^2 of the "mark" and to establish data for the blackening density, curves were plotted in the following manner.

1. All of the "marks" obtained on the plates were measured with a microphotometer at exactly the same relative point on each "mark" and which corresponded to the point of greatest blackening density. From this a blackening curve was drawn, $D = f(\lg N')$ where D is the optical density and N' is the number of quanta falling on the entire area of each "mark" during the time of exposure.

2. Along several of the "marks" the average width "b" was determined.

3. Several "marks" were measured with the microphotometer along the height. On the basis of what was obtained from the microphotometer the distributions of the optical densities were plotted as a function of the distribution of intensities. A graphical integration of these curves was then performed, and the effective height for each mark was determined, corresponding to the maximum optical density. These data were averaged for several "marks" and the average value of the height h was found.

4. After the determinations of b and h were made, blackening curves of the form $D=f(\lg N)$ were plotted, where $N = N'/bh$ or the number of quanta falling on 1 mm^2 of each "mark" in the region of maximum density.

It might be noted that the error in the calculation of N, arising from the described method of obtaining the measurements, worked out to be about 30%.

In Figure 1 are shown the blackening curves for Spectral plates No. 3 which were used in a majority of the measurements. From Figure 1 it is seen that with an increase in wavelength the curves are displaced in the direction of greater values of N, that is the sensitivity decreases; also the rectilinear portion of the curve is shortened, and for the radiation $Be_{K\alpha}$ for smaller values of optical density, the plate saturates more rapidly. The exception is the curve for $C_{K\alpha}$. The results obtain reveal that, taking into account the presence of the gelatin in the photographic emulsion, the radiation $Be_{K\alpha}$ is the most strongly absorbed by the gelatin, while the radiations $B_{K\alpha}$ and $O_{K\alpha}$ were absorbed to a lesser degree and the $C_{K\alpha}$

adiation least of all because of the strong absorp-
ion of carbon on the short wave side of the line
K_α. The sensitizing agent for the radiation $B_{K\alpha}$
was sodium salicylate acid, which did not produce
an increase in sensitivity as can be seen from
Figure 1. However, the slope of the blackening
curve is increased, and apparently the length of
the rectilinear portion is also.

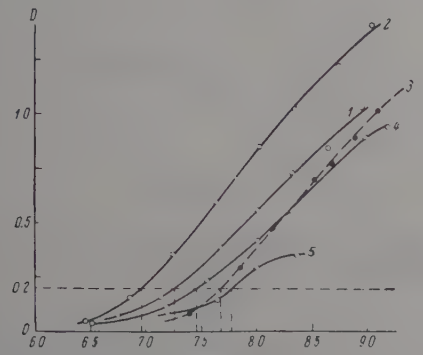

Figure 1. Blackening Curves for Spectral Plate No. 3.

Radiation wavelengths (in Å): 1- 23.6 ($O_{K\alpha}$), 2-
44 ($C_{K\alpha}$), 3- 4- 67($B_{K\alpha}$), 5- 113($Be_{K\alpha}$). Curve 4
was obtained with sodium salicylate acid on the photo-
graphic plate.

In Figure 2 are shown the blackening curves obtained for the NIKFI special plates which contained only very small amounts of gelatin. The curves depicting the sensitivity of this film to the radiations $O_{K\alpha}$, $C_{K\alpha}$, and $Be_{K\alpha}$ practically coincide, and exhibit very large rectilinear segments.

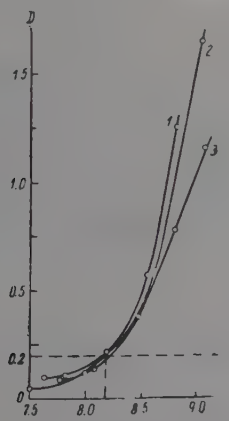

Figure 2. Blackening curves for NIKFI Special Films.

Radiation wavelengths (in Å); 1- 23.6, 2- 44,
3- 113.

In Figure 3 are shown the blackening curves for Schumann plates for the radiations $B_{K\alpha}$ and $Be_{K\alpha}$.

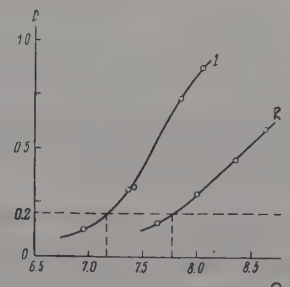

Figure 3. Blackening curves for Schumann plates.

Radiation wavelengths (in Å): 1- 67, 2- 113

In the following table is a tabulation of the values obtained for N corresponding to a blackening density of 0.2 These values allowed us to determine the characteristics of the absolute sensitivity of the photographic materials which were studied, to ultra- soft x-radiation.

Values of N, Corresponding to a Blackening Density of D=0.2 (in quanta per mm²)

Photographic Material	Wavelength of X-radiation (in Å)			
	23.6 ($O_{K\alpha}$)	44 ($C_{K\alpha}$)	67 ($B_{K\alpha}$)	113 ($Be_{K\alpha}$)
Spectral Plates No.3	$1.8\cdot10^7$	$9\cdot10^6$	$3\cdot10^7$	6.10^7
Spectral Plates No.3 sensitized with sodium salicylic acid	–	–	$5\cdot10^7$	–
NIKFI Special Films	$1.6\cdot10^8$	$1.6\cdot10^8$	–	$1.6\cdot10^8$
Schumann Plates	–	–	$1.5\cdot10^7$	$6\cdot10^7$

It is seen from the reduction of the data given in the table that for the obtaining of an appreciable blackening density of the emulsions studied under ultra-soft x-radiation, there are required between 10^7 and 10^8 quanta per mm².

July 31, 1958

References

1. A. P. LUKIRSKII, M. A. RUMSH, L. A. SMIRNOV: ZTF (in press) (See Soviet Physics, Technical Physics)

ТОМ VI, Vyp. 5
VOL. VI, No. 5

OPTIKA I SPEKTROSKOPIIA
OPTICS AND SPECTROSCOPY

Mai, 1959
May, 1959

Hydrogen and Mercury-Helium Light Sources for SF-4 Spectrophotometers

S. I. LEVIKOV AND L. P. SHISHATSKAIA

Structural, electrical, spectroscopic, and other characteristics of the VSFU-3 hydrogen lamp and RSFU-2 Mercury-helium lamp, usable in SF-4 spectrophotometers are described. Certain information on the practical use of these lamps are given.

In recent laboratory practice wide use has been made of the SF-4 quartz photoelectric photometer, which was designed for measurement of optical densities or transmission coefficients of liquids and solids in a wide range of the spectrum - from 220 to 1100 mμ . For such measurements there are two sources in the instrument for continuous illumination - incandescent lamp A-7 and a hydrogen lamp VSFU-3, supplied by line voltage through a special electronic regulator EPS-86. A third lamp, a mercury-helium RSFU-2, is used for periodic calibration of the SF-4 measurement scale. This article concerns certain information on the VSFU-3 and RSFU-2 lamps.

HYDROGEN LAMP VSFU-3

We know that molecular hydrogen, excited in a low pressure tube by an electrical discharge, gives an intense continuous spectrum beginning in the visible (about 480 mμ) and extending far into the short wave ultraviolet region (to 130 mμ).

The problem of constructing a lamp for the SF-4 was solved on the basis of the following assumptions:

a) the lamp is a low-voltage arc type with a directly-heated oxide cathode designed for constant or rectified current;

b) the type of lamp selected as the basis of the construction was the one known as the "light spray"; in lamps of this type the discharge between the electrodes passes through a narrow slit in a screen between the cathode and anode;

c) introduced into the narrow slit in the screen is a small tube wound of thin wire. Because of this tube the illumination of the gas becomes more intense (approximately double) than what it would be if the tube were absent;

d) a special procedure was developed for depositing the oxide layer on the cathode base, which assured increased stability of the radiation intensity.

The envelope of the lamp is made of ZS-5 glass, and the window of special uviol glass. The thickness of the glass window in the middle is not more than 0.2 mm. Its working part, which passes a 45° light cone, has an absolutely clean surface, without bubbles, waviness, or other defects. The average spectral curve of window transparency of several typical lamps is shown in Figure 1. The change in spectral absorption of the boron silicate uviol glass under the influence of ultraviolet radiation (solarization) is insignificant, and is observed primarily in the near ultraviolet region. This assures a very small shift in the initial values of the working shortwave boundary (215 mμ) to the end of the tube's life span. The envelope is filled with thoroughly dried and purified hydrogen gas to 4 mm Hg . The over-all appearance of the lamp is shown in Figure 2.

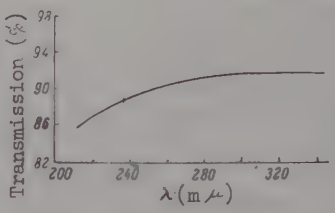

Figure 1. Averaged spectral curve of window transparency of several typical lamps.

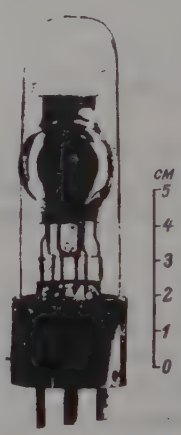

Figure 2

External view of a Hydrogen Lamp.

The electrical characteristics of the lamp are as follows: the cathode heater voltage is not more than 2 volts, maximum heater current is 4 amp, the working arc current through the lamp is 0.3 amp at a voltage on its electrodes of 80 to 90 V (at the beginning of operational use). To start the tube, 250 v of direct or rectified voltage and a heater current of 3.5 amp are required. After the lamp is lit, it is necessary to lower the heater current to 0.8 amp. The lamp can operate with alternating current also. In this case the ignition current decreases somewhat. The lamp, in operation, acts as a rectifier.

Shown in Figure 3 is a curve of relative change in radiation intensity during its life (for the 300 mμ region).

The radiation stability of the lamp is achieved with an EPS-36 electronic regulator which maintains constant discharge current with an accuracy of 0.1%. Unfortunately, the regulator does not include a circuit which could be used to regulate the cathode heater current.

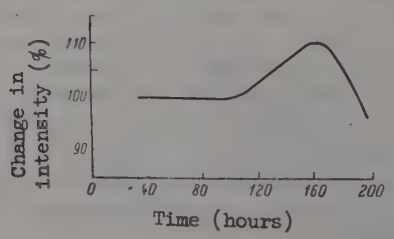

Figure 3. Curve of relative change in radiation intensity of a hydrogen lamp during its service life.

In this connection, if there are frequent noticeable voltage transients in the line, it is recommended that the device should be supplied through a ferro-resonance regulator. For greater accuracy in measurements the cathode should be supplied from a storage battery. If this is done, the supply circuit of the lamp should be modified as shown in figure 4.

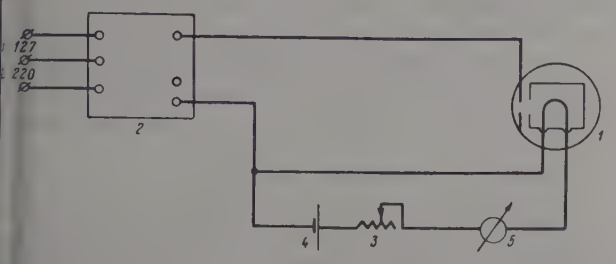

Figure 4. Diagram of the power supply for the hydrogen lamp with a regulator and storage batteries.

1) hydrogen lamp; 2) electronic regulator EPS-86; 3) adjustable resistor of 5 to 10 ohms and 3 to 5 amp; 4) 6-v, 135 ampere-hour storage batteries; 5) 5 amp ac ammeter.

If for any reason it should be impossible to regulate the cathode heater current, it will be necessary to determine for each lamp the dependence of the relative change in radiation intensity on the heater current, varying the latter from 0.1 to 1.5 amp, and selecting the current in the segment of the curve obtained which would give the minimum change in intensity.

MERCURY-HELIUM LAMP RSFU-2

The mercury vapors in this lamp radiate many intense lines in the visible and ultraviolet regions of the spectrum, and the helium acts similarly in the visible and infrared regions. Therefore this lamp is used periodically to check the calibration of the SF-4 scale. In structure and size this lamp is similar to the hydrogen lamp, differing only by the absence of the spiral in the opening in the screening cylinder. The envelope of the lamp is filled with helium at a pressure of 10 to 12 mm Hg, and contains, in addition, a certain quantity of mercury. The electrical characteristics of this lamp are the same as those of the hydrogen lamp, except that the voltage on the electrodes of the mercury-helium lamp during operation is 35 to 45 volts. A direct current of about 150 volts is required to ignite the lamp. The lamp can also operate with alternating current. In this case the ignition voltage is somewhat decreased. In operation the lamp functions as a rectifier. The envelope of the lamp has a window made of the same uviol glass as that of the hydrogen lamp. The radiation of the RSFU-2 lamp can be stabilized in the same manner as that for the hydrogen lamp.

In the following table are shown the most intensive helium and mercury lines which can be used for calibration.

Element	Wavelength (in mμ)	Element	Wavelength (in mμ)	Element	Wavelength (in mμ)
Mercury	226.0	Mercury	302.0	Helium	492.0
	248.0		313.0		502.0
	258.7	Helium	319.0	Mercury	546.0
	265.0	Mercury	334.0	Mercury	579.0
					580.0
	275.0		365.0	Helium	588.0
	280.0	Helium	389.5		668.0
	285.0	Mercury	405.0	Mercury	708.0
					709.0
Helium	294.0		436.0		1014.0
Mercury	297.0	Helium	447.0	Helium	1083.0
			471.0		

The life of both lamps - hydrogen and mercury-helium - is not less than 200 hours. The intensity of the general radiation of the hydrogen lamp is more or less constant at first, then increases because of lowered hydrogen pressure, reaches a maximum value, and then falls quickly. After a period of operation an RSFU-2 lamp can become unstable, and the intensity of the shortwave length lines will decrease somewhat, making it necessary to widen the slit of the apparatus. Both lamps require attention. Before using the lamps, it is necessary to wipe the windows with alcohol-moistened cotton, because greasy deposits on the glass strongly absorb ultraviolet rays.

In conclusion let us note that both the hydrogen and mercury-helium lamps can be used in various spectroscopic devices and equipment. In doing so, if radiation stability is not important, the lamp should be ignited as shown in Figure 5.

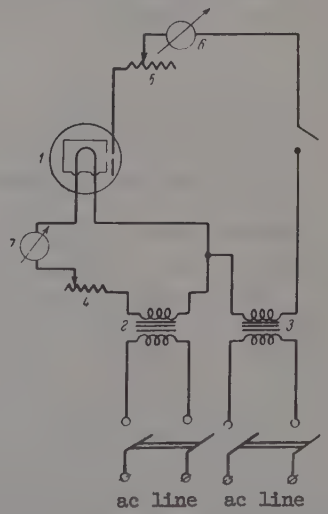

Figure 5. Ignition circuit for the hydrogen and mercury-helium lamps without discharge current regulation.

1) lamp; 2) step-down transformer with power of not less than 15 watts; 3) 450-v step-up transformer; 4) and 5) adjustable resistors; 6) and 7) ammeters for check of discharge and heater currents.

Some lamps ignite at a line voltage of 220 volts. For such lamps the same circuit is used, except for the step-up transformer. If the lamp does not ignite when the anode voltage is switched on, then it is recommended that a Tesla or Rukorf coil be used. In such rheostat circuits the discharge current of the lamp can be increased to 0.5 amp, and for short durations (not over 5 min.) it is permissible to bring the current up to 1.0 amp. In doing this the intensity of radiation increases sharply. The lamp should be switched off in reverse order: first the anode voltage should be removed, then the cathode heater current reduced to a minimum, and then the lamp is switched off.

June 4, 1958

TOM VI, Vyp. 5 OPTIKA I SPEKTROSKOPIIA Mai, 1959
VOL. VI, No. 5 OPTICS AND SPECTROSCOPY May, 1959

BRIEF REPORTS

Accuracy of Wavelength Determination on a DFS-3 Grating Spectograph with Various Interpolation Formulas

V. A. LOGINOV

An estimate of the interpolation error in the accurate measurement of spectrograms obtained on the DFS-3 grating spectrograph [1] is of interest in the investigation of the fine structure of molecular spectra.

The present paper gives the magnitudes of wavelength intervals over which the error of linear and quadratic interpolation does not exceed a given quantity.

The condition for the formation of the principal maxima is

$$m\lambda = d\,(\sin\psi + \sin\varphi), \tag{1}$$

where ψ is the angle of incidence, φ the angle of diffraction, d the grating spacing, λ the wavelength, and m the order of the spectrum. Denoting the microscope readings for the lines of the spectrum by x and taking into account that

$$x - x_0 = f \operatorname{tg} \alpha,$$

where $\alpha = \varphi - \psi$, a few simple rearrangements give the following expression for λ:

$$\lambda = \lambda_1 + a(x - x_1) - b(x - x_1)^2 - c(x - x_1)^3, \tag{2}$$

In the above expression,

$$a = a_0 - 2b_0(x_1 - x_0) - 3c(x_1 - x_0)^2,\quad b = b_0 + 3c(x_1 - x_0),\quad a_0 = k_m \cos\psi; \tag{3}$$

$$b_0 = \frac{\lambda_0}{4f^2},\quad c = \frac{a_0}{2f^2},\quad k_m = \frac{d}{mf},$$

$$\lambda_0 = \frac{\lambda_0^*}{m} = 2\,\frac{d}{m}\sin\psi,$$

λ_0^* – is the wavelength established on the wavelength scale; f is the focal length of the spherical mirror and λ, λ_1, and x, x_1 are the wavelengths and microscope readings for the unknown and comparison lines.

Computation shows that the deviation of (2) from (1) is 0.0004 Å over a range of $x - x_0 = 80$ mm; consequently, (2) can be considered as a practically exact dispersion formula for the DFS-3 spectrograph over an interval of this size.

In practice, it is important to know the magnitude of the wavelength interval l for which the limit of the interpolation error N is given [2].

In the simplest case, when linear interpolation is used to measure small section of the spectrum, we will have*

$$l = \frac{K}{\sqrt{\lambda_0}} \qquad (K = 4f\sqrt{N} = \text{const.}). \tag{4}$$

If it is required to determine the wavelengths of a large number of spectral lines, as is important in investigations of the fine structure of molecular spectra, linear interpolation is too cumbersome, requiring the identification of numerous standard lines located sufficiently close to each other. In this case, it is expedient to use quadratic interpolation. The remainder term of the interpolation

$$R(\mu, \mu_2) = -cl^3 f(\mu, \mu_2) \quad (0 < \mu_2 < 1) \tag{5}$$

becomes zero for $\mu = 0$, $\mu_2 = 1$.

The function $f(\mu, \mu_2)$ in (5) equals $\mu(\mu - \mu_2)(\mu - 1)$, where $\mu = \dfrac{x - x_1}{l}$, $\mu_2 = \dfrac{x_2 - x_1}{l}$, $l = x_3 - x_1$ are the intervals of the comparison spectrum and x_1, x_2, x_3 are the microscope readings for the comparison lines with wavelengths λ_1, λ_2, λ_3, respectively.

The extremum value $f(\mu_{cr}, \mu_2)$ equals 0.1 at $\mu_2 = 0.8$ and has its minimum value 0.048 for $\mu_2 = 0.5$; consequently, the equality $\lambda_2 \approx \dfrac{\lambda_1 + \lambda_3}{2}$ must be complied with if possible in selecting λ_2. If the limit of error $N \geq |R(\mu, \mu_2)|$ is known, expressions (3) and (5) give us

$$l \leq l_0 \sqrt[3]{\sec\psi}, \tag{6}$$

where

$$l_0 = f\sqrt[3]{\frac{2mN}{df(\mu_{cr.}, \mu_2)}}.$$

NUMERICAL DATA FOR THE DFS-3

1. For a 1200 lines/mm grating, $m = 1$, $\lambda_0 = 5000$ Å, $f = 4000$ mm, we have from (3)

$k_m = 2.0833$ Å/mm, $l = x - x_0 = 40$ mm,

$a = a_0 = 1.9874$ Å/mm, $al = 79.495$ Å,

$b = b_0 = 7.813 \cdot 10^{-5}$ Å/mm^2, $bl^2 = 0.125$ Å,

$c = 6.2 \cdot 10^{-8}$ Å/mm^3, $cl^3 = 0.004$ Å,

i. e., the influence of the third power term in (2) is insignificant.

2. Linear Interpolation. The constant K is 506 for $N = 0.001$ Å, $f = 4000$ mm and is independent of the order of the spectrum.

The numerical values of l over which linear interpolation is permissible are determined from (4), and are presented in Table 1. This table shows that linear interpolation is permissible for $N = 0.001$ A over intervals of approx. 5-11 mm, in different regions of the spectrum.

*See [3, 4] for the procedure for using interpolation formulas to measure spectrograms.

These figures are equivalent to intervals of 10 - 22 Å and 20 - 44 Å in the first orders of the 1200 and 600 lines/mm gratings, respectively.

3. Quadratic Interpolation. Putting $m = 1$, $N = 0.001$ Å, $f(\mu_{cr}, \mu_2) = 0.1$ (for $\mu_2 = 0.8$), $f = 4000$ mm, we find $l_0 = 53.6$ and 42.5 for 1200 and 600 lines/mm gratings, respectively. Table 2 gives numerical values of l as a function of λ_0, determined from (6). It is seen that quadratic interpolation is permissible over intervals of approximately 54 and 43 mm, (covering 108 Å and 172 Å in the first order) of the 1200 and 600 lines/mm gratings, respectively. It is also seen that l is practically independent o

It is important to note that the actual accuracy of a wavelength determination depends not only on the interpolation formula, but also on a number of other factors which must also be taken into account (spectrograph stability, accuracy of the standard lines, quality of spectral line images, line shapes accuracy of the comparator, etc.)

Formulas (4) and (6) for determining permissible interpolation intervals for a prescribed limiting error, and Tables 1 and 2 may prove useful for approximation purposes.

The author is grateful to Prof. V. M. Tatevsk for valuable remarks and comments.

May 21, 1958

Table 1

Spectrum Intervals Permissible For Linear Interpolation

$N = 0.001$ Å, $K = 506$

λ_0 (in Å)	l (in mm) according to (4)
2000	11.3
4000	8.0
5000	7.2
6000	6.5
8000	5.7
9000	5.3
10000	5.1

Table 2

Spectrum Intervals Permissible For Quadratic Interpolation

$N = 0.001$ Å, $m = 1$

λ_0 (in Å)	1200 lines/mm grating		600 lines/mm grating	
	φ	l (in mm) according to (6)	φ	l (in mm) according to (6)
2000	6°54′	53.7	3°26′	42.5
4000	13 53	54.1	6 54	42.6
5000	17 27	54.4	8 38	42.7
6000	21 06	54.9	10 22	42.8
8000	28 41	56.0	13 54	42.9
10000	36 52	57.7	17 27	43.2

References

1. V. K. PROKOF'EV: IAN USSR, SF, 18(6), 643 (1954) (See CTT Bulletin, p. 330)
R. I. TVERIANKINA: IAN USSR, SF, 19(1), 28 (1955) (See CTT Bulletin, p. 36)
2. V. L. GONCHAROV: Teoriia interpolirovaniia i priblizheniia funktsii (Theory of interpolation and approximation of functions). GITTL, Moscow, 1954
3. R. A. SAWYER: Experimental Spectroscopy. N.Y. Prentice-Hall, 1951 (IL, Moscow, 1953)
4. S. E. FRISH: Tekhnika spektroskopii (Spectroscopic Techniques) KUBUCH, Leningrad, 1936

TOM VI, Vyp. 5 OPTIKA I SPEKTROSKOPIIA Mai, 1959
VOL. VI, No. 5 OPTICS AND SPECTROSCOPY May, 1959

On the Temperature Dependence of the Intensities of the Summation Tones $\nu_1 + \nu_3$ and $\nu_1 + (\nu_1 + \nu_4)$ of Gaseous CCl_4

M. P. LISITSA AND V. N. MALINKO

Quantitative measurements of the intensities of vibrational bands of gases occupy a special place among temperature studies of infrared absorption spectra. From the results of such measurements it is possible to obtain valuable information concerning the probabilities of transitions between vibrational levels of the free molecule, the population densities of these levels, and so on. In spite of the fact that the theory of the temperature variation of the intensities of vibrational absorption bands was worked out some time ago [1], the theory has remained unverified up to the present. This situation is due to the substantial experimental difficulties involved, particularly for the spectral region in which glass or quartz cannot be employed for the windows of the gas absorption cell.

A first attempt to obtain an experimental verification of the theory has been undertaken by the authors of the present note. The investigation was concerned with the summation tones $\nu_1 + \nu_3$ and $\nu_1 + (\nu_1 + \nu_4)$ of carbon tetrachloride [2], the temperature dependence of which in the liquid state had been established previously [3].

According to the theory [1] the temperature factors for these vibrations can be expressed in the form :

$$f_1(T) = \left[1 - \exp\left(-\frac{h\nu_1}{kT}\right)\right]^{-1} \cdot \left[1 - \exp\left(-\frac{h\nu_3}{kT}\right)\right]^{-1} \quad (1)$$

$$f_2(T) = \left[1 - \exp\left(-\frac{h\nu_1}{kT}\right)\right]^{-2} \cdot \left[1 - \exp\left(-\frac{h\nu_4}{kT}\right)\right]^{-1}$$

From these equations it is easy to construct eoretical curves for each vibration separately. wever it is difficult in the present case to com- re these theoretical curves with the experimental rves, since the bands $\nu_1 + \nu_3$ and $\nu_1 + (\nu_1 + \nu_4)$ erlap strongly, forming a close doublet. Although room temperature the doublet can be separated cely into two completely symmetrical components, temperatures above 100° C such a separation is t possible. This situation is due to an asym- trical broadening of the bands with increasing mperature. In the circumstances it is expedient determine the total integrated absorption of the ublet and compare it with the corresponding cal- lated values. To carry out this procedure it is fficient to know the absorption associated with ch individual component for any one temperature, r example, room temperature.

We will express the integrated absorptions of e bands $\nu_1 + \nu_3$ and $\nu_1 + (\nu_1 + \nu_4)$ at temper- ure T in terms of the corresponding absorptions temperature T_o, which will be taken as zero:

$$S'_T = S'_{T_o} f_1(T), \qquad S''_T = S''_{T_o} f_2(T).$$

re S' and S" refer to the vibrations $\nu_1+\nu_3$ nd $\nu_1 + (\nu_1 + \nu_4)$, respectively. For room mperature T_1 these relations have the form

$$S'_{T_1} = S'_{T_o} f_1(T_1), \qquad S''_{T_1} = S''_{T_o} f_1(T_1).$$

It is now possible to write down the ratio of he integrated absorption coefficients of the whole oublet at an arbitrary temperature T and room emperature T_1 as follows:

$$\frac{S_T}{S_{T_1}} = \frac{S'_{T_o} f_1(T) + S''_{T_o} f_2(T)}{S'_{T_1} + S''_{T_1}} \tag{3}$$

From (2) and (3) we obtain

$$S_T = S_{T_1} \frac{\dfrac{f_1(T)}{f_1(T_1)} + \dfrac{S''_{T_1}}{S'_{T_1}} \dfrac{f_2(T)}{f_2(T_1)}}{1 + \dfrac{S''_{T_1}}{S'_{T_1}}} . \tag{4}$$

Thus, having measured S'_{T_1} and S''_{T_1} (and of course also S_{T_1}) and using (1), it is easy with the aid of (4) to construct the theoretical temperature dependence S_T for the whole doublet and then compare it with the experimental dependence.

Absorption curves * for the bands in question were obtained in the temperature interval 20-200° C.

Three of these profiles, for 20, 135 and 200 ° C , are shown in figure 1. It seen from figure 1 that a rise in temperature produces an increase in the total intensity, each component being broadened individually along with a noticeable increase in the peak absorption of the long wavelength component. At the lowest temperatures the long wavelength maximum splits into three components; these are due to isotopic shifts of the frequency $\nu_1 + (\nu_1 + \nu_4)$, resulting from the presence of molecules of carbon tetrachloride with different structures with respect to the two isotopes of chlorine Cl^{35} and Cl^{37}. Increasing the temperature leads to a broadening of the separate components and hence to the disappearance of the structure of the band.

The data in figure 1 indicate qualitative agreement between theory and experiment; however, completely quantitative agreement is lacking. This is borne out by the trend of the graphs in figure 2, where curve 1 refers to the experimental data and curve 2 to the theoretical calculations. Each experimental point corresponds to a given absorption profile ** of the type shown in figure 1.

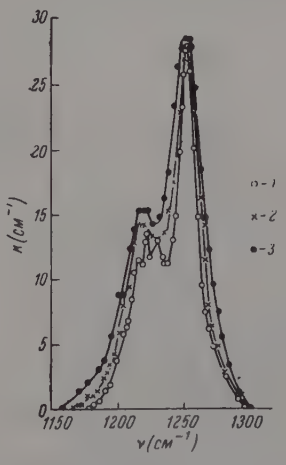

Figure 1.

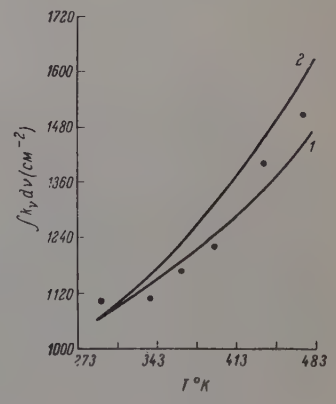

Figure 2.

Figure 1. Absorption curves of CCl_4 in the region of the summation tones $\nu_1 + \nu_3$ and $\nu_1 + (\nu_1 + \nu_4)$: 1 - 20° C, 2 - 135° C, 3 - 200° C.

Figure 2. Temperature dependence of the intensity of the doublet $\nu_1 + \nu_3$ and $\nu_1 + (\nu_1 + \nu_4)$ of CCl_4 : 1 - experimental, 2 - theoretical.

Although theory and experiment lead to the same qualitative result, namely, increasing absorption with increasing temperature, the theory gives in all cases a greater temperature effect than that observed experimentally.

* The error in the determination of the absorption coefficient in the most unfavorable experimental conditions did not exceed 10 % .

** Only three are reproduced.

At the moment it is premature to seek the reason for the discrepancy. Further elucidation will depend on the accumulation of much more data from investigations of single fundamentals, summation tones and overtones, which do not interact with other frequencies as do the vibrations $\nu_1 + \nu_3$ and $\nu_1 + (\nu_1 + \nu_4)$ which are in Fermi resonance [2 - 4] . However one can state immediately that it is hardly likely that the variation of the vapor pressure of carbon tetrachloride with temperature is the cause of the effect. At the highest temperature the the vapor pressure did not exceed 300 mm Hg, and preliminary experiments carried out by the authors at room temperature have shown no change in the intensities of the bands in question in the pressure range from 20 to 200 mm Hg.

It is interesting to note that the temperatur dependence of these same bands in liquid CCl_4 , is entirely different. As generally observed with other infrared bands, their intensities in the liq decrease linearly with rising temperature [3].

October 8, 195

References

1. M. V. VOL'KENSHTEIN, M. A. EL'IASHEVICH, B. I. STEPANOV: Kolebaniia molekul (Vibration of molecules), 2. GITTL, Moscow-Leningrad, 1949 .
2. M. P. LISITSA, V. N. MALINKO: OiS, 4, 455 (1958
3. M. P. LISITSA, V. N. MALINKO: IAN USSR, SF, 22(9), 1117 (1958) (See CTT Bulletin, p. 1106)
4. M. P. LISITSA, V. N. MALINKO: UFZ, 3, 482 (1958

TOM VI, Vyp. 5 OPTIKA I SPEKTROSKOPIIA Mai, 195
VOL. VI, No. 5 OPTICS AND SPECTROSCOPY May, 195

The Influence of Electron-donating Solvents on the C-H Stretching Absorption Band of Acetylene

by

E. V. SHUVALOVA

The very high solubility of acetylene in a number of organic solvents is well known. This property is used for storage of acetylene in cylinders as its acetone solution, and for its separation from gas mixtures with the aid of solvents.

Nieuwland and Vogt [1], citing the data of Copley and Holley [2], explained the high solubility as due to the formation of a complex between the acetylene and donor solvent molecules. These latter authors observed negative deviations from Raoult's law in solutions of phenylacetylene in nitrogen and oxygen-containing substances. From determinations of the heat of mixing of the components, they concluded that a hydrogen bond forms between the labile hydrogen of the acetylene group and the nitrogen or oxygen atom of the solvent,

Investigation of the structure and properties of the alkines also suggests the possibility of a hydrogen bond between electron-donating solvents and the acetylenic CH group. According to the modern view [3,4], the hydrogen bond is an expression of acid-base interaction and arises between the electron-accepting XH group (where X is carbon, nitrogen or oxygen) of an acid and the atom of the base acting as donor. The acidity of the CH group of acetylene and phenylacetylene results from the nearness of the triple bond and the phenyl group; this is confirmed by the possibility of replacing the alkine H by a metal or by deuterium [3] . The electron-accepting property of phenylacetylene was used by Cook [5] in studying the donor properties of the carbonyl group in different substances.

In studying the hydrogen bond, we usually have to deal with systems in which the electron-accepting groups are NH, OH or FH in the majority of cases. Clarification of the question of the formation of hydrogen bonds in solutions of acetylene is hence of special interest since this is one of the few cases of a hydrogen bond involving a CH (or CD) group. A second example of such a bond is found in intermolecular effects in chloroform solutions [6] In the present work, molecular interaction between acetylene and solvents (acetone, dioxane and pyridine) was investigated by means of infrared spectroscopy. The work was performed on a Perkin-Elmer Model 12B Spectrometer with an LiF prism, an FEOU-1 amplifier and an EPP-09 electronic potentiometer.

Figure 1 shows the infrared absorption spectrum of acetylene in CCl_4, acetone, dioxane and pyridine in the region of the CH stretching band. It will be seen that with increasing donor strength of the solvent (acetone, dioxane, pyridine[7]), the CH band shifts to lower frequencies and its half-width increases. Table 1 gives the frequencies ν and half-widths $\Delta\nu_{1/2}$ of the CH band of acetylene in the solvents studied. The difference $\Delta\nu$ between the absorption band frequency in the donor solvent and in CCl_4 is also given.

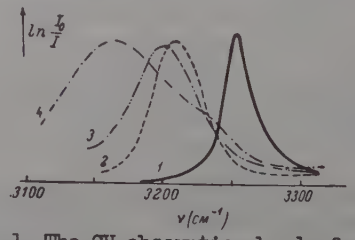

Figure 1. The CH absorption band of acetylene in various solvents: 1 - in CCl_4, 2 - in acetone 3 - in dioxane, 4 - in pyridine.

Table 1

olvent	ν(cm^{-1})	$\Delta\nu$ (cm^{-1})	$\Delta\frac{1}{2}$(cm^{-1})
	3265	—	25
$_3)_2CO$	3220	45	40
$_2H_4O_2$	3213	52	55
$_5N$	3180	85	100

Table 2

Solvent	ν_m(cm^{-1})	ν_a(cm^{-1})
$(CH_3)_2CO+CCl_4$	3260	3240
$(CH_2)_4O_2+CCl_4$	3260—3265	3232—3238
$C_5H_5N+CCl_4$	3260	3195

To help explain the nature of the shifts observed, the spectra of ternary mixtures, C_2H_2 + Cl_4 + donor solvent were also investigated. The mounts of donor solvent in the solutions were ..7 mol/l of acetone, 1.2 and 2.3 mols/l of dioxane nd 3.1 mols/l of pyridine. In all cases two osorption band maxima were observed in the acetylene pectrum (fig. 2) indicating molecules of acetylene n two different states in these solutions. The igh frequency band maximum (3260-65 cm^{-1}) of the ernary mixture corresponds to the acetylene absorpion band in pure CCl_4 and hence may be attributed o absorption of acetylene molecules free of the H ond. The low-frequency band maxima in the ternary ixtures are near the C_2H_2 absorption bands in the orresponding pure donor solvents and can be attriuted to absorption of acetylene molecules associated y means of a hydrogen bond to the acetone, dioxane r pyridine molecules.

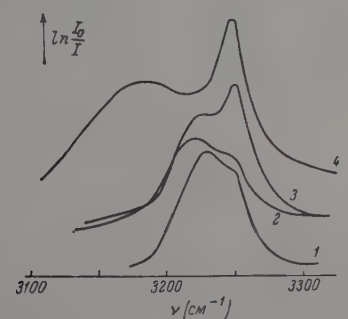

Figure 2. The CH absorption band of acetylene in mixed solvents : 1 - 2.7 mols/l acetone in CCl_4, 3 - 1.2 mols/l of dioxane in CCl_4, 4 - 3.1 mols/l of pyridine in CCl_4.

Table 2 gives the frequencies of monomer (ν_m) and of associated (ν_a) absorption bands in the mixtures of CCl_4 with each of the three donors. It may be seen that the position of the monomer is almost unchanged on addition of the donor solvent, while the position of the association band differs considerably (by 15-25 cm^{-1}) from its position in the corresponding pure electron-donating solvent. It is clear that this shift cannot be explained simply by the superposition of the two fairly close bands. Further experiments are necessary to explain the effect.

All of these phenomena, the simultaneous existence of the CH band of both free and associated molecules, in mixed solvents, the shift of the "associated" band to a frequency lower than that of the monomer, and the increased half-width of the association band , all indicate the formation of a hydrogen bond between the CH group of acetylene and the solvents. To characterize more fully the hydrogen bonds involving the CH group of acetylene it is necessary to obtain information on the integrated absorption intensities of the monomer and association bands, the equilibrium constant for the formation of complexes at various temperatures, and the energy of the bond.

Thanks are expressed to Prof. V. M.Chulanovskii for supervision of this work.

October 27, 1958

References

1. J. A. NIEUWLAND, R. R. VOGT: The Chemistry of Acetylene, New York, Reinhold Publ. Co., 1945 (IL, Moscow, 1947)
2. M. J. COPLEY, C. E. HOLLEY, Jr.: J. Amer. Chem. Soc., 61, 1599 (1939)
3. A. I. SHATENSHTEIN: UKh, 24, 377 (1955) (See ATS 80L28R)
4. C. G. CANNON: Spectrochim. Acta, 10, 341 (1958)
5. D. COOK: J. Amer. Chem. Soc., 80, 49 (1958)
6. C. M. HUGGINS, G. C. PIMENTEL: J. Chem. Phys., 23, 896, 1244 (1955)
   V. M. CHULANOVSKII, M. P. BURGOVA: OiS, 2, 330, 433 (1957)
   L. W. REEVES, W. G. SCHNEIDER: Canad. J. Chem., 35, 251 (1957)
7. W. GORDY: J. Chem. Phys., 7, 93 (1939)

TOM VI, Vyp. 5 OPTIKA I SPEKTROSKOPIIA Mai, 1959
VOL. VI, No. 5 OPTICS AND SPECTROSCOPY May, 1959

The Form of the Correlation Function for the Helium Atom

V. B. GLASKO, V. P. MASLOV, V. I. PANIKAR, N. D. SOKOLOV

In molecular calculations, correlation of the motions of electrons are taken into account by introducing an additional factor into the wave function which depends on the inter-electron distances r_{ij} [1] . By analogy with the first approximation in calculating the helium atom wave function carried out by Hylleraas [2], this factor may be written in the case of a two-electron system in the form

(1) $$f(r_{12}) = 1 + \alpha r_{12} ,$$

where α is a variational parameter. In the general case the correlation function must depend not on one, but on three correlation variables, where-upon f may be put in the form of a power series in these variables [2, 3] . On restricting ourselves to one correlation variable the choice of the function $f(r_{12})$ to be of the form (1) turns out to be arbitrary. The question naturally arises as to whether or not this choice is optimal.

In order to solve this problem, we have determined the correlation function $f(r_{12})$ for the helium atom by a variational method. Corresponding to what was said above, we write the wave function for the system of two electrons of the He atom in the form

$$\psi = f(u) \exp\left(-\frac{k}{2} s\right) \tag{2}$$

where $s = r_1 + r_2$, $u = r_{12}$, and r_1 and r_2 are the distances of the first and second electrons from the nucleus.

The problem of the determination of $f(u)$ may be solved by the method of Kantorovich [4].

The variational equation

$$\delta \int \left(L - E\,\psi\psi^*\right) d\tau = 0 , \tag{3}$$

where

$$L = \frac{1}{2} \sum_{i=1}^{2} (\nabla_i \psi)^2 + V\psi^2 \tag{4}$$

in the coordinate system s, u and $t = r_1 - r_2$, has the form (in atomic units)

$$\delta \int_0^\infty ds \int_0^s du \int_0^u dt \left\{ u(s^2 - t^2)\left[\left(\frac{\partial\psi}{\partial s}\right)^2 + \left(\frac{\partial\psi}{\partial u}\right)^2 + \left(\frac{\partial\psi}{\partial t}\right)^2\right] + \right. \tag{5}$$

$$+ 2\frac{\partial\psi}{\partial u}\left[s(u^2 - t^2)\frac{\partial\psi}{\partial s} + t(s^2 - u^2)\frac{\partial\psi}{\partial t} \right] -$$

$$\left. (4zsu - s^2 + t^2)\psi^2 - Eu(s^2 - t^2)\psi^2 \right\} = 0$$

where z is the nuclear charge.

Having substituted (2) into (5) and interchanged the order of integration, after integrating over t and s we obtain an Euler equation for the function $f(u)$

$$\left(u^3 + \frac{3u^2}{k} + \frac{3u}{k^2}\right) f'' + \left(-ku^3 + u^2 + \frac{6u}{k} + \frac{6}{k^2}\right) f' + \tag{6}$$

$$+ \left[\left(\frac{k^2}{4} + E\right) u^3 + \left(\frac{3E}{k} + 6z - 1 - \frac{9k}{4}\right) u^2 + \right.$$

$$\left. + \left(\frac{3E}{k^2} + \frac{6z-3}{k} - \frac{9}{4}\right) u - \frac{3}{k^2} \right] f = 0 .$$

Setting $f(u) = \varphi(u) \exp\left(\frac{ku}{2}\right)$, we transform to the following equation for $\varphi(u)$:

$$\left(u^3 + \frac{3}{k} u^2 + \frac{3}{k^2} u\right) \varphi'' + \left(4u^2 + \frac{9}{k} u + \frac{6}{k^2}\right) \varphi' + \tag{7}$$

$$+ \left[Eu^3 + \left(\frac{3}{k} E + 6z - 1 - k\right) u^2 + \left(\frac{3}{k^2} E - \frac{3-6z}{k} + \frac{3}{2}\right) u + \right.$$

$$\left. + \frac{3}{k} - \frac{3}{k^2} \right] \varphi = 0 .$$

The solution of this equation bounded at $u =$ and tending to zero as $u \to \infty$ is an eigenfunction of the boundary value problem depending on the two parameters k and E.

Analysis of this problem was carried out with the aid of the high-speed electronic computer "Stre of the Moscow State University Computation Center.

For small values of u the solution is expresse in the form of a series:

$$\varphi(u) = A\left\{1 + \frac{1-k}{2} u + \frac{1}{6}\left[\frac{3}{2} k^2 - \left(\frac{3}{2} + 2z\right)k + \left(\frac{1}{2} - E\right)\right]u^2 + \right. \tag{8}$$

which permits the removal of the singular point $u = 0$. The factor A is determined from the condition

$$\frac{4}{3}\frac{\pi^2}{k^3} \int_0^\infty \varphi^2(u) u^2 (k^2u^2 + 3ku + 3) du = 1 , \tag{9}$$

which follows from the normalization of the functio ψ.

We shall examine the Cauchy problem for equation (7) with initial conditions for some $u = u_0$ (in our case $u_0 = 10^{-3}$) and the two variational parameters k and E. The ballistic method for finding the eigenfunctions of the initial problem wa utilized [5, 6].

It turns out that for each value of the parameter k, at least in the region $3.5 \; k \; 5$, there exists an eigenvalue of E, whose dependence on k is given by the formula :

$$E = 0.133998\, k^2 - 0.990815\, k - 1.059669 . \tag{10}$$

Hence, for some value $k = k_0$ the quantity E takes on a smallest value, which is the object of our investigation.

Numerical calculation shows that $k_0 = 3.70$, and $E_{min} = -2.891252$. This is in good agreement with the results of Hylleraas [2] ($k_0 = 3.7$, $E = -2.8912$), obtained under the assumption of a lin dependence of f on u.

The corresponding eigenfunctions were tabulate with a relative acuuracy of $10^{-6} - 10^{-4}$. The normalizing factor is $A = 4.2607$. A graph of $f(u)$ is presented in the figure (curve I).

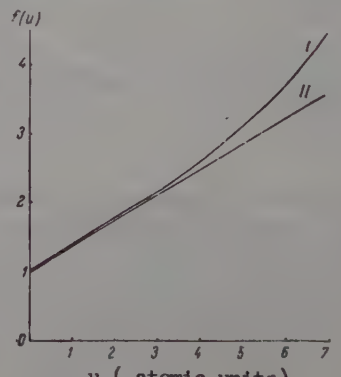

Correlation functions for the He atom dete mined by the variational method (I) and by Hylleraas (II).

ver the particular interval $0.974 \leqslant u \leqslant 3.278$ the unction $f(u)$ is represented well by the linear unction $f(u) = \alpha_0 + \alpha_1 u$, where $\alpha_0 = 1.05$, $\alpha = 0.3686$, hich also agrees sufficiently well with the values f Hylleraas ($\alpha_0 = 1, \alpha = 0.3675$). For large sis distances ($u > 5$) $f(u)$ is represented with a recision of at least 0.1% by the asymptotic ormula.

$$f(u) = C_0 u^{\sigma} \exp\left[\left(\frac{k}{2} - \lambda\right) u\right],$$

here $\lambda = 1.700368$, $\sigma = 0.146594$, $C_0 = 1.172463$.

The straight line (II) in the figure is the raph of $f(u) = 1 + \alpha u$ according to Hylleraas [2]. s is seen from the figure, for $u < 4 - 5$ the correlation function $f(u)$ in general differs little rom the function of Hylleraas (1). For $u > 5$ he difference between them becomes significant; owever, as the calculation shows, the contribution f this region to the energy is small, and therefore he divergence of the functions is almost undetectable in the results of computations.

On the whole, one may conclude that on restricting ourselves to the one correlation variable r_{12} he linear approximation correlation function (1) s practically optimal (at least for atoms).

The ballistic method utilized in the investigation consists in the following: by means of numerical integration of the equation for the given initial conditions for fixed k, a pair of integral curves $y_1(u, E)$ and $y_2(u, E)$ is sought of which one is positive and the other is negative for asymptotic values of u. Then, because of continuity of the eigenfunction the following inequality is satisfied, at least asymptotically:

$$y_1(u, E_2) < y_0(u) < y_2(u, E_1),$$

and similarly for the eigenvalue

$$|E_2| < |E| < |E_1|.$$

It can be shown [6] that the eigenvalue is the limit of a sequence of embedded intervals $[E_1^{(i)}, E_2^{(i)}]$, as $i \to \infty$, and hence it could be determined as accurately as desired by means of a contraction on the intervals found, for example by successive halvings.

November 29, 1958

References

1. A. A. FROST, J. BRAUNSTEIN, W. SCHWEMER: J. Amer. Chems. Soc., 70, 3292 (1948)
2. E. A. HYLLERAAS: Zs. f. Phys., 54, 347 (1929)
3. T. KINOSHITA: Phys. Rev., 105, 1490 (1957)
   V. A. FOCK: IAN USSR SF, 18(2), 161 (1954) (See NRCL: TT 503)
   P. PLUVINAGE: J. Phys. Radium, 18, 474 (1957)
   E. A. HYLLERAAS, J. MIDTDAL: Phys. Rev., 103, 829 (1956)
4. L. V. KANTOROVICH: IAN USSR, No. 5, 647 (1933); L. V. KANTOROVICH, V. N. KRYLOV: Priblizhennye metody vysshego analiza (Approximate methods of higher analysis). In English from P. NOORDHOFF, Groningen, The Netherlands, 1958
5. V. B. GLASKO, F. L. LERIUST, IA. P. TERLETSKII: ZETF, 35(2), 452 (1958) (See Soviet Physics JETP, p. 312 Feb. 1959)
6. V. L. BONCH-BRUEVICH, V. B. GLASKO: ZFKh (In press)

TOM VI, Vyp. 5 OPTIKA I SPEKTROSKOPIIA Mai, 1959
VOL. VI, No. 5 OPTICS AND SPECTROSCOPY May, 1959

The Measurement of Birefringence of Fibers

A. N. ZAKHAR'EVSKII AND L. A. FEDIN

Double refraction, that is, the difference of the indices of refraction $(n_{\parallel} - n_{\perp})$ in polarized light whose vibrations are parallel $(n_{\parallel})$ and perpendicular $(n_{\perp})$ to the length of a fiber, is an important characteristic of artificial synthetic fibers.

A convenient method of detection and measurement of birefringence in fibers consists of the following. The fiber F, together with an immersion medium of suitable refractive index, is placed on the stage of a polarizing microscope. In Figure 1 are represented the basic parts of the microscope: P - the polarizer, K - the condenser, Ob - the objective, Oc - the ocular, and A- the analyser. In the plane of the image F' is placed a Wollaston prism W with small refracting angle. The orientation of the axis of P, A, and the edges of the halves of the Wollaston prism W with respect to the fiber F are shown in the right side of the illustration. For fibers of thickness 0.01-0.02 mm microscope magnifications of about 500 x are necessary.

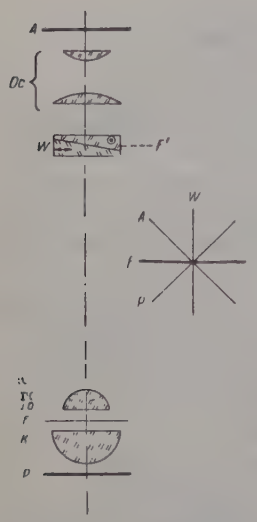

Figure 1. The Polarizing Microscope with a Wollaston Prism.

The scheme described gives straight interference fringes in the field of the microscope visible in white light and oriented perpendicularly to the fiber. In the part occupied by the fiber the interference fringes are displaced by the amount ΔN corresponding to the equation

$$\Delta N = \frac{a(n_{\parallel} - n_{\perp})}{\lambda}, \qquad (1)$$

where a is the fiber thickness and λ the wavelength.

As an example, Figure 2 is a reproduction of a photomicrograph of a preparation of five different types of fiber, exposed in green light (λ=546 mμ). The greatest birefringence is possessed by the lavsan fiber (filament 2). From observation in white light it was possible to determine that the shift of the achromatic (null) fringe is $\Delta N = 8$. There follows in order capron (filament 1; $\Delta N = 2.6$) and viscose silk (filament 5; $\Delta N = 0.7$). The fiber of viscose silk, in contrast to the others, is covered with fine spots. The interference fringes of the nitron fiber (filament 3) have a zigzag form that may have arisen either from different birefringence in the several layers of the filament or from the irregular form of the cross section of the filament. The copper-ammonium staple fiber (filament 4) has a weak birefringence of reversed sign.

More accurate measurements of the shift of the interference fringes (to 0.01-0.02 of a fringe) may be made with the help of a filar micrometer eyepiece, the traveling wire of which is seen at a in Figure 2.

Figure 2. Birefringence in fibers.

1 - Capron fiber. 2 - Lavsan fiber. 3 - Nitron fiber. 4 - Copper-ammonium staple fiber. 5 - Viscose rayon.

However, the simple scheme for this as shown in Figure 1 is not fully satisfactory since the interference fringes are localized in the plane of the cement layer of the prism W where the micrometer wire cannot be placed. The arrangement for moving the plane of the fringes outside proposed by L. A. Fedin (author's claim No. 604720/26 with priority from 25 June 1958 *) is represented in Figure 3A, and consists of two Wollaston prisms W_1 and W_2.

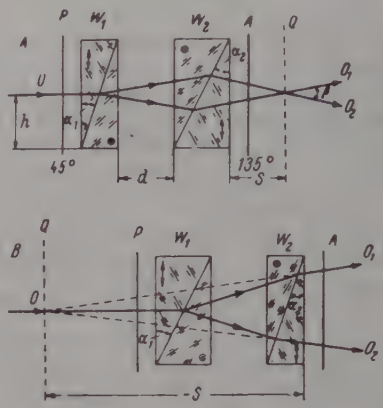

Figure 3. Wollaston prisms with external image planes: A - first type; B - second type.

The wedge angle of the first prism (α_1) is smaller than the wedge angle of the second prism (α_2). Light incident on the system is first divided at the cemented plane of the prism W_1 and gives two deviated beams. At the cemented plane of the prism W_2 these beams are refracted a second time, coming together and intersecting at a new plane Q, lying outside the prism W_2. Full contrast is preserved in the interference field at the plane Q for relatively large apertures of the illuminating beams. The angle β between the emerging beams, on which depends the width of the interference fringe, is equal to

$$\beta = 2(n_e - n_o)(\alpha_2 - \alpha_1), \qquad (2)$$

where n_e and n_o are the principal indices of refraction of crystalline quartz. The distance S from the last surface of the prism W_2 to the plane Q is given by the approximate formulae

$$S \approx \frac{\alpha_1}{\alpha_2 - \alpha_1} \cdot d + \frac{\alpha_1^2 + 2\alpha_1\alpha_2 - \alpha_2^2}{n_o(\alpha_2 - \alpha_1)} \cdot h \approx \frac{\alpha_1}{\alpha_2 - \alpha_1} \cdot d \qquad (3)$$

where h is the distance from the edge of the prism to the optical axis, and d is the air separation of the prisms.

A possible second variant of a similar arrangement is shown in Figure 3B, in which the plane of the fringes Q falls in front of the prism W_1.

* A corresponding arrangement was proposed independently of this by Nomarski [1].

If the fiber is so uniform that the birefringence $(n_{\parallel} - n_{\perp})$ has the same value at every point in the transverse section, then the form of the interference fringes depends only on the shape of the fiber section. In this case the difference $(n_{\parallel} - n_{\perp})$ may be established for any complicated shape of interference fringe. In Figure 4 are shown: A - a microphotograph of a fiber with its intersecting interference fringe, the width of which is equal to E; B - the cross section of the fiber.

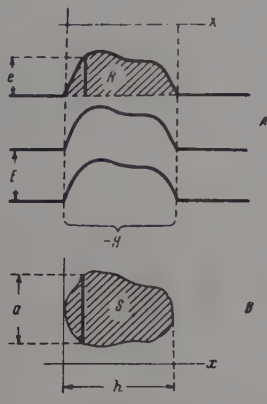

Figure 4. The computation of birefringence in fibers.

If M is the image scale (magnification), H is the width of the fiber in the photograph, h is its actual width, then

$$M = \frac{H}{h} \qquad (4)$$

and generally

$$X = Mx \qquad (4')$$

The displacement N at each point of the curve of the interference fringe is equal to [see (1)]

$$\Delta N = \frac{e}{E} = \frac{\alpha(n_{\parallel} - n_{\perp})}{\lambda} . \qquad (5)$$

The area R, bounded by the interference fringe, equals

$$R = \int edX = \int \frac{\alpha(n_{\parallel} - n_{\perp})E}{\lambda} Mdx$$

$$= \frac{(n_{\parallel} - n_{\perp})EM}{\lambda} \int adx = \frac{(n_{\parallel} - n_{\perp})\,EMS}{\lambda} , \qquad (6)$$

where S is the cross-sectional area of the fiber.

In this way, the birefringence is equal to

$$(n_{\parallel} - n_{\perp}) = \frac{R\lambda}{EMS} . \qquad (7)$$

The area of R is measured in the photomicrograph in the usual way. The magnitude of the area S must be determined by an indirect method, for example through the weight of a definite length of fiber and the specific gravity of the material from which the fiber is made.

The birefringence of fibers as it follows from the general notion of polarized light is determined by their chemical nature and the degree of molecular orientation, on which in turn depend the strength, elasticity and moisture and heat resistance and other technical properties of the fibers. Consequently the observation of birefringence may prove a useful method for the study of fibers.

December 4, 1958

References

1. W. GÄRTNER: Optik, 15, No. 5, 281 (1958)
2. S. C. SIMMENS: Nature, 181, No. 4618, 1260 (1958)

OM VI, Vyp. 5 OPTIKA I SPEKTROSKOPIIA Mai, 1959
OL. VI, No. 5 OPTICS AND SPECTROSCOPY May, 1959

On the Theory of Electromagnetic Wave Propagation in Gyrotropic Media

G. S. KRINCHIK, M. V. CHETKIN

Recently, investigations have been extended in gyrotropic media, i. e., media for which either ϵ or μ are tensors with the following components

$$\epsilon_{xx} = \epsilon_{yy} = \epsilon \; ; \quad \epsilon_{xy} = -\epsilon_{yx} = -i\epsilon M \; ;$$

$$\epsilon_{zz} = \epsilon_0 \; ; \quad \epsilon_{xz} = \epsilon_{yz} = \epsilon_{zx} = \epsilon_{zy} = 0 \; ;$$

$$\mu_{xx} = \mu_{yy} = \mu \; ; \quad \mu_{xy} = -\mu_{yx} = -i\mu M' \; ;$$

$$\mu_{zz} = \mu_0 \; ; \quad \mu_{xz} = \mu_{yz} = \mu_{zx} = \mu_{zy} = 0 .$$

The same substance can be gyroelectric at optical frequencies and gyromagnetic in the microwave band [1, 2]. Apparently substances exist which have both gyromagnetic and gyroelectric properties at certain frequencies. Let us show how it is possible to determine experimentally whether a medium is gyromagnetic, gyroelectric or has these properties simultaneously at a prescribed frequency. To do this, it is necessary to find the refractive index n^* of the medium which is characterized by the above mentioned tensors ϵ and μ.

Let us look at the solution of the Maxell equations in the form of plane waves

$$\vec{H} = \vec{H}_0 e^{i\omega\left(t - n^* \frac{\alpha^* x + \beta^* y + \gamma^* z}{c}\right)}$$

Then the following system of equations can be obtained to determine H_x, H_y and H_z

(1)

$$H_x - \alpha^* \Delta H = p\left\{B_y\left[m + \frac{\epsilon_0}{\epsilon}(iMn_\alpha - 1)\right] + B_x\left[\frac{\alpha^*}{\beta^*} m + \frac{\epsilon_0}{\epsilon}(n_\alpha - iM)\right]\right\}$$

$$H_y - \beta^* \Delta H = p\left\{B_x\left[m + \frac{\epsilon_0}{\epsilon}(iMn_\beta - 1)\right] + B_y\left[\frac{\beta^*}{\alpha^*} m + \frac{\epsilon_0}{\epsilon}(n_\beta - iM)\right]\right\},$$

$$H_z - \gamma^* \Delta H = pM\left[i\frac{\epsilon_0}{\epsilon}\left(\frac{\gamma^*}{\beta^*} B_y - \frac{\gamma^*}{\alpha^*} B_x\right) - \mu_0 Mn_\gamma H_z\right] + \frac{\epsilon\mu_0}{n^{*2}} H_z ,$$

where

$$\Delta H = \alpha^* H_x + \beta^* H_y + \gamma^* H_z, \quad B_x = \mu H_x - i\mu M' H_y, \quad B_y = i\mu M' H_x + \mu H_y,$$

$$m = 1 - M^2, \quad n_l = \frac{1 - l^{*2}}{\alpha^* \beta^*}, \quad p = \frac{\epsilon^2 \alpha^* \beta^*}{n^{*2}[\epsilon_0 \gamma^{*2} + \epsilon(\alpha^{*2} + \beta^{*2})]} .$$

This system has a non zero solution under the condition

$$[\mu_0 \gamma^{*2} + \mu(\alpha^{*2} + \beta^{*2})][\epsilon_0 \gamma^{*2} + \epsilon(\alpha^{*2} + \beta^{*2})]n^{*4}$$

$$- [\epsilon^2 \mu\mu_0 (1 - M^2)(\alpha^{*2} + \beta^{*2}) + \epsilon_0 \epsilon\mu^2 (1 - M'^2)(\alpha^{*2} + \beta^{*2})$$

$$+ 2\epsilon_0 \mu_0 \epsilon\mu (1 + MM')\gamma^{*2}]n^{*2} + \epsilon_0 \mu_0 \epsilon^2 \mu^2 (1 - M^2)(1 - M'^2) = 0 ,$$

from which the refractive index n^* is also determined.

Now, let us turn to a consideration of electromagnetic wave reflection from a gyrotropic medium when the magnetization vector (directed along the z axis) is parallel to the reflecting plane (y, z) and perpendicular to the light incidence plane (equatorial magnetization). In this case $\gamma^* = 0$ and we obtain from (2)

(3) $$n_1^{*2} = \epsilon\mu_0(1 - M^2), \quad n_2^{*2} = \epsilon_0\mu(1 - M'^2) .$$

It is seen from (1) that n_1^* refers to a wave whose electrical vector is parallel to the incident plane (p-wave), n_2^* to a wave whose electrical vector is perpendicular to the incident plane (s-wave).

The conditions of continuity of the tangential components of the electrical and magnetic fields on the interface together with the condition $\operatorname{div} \vec{B} = 0$ lead to the following reflection coefficients:

(4a) $$\frac{R_p}{A_p} = \frac{\alpha n_1^* - \mu_0(\alpha^* + i\beta^* M)}{\alpha n_1^* + \mu_0(\alpha^* + i\beta^* M)} ;$$

(4b) $$\frac{R_s}{B_s} = \frac{\alpha n_2^* - \epsilon_0(\alpha^* + i\beta^* M')}{\alpha n_2^* + \epsilon_0(\alpha^* + i\beta^* M')} ,$$

where R and A are the amplitudes of the reflected and incident waves, $\alpha = \cos\varphi$, φ is the angle of incidence. When the medium is gyroelectric, the effect is determined by (4a) and when it is gyromagnetic, by (4b); if it is bi-gyrotropic then using (4) the influence of the gyromagnetic and the gyroelectric parts can be isolated. Assuming that

$$\epsilon = \epsilon_0 (1 + bM^2 + \ldots), \quad \mu = \mu_0(1 + b' M'^2 + \ldots),$$

$M \ll 1$, $M' \ll 1$ and being limited by the linear terms concerning M, M', we obtain from (4) and

(5a) $$\frac{R_p}{A_p} = \frac{\alpha n - \alpha^* \mu_0}{\alpha n + \alpha^* \mu_0} - 2iM \frac{\alpha\beta\mu_0}{(\alpha n + \alpha^* \mu_0)^2} ,$$

(5b) $$\frac{R_s}{A_s} = \frac{\alpha n - \alpha^* \epsilon_0}{\alpha n + \alpha^* \epsilon_0} - 2iM' \frac{\alpha\beta\epsilon_0}{(\alpha n + \alpha^* \epsilon_0)^2} .$$

We obtain the formula for the relative change of the reflected light intensity for a gyromagnetic medium from (5b)

$$\delta = \frac{I - I_0}{I_0} = \frac{2 \sin 2\varphi}{(1 - \epsilon_1)^2 + \epsilon_2^2}\left[M_1' \epsilon_2 - M_2' (1 - \epsilon_1)\right] ,$$

where $\epsilon = \epsilon_0 = \epsilon_1 - i\epsilon_2$, $\mu = \mu_0 = 1$, $M' = M_1' - iM_2'$.

The formula for the relative change in the reflected light intensity of a p-wave has been obtained in Reference [2], where, however, it was erroneously considered that it is also applicable for a gyromagnetic medium. Returning once again to (3), we see that the refractive index for the passage of p- and s- waves through a transversely magnetized gyrotropic medium (the Cotton-Mouton effect) depends only on M in the first case and on M' in the second*+. Hence, measuring the phase path of the p- and s- waves, it is possible to determine whether a medium has gyromagnetic or gyroelectric properties. Whereas, there is no limitation here on the smallness of M, M', this method can be used for ferrites in the microwave band.

*+ Let us note that the formulas for the Cotton-Mouton effect obtained in [3] are wrong because the commutator μ and rot were equated to zero. The equations similar to (1) and (2) are wrong for the same reason.

In addition to the effects considered, there lso exist magnetooptic effects and their analogs n the radio frequency band (Faraday effect, polar nd meridian Kerr effect) in which it is impossible o separate the influence of the parameters M and . Formulas for these effects can be obtained ? an expression is known for the refractive index ? a circularly polarized wave $n^*_{\pm}$. Being limit-

1 to linear terms in M, M', we obtain from 2)

$$n^{*2}_{\pm} = \epsilon_0\mu_0\left[1 \pm \gamma^*(M + M')\right]$$

from which it is seen that the parameters M and M' enter additively and it is impossible to separate the gyromagnetic and gyroelectric parts.

December 29, 1958

References

1. M. BORN: Optik, Berlin, Springer, 1933 (ONTI, 402, 1937)
P. EPSTEIN: UFN, 65, 283 (1958) (Translated from English)
2. G. S. KRINCHIK, V. I. RIABCHENKO: OiS, 2, 537 (1957)
G. S. KRINCHIK: Vestnik, Moscow Univ., No. 6, 87 (1957) (Translation exists)
3. A. V. SOKOLOV: FMM, 3, 208 (1956)

M VI, Vyp. 5 OPTIKA I SPEKTROSKOPIIA Mai, 1959
L. VI, No. 5 OPTICS AND SPECTROSCOPY May, 1959

The Theory of Resonance Radiation of a Gas Discharge

B. A. VEKLENKO

The theory of resonance emission of a gas discharge leads to the following integral equation or the distribution of concentrations of excited toms $n_a(r)$

$$1) \quad y_a(\vec{r}) - \frac{1}{4\pi}\int_V\int_0^\infty \epsilon_\nu k_\nu y_a(\vec{r}')\frac{\exp[-k_\nu|\vec{r}-\vec{r}'|]}{|\vec{r}-\vec{r}'|^2}\,d\nu dV + y_a(\vec{r})\,\beta(\vec{r}) = \beta(\vec{r}),$$

here $y_a(\vec{r}) = \frac{n_a(\vec{r})}{n^0}$, n^0 is the concentration of excited atoms under thermodynamic equilirium conditions, ν is the frequency of the photon, nd ϵ_ν and k_ν characterize the shapes of the mission and absorption lines, respectively. The unction $\beta(\vec{r})$ is defined by the equality

$$\beta(\vec{r}) = \tau\sigma n_e(\vec{r})$$

here $n_e(\vec{r})$ is the electron concentration (it s assumed that the latter have a Maxwellian velocity distribution,) τ – is the average lifetime of he excited state of the atom and σ – is the probability of a quenching collision per excited atom er unit time.

Equation (1) was formulated by L.M.Biberman [1] n 1947. The only attempts to solve it so far have een by numerical methods. The only xception is the attempt of Walsh [2] to deterine $n_a(\vec{r})$ by expanding it in a series of eigenfunctions of equation (1). The first eigen-value and the first eigenfunction were borrowed from the work of Holstein [3]. Such a means of determining the concentration of excited atoms is extremely tedious and the author did not succeed completely.

In this connection, it seems expedient to us to turn attention to the possibility of seeking the desired solution by constructing an extremum functional for the inhomogeneous equation (1). A similar functional was introduced into transport theory by Marshak [4] and Su Shu-Huang [5].

Let us write (1) in symbolic form

$$(2) \qquad Ky_a + \beta y_a = \beta \quad ,$$

where K – is the self-conjugate integral operator. The following extremum functional corresponds to (2)

$$(3) \qquad F = (y_a;\ Ky_a + \beta y_a) - 2(\beta;\ y_a) \quad .$$

The symbol $(f; g)$ denotes the scalar product of the functions f and g. Using the Ritz method, let us look for the solution in the form

$$(4) \qquad y_a = \sum_{i=o}^{n} a_i y_{ai}$$

where y_{ai} – are known functions. Substituting (4) into (3), we find

$$F = \sum_{i,j=o}^{n} a_j (K^a_{ij} + M^a_{ij}) - 2 \sum_{i=o}^{n} a_i M^a_{io},$$

where

$$K^a_{ij} = (y_{ai} ; Ky_{aj}) ; \quad M^a_{ij} = (y_{ai}; \beta y_{aj}) .$$

The extremum condition leads to the following system of equations determining the coefficients a_i

$$\frac{\partial F}{\partial a_i} = 0 ; \quad (i = 0, 1, \ldots n) .$$

Expression (4) affords the possibility of obtaining all of the optical characteristics of a discharge, some of which are the average concentration of the excited atoms (proportional to $\bar{y}_a$) and the average time $\bar{t}$, required for the photons emitted in the radiating volume V to diffuse to the boundaries [2] :

(5)
$$\bar{y}_a = \frac{1}{V}\int_V y_a(\vec{r})dV = \frac{1}{V}\sum_{i=o}^{n} a_i H^a_{io}; \quad \bar{t} = \tau \frac{\bar{y}_a}{K y_a} = \frac{\sum_{i=o}^{n} a_i H^a_{io}}{\sum_{i=o}^{n} a_i K^a_{io}},$$

where

$$H^a_{ij} = (y_{ai} ; y_{aj}) .$$

Let us consider a gas discharge in a space bounded by two parallel planes separated by the distance L. Let us consider that the spectral line broadening is determined by Doppler effect. Let us introduce the new function $y(x)$

$$y(x) = y_a\left(x \frac{d}{2}\right), \quad -1 \leqslant x \leqslant 1 .$$

Let $\beta(x) = \beta(0)e(x)$, where $e(x)$ – is an even function and $e(0) = 1$. The coefficients K_{ij} have been computed by Holstein [3] and Walsh [2] for the function $y(x) = a_o + a_1 (1-x^2) + a_2 (1-x^4)$:

$$Kij = \frac{K^p_{ij}}{k_o L \sqrt{\pi \ln k_o \frac{L}{2}}}; \quad K^p_{ij} = \begin{pmatrix} 2 \ln k_o \frac{L}{2} & 2 & 8/5 \\ 2 & 2 & 20/9 \\ 8/5 & 20/9 & 8/3 \end{pmatrix}$$

Let us be limited to a parabolic approximation. Then

(6) $$a_o = \frac{A_{11}M_{00} - A_{10}M_{10}}{A_{00}A_{11} - A^2_{10}}; \quad a_1 = \frac{A_{00}M_{10} - A_{10}M_{00}}{A_{00}A_{11} - A^2_{10}} ,$$

where $A_{ij} = K_{ij} + M_{ij}$

We find that $a_o \to 1$, $a_1 \to 0$ as $k_o L \to \infty$ or $\beta(0) \to \infty$, which means that the discharge approaches thermodynamic equilibrium. If the change $\sqrt{\ln k_o \frac{L}{2}}$ is neglected, then the distribution $y(x)$ will depend only on the product $\beta(0)k_o$ but not on each of the parameters individually.

Substituting (6) into (5), we arrive at an explicit expression for $\bar{t}$. Let us turn to the limiting cases. Let $\beta(0) \to \infty$, then

$$\bar{t} = \tau \frac{H_{00}}{K_{00}} = \tau k_o L \cdot \sqrt{\frac{\pi}{\ln k_o \frac{L}{2}}} .$$

Hence, the time $\bar{t}$ obtained agrees with the volume-averaged effective lifetime of the excited state of the atom introduced by L. M. Biberman [6].

If $\beta(0) \to 0$, then the expression for $\bar{t}$ can be reduced to

(7)
$$\bar{t} = \frac{2}{3}\tau k_o L \sqrt{\pi \ln k_o \frac{L}{2}} \frac{m_{10}}{m_{00}} \left[1 + \frac{m_{00} - m_{10}}{2m_{10}\left(\ln k_{o\frac{L}{2}} - 1\right)}\right]$$

in which $m_{ij} = (y_i; ey_j)$. For $e(x) = 1 - x^2$, formula (7) agrees with the expression obtained by T. Holstein [3].

In conclusion, I am grateful to L. M. Biberman for discussions and helpful comments.

December 31, 1958

References

1. L. M. BIBERMAN: ZETF, 33, 416 (1957) (See Soviet Physics, JETP)
2. P. T. WALSH: Phys. Rev., 107, 338 (1957)
3. T. HOLSTEIN: Phys. Rev., 72, 1212 (1947)
4. R. E. MARSHAK: Phys. Rev., 71, 688 (1947)
5. SU SHU-HUANG: Phys. Rev., 88, 50 (1952); Astrophys. J., 117, 211, 213, 221 (1953)
6. L. M. BIBERMAN: DAN USSR, 59, 659 (1948)

TOM VI, Vyp. 5 OPTIKA I SPEKTROSKOPIIA Mai, 1959
VOL. VI, No. 5 OPTICS AND SPECTROSCOPY May, 1959

Investigation of Linear Fluorescence and Absorption of Pure Cadmium Sulfide Crystals at a Temperature of 4.2° K

M. BANCIE-GRILLOT, E. F. GROSS, E. GRILLOT, B. S. RAZBIRIN

Abstract: Results of an investigation of blue linear fluorescence at t = 4.2°K in samples of pure cadmium sulfide prepared by sublimation in a high temperature gradient [1,2] were made more precise by using high disperson spectral apparatus and were compared with results obtained in investigations of the absorption of light in the same crystals. The identical state of the fluorescence line polarization shows that they are all probably caused by the same system.

It has been shown by two of the authors that certain characteristic features of the linear fluorescence of pure cadmium sulfide at very low temperatures depend noticeably on the method of chemically preparing the sample [1]. In particular, the green fluorescence, usually observable at 77° K [3] was not observed [2] for crystals produced by sublimation in a very high temperature gradient. This fluorescence is very weak at 20°K and an intense new emission in the blue region of the spectrum, consisting of nine clear lines, is observed simultaneously. Six of these lines, located in the high frequency range, form a quasi-hydrogen-like series running down to the fundamental absorption edge of the crystal [2]. New emission lines in the form of three triplets and a doublet which adjoin a system of three lines beyond the limits of the quasi-hydrogen-like series appear at 4.2°K. This unique fluorescence was interpreted [2] as the appearance of exciton annihilation.

On the other hand, one of us has observed a complex absorption spectrum near the fundamental absorption edge of a crystal [4] during a study of cadmium sulfide crystals produced by synthesis in the gas phase and cooled to 4.2°K. Later, it appeared possible to classify these lines into two groups [5]. The first group, including the intense lines, is observed in all the samples investigated and its lines maintain an invariant position in the spectrum. The lines of the second group, less intense and located in the longer wavelength part of the spectrum, vary from sample to sample depending on the method of preparing the crystal. Apparently they do not belong to the fundamental CdS lattice. On the other hand, the first group of lines was ascribed to the fundamental lattice and related to the exciton states of the crystal [5].

In order to compare these results, we undertook a joint additional investigation of this question.

The CdS single crystals studied showed the above mentioned linear fluorescence at 4.2°K [2]. The crystal thickness was such (50 μ) that it was possible to observe both fluorescence and absorption in the sample. In this note are described the results, obtained on a spectrograph, whose dispersion is 8 times larger than that used in the first investigations of fluorescence in CdS [2] and which is about 4 Å/mm in the spectral region being studied. This permitted us to determine the spectral location of the fluorescence lines in the crystal spectrum with great accuracy (diagram A in the figure). Besides the lines already known, an additional fine line λ = 4868 Å was found. The temperature variation of the intensity of the very bright line λ = 4870.0, which masked the line at λ = 4868.2 Å in the previous experiments, was seemingly not subject to the same law as were the other lines we observed. Consequently, it may be thought that one of these two adjacent lines can arise from a mechanism different from that which causes all the other lines of the system. However, the polarization of these lines (see below) as well as the effect of an electric field thereon (this is the subject of later reports) show that they almost all apparently have a common origin.

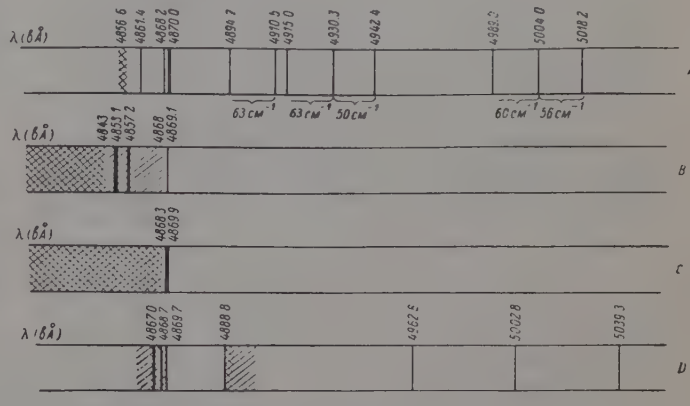

Crystals of pure CdS yielding blue fluorescence (and very weak green fluorescence)

A - Fluorescence spectrum, B - Absorption spectrum (unpolarized light), C- absorption spectrum (polarized E⊥C)
Crystals of pure CdS yielding intense green fluorescence at 4.2°K, which is accompanied by comparatively slightly intense lines in the blue range of the spectrum D - luminescence spectrum in the blue region of the spectrum

Moreover, we could establish that all the fluorescence lines are strongly polarized perpendicular to the optical axis of the single crystal: They are almost all completely quenched in observations with a Nicol E||C. The very same thing also occurs with the complex background (much less intense than the lines), which is located between λ = 4870 and 4942 Å [2]. This fact apparently can be considered as partial confirmation of the hypothesis that they are all caused by a single system. It also indicates the orientation of the system with respect to the crystallographic directions.

It has been found that the absorption spectra of all the samples of cadmium sulfide single crystals we investigated are identical. Moreover, it appears remarkable that this spectrum is particularly simple. As diagram B of the figure shows, it consists of just three absorption lines in nonpolarized light: λ = 4853.1, λ = 4857.2 and λ = 4869.1 Å. These

absorption lines occupy a position in the spectrum which is very close to the three fluorescence lines corresponding to the three highest levels. Their wave numbers exceed the respective wave numbers of the fluorescence lines λ_8 = 4856.6, λ_7 = 4861.4 and λ_6 = 4870.0 Å by 15, 18 and 3 cm^{-1}. In addition, we observed that light emerging from the crystal in the range where the complex absorption diminishes and absorption lines are located is polarized completely parallel to the optical axis of the crystal. If the Nicol is oriented E ∥ c, then the complex absorption edge is shifted to 4868 Å (diagram C of the figure) so that only the line λ (which is broadened on the figure and extends from 4868.3 to 4869.9 Å) can be observed.

In addition, for comparison purposes, we investigated cadmium sulfide single crystals prepared by another method under the same conditions, whereupon several comparatively weak lines in the blue range of the spectrum and an intense green band with a classical structure [3] but consisting of two series of luminescence maxima [1], is observed at 4.2°K in the fluorescence spectrum. Diagram D of the figure shows the position of the blue lines observed in the spectrum; it is seen that they form a system completely different from that which had been observed for the crystals sublimed in a high temperature gradient. Moreover, neither the green band nor the blue lines exhibit a polarization similar to that described above. Observation with the aid of a Nicol oriented E∥c shows that only lines with wavelength less than 4869 Å have greatly reduced intensities. All the remaining lines, as well as the green luminescence band, are rather more intense.

Dec. 31, 1958

References

1. E. GRILLOT: International Colloquium "Semiconductors and Phosphors", Garmisch-Partenkirchen, 1956. Interscience, N.Y., 1958
J. de chimie phys., 54, 118 (1957)
E. GRILLOT, M. BANCIE-GRILLOT: Kolloquium über Festkörperphysik, Erfurt, 1957 (in press); IAN USSR SF, 22 (1958) (See CTT BULLETIN)
2. E. GRILLOT, M. BANCIE-GRILLOT, P. PESTEIL, A. ZMERLI: C.R., 242, 1794 (1956)
E. GRILLOT: J. Phys. et Rad., 17, 822 (1956)
3. F. A. KROEGER; Physica (Pays Bas), 7, 1 (1940)
4. E. F. GROSS, M. A. IAKOBSON: DAN USSR, 102, 485 (1955)
5. E. F. GROSS: Congress of Czech Physicists, Prague, 1957
E. F. GROSS, B. S. RAZBIRIN, M. A. IAKOBSON: ZTF, 27, 1149 (1957) (See Soviet Physics Technical Physics)

TOM VI, Vyp. 5 OPTIKA I SPEKTROSKOPIIA Mai, 1959
VOL. VI, No. 5 OPTICS AND SPECTROSCOPY May, 1959

Influence of a Magnetic Field on the Blue Fluorescence Lines and On the Absorption Lines of Certain Pure Cadmium Sulfide Crystals at a Temperature of 4.2° K

E. F. GROSS, E. GRILLOT, B. P. ZAKHARCHENIA, M. BANCIE-GRILLOT

Abstract: Zeeman splitting into a doublet was detected in three fluorescence lines of cadmium sulfide crystals produced by sublimation in a high temperature gradient, at a temperature of 4.2° K in a magnetic field. This Zeeman splitting is not accompanied by a diamagnetic shift [1].

In previous work [2], we presented additional data on a new kind of fluorescence, which can be observed at 4.2° K for certain pure cadmium sulfide crystals and which two of the authors had observed earlier and had interpreted as the appearance of exciton annihilation [3]. We also investigated the absorption spectra at 4.2° K which appeared to be less complex than the spectrum of CdS crystals prepared by other methods [4]. Moreover, we reported that all the fluorescence and absorption lines are polarized with the electric vector perpendicular to the optical axis of the crystal.

It seemed to be of interest to study the influence of a strong magnetic field on these fluorescence and absorption lines. These experiments were conducted at the Physical Technical Institute AN USSR in Leningrad.

The sample studied was a CdS single crystal 4 mm x 2 mm x 50-60 μ. Its fluorescence and absorption spectra were described earlier [2]. While clamped in a selected crystallographic orientation, the crystal was submerged in a cryostat containing liquid helium and placed between the poles of an electromagnet. The fluorescence was excited by the mercury line at 3650 Å. The investigation was conducted by using a grating spectrograph with a 2 m focal length in the first and second orders. The second order dispersion was 1.7 Å/mm in the spectral range studied. The necessity of using a very narrow entrance slit width (0.03 mm) and of limiting the photographic exposure to the time between two fillings of the cryostat with liquid helium led to our being able to observe the influence of the magnetic field only on the finest and most intense lines of the fluorescence spectra.

MAGNETIC FIELD PERPENDICULAR TO THE OPTICAL AXIS OF THE CRYSTAL

In the first series of experiments, we placed the crystal with its optical axis perpendicular to the magnetic field. The most intense fluorescence

ine at λ = 4870 Å and also the considerably ess intense neighboring line at λ = 4868 Å ppear to be split on photograph 1 (fig. 1), obtained sing a magnetic field of 28,000 Oe.

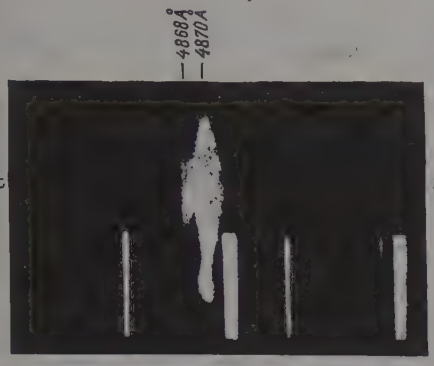

Figure 1

On the original photograph, it can also be een, although with difficulty, that the λ = 4861 A ine is also split. The spacings between the two oublet components are, respectively, 0.58 Å, .8 Å and 1.2 - 1.3 Å .

As with the unsplit lines observed in the ab- ence of a magnetic field [2], the components of hese doublets are polarized perpendicular to the ptical axis of the crystal. Actually, they are learly observed through the Nicol oriented so that ⊥ c (i.e., E || H); conversely, they are al- ost completely quenched if the Nicol is rotated hrough 90° . Therefore, these doublets are the π - components. The σ - components are not observ- d for this orientation of the crystal relative to he magnetic field.

MAGNETIC FIELD PARALLEL TO THE OPTICAL AXIS OF THE CRYSTAL

On the other hand, observation of the σ com- onents will be possible if the crystal is located o that its optical axis is parallel to the magnetic ield. However, under these conditions none of the luorescent lines mentioned shows Zeeman splitting, s shown in figure 2, which gives spectra at H=0 nd H=28000 Oersteds.

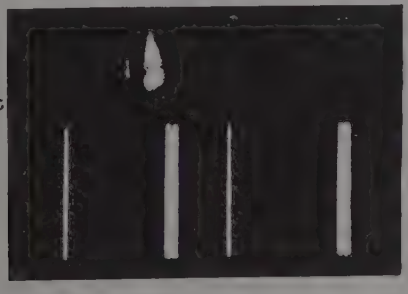

Figure 2

Thus, depending on the crystal orientation, the magnetic field can cause either a doublet in the π - component or an unsplit line corresponding to the σ component. This result is in agreement with what has been observed in certain crystals containing rare-earth ions.

On the other hand, no matter what the crystal orientation relative to the magnetic field, the center of gravity of the Zeeman components does not exhibit a shift toward longer wavelengths. Such a shift was observed in cuprous oxide [1], which indicates that the system causing the appearance of the series in the Cu_2O crystal has an electron in an orbit, which in this case is very large in comparison to the lattice parameters. On the other hand, if it is assumed that the series of luminescence lines observed in the cadmium sulfide crystals we studied was due to the annihilation of excitons, then the absence of a diamagnetic shift would mean that the orbital radii of these excitons are considerably less than in the cuprous oxide crystal.

We also carried out certain investigations on the influence of a magnetic field on the absorption lines in the same crystals. The absorption line at λ = 4869.1 Å is so weak with the Nicol oriented E || c and in nonpolarized light that the Zeeman effect could clearly be observed. The complex absorption edge is displaced [2] for the Nicol oriented E ⊥ c and only one of the lines mentioned above is observed; it becomes considerably more intense and its width is 1.62 Å . This absorption line, in a H = 28,000 Oe magnetic field directed perpendicular to the optical axis of the crystal, is broadened greatly, has very clear edges and its width becomes 2.24 Å . This broadening possibly occurs because of splitting of the levels into two components, which are superimposed. Since the orientation is E || H in this case, then we may speak of a doublet, exactly as has been established in the fluorescence case. Further experiments are required to confirm this result.

December 31, 1958

References

1. E. F. GROSS, B. P. ZAKHARCHENIA: J. Phys. et Rad., 18, No. 1, 68 (1957)
2. M. BANCIE-GRILLOT, E. F. GROSS, E. GRILLOT, B. S. RAZBIRIN: C.R. (in press)
M. BANCIE-GRILLOT, E. F. GROSS, E. GRILLOT, B. S. RAZBIRIN: OiS (See preceding article)
3. E. GRILLOT, M. BANCIE-GRILLOT, P. PESTEIL, A. ZMERLI: C.R., 242, 1794 (1956)
E. GRILLOT: J. Phys. et Rad., 17, 822 (1956)
4. E.F. GROSS, M. A. IAKOBSON: DAN USSR, 102, 485 (1955)

TOM VI, Vyp. 5
VOL. VI, No. 5

OPTIKA I SPEKTROSKOPIIA
OPTICS AND SPECTROSCOPY

Mai, 1959
May, 1959

The Crookes Radiometer as a Radiation Chopper

M. L. VEINGEROV, A. A. SIVKOV, A. P. PETROV

In certain cases, it is impossible to use a radiation chopper driven by an electric motor; e.g. because of interference of the latter with the measuring apparatus, or because of the necessity of avoiding sparking, if a dc motor were to be used.

Our experiment have shown that a somewhat altered Crookes radiometer can operate as a radiation chopper.

A radiometer was prepared whose moving parts rotated, as is usual, on the point of a needle. The mica vanes, however, blackened on one side and aluminized on the other, were clamped at a 45^{o} angle to the vertical rather than vertically. The radiation flux which set the radiometer rotating was directed to the blackened side of the vanes in the horizontal plane. The radiation flux to be modulated was directed vertically to the aluminized side of the vanes and was thus chopped by the rotation. The angular velocity of the radiometer depends on the degree of vacuum and on the magnitude of the driving flux. The greatest angular velocity achieved was 13 revolutions per second for 2.10^{-2} mm Hg pressure and for a driving flux of 0.5 watt directed at the vanes by means of a lens.

Hence, the modulation frequency for four vanes was 52 cps.

By decreasing the driving flux, the frequency of the interruptions could be smoothly reduced to zero. When the radiation to be chopped is constant and sufficiently intense, this radiation can be used to drive the radiometer. To do this, it is necessary to direct the radiation vertically, as before, but in the opposite direction, i,e., toward the blackened side of the vanes.

The maximum diameter of the transverse cross-section of the radiation beam to be modulated is determined by the size of the radiometer vanes. In our case, it was 10 mm.

Still another possible variation of the Crookes radiometer is an instrument having two sets of vanes situated one above the other. One series of vanes is clamped vertically as usual and is used for rotation; the other set is used to modulate the radiation. The angular momentum for this design will be corespondingly larger than in the previous case

January 9, 1959

TOM VI, Vyp. 5
VOL. VI, No. 5

OPTIKA I SPEKTROSKOPIIA
OPTICS AND SPECTROSCOPY

Mai, 1959
May, 1959

Letter to the Editor

In my paper [1], I gave a value, mentioned in [2] for the radius of curvature of the knife-edge of the entry slit of the IKS-11 monochromator of $r_o = 105$ mm, in connection with which some conclusions were drawn about the incomplete compensation of distortion of the spectral lines in this instrument. Actually, according to the working sketches of the factory, $r_o = 158$ mm, which compensates almost completely for both the dispersion and aberration curvatures of the lens for all interchangeable prisms.

References

1. I. V. PEISAKHSON: OiS, 4, 481 (1958)
2. S. G. RAUTIAN: OiS, 1, 1000 (1956)

ОМ VI, Vyp. 5
ol. VI, No. 5

OPTIKA I SPEKTROSKOPIIA
OPTICS AND SPECTROSCOPY

Mai, 1959
May, 1959

BOOK REVIEW

Optics of Anisotropic Media by F. I. Fedorov

AN BSSR Press, Minsk, 1958

D. IU. GAL'PERN

In this book by F. I. Fedorov a number of roblems of electromagnetic optics is investigated. he presentation is based on Maxwell's equations nd relationships between electric intensity and lectric induction, magnetic intensity and magnetic nduction, and electric intensity and current ensity.

The author limits himself to considering the ropagation of plane wave fronts in an unbounded edium, and also the reflection and refraction of lane wave fronts from a plane interface between wo unbounded media, and as a result all highly mportant problems of diffraction drop out of the nvestigation.

Propagation of light is studied, in succession, n an isotropic non-conducting and non-magnetic edium, anisotropic non-conducting and non-magnetic edium, isotropic conducting and non-magnetic medium, nd, thus, in the monograph there are chapters orresponding to all problems covered in courses f optics and crystal optics.

In the initial chapters, devoted to the optics f isotropic media, it is assumed as usual, that: he electric intensity vector is proportional to lectric induction vector, magnetic intensity ector to magnetic induction vector, and current ensity vector to electric intensity vector. In ubsequent chapters, devoted to optics of aniso- ropic media, it is assumed that the proportionally oefficients, relating the electric induction ector to the electric intensity vector, magnetic nduction vector to magnetic intensity vector, tc., are replaced by tensors. Thus, the problem s treated as in all modern courses of optics. he fact that F. I. Fedorov considers only the ases in which the function relating the basic ectors is a tensor, deprives him of the possibility f examining phenomena more complex than anisotropy, or instance optical activity. A feature of the onograph is that the author presents the material n both vector and tensor forms, without being estricted to any definite system of coordinates. he author's conclusions are correct to the same egree in any coordinate system, if all the lements of the corresponding tensors are known.

This method of presentation is both natural nd modern. However, studying from the book equires experience in using vectors and tensors, hich will present difficulties for some readers. A short description of tensors is given in the ook, but it is the opinion of the reviewer that t is insufficient for a good understanding of the ook. The formulas cited in the book, are of a imple form, due to the use of vectors and tensors, ut in order to use these formulae the reader must ompute all the vector and tensor components.

In the process of translating the optics of rystals into the language of vectors and tensors, F. I. Fedorov obtained some new and interesting results, and the mistakes of his previous presentation are corrected. Of the new results one must note the simple, and to the reviewer's knowledge original, formulas for computing the phase and and amplitude of the vectors of the rays refracted and reflected from the boundary of two crystals, and a set of conditions set up for magnetic and conducting anisotropic bodies.

In an overwhelming majority of the cases, the tensors of the dielectric constant and of the magnetic permeability and conductivity are given in the coordinate system coinciding with the principal axes of these tensors. Therefore, it would seem more advantageous to use the main axes of one of the tensors for the coordinate system and present other tensors in the same system.

For practical use, the formulas for solving a given problem should have been given in the book. It may be assumed that the method of transformation is known, or that it may be found in textbooks, but of course it is more convenient to have all the necessary formulas in the same book.

Contrary to F. I. Fedorov's opinion, the use of vector and tensor methods, generally speaking, does not reduce the number of transformations in deriving the formulas, but permits breaking up the derivation into several independent parts, thereby simplifying the derivations for magnetic or conducting crystals.

The book, apparently, is not a textbook of crystal optics but a monograph, the study of which is useful for persons familiar with its presentation. Therefore, a logical presentation of simpler cases of plane wave propagation in anisotropic magnetic media first, followed by more complex cases of light propagation in anisotropic magnetic media, which is quite proper for a textbook, could be replaced by considering the most general case. Particular solutions, pertaining to elementary problems, could have been obtained by making corresponding simplifying assumptions in general formulas.

In the book, it should have been pointed out more clearly that all derivations, with regard to refraction and reflection, refer to an indefinitely large plane refracting surface. The beginning of the sixth paragraph permits one to infer that reflection from any surface is being examined.

The book is a very valuable contribution to the extremely limited literature of crystal optics. The study of it is useful for everyone seriously occupied with electromagnetic optics, and the first chapter, containing a very clear presentation of basic concepts, may be recommended even to the beginning students of optics. The other chapters are intended for a mature reader.

D. IU. Galpern.

TOM VI, Vyp. 5
VOL. VI, No. 5

OPTIKA I SPEKTROSKOPIIA
OPTICS AND SPECTROSCOPY

Mai, 1959
May, 1959

OBITUARY

M. F. ROMANOVA

Soviet science has sustained a great loss. Mariia Fedorovna Romanova, Professor and Doctor of Technical Sciences, member of the Communist Party of the Soviet Union and well known specialist in the field of optical measurement, passed away on March 1 of this year, at the age of 67. In our country the name of M. F. Romanova was connected with the development of interferometry and its application to metrology.

After graduating with honors from the Womens Pedagogical Institute in 1916, Mariia Fedorovana was assigned to the institute in the capacity of assistant professor of physics. This was the beginning of her career.

At the Government Optics Institute, where she was accepted together with other talented young people soon after the founding of the institute, M. F. Romanova began her studies under the supervision of D. S. Rozhdestvenskii and A. A. Lebedev. Her first work was devoted to the development and thorough study of the Hartman method in its application to the testing of parabolic mirrors. Later on she switched to the search for more monochromatic spectral lines in order to extend the limits of visibility of the interferential picture The presence of a hyperfine structure of the red line of cadmium, observed by M.F. Romanova in 1933 and which had been regarded as simple up until then, for the first time placed in doubt the suitability of this line for its further utilization as a primary standard and proved to be a stimulus for the development of research dealing with spectra of even-even elements. Mariia Fedorovna was one of the first in the Soviet Union to initiate studies dealing with the production of highly reflecting thin coatings and research into the qualities of surfaces of mirrors for instruments of high resolving power. She developed an exact method of studying surfaces by increasing their reflectivity by silver plating. (This method was developed by her independently of Tolansky, to whom this method is generally ascribed.

Concurrently with research in the field of high resolution spectroscopy , Mariia Fedorovna also worked on problems concerning the application of interference to measure-length. Her monograph, written in 1937, entitled "Light Interference and its Technical Applications", to this day remains a reference book for all who utilize optical measurements of length. In 1938, Mariia Fedorovna transferred her studies to the All-Union Research and Scientific Institute for Metrology named after D. I. Mendeleev. Here, under her supervision and with her direct assistance, took place the comparison of the prototype of meter No.28 with the light wave length of the red line of cadmium. This study was the basic reason why the Soviet Union changed to a new length standard by utilizing the length of light waves. Being a supporter of the development of progressive ideas in metrology, Mariia Fedorovna attempted in her studies to establish a basis for a practical change to atomic constants. Therefore, side by side with pure scientific research, she also worked on the development of interferometers for the measurement of large end measurement of length.

Being an enthusiastic and active supporter of ideas of creative cooperation with industry during the difficult years of World War II, Mariia Fedorovna promptly responded to the requirements of industry and was decorated with the " Red Order of Labor" for her work in the solution of a series of problems concerning exact optical measurements connected with the defense effort.

Mariia Fedorovna was one of the leading metrologists of our country. She was able to train and gather around her a group of physicists and engineers engaged in the exact measurement of length. The efforts of this group placed Soviet metrology in a leading position in the field of interferential measurement of length.

Being very devoted to young people, Mariia Fedorovna, her great scientific activity notwithstanding, was throughout her life extremely active in pedagogical work in several Leningrad institutes of higher learning.

A highly cultured woman, her attributes were broad erudition and a thorough knowledge of special problems.

Those who knew her will always retain in their memory the bright image of Mariia Fedorovna.

ABBREVIATIONS OFTEN ENCOUNTERED AND USED HEREIN

DAN USSR	Doklady Akademii Nauk	(Reports of the Academy of Sciences of the USSR)
DAN UkrSSR	Dopovidi Akademii Nauk UkrSSR	(Reports of the Academy of Sciences of the Ukraine SSR)
DAN ArmSSR	Doklady Akademii Nauk ArmSSR	(Reports of the Academy of Sciences of the Armenia SSR)
IAN USSR	Izvestiia Akademii Nauk USSR	(Bulletin of the Academy of Sciences of the USSR)
	SF Seriia fizika	(Physics series)
	SM Seriia matematika	(Mathematics series)
	OKhN Otdelenie khimicheskikh	(Section of chemical sciences)
OiS	Optika i Spektroskopiia	(Optics and Spectroscopy)
PiTE	Pribory i Tekhnika Eksperimenta	(Instruments and Techniques of Experiment)
AE	Atomnaia Energiia	(Atomic Energy)
AZ	Astronomicheskii Zhurnal	(Astronomy Journal)
FMM	Fizika Metallov i Metallovedenie	(Physics of Metals and Metallography)
Radiotekh.	Radiotekhnika	(Radio Engineering)
RiE	Radiotekhnika i Elektronika	(Radio Engineering and Electronics)
UK	Uspekhi Khimii	(Progress in Chemistry)
UFN	Uspekhi Fizicheskikh Nauk	(Progress in Physical Sciences)
UFZ	Ukrainskii Fizichni Zhurnal	(Ukraine Physical Journal)
ZETF	Zhurnal Eksperimental'noi Teoreticheskoi Fiziki	(Journal of Experimental Theoretical Physics - JETP)
ZTF	Zhurnal Tekhnicheskoi Fiziki	(Journal of Technical Physics)
FTT	Fizika Tverkogo Tel	(Solid State Physics)
ZFKh	Zhurnal Fizicheskoi Khimii	(Journal of Physical Chemistry)
ZOKh	Zhurnal Obshchee Khimii	(Journal of General Chemistry
ZNKh	Zhurnal Neorganicheskoi Khimii	(Journal of Inorganic Chemistry)
ZPKh	Zhurnal Prikladnoi Khimii	(Journal of Applied Chemistry)
Tr.	Trudy	(Transactions, as for instance, Tr. FIAN)
FIAN	Fizicheskii Institut Akademii Nauk USSR	(P.N. Lebedev Physical Institut of the Academy of Sciences USSR)
Sb.	Sbornik	(Collection, as for instance, Fizich. sb. L'vovskogo Universitet) Fizich. sb. Fizicheskaia sbornik (Physics Collection)
Uch. Zap.	Uchenye Zapiskii	(Scientific Records)
Vestn.	Vestnik	(Herald or Messenger)
FTIAN	Fiziko-Tekhnicheskii Institut Akademii Nauk	(Physical-Technical Institute of the Academy of Sciences)
GOI	Gosudarstvennyi Opticheskii Institut	(State Optical Institute)
VEI	Vsesoiuznyi Elektrotechnicheskii Institut	(All-Union Electrotechnical Institute)
MFTI	Moskovskaia Fiziko-Tekhnicheskii Institut	(Moscow Institute of Physics and Technology)
NIZMIR	Nauchno-Issledovatel'skii Institut Zemnogo Magnetizma, Ionosfery i Rasprostraneniia	(Research Institute of Terrestrial Magnetism and Ionospheric Propagation)
GIFTI	Gor'kovskii Issledovatel'skii Fiziko-Tekhnicheskii Institut	(Gor'kii Research Institute of Physics and Technology)
NIFI	Nauchno-Issledovatel'skii Fizicheskii Institut	(Scientific Research Institute of Physics, Leningrad Univ.)
NIRFI	Nauchno-Issledovatel'skii Radio-fizicheskii Institut	(Scientific Research Institute of Radiophysics, Gor'kii Univ.)
GITTL	Gostekhizdat - Gosudarstvennoe Izdatel'stvo Tekhniko-Teoreticheskoi Literatury	(State Publishers of Technical-Theoretical Literature)
GIFML	Fizmatgizdat - Gosudarstvennoe Izdatel'stvo Fiziko-Matematicheskoi Literatury	(State Publishers of Physical-Mathematical Literature, formerly Gostekhizdat)
IL or IIL	Izdatel'stvo Inostrannoi Literatury	(Publishers of Foreign Literature)
Izd. AN USSR	Izdatel'stvo Akademiia Nauk USSR	(Academy of Sciences Press)
ZL	Zavodskaia Laboratoriia	(Factory Laboratory)
GOST	Gosudarstvennyi Obshchesoiuznyi Standart	(All - Union State Standard)
LIPAN USSR	Laboratoriia izmeritel'nykh priborov AN USSR	(Laboratory of Measuring Instruments)
IFAN UkrSSR	Institut Fiziki AN UkrSSR, KIEV	(Physics Institute AN Ukr SSR)
SFTI	Sibirskii Fiziko-Tekhnicheskii Institut, Tomsk	(Siberia Physical-Technical Institute)
IFAAN ESSR	Institut Fiziki i Astronomii AN ESSR, Tartu	(Institute of Physics and Astronomy)
IFA AN USSR	Institut fiziki atmosfery AN USSR	(Institute of the Physics of the Atmosphere)

TOM VI, Vyp. 5
VOL. VI, No. 5

OPTIKA I SPEKTROSKOPIIA
OPTICS AND SPECTROSCOPY

Mai, 195
May, 195

AFFILIATIONS OF AUTHORS FROM ISSUE 5

F. I. FEDOROV — BELORUSSKII GOSUDARSTVENNYI UNIVERSITET, MINSK
(Belorussian State University, Minsk)

A. I. FINKEL'SHTEIN — DZERZHINSKII FILIAL NAUCHNO-ISSLEDOVATEL SKOGO I PROEKTNOGO INSTITUTA AZOTNOI PROMYSHLENNOSTI
(Dzerzhinskii Branch of the Scientific Research and Planning Institute of the Nitrogen Industry)

P. A. BAZHULIN — FIZICHESKII INSTITUT im P. N. LEBEDEVA AN USSR
(P. N. Lebedev Physics Institute)

I. V. PEISAKHSON
A. A. SIVKOV
N. A. TOLSTOI
M. L. VEINGEROV
— GOSUDARSTVENNYI OPTICHESKII INSTITUT
(State Optical Institut)

O. N. KAZANKIN — GOSUDARSTVENNYI INSTITUT PRIKLADNOI KHIMII

L. S. MAIANTS — INSTITUT ELEMENTOORGANICHESKIKH SOEDINENII AN USSR

M. S. BRODIN — INSTITUT FIZIKI AN UkrSSR
(Ukrainian Institute of Physics)

I. N. SHKLIAREVSKII — KHAR'KOVSKII GOSUDARSTVENNYI UNIVERSITET

M. P. LISITSA
V. N. MALINKO
— KIEVSKII GOSUDARSTVENNYI UNIVERSITET
(Kiev State University)

I. F. KOVALEV — SARATOVSKII PEDAGOGICHESKII INSTITUT

SYMBOLS FOR SOURCES OF TRANSLATIONS

AIP
American Institute of Physics
335 East 45th Street
New York 17, New York

ATS
Associated Technical Services, Inc.
P.O. Box 271
East Orange, New Jersey

CB
Consultants Bureau, Inc.
227 West 17th Street
New York 11, New York

CCT
Consultants Custom Translations, Inc.
227 West 17th Street
New York 11, New York

CTT
Columbia Technical Translations
5 Vermont Avenue
White Plains, New York

HB
Henry Brutcher
P.O. Box 157
Altadena, California

LC
Photoduplication Service
Publication Board Project
Library of Congress
Washington 25, D. C.

MDF
Morris D. Friedman, Inc.
P.O. Box 35
New Newton 65, Mass.

NRCC
National Research Council, Library
Ottawa 2, Canada

OTS
Office of Technical Services
Department of Commerce
Washington 25, D.C.

PS
Primary Sources
11 Bleecker Street
New York 12, New York

RIS
Research Information Service
40 East 23rd Street
New York 10, New York

SLA
SLA Translation Center
The John Crerar Library
86 East Randolph Street
Chicago 1, Illinois

N. A. TOLSTOI
Formal'nyi analiz teorii dvukhstupenchatogo vozbuzhdeniia fosforestsentsii i fotoprovodimosti. III. Sravnenie teorii s opytom (svechenie ZnS-Cu) 665
O. N. KAZANKIN, F. M. PEKERMAN, L. N. PETOSHINA
Elektroliminofory na sul'fidselenidnoi osnove 672
I. N. SHKLIAREVSKII, A. A. AVDEENKO
Prosvetlenie metallicheskikh pokrytii 678
A. P. LUKIRSKII AND I. A. KARPOVICH
Opredelenie absoliutnoi chuvstvitel nosti nekotorykh fotomaterialov k ul tramiagkomu rentgenovskomu izlucheniiu 685
S. I. LEVIKOV AND L. P. SHISHATSKAIA
O vodorodnoi i rtutno-gelievoi lampakh dlia spektrofotometrov SF-4 688

KRATKIE SOOBSHCHENIIA

V. A. LOGINOV
Tochnost' opredeleniia dlin voln pri razlichnykh formulakh interpolirovaniia na difraktsionnom spektrografe DFS-3 692
M. P. LISITSA, V. N. MALINKO
O temperaturenoi zavisimosti intensivnostei sostavnykh tonov $\nu_1 + \nu_3$ i $\nu_1 + (\nu_1 + \nu_4)$ gazoobraznogo CCl_4 694
E. V. SHUVALOVA
Vliianie elektronodonornykh rastvoritelei na polusu pogloshcheniia valentnogo CH-kolebaniia atsetilena 696
V. B. GLASKO, V. P. MASLOV, V. I. PANIKAR, N. D. SOKOLOV
O vide korreliatosionnoi funktsii dlia atoma gelii 698
A. N. ZAKHAR'EVSKII, L. A. FEDIN
Izmerenie dvoinogo lucheprelomleniia volokon 701
G. S. KRINCHIK, M. V. CHETKIN
K teorii rasprostraneniia elektromagnitnykh voln v girotronykh sredakh 703
B. A. VEKLENKO
K teorii rezonansnogo isluchenija gazovogo razriada 705
M. BANCIE-GRILLOT, E. F. GROSS, E. GRILLOT B. S. RAZBIRIN
Issledovanie lineichaoi fluorestsentsii i pogloshcheniia kristallov chistogo sernistogo kadmiia pri temperature 4.2°K 707
E. F. GROSS, E. GRILLOT, B.P. ZAKHARCHENIA, M. BANCIE-GRILLOT
Vliianie magnitnogo polia na linii sinei fliuorestsentsii i na linii pogloshcheniia nekotorykh kristallov chistogo sernistogo kadmiia pri temperature 4.2°K 710
M. L. VEINGEROV, A. A. SIVKOV, A. P. PETROV
Radiometr Kruksa v kachestve modulatora izlucheniia 713
I. V. PEISAKHSON
Pis'mo v redaktsiiu 713

RETSENZII

D. IU. GAL PERN
Optika anizotropnykh sred. F. I. Fedorov 714

NEKROLOG

M. F. ROMANOVA 716

Formal Analysis of the Theory of Two-Step Excitation of Phosphorescence and Photo Conduction III. Comparison of Theory and Experiment (ZnS-Cu Luminescence) 430

Electro-luminophors on a Sulphide-Selenide Base 435

Increasing the Transparency of Metallic Coatings 439

Determination of the Absolute Sensitivity of Certain Photographic Materials to Ultra-Soft X-Radiation 444

Hydrogen and Mercury-Helium Light Sources for SF-4 Spectrophotometers 446

BRIEF REPORTS

Accuracy of Wavelength Determination on a DFS-3 Grating Spectograph with Various Interpolation Formulas 449

On the Temperature Dependence of the Intensities of the Summation Tones $\nu_1 + \nu_3$ and $\nu_1 + (\nu_1 + \nu_4)$ of Gaseous CCl_4 450

The Influence of Electron-donating Solvents on the C-H Stretching Absorption Band of Acetylene 452

The Form of the Correlation Function for the Helium Atom 453

The Measurement of Birefringence of Fibers 455

On the Theory of Electromagnetic Wave Propagation in Gyrotropic Media 457

The Theory of Resonance Radiation of a Gas Discharge 459

Investigation of Linear Fluorescence and Absorption of Pure Cadmium Sulfide Crystals at a Temperature of 4.2°K 461

Influence of a Magnetic Field on the Blue Fluorescence Lines and On the Absorption Lines of Certain Pure Cadmium Sulfide Crystals at a Temperature of 4.2°K 462

The Crookes Radiometer as a Radiation Chopper 464

Letter to the Editor 464

BOOK REVIEW

Optics of Anisotropic Media by F. I. Fedorov AN BSSR Press, Minsk, 1958 465

OBITUARY

M. F. ROMANOVA 466

Abbreviations Often Encountered and Used Herein 467

Affiliations of Authors from Issue 5 468

Lithoprinted in the U.S.A. by Blackburn Printing Co., West Concord, Mass.

TOM VI, Vyp. 5 OPTIKA I SPEKTROSKOPIIA Mai, 1959
VOL. VI, No. 5 OPTICS AND SPECTROSCOPY May, 1959

SODERZHANIE

Plan razvitiia narodnogo khoziaistva SSSR i zadachi sovetskoi optiki 573

F. A. KOROLEV, B. A. KOZLOV, A. I. ODINTSOV
K voprosu o forme kontura linii v atomnom puchke 576

S. M. KISHKO, M. IU. KUCHINKA
Funktsii vozbuzhdeniia nekotorykh polos vtoroi polozhitel'noi sistemy N_2 580

I. N. GODNEV, I. V. ORLOVA
O sviazi matritsy kinematicheskikh koeffitsientov s obratnymi matritsami kineticheskoi energii v zadache o kolebaniiakh v molekule 583

L. S. MAIANTS, E. M. POPOV, M. I. KABACHNIK
Raschet kharakteristichnykh kolebanii soedinenii fosfora. Kharakteristichnye kolebaniia molekul $POCl_3$, $POBr_3$, $PSCl_3$ i $PSBr_3$ 589

I. F. KOVALEV
Raschet i interpretatsiia kolebatel'nykh spektrov tetrametilsilana i tetrametilsilana--d_{12} 594

M. S. BRODIN, M. S. SOSKIN
Issledovanie spektra pogloshcheniia monokristalla 1,2-benzantratsena v oblasti nizhaishikh elektronnykh perekhodov 600

M. P. LISITSA, IU. P. TSIASHCHENKO
Kolichestvennye issledovaniia infrakrasnogo pogloshcheniia i dispersii khloroforma 605

V. E. ESKIN, I. A. BARANOVSKAIA
Akusticheskoe dvoinoe lucheprelomlenie fenil-etilovogo spirta pri nizkikh temperaturakh 616

V. M. PIVOVAROV, N. D. ORDYNTSEVA
Vliianie kontsentratsii i tipa rastvoritelia na intensivnost' linii kombinatsionnogo rasseianiia polnosimmetrichnogo kolebaniia nitrogruppy i na elektronnye spektry pogloshcheniia aromaticheskikh nitrosoedinenii 620

P. A. BAZHULIN AND L. P. OSIPOVA
Raznost' energii povorotnykh izomerov v zhidkom i gazoobraznom 1, 2 -ftorkhloretane 625

I. V. ASTAF'EV, A. I. SHATENSHTEIN
Spektry pogloshcheniia karbanionov 631

B. I. SUKHORUKOV, A. I. FINKEL'SHTEIN
Opticheskoe issledovanie molekuliarnogo stroeniia tsianamida i ego proizvodnykh. I. Molekuliarnoe stroenie ditsiandiamida 637

V. L. ERMOLAEVA
Zavisimost' veroiatnosti perenosa energii pri sensibilizovannoi fosforestsentsii ot sily ostsilliatora triplet-singuletnogo perekhoda v molekule aktseptora energii 642

V. M. AGRANOVICH, IU. V. KONOBEEV
Vliianie reabsorbtsiina vykhod i dlitel'nost' liuminestsentsii molekuliarnykh kristallov. I. 648

N. A. TOLSTOI, A. M. TKACHUK
Issledovanie spektraal'nogo raspredeleniia vremeni zatukhaniia svecheniia rubina metodom impul'snogo taumetra 659

CONTENTS

The Plan for the Development of the National Economy of the USSR and the Tasks of Soviet Optics 373

On the Line Shape in an Atomic Beam 375

Excitation Functions of Certain Bands of the Second Positive System of N_2 378

On the Relation Between the Matrix of Kinematic Coefficients and the Inverse Kinetic Energy Matrices in the Problem of Molecular Vibrations 380

Computation of the Characteristic Vibrations of Phosphorus Compounds. Characteristic Vibrations of the Molecules $POCl_3$, $POBr_3$, $PSCl_3$ and $PSBr_3$ 384

Calculation and Interpretation of the Vibrational Spectra of Tetramethylsilane and Tetramethylsilane--d_{12} 387

Investigation of the Absorption Spectra of 1,2-Benzanthracene Single Crystals in the Region of Lowest Electronic Transitions 392

Quantitative Investigations of the Infrared Absorption and Dispersion of Chloroform 396

Acoustic Birefringence of Phenylethyl Alchohol at Low Temperatures 401

The Influence of Concentration and Type of Solvent on the Raman Line Intensity of Totally Symmetric Vibrations of the Nitro Group and on the Electronic Absorption Spectra of Aromatic Nitro Compounds 403

Difference in Energy of Rotational Isomers in Liquid and Gaseous 1,2-Chlorofluoroethane 406

Absorption Spectra of Carbanions 410

Optical Investigation of the Molecular Structure of Cyanamide and its Derivatives I. Molecular Structure of Dicyanamide 414

Dependence of the Probability of Energy Transport in Sensitized Phosphorescence on the Oscillator Strength of a Triplet-Singlet Transition in an Energy Acceptor Molecule 417

Influence of Reabsorption on the Yield and Duration of Luminescence of Molecular Crystals. I. 421

Investigation of the Spectral Distribution of the Luminescence Decay Time of Ruby by The Pulse Taumeter Method 427